Modeling the effect of exogenous Interleukin 7 in HIV patients under antiretroviral therapy with low immune reconstitution

Ana Jarne Munoz

DOCTEUR DE
L'UNIVERSITÉ DE BORDEAUX

Ana JARNE MUÑOZ

Modeling the effect of exogenous Interleukin 7 in HIV patients under antiretroviral therapy with low immune reconstitution

Sous la direction de: Daniel COMMENGES
(co-directeur: Rodolphe THIÉBAUT)

Présentée et soutenue publiquement le 10 Décembre 2015

Membres du jury:

François DUFOUR	Président
Robin CALLARD	Rapporteur
Fabien CRAUSTE	Rapporteur
Francisco GUILLÉN	Examinateur
Daniel COMMENGES	Directeur
Rodolphe THIÉBAUT	Directeur

A mi familia
À Séb

Acknowledgements

Un grand **merci aussi** aux membres des équipes Biostat et SISTM, ainsi qu'à l'ensemble de l'ISPED pour les bons moments passés dans le centre. Ce fut un plaisir de travailler avec une si bonne ambiance. Merci à Mélanie Prague pour son temps et son attention constante. Merci à Camille, à Mél, à Juan... à tous ceux qui ont fait de cette expérience professionnelle remarquable une expérience personnelle inoubliable.

Finalement, j'exprime ma **profonde gratitude** au VRI (Institut de Recherche Vaccinale) qui a entièrement financé cette thèse.

Scientific production

PUBLICATIONS:

Papers published:

Thiébaut, R., Drylewicz, J., Prague, M., Lacabaratz, C., Beq, S., Jarne, A., Croughs, T., Sekaly, R.P., Lederman, M.M., Sereti, I., Commenges, D., Lévy, Y. (2014). **Quantifying and predicting the effect of exogenous interleukin-7 on CD4+ T cells in HIV-1 infection.** *PLoS computational biology, 10(5), e1003630.*

Toutain, J., Prochazkova-Carlotti, M., Cappellen, D., Jarne, A., Chevret, E., Ferrer, J., Idrissi, Y., Pelluard, F., Carles, D., Maugey-Laulon, B., Lacombe, D., Horovitz, J., Merlio, J.P., Saura, R. (2013). **Reduced placental telomere length during pregnancies complicated by intrauterine growth restriction.** *PloS one, 8(1), e54013.**

* This paper was the object of a punctual collaboration, and it is not related with the rest of the thesis work.

Papers under review (minor revisions):

Thiébaut, R., Jarne, A., Routy, J.P., Sereti, I., Fischl, M., Ive, P., Speck, R., D'Offizi, G., Casari, S., Commenges, D., Foulkes, S., Croughs, T., Delfraissy, J.F., Tambussi, G., Levy, Y., & Lederman, M.M. **Repeated cycles of recombinant human Interleukin 7 in HIV-infected patients with low CD4 T cell reconstitution on antiretroviral therapy: Results of two Phase II multicentre studies.** *Submitted to Clinical Infectious Diseases (August 2015)*

Papers in preparation:

Jarne, A., Commenges, D., Prague, M., Levy, Y., Thiébaut, R. for INSPIRE 2&3 study group. **Modeling CD4 dynamics in HIV-infected patients receiving repeated cycles of exogenous Interleukin 7.** *For Annals of Applied Statistics*

ORAL COMMUNICATIONS:

July 2014: *27th International Biometric Conference*, Florence, Italy **Using mechanistic models to analyze the effect of Interleukin 7 treatment in HIV infected patients.** Jarne, A., Thiébaut, R., Prague, M., Commenges, D.

June 2014: *2nd Bordeaux Modelling Workshop*, Bordeaux, France **Modeling the effect of exogenous IL-7 in HIV infected patients.** Jarne, A., Thiébaut, R., Commenges, D.

June 2013: *1st Bordeaux Modelling Workshop*, Bordeaux, France **Modeling the response to IL-7 therapy in HIV infected patients** Jarne, A., Commenges, D., Prague, M., Thiébaut, R.

POSTER COMMUNICATIONS:

February 2015: *CROI (Conference on Retroviruses and Opportunistic Infections)*, Seattle, USA **Repeated injections of r-hIL-7 in HIV patients receiving cART in INSPIRE 2&3 phase II trials.** Thiébaut, R., Jarne, A., Routy, J.P., Sereti, I., & Lederman, M.

May 2013: *20th International HIV Dynamics & Evolution Conference*, Utrecht, the Netherlands **Modeling the effect of Interleukin 7 on CD4+ T cells.** Jarne, A., Prague, M., Thiébaut, R., Commenges, D.

October 2013: *Early-stage researchers on HIV Summer School*, Carry-en-Rouet, France **Modeling the effect of IL-7 on CD4$^+$ T lymphocytes count.** Jarne, A., Thiébaut, R., Prague, M., Commenges, D.

November 2014: *Bordeaux Computational Biology and Bioinformatics*, Bordeaux, France **Modeling the effect of r-hIL-7 on CD4$^+$ lymphocytes dynamic.** Jarne, A., Thiébaut, R., Commenges, D.

Contents

List of Figures

List of Tables

Chapter 1

Introduction

The introduction of cART (combined antiretroviral therapy) has resulted in the recognition of HIV as a chronic condition, with major improvements in the life quality of HIV-infected patients. Generally, viral load dramatically decreases a few weeks after starting antiretroviral therapy, until it becomes undetectable. This usually leads to an adequate reconstitution of $CD4^+$ T cells pool with the consequent improvement in the immunenity, but sometimes this is not true. This work has been focused on these "low responder patients", who fail to achieve a good enough improvement in $CD4^+$ T cells count despite undetectable viral load after at least 6 months of cART therapy. The $CD4^+$ cells count remaining the best single indicator of immunodeficiency related to infection with HIV, novel therapeutic approaches and more concretely immunotherapeutic approaches are being considered for improving immune competence. In our days, the scientific

community is interested in Interleukin 7, a cytokine naturally secreted in the bone marrow and the thymus, as a promising adjutant therapy to boost the immune system of these patients.

The HIV infection is paradoxically a slow progressive pathogenic process including rapid, highly dynamic mechanisms. Dynamical models based on systems of ordinary differential equations have been widely used and particularly useful to study these mechanisms, as well as the interaction between HIV virions and $CD4^+$ T cells. During this thesis work, we have placed us in an scenario with undetectable viral load, and we have modeled the effect of exogenous Interleukin 7 on $CD4^+$ T cells. We have studied some amendments to an existing mathematical model based on a system of ordinary differential equations. This system distinguishes two main sub-populations of $CD4^+$ T lymphocytes, quiescent ($CD4^+Ki67^-$) and proliferating ($CD4^+Ki67^+$), according to the presence or not of the Ki67 proliferation biomarker. Also, we have used a complex statistical theory developed in the team in recent years for considering some different statistical models for the effect of the Interleukin 7. These models have been compared according to different comparison criteria, fits of real data or predictive abilities.

Second chapter provides a sufficiently wide background of HIV, antiretroviral therapy and immune response to cART. After a brief look at the state of the global HIV/AIDS pandemic in 2015, we focus on biological basis of the interaction HIV/immune system. Once we have a description of the HIV virus nature and behavior, a historical look at the antiretroviral drugs birth and cART use are exposed with a particular emphasis on mechanisms of reconstitution following therapy. Finally, we focus on normal and pathological immune responses to cART, with a bibliographic summary of figures and related parameters that have been published in relation to the target population: the "low immunological responders".

Chapter three is dedicated to immune-based interventions. After a background about the utility of developing adjuvant therapies for these "immunological low responder" patients, there is a presentation of the cytokine signaling as a fundamental process for human body regulation. An overview of the Interleukin-2 case (which was considered as a promising intervention for low immune responders) precedes the review of the Interleukin 7 (IL-7). Here we care about endogenous IL-7 production and behavior, as well as some opportunities for its clinical application. We have revised the clinical trials involving exogenous IL-7 in HIV infection to date, and we have fully entered into the INSPIRE 2 and INSPIRE 3 studies, to which analysis we have contributed in this thesis work. INSPIRE 2 and INSPIRE 3 trials are, to our knowledge, the first studies where repeated cycles of exogenous IL-7 are administrated to HIV infected patients.

The fourth chapter presents a background on mathematical modeling, with a special look to history and behavior of dynamic models focused on the interaction between the HIV virus and the immune system. We have extensively revised the theory underlying mixed effect models based on ODE systems, by looking in depth the " "half-Bayesian" statistical approach that has been used to estimate the unknown parameters. We present the existent mathematical model we have used, conceived for modeling data from patients receiving a single cycle of exogenous IL-7. It has been our "original model", from which we have adapted different mathematical and statistical patterns.

The fifth chapter slightly modifies the previous model to transform it into our "'basic model", that has been studied deeply in terms of statistical results and goodness of fits. Then, it has been modified again for letting introduce a feedback term. Different models have been studied and they are proposed with the obtained results. For instance, the "pharmacokinetic/pharmacodynamic model", which takes into account the estimated concentration of exogenous IL-7 at each time instead of the dose received. Also, a "four-compartment model" involving naive and memory CD4$^+$ T cells, as well as the "three-β's model", that has finally been kept for future analysis. Finally, the "three-compartment model" is shown with its modifications and obtained results, that tried unsuccessfully to explain the biological background for the improvement obtained with the "three-β's model".

Chapter six incorporates data from patients receiving repeated cycles from the INSPIRE 2 and INSPIRE 3 trials, assessing the theoretical long-term efficacy of this immune therapy. We have applied previous models to this data set, and also a new statistical model is proposed to compare the effect of repeated cycles with respect to the effect of the initial one. This "cycle effect" is found to be significant and slightly lower than 1. Some hypotheses have been suggested for trying to explain this phenomenon, as the so-called feedback effect or the presence of antibodies. In this Chapter, we have also predicted the effect of exogenous IL-7 when administered throughout different scenarios (different number of injections in a cycle). Predicted trajectories of a regular patient (with both random effects equal to zero) and two real patients have been displayed for 4 years. We have ended up concluding that repeated complete cycles are perhaps not necessary for all patients, and an adaptive treatment in function of the response to the first cycle could be considered.

Chapter seven concludes, and a French abstract can be found in Chapter eight. To finish, during this thesis work I have had the opportunity of doing a 3 months internship at the Universidad de Navarra (Spain) in the framework of the Mérimée program. There, I took part of a team that is searching to describe the epidemiology of HIV in Navarra and to estimate in this region the number of HIV infections that are currently without diagnosis. This is explained in Appendix F.

Chapter 2

HIV infection and cART therapy

2.1 Introduction: HIV pandemic in 2015

The end date for both the *Millennium Development Goals (MDGs)* and the *2011 Political Declaration on HIV and AIDS* is the year 2015. For this occasion, UNAIDS (Joint United Nations Program on HIV and AIDS) has presented a report in order to review progress and start preparing for the final reporting towards these targets. As the main statistics, there were 2.3 million people newly infected in 2012, even though new HIV infections drop by 30% since 2002 (Maartens et al., 2014). There are 35 million people living with HIV in the world (and the trend is on the rise), of which 19 million do not know their HIV-positive status (Kelly and Wilson, 2015). In 2012 there were 1.6 million AIDS-related deaths. Overall, almost 78 million people have been infected and about 39 million people have died of HIV since the beginning of the pandemic (according to the World Health Organization).

In 2011, the United Nations Political Declaration on HIV and AIDS recognized that HIV and AIDS constitute a global emergency, posing one of the most formidable challenges to the development, progress and stability of societies and the world at large. They noted that despite substantial progress over the three decades since AIDS was first reported, the HIV pandemic remains an unprecedented human catastrophe.

2.2 Human Immunodeficiency Virus

2.2.1 Background: Immunity and CD4$^+$ T cells

Immune system comprises small cells called lymphocytes, that can be divided into B and T cells. B cells are produced in the bone marrow and they carry extremely diverse antibody molecules. When a foreign pathogen like a virus enters the body, the B cells that have antibody receptors of the correct specificity will become activated. They will start to multiply providing even more specific interaction with the virus. Antibody molecules of B cells can bind to the virus particle and mark it as a foreign structure for elimination by other cells of the

immune system (Nowak and May, 2000). T cells are produced in the thymus and they can be roughly classified according to the quantity of surface proteins into CD8 positive (CD8$^+$) cells and CD4 positive (CD4$^+$) cells. There are also some functionally distinct populations: Helper T cells can secrete cytokines (proteins acting as the messenger molecules of the immune system); cytotoxic T lymphocytes (CTLs) kill infected cells; natural killer (NK) cells are involved in innate immunity; regulatory T cells (Treg) inhibit immune responses.

HIV virus infect CD4$^+$ T cells leading to a progressive depletion of the number and functionality of these cells, together with progressive impairment of cellular immunity and increasing susceptibility to opportunistic infections (Okoye and Picker, 2013). CD4$^+$ T cells count (CD4 count) is then used as an indicator of HIV and AIDS disease progression.

Two distinct populations of T lymphocytes can be distinguished by phenotypic criteria: naive and memory cells. Mature T cells are produced in thymus and the bone marrow, and then they migrate into lymph nodes, spleen and mucosa-associated lymphoid tissue (Male and Brostoff, 2007). Those who are immunologically inexperienced are called naive lymphocytes, and they will die as naive cells if they do not recognize MHC-peptide complexes for which their T-cell receptors (TCR) have high affinity (Berard and Tough, 2002). In the steady state, the generation of new cells and the spontaneous death of these cells maintain the pool of naive lymphocytes at a fairly constant number. After naive lymphocytes are activated in specialized lymphoid organs they become larger and proliferate and are called lymphoblasts, some of which differentiate into effector lymphocytes (having the ability to produce molecules capable of eliminating foreign antigens). On the other hand, memory cells may survive in a functionally quiescent or slowly cycling state for months or years. Although it is still not clear which surface proteins are definitive markers of memory populations, they have long been classified into central memory T cells (restricted to the secondary lymphoid tissues and blood) and effector memory T cells (which can migrate between peripheral tissues). Recently, another player has been highlighted: the tissue-resident memory T cells, that occupies tissues without recirculating (Mueller et al., 2013; Shin and Iwasaki, 2013; Sathaliyawala et al., 2013).

2.2.2   What is the HIV virus?

Human Immunodeficiency Virus (HIV) is a retrovirus (their RNA genome is transcribed into DNA by means of the enzyme reverse transcriptase: RT) firstly isolated in 1983. As a member of the lentivirus family, it generally produces a long-term latent infection and slowly progressive, fatal diseases. Two major types have been identified: HIV-1 and HIV-2. HIV-2 has the same modes of transmission but a lower infectivity potential than HIV-1 (Kanki et al., 1994) and a slower progression to AIDS (Campbell Yesufu and Gandhi, 2011). These two types may be further divided into groups, where HIV-1 group M is the most common cause of AIDS. Henceforth in this work we will only reference to HIV-1, even if only HIV is written for clarity purposes.

Primary target of HIV are CD4$^+$ T cells, in which the virus can replicate and thereby exhaust the lymphocytes, producing profound immunodeficiency (Kurth and Bannert, 2010). In retroviruses, frequent ARN variations produce new viral genotypes that can mutate into new viral quasispecies. For HIV,

about three base exchanges were estimated in a single reverse transcription of the genome (see Unger et al. (2000)).

2.2.3 HIV discovery

Warning signs began in 1981 with the publication of Gottlieb et al. (1981), where a medicine assistant professor from Los Angeles presented the case of four previously healthy homosexual men who had contracted *Pneumocystis carinii* pneumonia, extensive mucosal candidiasis, and multiple viral infections. In 1982, Stahl et al. (1982) warned that an epidemic of a fulminant variety of Kaposi's sarcoma had recently appeared among young and middle-aged men in the United States.

The HIV virus was firstly isolated thanks to a biopsied lymph node of a patient with "signs and symptoms that often precede the acquired immune deficiency syndrome" in 1983 (Barré-Sinoussi et al., 1983). This earned François Barré-Sinoussi and Luc Montagnier the 2008 Nobel Prize in Physiology or Medicine. By the summer of 1983, evidence was obtained for a retrovirus related to HTLV (human T-lymphotropic virus) in many patients with AIDS (Gallo, 2002). Soon after the isolation of HIV, its main receptor (CD4 cell surface molecules) was identified (Dalgleish et al., 1984; Klatzmann et al., 1984). This discovery reinforced the idea of monitoring of the quantity of $CD4^+$ T lymphocytes (CD4 count) together with the concentration of HIV RNA in plasma (viral load) in the follow up of infected patients. A complete review of these three decades of HIV research can be found in Barré-Sinoussi et al. (2013).

2.2.4 Natural evolution of untreated HIV infection

Natural history of untreated HIV infection can be divided into three well differentiated phases, as detailed in Figure 2.1

Primary or Acute HIV Infection starts immediately after infection, and it is characterized by an initial burst of viremia. Although anti-HIV-antibodies are still undetectable, Viral load is already present in the first weeks after the infection (Abu-Raddad, 2015). An important replication rate is accompanied by a significant decrease of the CD4 count. Most of patients in this phase experience symptoms similar to those of many other viral infection that usually go unnoticed. This short phase (6-12 weeks) is followed by the **clinically asymptomatic stage**, where viral load remains stable and CD4 count falls relentlessly. The length of the asymptomatic phase is very heterogeneous, with an average of about 10 years (Nowak and May, 2000). After that, a **severe immunodeficiency** appears, where viral load increases and CD4 count drastically goes down. The development of AIDS announces the final phase of the disease, when the immune system is exhausted and patients die from opportunistic infections.

2.2.5 Virus replication

HIV replication cycle (see Figure 2.2) begins with the binding of the virus in a $CD4^+$ T cell. The viral external glycoprotein, gp120, recognizes the CD4 receptor and coreceptors (CXCR4, CCR5) present on the cell surface. Upon infection of the susceptible host cell, HIV-RNA and proteins are released into
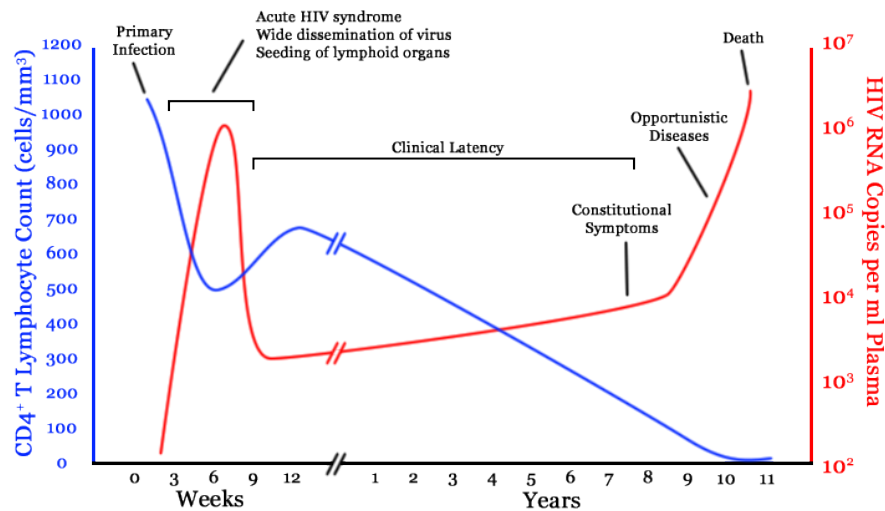
Figure 2.1: Stages of the natural history of HIV infection. *From: O Brien, Stephen J. & Hendrickson, Sher L. (2013) Host genomic influences on HIV/AIDS. Genome Biology 2013, 14:201. Retrieved 9 September 2015, from GenomeBiology. doi:10.1186/gb-2013-14-1-201*

the cytoplasm, and the enzyme reverse transcriptase (RT) uses this to synthesize double-stranded DNA in the process for which retroviruses have received their designation (Gupta, 1996). Synthesized DNA (designated the provirus) is subsequently integrated into the host chromosomal DNA by the enzyme viral integrase (IN). Then, host cell signals initiate the transcription of viral DNA into genomic RNA and messenger RNA (mRNA), thanks to a viral protein called *tat*. For its part, this mRNA will be therefore used to synthesize viral proteins like *tat*. Assembly of viral proteins and encapsidation of the viral ARN lead to the formation of new immature virus forms. Finally, the protease enzyme converts them into new infectious virions that are released into the extracellular environment and will be able to infect new cells (Girard et al., 2007).

2.3 Therapies against HIV virus

2.3.1 Antiretrovirals birth

In 1985 Zidovudine (AZT), belonging to a group of drugs known as NRTI (Nucleotide Reverse Transcriptase Inhibitors), showed potent effects on the inhibition of the infectivity and cytopathic effect of HIV *in vitro* (Mitsuya et al., 1985). A double-blind, placebo-controlled trial was subsequently conducted in order to establish the *in vivo* efficacy of AZT in patients with AIDS (see Fischl et al. (1987)). In this study, 282 subjects were stratified according to CD4 count and were randomly assigned to receive AZT (N=145) or placebo (N=137) for a total of 24 weeks. When all subjects had completed at least 8 weeks, 19 placebo patients and only 1 AZT patient had died; the study was stopped and all subjects were put on AZT. In an unusually short period the FDA (Food and Drug Administration) recommended the approval of AZT for use as a treatment of
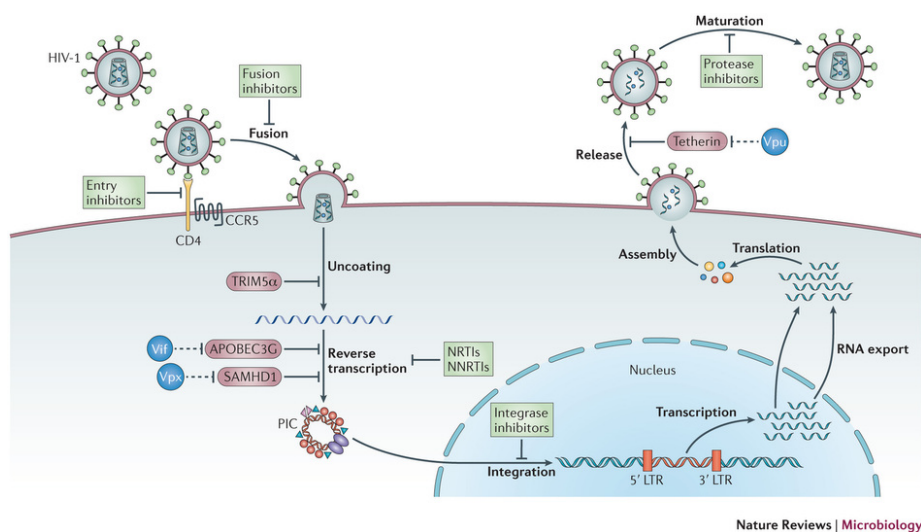
Figure 2.2: Main steps in the HIV replication cycle with antiretroviral drugs blocking them. *From: Barré-Sinoussi, F. & Ross, A.L. & Delfraissy, J.F. (2013) Past, present and future: 30 years of HIV research. Nature Reviews Microbiology 11, 877-883 (2013). Retrieved 5 September, 2015, from Nature. doi:10.1038/nrmicro3132*

selected patients with AIDS (Brook, 1987).

Different studies showed how Zidovudine decreased the rates of progression to AIDS as well as significant increased CD4 count in adults with asymptomatic HIV infection (Volberding et al., 1990; Cooper et al., 1993). Simultaneously, other studies advised about drug resistance estimated in about 89% of persons with late-stage HIV infection and 31% of persons with early stage disease after 12 months of AZT therapy (Larder et al., 1989; Richman et al., 1990). It was not until October 1991 that a second drug was approved for the treatment of HIV infection: the Didanosine (ddI). Patients developing AZT resistance mutations were switched to this new monotherapy, but also Didanosine resistances soon appeared (Kozal et al., 1994). Other NRTIs followed in following years, and therapies based on a combination of two of these drugs improved survival by delaying disease progression (Yarchoan et al., 1994; Darbyshire et al., 1996).

2.3.2 Combined Antiretroviral Therapy

The treatment of HIV infection was even more revolutionized in late 1995 and 1996, where two different types of antiretroviral drugs were added to the fight against HIV/AIDS: the PI (Protease Inhibitors) and the NNRTI (Non-Nucleotide Reverse Transcriptase Inhibitors). Several results supported the development of combinations of more than two antiretroviral drugs to increase and prolong HIV suppression while restricting mutations (D'Aquila et al., 1996; Staszewski et al., 1996). The advent of combined antiretroviral therapy (cART) for the treatment of HIV infection was seminal in reducing the morbidity and mortality associated with HIV infection and AIDS thanks to an important reduction in HIV replication and increase of CD4 count (Collier et al., 1996).

Nowadays, there are more than one hundred of antiretroviral drugs (see Table 2.1 for a review of drug currently used in the treatment of HIV infection).

Table 2.1: Brand name and active ingredients of the drugs currently used in the treatment of HIV infection. *From: U.S. Food and Drug Administration (FDA). Retrieved 9 September, 2015, from fda.gov.* Updated 25 September 2014

TYPE	BRAND NAME AND ACTIVE INGREDIENTS
Multi class	Atripla *(efavirenz, emtricitabine and tenofovir)*, Complera *(emtricitabine, rilpivirine and tenofovir)*, Stribild *(elvitegravir, cobicistat, emtricitabine and tenofovir)*
NRTIs	Combivir *(lamivudine and zidovudine)*, Emtriva *(emtricitabine, FTC)*, Epivir *(lamivudine, 3TC)*, Epzicom *(abacavir and lamivudine)*, Hivid *(zalcitabine, dideoxycytine, ddC)*, Retrovir *(zidovudine, azidothymidine, AZT, ZDV)*, Trizivir *(abacavir, zidovudine and lamivudine)*, Truvada *(tenofovir and emtricitabine)*, Videx EC *(enteric coated didanosine, ddI EC)*, Videx *(didanosine, dideoxynosine, ddI)*, Viread *(tenofovir, TDF)*, Zerit *(stavudine, d4T)*, Ziagen *(abacavir sulfate, ABC)*
NNRTIs	Edurant *(rilpivirine)*, Intelence *(etravirine)*, Rescriptor *(delavirdine, DLV)*, Sustiva *(efavirenz, EFV)*, Viramune *(nevirapine, NVP)*, Viramune XR *(nevirapine, NVP)*
PIs	Agenerase *(amprenavir, APV)*, Aptivus *(tipranavir, TPV)*, Crixivan *(indinavir, IDV)*, Fortovase *(saquinavir)*, Invirase *(saquinavir mesylate, SQV)*, Kaletra *(lopinavir and ritonavir, LPV/RTV)*, Lexiva *(fosamprenavir calcium, FOS-APV)*, Norvir *(ritonavir, RTV)*, Prezista *(darunavir)*, Reyataz *(atazanavir sulfate, ATV)*, Viracept *(nelfinavir mesylate, NFV)*
Fusion Inhibitors	Fuzeon *(enfuvirtide, T-20)*
Entry Inhibitors	Selzentry *(maraviroc)*
Integrase transfer Inhibitors	Isentress *(raltegravir)*, Tivicay *(dolutegravir)*

Controversial in evaluations of the associated short- and long-term complications and costs has been that the start of the antiretroviral therapy was delayed, for many years, until a patient's CD4 count fell below 200 cells per cubic millimeter, which led to frequent opportunistic infections. Today, we know that the use of combined antiretroviral treatment allows also to reduce the spread of HIV

infection. These therapies have shown to reduce the amount of HIV in blood and in genital secretions, which is strongly correlated with sexual transmission of HIV (Cohen et al., 2011).

In our time, first-line ART should consist of two Nucleotide Reverse-Transcriptase Inhibitors (NRTIs) plus a Non-Nucleotide Reverse-Transcriptase inhibitor (NNRTI). Consolidated ARV guidelines presented by the World Health Organization in June 2013 recommend TDF + 3TC (or FTC) + EFV as a fixed-dose combination as the preferred option to initiate ART. In most cases, effective therapy can dramatically reduce the risk of the classically defined AIDS complications (Li et al., 1998). The latest news about HIV treatment appeared on 15 September 2015, when the WHO proposed to begin the antiretroviral treatment as soon as possible, without waiting for achieving any CD4 count threshold.

2.3.3 Main goals of cART

Immunodeficiency results from viral replication, as well as dysregulation and ultimately failure of host homeostatic mechanisms and cellular immune networks (Okoye and Picker, 2013). The majority of patients who are able to access and adhere to combination therapy will achieve durable viral suppression together with an increase in the number of CD4 cells and the functional reconstitution of the immune system (Battegay et al., 2006).

Life expectancy for HIV-positive patients accessing ART is improving over time, but it remains below the life expectancy of the general population (Patterson et al., 2015). A patient's overall prognosis approaches the one of an HIV-negative individual only if CD4 count is consistently maintained over 500 cells/μL (Kelley et al., 2009; Saison et al., 2014).

The key objectives of antiretroviral therapy are to minimize the viral load and to recover and maintain an adequate CD4 count while maintaining a good quality of life and minimizing toxicity and side effects. Then, the target of antiretroviral therapy is to keep viral load below detection levels (usually between 20 and 50 copies/mL) and CD4 count above 500 cells/μL.

2.3.4 Immune reconstitution by CD4 count and viral load

From the beginning, the use of cART was linked to marked reductions in morbidity and mortality associated with the acquired immunodeficiency syndrome (AIDS). Firstly, the routine use of this combined therapy resulted directly in dramatic improvement in life-expectancy among HIV-infected patients with advanced immune depletion (Autran et al., 1997; Carr et al., 1996; Hammer et al., 1996; Palella Jr et al., 1998), and progressively the beneficial effect of the early initiation of cART reached a global consensus. Kitahata et al. (2009) studied the change of the risk of death in 17517 patients starting cART before the CD4 count fell below 350 or 500 cells/μL. They found that patients in the deferred-groups had an increase in the risk of death of 94% and 69%, respectively.

Opportunistic Infections Project Team COHERE et al. (2012) adjusted a Cox proportional hazards model for time to a first new AIDS event or death for patients on cART with a suppressed viral load. They showed that the relationship between the improvement in CD4 count and the risk of illness progression strongly varies according to the CD4 count stratum. Absolute risk reduction

for patients with a CD4 count above 500 cells/μL was found to have few clinical relevance, whereas it was intermediate for CD4 count from 200 to 350 and from 350 to 500 cells/μL. Importantly, in the category of patients below 200 cells/μL, small improvements of CD4 count showed great decreases in the risk of progression.

In the UK, May et al. (2014) conducted a study relating viral load and CD4 count with life expectancy in HIV-positive persons. They found that, after 5 years of ART, expected age at death of 35-year-old men varied from 54 (48-61) to 80 (76-83) years for those with CD4 count less than 200 cells/μL and no viral suppression versus CD4 count at least 350 cells/μL and suppressed.

Lewden et al. (2007) compared mortality rates in cART treated patients with mortality rates in the general population according to the level of CD4 count and the duration of exposure to cART. They also found that overall mortality for HIV infected patients was 7 times higher than in the general population. However, mortality reached the level of the general population in patients maintaining a CD4 count > 500 cells/μL after the sixth year after initiation of cART. A few years later, they compared mortality rates from data from the study COHERE (Collaboration of Observational HIV Epidemiological Research in Europe) comprising more than 80000 cART-treated HIV-infected people. They found that in a special subgroup (men who do not inject drugs) mortality rate was also similar to the general population when CD4 count > 500 cells/μL (Lewden et al., 2011).

2.3.5   Conclusion

A clear inverse relation exists between the number of CD4 cells in peripheral blood and the risk of HIV-1 associated diseases and mortality. The frequency of opportunistic infections dramatically declines upon initiation of antiretroviral therapy and the subsequent increase in CD4 cell count (Battegay et al., 2006).

Even if the routine measures of CD4 cell count in virologically suppressed patients have been questioned in these late years (see a review in Ford et al. (2015)), it continues to be the most important predictor in people with HIV infection.

In the next chapter, we see that there is no clear consensus with regard to how to best define immunological success or failure in the context of sustainable treatment-associated viral suppression.

2.4   Immune response to HAART

2.4.1   Different immunological responses to cART

There is no doubt that AIDS-defining morbidity and mortality has dramatically decreased since the introduction of cART. Several phases of T cell reconstitution can be distinguished: During the first weeks/months, a rapid increase of the CD4 count in plasma is observed, with a specifically rise of memory CD4 cells and destruction of optimal $CCR5^+$ viral targets (Autran et al., 1997; Okoye and Picker, 2013). After that, mainly the sub-population of memory CD4 lymphocytes contributes to maintain a slower increase of CD4 count; increase in naive T cells exists but is very limited in adults (Pakker et al., 1999).

Considerable individual variation in the reconstitution of CD4 lymphocytes has been noted. The majority of patients have a good virological response to therapy and exhibit sustained increases in their peripheral CD4 cell count, with most individuals achieving a normal CD4 cell count (Kelley et al., 2009). In few cases there is a virological failure of the therapy, the viral load remains high and this leads to overt AIDS (Okoye and Picker, 2013). Finally, in a significantly fraction of individuals, however, ART fails to effectively reconstitute CD4+ T cells to pre-infection levels despite fully suppressed viral replication (Pakker et al., 1999).

2.4.2 Consequences at short and long term

There is no doubt that individuals without evidence of increases in their CD4 cell count over time take a higher risk of non-AIDS-related morbidity and mortality Chêne et al. (2003); Kelley et al. (2009); Kantor et al. (2009); Saison et al. (2014).

This risk in clinical progression is observed both at short- and long-term. Grabar et al. (2000) noticed that patients with only a virologic response had significantly higher risks for clinical progression at 6 months (relative risk 1.98) whereas Lewden et al. (2007) found that differences in mortality remain higher even 7 years after starting the cART.

2.4.3 Immunological response through time

Patients not achieving an adequate immunologic response despite undetectable viral load are the target population within this work. There is no universal term for designating such patients (for instance Immunological Non Responders: INRs or Inadequate Immunological Responders have been used), and the main reason is the difficulty for finding universal criteria to classify the immune response. It goes without saying that the achieved CD4 count must be the main criterion, but, what is the threshold to determine a good response? (For instance CD4 count<200 cells/μL, CD4 count<350 cells/μL, CD4 count<500 cells/μL, CD4 recovery≤25%, CD4 recovery≥100 cells/μL...). And in terms of time, how long must it take after beginning cART? In fact, whether such patients will experience normalization of their CD4 count with time is a key question.

There are findings consistent with the idea of an asymptomatic effect, where patients would continue to have significant but progressively smaller increases in CD4 count after long time (Mocroft et al., 2007). For example, Lewden et al. (2007) found significant rises in CD4 count after 5 years of cART for patients beginning the treatment with CD4<200 cells/μL whenever viral suppression can be maintained for a sufficiently long period of time. On the other hand, Kelley et al. (2009) could not detect strong evidence of ongoing increases in CD4 count after year 7 among those who had yet to achieve a normal CD4 count, supporting the theory of a "plateau effect".

2.4.4 Immunological "low" responders

The lack of agreement on defining an immunological low response does not help for estimating the percentage of persons in this situation. In spite of that,

many authors have shed light on this issue. Here we present some of the figures that can be found estimating the number of "low immunological responders" to cART while adequate viral control. However, the mentioned differences in the definition of "low immunological responders" do not let to properly compare them. In any case, every figure must be assessed considering what is the study population and specially the amount of time spent under cART:

- 30% (Marchetti et al., 2008)

- 10-25% (de Kivit et al., 2015)

- 17% (Grabar et al., 2000)

- 9%-45% (Rusconi et al., 2013)

- 5-30% (Saison et al., 2014)

- 36% (Battegay et al., 2006; Kaufmann et al., 2005)

In 2009, Kelley et al. (2009) presented one of the most durable studies, in terms of time, regarding the immune response. They classified 366 virologically suppressed patients according to the CD4 count and they found that 25% of patients that began therapy between 100-200 cells/μL could be considered as "low immunological responders". This figure increases to 44% for patients with a baseline < 100 cells/μL and it decreases to 5% for those starting therapy with CD4> 300 cells/μL.

2.4.5 Parameters associated with immunological response to cART

Mechanisms underlying the immune recovery in HIV-infected patients upon long-term effective combined antiretroviral therapy remain elusive (Saison et al., 2014). Factors are only partly known and depend on both the host and the virus. Some of these factors linked to impairment of CD4$^+$ T cells reconstitution under cART are widely recognised, as **baseline CD4 count**, **pre-therapy nadir CD4 count**, **age** (consistent with the effect of age on thymic function), **degree of viral suppression** (possibly due to viral reservoirs) and especially when initiation of cART during **primary infection** rather than later in chronic infection (Battegay et al., 2006; Mocroft et al., 2007; Egger et al., 2002; Kaufmann et al., 2005; Okoye and Picker, 2013).

As for the drugs, cART intensification with Maraviroc in "low immunological responders" showed a slight increase of the CD4 count at week 12, which was not confirmed at week 48 (Rusconi et al., 2013). Also, a negative impact of the combination of tenofovir and didaonsine at high dose on the recovery of CD4$^+$ T cells was observed (Karrer et al., 2005).

In the last years, other factors have been proposed as having also an impact on immunological response to cART, as microbial translocation (Marchetti et al., 2008), levels of T regulatory cells (Gaardbo et al., 2014; Saison et al., 2014) or levels of the CC chemokine macrophage inflammatory protein 1β (Prebensen et al., 2015).

Also, within this year 2015, Jarrin et al. (2015) found that optimal restoration after cART was significantly lower for patients having a rapid progression

of the infection before treatment, but these differences disappeared after adjusting for baseline CD4 count. These results are in line with Kaufmann et al. (2005), when saying that long-term $CD4^+$ T cells changes during ART were not associated with the natural course of $CD4^+$ T cells depletion in untreated HIV-infected people before ART initiation. As another example of the variability of the considered factors, Allen et al. (2015) studied the association between the response to the Hepatitis B virus and CD4 gains during the first year of cART without conclusive results.

Chapter 3

Adjuvant interventions for HIV: Immunotherapy

3.1 Immunotherapies

In the previous Chapter, we have talked about the "immunologial low responder" patients. Here, we focus on novel immune-based therapeutic approaches that may be necessary to restore immunocompetence in these individuals.

3.1.1 Adjuvant therapies for HIV

It is not certain that prolonged cART would succeed to eradicate the infection on the long term, despite the fact that cART can reduce plasma virus to undetectable levels relatively fast. The reason is that HIV can persist in the body in several cellular and anatomical reservoirs that are established early in the infection, and contribute to long-term persistence of the virus. One of these reservoirs comprises latent infected resting $CD4^+$ T cells with a very long half-life (about 4 years). At this rate, eradication of this reservoir has been estimated over 60 years of cART treatment (Finzi et al., 1999; Pierson et al., 2000).

The fact that antiviral therapy does not restore effective defenses capable of controlling HIV replication (Pantaleo and Lévy, 2013) opens the way for complementary therapies in the search of a functional cure and ultimately eradication of the HIV. In addition to the search for an effective vaccine, immune based interventions are being considered as a key factor in HIV therapy in recent years. Development of an immunotherapy able to restore an effective immune response could have a crucial role in the fight against the virus.

3.1.2 The role of cytokines

Understanding HIV-specific immunity and its failure is needed for the development of these immunotherapies, that may one day lead to immune control of HIV infection (Lange and Lederman, 2003). Interleukins are part of the family of cytokines, that are communication tools between the lymphocytes for establishing and coordinating an adequate immunological response. Immune cells

15

as well as other cells of the lymphoid organs send information about the infection that will be received by cells having specific receptors. This is a complex process, where lymphocytes communicate through these interleukins for various purposes: they send signals for activating lymphocytes, stimulating production and proliferation of $CD4^+$ T cells, and also for slowing cellular activity when danger is finished, by means of apoptosis or controlled cellular death.

When HIV infects lymphocytes CD4, the homeostasis of the system is lost. Regulation mechanisms are disturbed, both at cellular and immune system levels. The number and function of $CD4^+$ T cells is seriously perturbed, and signals are incorrectly send and received. Infected $CD4^+$ T cells continue to produce new virus, and the system is no longer able to preserve the equilibrium, leading to a progressively destruction.

Immune therapy is proposed as an adjuvant of antiretroviral therapy in order to help the immune system to regain control of the situation.

3.1.3 Interleukin 2 therapy

Interleukin 2 (IL-2) is known to have a decisive influence in immune responses and homeostasis. Before the appearance of the HIV, the *in vitro* T cell-stimulatory capacity of the Interleukin 2 had already been documented (Morgan et al., 1976). Its role in influencing various lymphocyte subsets, as the differentiation of $CD4^+$ T cells into defined effector T cell (Boyman and Sprent, 2012; Zhu et al., 2010) converted the Interleukin 2 into a powerful and promising candidate for immunotherapy against the HIV virus.

First results showed that intermittent infusions of IL-2 produced substantial and sustained increases in CD4 count (Kovacs et al., 1995, 1996; Levy et al., 1999, 2012). For instance, Stellbrink et al. (2002) studied the effect of IL-2 on virus replication and reservoirs in 56 asymptomatic HIV-infected subjects with CD4 count>350 cells/μL. They found a CD4 count normalization in ∼90% of IL-2-treated patients whereas only ∼50% in cART-only subjects. Interestingly, they do not found an impact on virus production or latency. Also, Chun et al. (1999) noticed a reduction in the size of the pool of resting $CD4^+$ T cells containing HIV in the blood in patients receiving intermittent IL-2 in addition to cART.

Despite the demonstrated role of the IL-2 in regulating proliferation, differentiation and survival of T cells (Abrams et al., 2009), the clinical impact of $CD4^+$ increase associated with its use still remained to be seen.

The question was answered in 2009, at the 16th Conference on Retroviruses and Opportunistic Infections (CROI) in Montreal, where Pr Yves Levy and Pr Marcelo Losso presented the primary results of two large clinical trials: SIL-CAAT (Levy et al., 2009b) and ESPRIT (Losso and Abrams, 2009), respectively. These trials involved more than 5800 patients in the world, that were randomized into two groups: those who received repeated injections of IL-2 associated to combined retroviral therapy and those who received cART alone. Despite the significantly increase of CD4 count shown in both cases, no differences were observed in terms of the risk of opportunistic diseases or death.

Initially, it was difficult to understand the reasons for this disappointing performance. Shortly after, Weiss et al. (2010) found that the principal effect of long-term IL-2 therapy was the expansion of $CD4^+CD25^{lo}CD127^{lo}FOXP3^+$ and $CD4^+CD25^{hi}CD127^{lo}FOXP3^{hi}$ T cells population, which are part of the

regulatory T cells. Tregs represent a regulatory subset within the CD4$^+$ lineage involved in inhibiting the activation, proliferation and cytokine production of effector T cells (Okoye and Picker, 2013). The increase in the subset of Tregs is today the most accepted hypothesis for the failure of the IL-2 therapy in HIV infection. However, such behavior can result in very promising results, since IL-2 is being used in autoimmune diseases (Rosenzwajg et al., 2015; Klatzmann and Abbas, 2015).

3.2 Endogenous Interleukin 7

3.2.1 Introduction

Interleukin 7 (IL-7) was firstly characterized in 1988 as a pre-B cell growth factor (Namen et al., 1988), and it has since found to be indispensable for T-cell development in humans. Now, it is known to play an essential role in both T-cell and B-cell maturation (Beq et al., 2004; Fry and Mackall, 2002).

IL-7 is produced by stromal tissues and dendritic cells within the lymph node (Hofmeister et al., 1999; de Saint-Vis et al., 1998). The complete set of physiologic roles for this cytokine are still being elucidated, but we know the essential role of the IL-7 in enhancing both thymic-dependent and independent T-cell regeneration (Fry et al., 2001), proliferation (Vieira et al., 1998) and survival of mature cells (Vella et al., 1998; Seddon et al., 2003). See Lundström et al. (2012) for a review of the evidence implicating IL-7 as an important modulator of peripheral T-cell homeostasis. More recently, Dooms (2013) set out two mechanisms of IL-7 promotion of naive T cells survival: inhibition of the mitochondrial death pathway and stimulation of glucose uptake and metabolism.

IL-7 has been involved in the pathophysiology of a variety of diseases: Rheumatoid arthritis (van Roon et al., 2005), systemic lupus erythematosus (Badot et al., 2012), type 1 diabetes (Harrison, 2012) or multiple sclerosis (Gregory et al., 2007). Some of the opportunities for clinical application of this cytokine are summarized in Mackall et al. (2011).

3.2.2 Endogenous IL-7 in lymphopenia

Normal ranges for IL-7 oscillate from 0.3 to 8.4 pg/mL. Interestingly, there is a strong inverse correlation between IL-7 levels and CD4 count in HIV-infected patients (Fry et al., 2001). Actually, patients with a low CD4 count experience elevated circulating and tissue levels of IL-7, and Lundström et al. (2012) showed that this increased IL-7 availability plays a major role in mediating the enhanced cycling of naive and memory T cells. Mastroianni et al. (2001) found that treated patients who responded to cART had IL-7 concentrations below the detection limit, while patients with evidence of cART failure had increased concentrations of IL-7 (comparable to those found in the untreated group with progressive disease). Hodge et al. (2011) established that increased levels of IL-7 during lymphopenia can be the consequence of a decreased receptor-mediated clearance of IL-7 as the availability of receptors diminishes.

Saidakova et al. (2014) divided 80 HIV infected patients into two groups, according to the level of immunological response after at least two years of cART. They found that the amount of IL-7 in blood plasma was significantly

lower in immunological low responders (< 350 cells/μL) than in patients with an adequate immunological response, pointing to the insufficient amount of this cytokine as a factor blocking the increase in the number of CD4$^+$ T cells during cART. Also, the relative number of CD4$^+$CD127$^+$ T cells (expressing the IL-7 receptor) in low immunological responders was lower; thus, they concluded that these patients would have a deficiency of not only the amount of IL-7 but also of the number of cells producing a response to IL-7.

3.3 Exogenous IL-7 therapy

3.3.1 IL-7 in other diseases

Exogenous IL-7 has been evaluated as immunoadjuvant in a large number of illnesses in animals and humans for more than 20 years (Talmadge et al., 1993; Valenzona et al., 1998). IL-7 is currently being evaluated in the therapy of sepsis (Shindo et al., 2015), as well as in cancer (Sportès et al., 2010; Fritzell et al., 2013) or in the context of stem cell transplantation (Perales et al., 2012), among others.

3.3.2 IL-7 therapy in HIV infection

The relationship between IL-7 and modulation of immune function in patients with lymphocyte depletion suggests potential usefulness of exogenous IL-7 in the framework of the HIV infection. As far as we know, in 2009 were presented the first trials studying the safety and efficacy of the administration of Recombinant Human IL-7 (r-hIL-7).

Sereti et al. (2009) conducted a consecutive dose escalation design in order to determine the effect of a single dose of non-glycosylated r-hIL-7. Participants were HIV-infected persons under cART with HIV-RNA under 50000 cp/mL and CD4 count over 100 cells/μL. They found demonstrable biologic activity since 3 μg/kg with a maximum tolerated dose of 30 μg/kg and the most notable side effects were injection site reactions, transient increases in plasma HIV-RNA levels and transient elevations of liver function tests. Despite an initial decrease in circulating CD4 count on days 1 and 2 after IL-7 administration (possibly due to a redistribution of cells out of the circulation), they observed next statistically significant increases in almost all measured CD4 subsets, especially in central memory CD4. They also found that naive and all memory and effector subsets were induced to enter cell cycle after the injection (measured thanks to the proliferation marker Ki67). Importantly, they did not observe changes in the proportion of CD4$^+$ T cells with Treg phenotype.

Also in 2009, Levy et al. (2009a) presented another phase I/IIa trial, where the effect of 8 subcutaneous injections of non-glycosylated r-hIL-7 was evaluated. Here, participants were cART-treated HIV-infected patients with HIV-RNA under 50 cp/mL and CD4 count between 100 and 400 cells/μL. Patients received 3 or 10 μg/kg of r-hIL-7 every other day over 16 days. R-hIL-7 was well tolerated, with peaks of viral replication presented in 4 of the 7 patients in the highest dose group. As the main results, a sustained increase was observed in both naive and central memory CD4 subsets. Total CD4 count peaked at day 21 in both groups ,and the time to reach 500 cells/μL was equal to 7 days in average

in patients receiving IL-7 at 10 μg/kg doses. Also, the CD4$^+$ T cells gain 3 months after the first injection was strongly correlated with the CD4 count at baseline. Analysis of Ki67 expression showed an increase of cycling cells in all subsets except terminally differentiated effector cells.

3.3.3 INSPIRE (1) study

Subsequent studies were realized with a new glycosylated r-hIL-7 (CYT107), having a longer half-life, and they were called INSPIRE studies. These studies were carried out by Cytheris S.A. (which no longer exists), a bio-pharmaceutical company focused on research and development of new immunotherapies. Data are now managed by Revimmune Inc., a development stage biotechnology company that develops therapies for autoimmune diseases.

The first one was presented in Levy et al. (2012). INSPIRE (CYT-107-06) is a phase I/IIa randomized placebo controlled, single-blind multicenter dose-escalation study of subcutaneous intermittent r-hIL-7. Participants are chronically HIV-infected patients with CD4 count between 101-400 cells/μL and plasma HIV-RNA<50 copies/mL after at least 12 months of cART. This study provided information about 21 patients who received 3 weekly subcutaneous injections of r-hIL-7, at doses 10 μg/kg, 20 μg/kg or 30 μg/kg, plus two patients by dose level who were randomized to receive placebo (N=27). As the major findings, the maximal dose established as well tolerated was 20 μg/kg. This led to important dose-dependent increases in CD4 count, especially within naive and central memory subsets. CD4 count mean and percentage of CD4$^+$Ki67$^+$ mean by group are shown in Figures 3.1 and 3.2. No increase in Tregs was observed, and r-hIL-7 was contemplated as a real and powerful alternative to boost the immune system in cART-treated HIV-infected patients with inadequate immune response. The possibility of an intermittent therapy with repeated cycles of IL-7 in combination with cART was in the air.
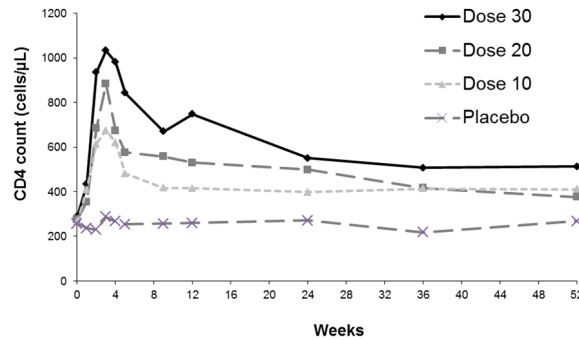
Figure 3.1: CD4 count by group for INSPIRE patients
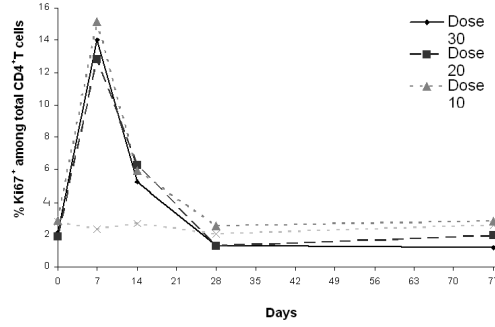
Figure 3.2: Percentage of $CD4^+Ki67^+$ cells by group for INSPIRE patients

3.3.4 Description of the INSPIRE 2 and INSPIRE 3 studies

These are the first studies considering repeated cycles of exogenous IL-7, conducted in HIV infected patients with a low immune response to cART despite undetectable viral load.

A first part of this thesis work was the contribution in analyzing data from INSPIRE 2 and 3 studies, that is the subject of an article submitted to *Clinical Infectious Diseases* and can be found in the Appendix D.

INSPIRE 2

INSPIRE 2 (CLI-107-13) was a single arm clinical trial conducted in the USA (Case Western Reserve, NIH/intramural NIAID, University of Miami) and in Canada (McGill University Health Centre). The study was approved by the ethics committees of the participating institutions, and all subjects provided written informed consent at screening. The study was registered in clinicaltrials.gov, NCT01190111.

Patients received a cycle of 3 weekly subcutaneous injections of r-hIL-7 at 20 μg/kg. The study was amended 12 months after its initiation to repeat cycles of r-hIL-7 in order to maintain CD4 count>500 cells/μL (see Figure 3.3).
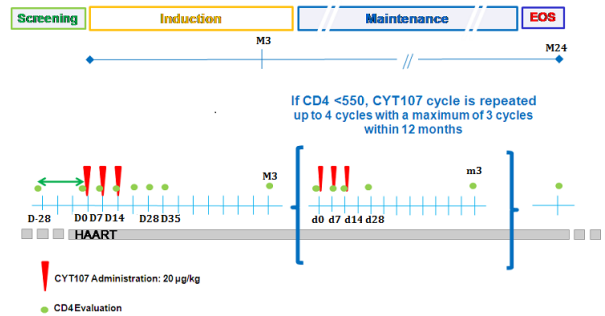
Figure 3.3: INSPIRE 2 design

INSPIRE 3

INSPIRE 3 (CLI-107-14) was an open-label, controlled, randomized trial conducted in Italy (Milano, Brescia, Roma), Switzerland (Zurich) and South Africa (Johannesburg and Bloemfontein). The study was approved by the ethics committees of the participating institutions, and all subjects provided written informed consent at screening. The study was registered in EudraCT, #2010-019773-15 and clinicaltrials.gov, NCT01241643. INSPIRE 3 was prematurely terminated because the Cytheris company was liquidated on June 18th 2013. All patients were however followed for at least 3 months after the last drug administration as per protocol.

While treated by cART, patients were randomized in two arms: CYT107 Arm and Control Arm with a ratio 3:1 (3 CYT107: 1 control). Patient randomized to the CYT107 Arm received induction treatment within 2 weeks and then were followed quarterly. A first cycle (3 weekly doses) of r- hIL-7 was administered at 20 μg/kg. A new cycle was administered if at any quarterly evaluation the CD4 count fell below 550 cells/μL. A maximum of four cycles were administered over 21 months and 3 over the first 12 months. Patients randomized to the Control Arm were followed without receiving study treatment for one year. If CD4 count were still below 500 cells/μL, an induction cycle was administered and then, repeated maintenance cycles of r-hIL-7 were given if quarterly evaluations showed CD4 count below 550 cells/μL (see Figure 3.4).
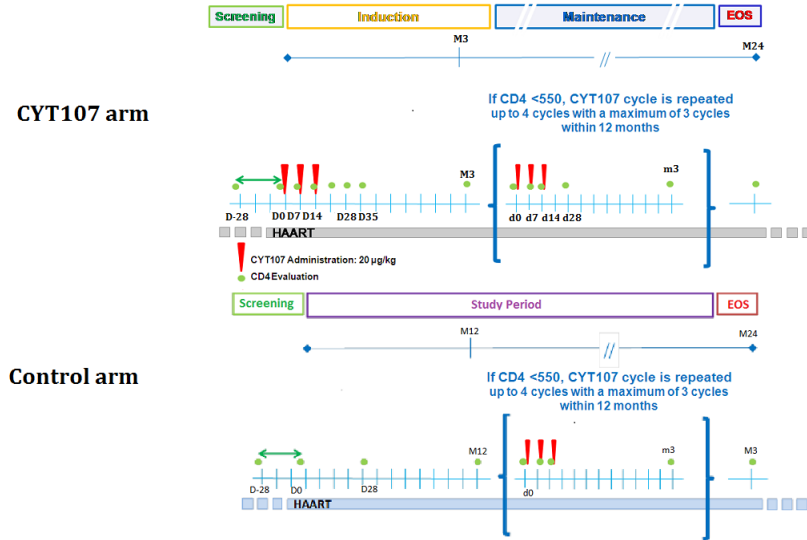
Figure 3.4: INSPIRE 3 design

Conditions for eligibility in INSPIRE 2 and 3 are summarized in Table 3.1.

A total of 111 patients were included in the two trials (23 in INSPIRE 2 and 88 in INSPIRE 3). Median CD4 count before the first cycle was 266 cells/μL, whereas it was 473 cells/μL and 373 cells/μL before the second and the third one, respectively. A total of 107 patients started the first cycle; 74 started the second cycle; 15 started the third cycle, and only one participant received 4 cycles. A total of 197 cycles were received, of which 42 were incomplete (one or

Table 3.1: Main eligibility criteria for INSPIRE 2 and 3 studies

Criterion	INSPIRE 2	INSPIRE 3
Age	≥ 18 years old	
cART	Minimum of one year	Minimum of two years
HIV-RNA plasma level	< 50 cp/mL	
CD4 count	101-400 cells/μL	101-350 cells/μL
Other	No hepatitis B or C nor HIV-2 or HTLV 1 or 2	

two injections instead of three).

3.3.5 Results of the INSPIRE 2 and INSPIRE 3 studies

Sereti et al. (2014) presented some results from the first cycle of the INSPIRE 2 study, where it was confirmed that r-hIL-7 administration leads to important increases of CD4 count in peripheral blood. They also showed results from 12 patients that underwent recto-sigmoid biopsies before and after r-hIL-7 administration, concluding an increase in the gut mucosa as well as an apparent improvement in gut barrier integrity after the treatment.

Here are some of the most important results of the analysis we did of both INSPIRE 2 and INSPIRE 3 studies (see Thiébaut et al. (2015 in revision) for more information): R-hIL-7 was overall well tolerated. A total of 1300 drug Related Adverse Events (RAEs) were reported, most (77.6%) were grade ≤ 1, 20.7% grade 2 and 1.7% grade ≥ 3.

For analyzing the time spent over 500 CD4 cells/μL we included all patients having a follow-up of 21-24 months after the first injection (N=76). The median time spent above 500 CD4 T cells/μL was found to be 13.7 months (8.4, 20.1). Half of these patients spent more than 63% of their follow-up with more than 500 CD4 T cells/μL.

Two major questions appear when analyzing data from these studies: Are complete cycles necessary or could similar effect be obtained with 2 or even a single injection? And also, have repeated cycles the same effect as the initial ones? During maintenance cycles, observed CD4 responses after 2-injection cycles and complete cycles seem similar, however, 1-injection cycles seem to have a weaker effect (see Figure 3.5). As for the responses after first and second cycles (for patients receiving complete cycles) we did not find differences (see Figure 3.6).

These results were confirmed with a survival study. We analyzed the influence of some covariates as age, gender or CD4 baseline into the time to drop of CD4 count below 550 cells/μL (the threshold for receiving a new cycle). Linear interpolation allowed us to estimate the time to drop below 550 when this drop was observed; otherwise, the observation was right-censored. A shared gamma frailty model was used, in order to take into account the inter-individual variability. A Weibull hazard function was fitted using a parametric model with the R package Frailtypack (Rondeau et al., 2012). The stronger predictor of dropping below 550 CD4$^+$ T cells/μL was CD4 count at baseline (p<0.001, HR=11.1 when CD4 below 200 cells/μL). The following variables were considered: age,
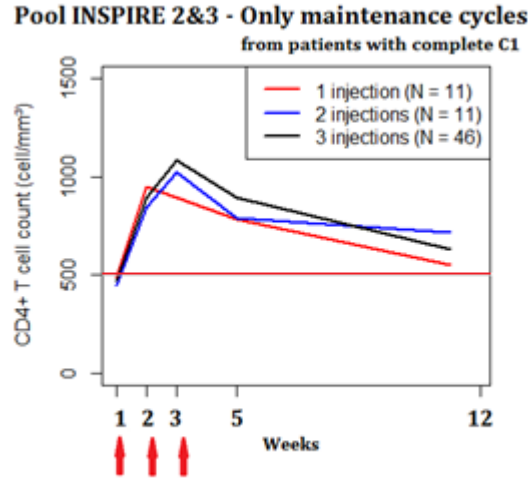
Figure 3.5: Observed CD4 responses for INSPIRE 2 & 3 patients when receiving 1-injection cycles, 2-injections cycles or complete cycles within repeated cycles with the number of observations at each time

sex, ethnic origin, type of cycle *initial/maintenance*, number of injections in a cycle, time since HIV diagnosis, duration of cART, stage at diagnosis and proviral HIV DNA levels at baseline. The only one that was found to have a significant effect was the number of injections in a cycle (see Table 3.2). After adjustment, there was still unexplained inter-individual variability in the probability of dropping below 550 cells/μL as the variance of the frailty parameter (0.822) was significantly different from 0 (p=0.006).

As for the sub-populations of $CD4^+$ T cells, the main increase was observed among naive and central memory cells, with a transient increase of $CD4^+Ki67^+$ (cycling) cells and without relative increase of Tregs. There was no impact of the presence of antibodies on the $CD4^+$ T cell dynamics. Nearly half of the patients had HIV-RNA blips exceeding 50 copies/mL; also 13% of the patients included in INSPIRE 2 and 17% of the patients included in INSPIRE 3 had HIV-RNA blips exceeding 200 copies/mL.

In conclusion, INSPIRE 2 and INSPIRE 3 studies show that repeated cycles of r-hIL-7 can improve and sustain CD4 restoration in cART-treated HIV-infected patients with a low immune response.
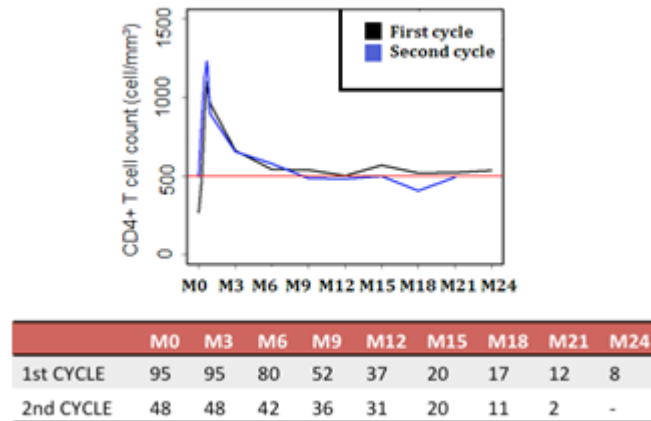
Figure 3.6: Observed CD4 responses for INSPIRE 2 & 3 patients when receiving initial and maintenance (complete) cycles

Table 3.2: Shared Gamma Frailty model using a Weibull hazard function. Data are based on 95 patients with a CD4 T cell count > 550 cells/μL two weeks after the last injection of r-hIL-7

Factor	Hazard Ratio	95 % CI	p-value
Baseline CD4 count			**<0.001**
CD4 > 200 cells/μL	1		
CD4 ≤ 200 cells/μL	11.10	(4.02, 30.66)	
Type of IL-7 cycle			0.57
Initial cycle	1		
Maintenance cycle	0.86	(0.51, 1.46)	
Number of injections in a cycle			**0.023**
Three injections	1		
Two injections	2.27	(0.79, 6.55)	
One injection	4.29	(1.32, 13.90)	

24

Chapter 4

Background: Modeling

4.1 Introduction

Throughout this work we have used dynamic models based on a system of ordinary differential equations (ODEs). We basically distinguish two sub-populations of CD4$^+$ T cells: quiescent and proliferating cells, according to the presence or not of the biomarker Ki67. A mixed effects model is applied on biological parameters in order to capture both populational and individual behavior. Statistical inference in such mechanistic models can be an arduous task, mostly because of the non-linearity of the ODE system and the presence of random effects. For this purpose, we have used a program called NIMROD (Prague et al., 2013a), based on the maximum *a posteriori* estimation of the penalized likelihood function.

In Section 4.2 there is an overview of the HIV modeling history, that has been a relevant tool to improve our knowledge about the viral dynamics in the last years. Section 4.3 explains our statistical approach, that is based on a mathematical model, a statistical model on the biological parameters and a model for the observations. Section 4.4 deals with parameter estimation in these types of models; we review some of the proposed methods and we develop the hierarchical approach that has been used during this thesis work. The NIMROD program is succinctly presented. Section 4.5 describes the basis of our work: the original model firstly presented in Thiébaut et al. (2014) and some minor changes which help us to shape our "basic model".

4.2 HIV modeling framework

According to Motta and Pappalardo (2013), "modeling" is the human activity consisting of representing, manipulating and communicating real-world daily life objects, and "system" is the collection of these interrelated objects. Generally speaking, a "model" can be any interpretable description of a system in terms of the objects constituting it and the relationships among them. In clinical research, mathematical models based on differential equations are especially useful; as biological systems. These simplified mathematical representations of the real world are especially useful in medicine, as biological systems interrelating different cellular populations.

A model can have different purposes. Descriptive models have been widely

used for analyzing HIV data, as classic linear mixed models describing viral load and CD4 count trajectories (Boscardin et al., 1998) or more complex bivariate mixed models taking into account left-censoring of viral load measurements(Thiébaut et al., 2005). Mechanistic models, on the other hand, search to translate the biological knowledge into equations, in our case a system of ordinary differential equations. This ODE system represents important characteristics of the underlying biological mechanisms, and we call this type of models "dynamic models". Unknown parameters involved in such a system of differential equations are called "biological" parameters, and they will condition the behavior of the system. ODE systems involve functions and their derivatives and they are, therefore, able to relate a continuous quantity and its rates of change throughout time.

Since 1995, our knowledge about viral dynamics has greatly increased thanks to dynamic models. The works of Ho et al. (1995) and Wei et al. (1995) were the start point of a success story for modeling. First models searched to determine the ratio between the destruction of cells and lack of their production in CD4 lymphocyte depletion seen in AIDS. Until then, HIV replication and clearance rates were thought to be relatively slow (because of the stable levels of viral load observed in patients following several years of infection). These models showed that HIV production and clearance in chronically infected patients take place at a rapid rate. The field of HIV research was also hugely influenced by Perelson et al. (1996), who estimated the half-life of the virus in plasma at only 6 hours or less, and the production rate was estimated at 10^{10} virions per day on average. There were many consequences to these findings, some of them of a fundamental importance. HIV was considered as a rapidly reproducing virus that could respond to therapy, but also as a virus that would repeat every single possible point mutation of the genome several times a day, so it could quickly become resistant to any single drug (Perelson, 2002).

These dynamic models became progressively more complex, as the biological knowledge about the infection and the immune system increased. Today, most HIV dynamic models describe the interaction between virions and $CD4^+$ T cells: a complete review of the existing models can be found in Xiao et al. (2013).

4.3   Parts of the theoretical model

Mechanistic approaches based on systems of ordinary differential equations with biological "compartments" (cell populations) have been widely used. The originality and complexity of our approach is in the statistical part. An elaborated method for the estimation of the parameters involved in these equations is implemented in our team since 2007. A mixed effect model is applied to biological parameters for distinguishing populational and inter-individual behavior, and a so-called "model for the observations" let us to deal with observations of only some of the system compartments and also with measurement errors. This is generally presented in this Section. A frequentist maximum likelihood approach based on an adaptation of a Newton-like method was initially proposed by Guedj et al. (2007). Hereafter, a maximum *a posteriori* estimation in a semi-Bayesian context was introduced by Drylewicz et al. (2012). This is furthered explained in Section 4.4. We describe now the different parts of our model:

ODE model for a population of subjects

For subject i, we can write

$$
\begin{cases}
\frac{d\mathbf{X}^i(t)}{dt} & = f(\mathbf{X}^i(t), \boldsymbol{\xi}^i) \\
\mathbf{X}^i(0) & = h(\boldsymbol{\xi}^i)
\end{cases}
\tag{4.1}
$$

where $\mathbf{X}^i(t) = [X_1^i(t), ..., X_K^i(t)]$ is the vector of the K state variables (or compartments), and $\boldsymbol{\xi}^i(t) = [\xi_1^i(t), ..., \xi_p^i(t)]$ is the p-vector of the parameters, having a biological interpretation.

We often assume that the system is in a stable state at time 0 (all the state variables are in equilibrium), but alternatively the start point can be fixed. In order to be able to estimate the parameters, a compromise has to be found to design a reasonably simple model which correctly fits the observed data.

Mixed effect model for $\boldsymbol{\xi}^{(i)}$

Biological parameters can be re-parametrized thanks to one-to-one functions $\phi_l[\xi_l^i(t)] = \tilde{\xi}_l^i(t)$, l=1,...,p. In our case, we take a logarithmic transformation to ensure positivity. A mixed effect model can be applied on some of the biological parameters, and this allows us to introduce covariates and to take into account inter-individual variability. For the patient i and the biological parameter l we have:

$$
\begin{cases}
\tilde{\xi}_l^i = \log(\xi_l^i) \\
\tilde{\xi}_l^i = \phi_l + z_l^i \beta_l + b_l^i
\end{cases}
\tag{4.2}
$$

where ϕ_l is the intercept, and z_l^i is the vector of explanatory variables associated to the fixed effects of the lth biological parameter. The β_l's are vectors of regression coefficients associated to the fixed effects. If b^i is the individual vector of random effects, we assume $b^i \sim \mathcal{N}(0, \Sigma)$.

In our model, we have not applied this statistical model for all parameters, but to some of them which are supposed to be affected by IL-7 injections. As for the random effects, we apply them for parameters that have shown a notable inter-individual variability.

Model for the observations

In practice, the vector $[X_1^i(t), ..., X_K^i(t)]$ is generally not directly observable. Instead, we have some discrete-time observations of some functions of its components. With relevant transformations used for obtaining normality and homocedasticity of measurement errors distributions, we note the observable components as follows (for the subject i at time j):

$$
Y_{ijm} = g_m(\boldsymbol{X}(t_{ijm}, \tilde{\boldsymbol{\xi}}^{(i)})) + e_{ijm}, \qquad e_{ijm} \sim N(0, \sigma_m^2)
$$

with independent normally distributed measurement errors.

So the vector of the parameters to estimate includes biological parameters, regression coefficients for the covariates, variances of random effects and variances of measurement errors.

4.4 Maximum likelihood estimation

Working with nonlinear mixed effect models in a population context involves two main numerical issues: the evaluation of the integrals involved when computing the log-likelihood function and a possibly non closed-form of the solution of the ODE system. Several attempts for approximating the likelihood function have been made (Pinheiro and Bates, 1995), but it may result in misleading conclusions (Ding and Wu, 2001). Also, purely Bayesian approaches relaying on the Markov Chain Monte Carlo (MCMC) algorithms have been proposed (Putter et al., 2002; Huang et al., 2006). In 2007, Guedj et al. (2007) proposed the algorithm that we have used for estimating parameters.

In an inferential approach, the presence of random effects implies a hierarchical approach, so this algorithm starts by considering individual likelihoods given the random effects. After that, marginal likelihood is computed by integrating over the random effects via the adaptive Gaussian quadrature (Genz and Keister, 1996; Pinheiro and Bates, 2000). The Fortran solver DLSODE (Hindmarsh, 1983) allows us to solve the ODE system, using backward difference formula and gear type method BDF (Radhakrishnan and Hindmarsh, 1993).

The approach of Guedj was subsequently adapted to compute the normal approximation of the posterior, allowing prior knowledge on biological parameters to be taken into account (Drylewicz et al., 2012). The Bernstein-von Mises theorem (Van der Vaart, 2000) justifies asymptotically the assumption of a normal approximation of the posterior (NAP). This amounts to compute the maximum of the posterior distribution when the variance matrix is approximated by the inverse of the Hessian of minus the logarithm of the posterior. Let $L(\theta)$ be the log-likelihood function; let $\pi(\theta)$ and $P(\theta|Y)$ be the prior and posterior distribution, respectively; and let C be the normalization constant. Bayes theorem gives:

$$\log[P(\theta|Y)] = L(\theta) + \log(\pi(\theta)) + C, \tag{4.3}$$

and the normal approximation of the posterior is obtained by maximizing the penalized log-likelihood $L^P(\theta) = L(\theta) - J(\theta)$. If we assume normal priors for the p biological parameters, where E_0 and v_0 are the expectation and the variance under these priors, the penalization term can be written as:

$$J(\theta) = \sum_{j=1}^{p} \frac{[\phi_j - E_0(\phi_j)]^2}{2\, v_0(\phi_j)}. \tag{4.4}$$

Penalized likelihoods can be compared thanks to the criterion so-called "LCVa", an extension of Akaike criterion (AIC) proposed by Commenges et al. (2007). It corrects for the number of parameters and for the penalization, and is normalized on the number of observations (Commenges et al., 2008, 2015). This criterion can be written as:

$$\text{LCVa} = -\,\text{n}^{-1}[\; \text{L}(\tilde{\theta}) - \text{Trace}(\text{H}_{L^P}^{-1}(\tilde{\theta})\text{H}_L(\tilde{\theta}))],$$

where H_L is the Hessian of minus the log-likelihood. Since LCVa estimates a risk, the smaller value the better model. When the response is univariate, difference in criteria values can be considered as "large" beyond 0.1; however this threshold must be higher when the response is multivariate, as in our case.

Finally, a Fortran program called NIMROD (Normal approximation Inference in Models with Random effects based on Ordinary Differential equations) was developed (Prague et al., 2013a) collecting this approach. As for the optimization procedure, the program is based on the Robust Variance Scoring (RVS) algorithm (Commenges et al., 2006).

After calculating the individual score $U_i(\theta)$ using Louis' formula (Louis, 1982), the observed log-likelihood $L_P(\theta)$ and the scores $U(\theta)$ are calculated as the sum over all the subjects. Finally, the Hessian of $-L^P(\theta)$ is approximated by

$$G(\theta) = \sum_{i=1}^{n} U_i(\theta) U_i^T(\theta) - \frac{1}{n} U(\theta) U^T(\theta) + \frac{\partial^2 J(\theta)}{\partial \theta^2}$$

To finish, for when the algorithm gets stuck, NIMROD is implemented with an optional switch to a classical Levenberg-Marquardt algorithm by using the Hessian matrix (Marquardt, 1963). This method will be more robust than the Newton-Raphson method far from the maximum, when the penalized log-likelihood is not very close to a quadratic form.

NIMROD has three convergence criteria or stopping rules: a threshold for the displacement in the parameters space, a threshold for the variation in log-likelihood and a main criterion named RDM (Relative Distance to Maximum), that can be interpreted as the ratio of the numerical error over the statistical error (Commenges et al., 2006):

$$\text{RDM}(\theta^{(k)}) = \frac{U^P(\theta^{(k)})^T G^{-1}(\theta^{(k)}) U^P(\theta^{(k)})}{p} \tag{4.5}$$

Once the algorithm has converged individual trajectories are computed thanks to Parametric Empirical Bayes (PEB) estimators (Morris, 1983; Kass and Steffey, 1989).

NIMROD is written in Fortran 90, and it has been implemented to let parallel computing over the subjects. An open source code is available in `http://etudes.isped.u-bordeaux2.fr/BIOSTATISTIQUE/NIMROD/documentation/html/index.html`.

During this thesis, we made some inquiries about NIMROD calculation time, that can be found in Appendix A.

4.5 Original model

4.5.1 Description of the original model

Note: During the remainder of this work, the term IL-7 is sometimes used instead of r-hIL-7 when there is no possibility of confusion.

As it has been said, the structure of the model must represent important characteristics of the underlying biological mechanisms. We have considered as starting point the mathematical model appeared in Thiébaut et al. (2014), including two populations of CD4$^+$ T-cell: non-proliferating cells (CD4$^+$Ki67$^-$, denoted Q) and proliferating cells (CD4$^+$Ki67$^+$, denoted P).

$$\begin{cases} \frac{dQ}{dt} = \lambda + 2\rho P - \mu_Q Q - \pi Q \\ \frac{dP}{dt} = \pi Q - \rho P - \mu_P P \end{cases} \tag{4.6}$$

The system is supposed to be in equilibrium at t=0. A graphical representation of the model can be found in Figure 4.1. Q cells (CD4$^+$Ki67$^-$) are produced at a constant rate λ. They become P cells (CD4$^+$Ki67$^+$) at rate π and die at rate μ_Q. Every P cell divides and produces 2 Q cells at a rate ρ, and dies at rate μ_P. Even if we call them *mortality rates*, the loss rates μ_Q and μ_P are also influenced by any redistribution between blood and other tissues.
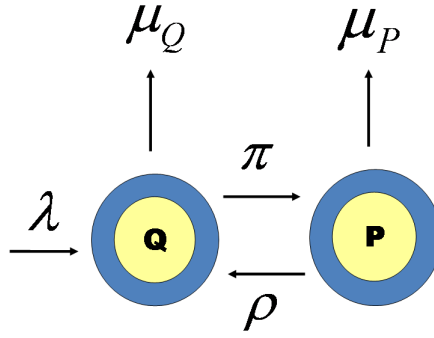
Figure 4.1: Graphical representation of the basic mathematical model

Table 4.1: Biological meaning of parameters from the original model

λ	Constant rate of production of the non-proliferating cells Q *(cells/day)*
ρ	Reversion rate *(/day)*
π	Proliferation rate *(/day)*
μ_Q	Mortality rate of non-proliferating cells Q *(/day)*
μ_P	Mortality rate of proliferating cells P *(/day)*

The biological parameters are defined in the table 4.1. For subject i we denote by $\xi^i = (\lambda^i, \rho^i, \pi^i, \mu_Q^i, \mu_P^i)$ the vector of individual biological parameters that appear in the ODE system.

As for the model for the observations, the state variables $(P^i(t), Q^i(t))$ are not directly observable. Let Y^i_{1j} and Y^i_{2k} be the CD4 count and the Ki67 count for patient i at times t_{ij} and t_{ik}, respectively. The following observation scheme is assumed:

$$\begin{cases} Y^i_{j1} = \sqrt[4]{(P+Q)(t^i_{j1}, \tilde{\xi}^i)} + \epsilon^i_{j1} \\ Y^i_{k2} = \sqrt[4]{P(t^i_{k2}, \tilde{\xi}^i)} + \epsilon^i_{k2} \end{cases} \tag{4.7}$$

where $\tilde{\xi}^i = (\tilde{\xi}^i_l, l = 1, ..., 5)$ and the ϵ^i_{j1} and ϵ^i_{k2} are independent Gaussian measurement errors with zero mean and variances σ^2_{CD4} and σ^2_P, respectively.

Thiébaut et al. (2014) considered data from 53 patients receiving a complete cycle of (glycosylated and not glycosylated) r-hIL-7. Their objective was to use mathematical modeling to test whether an improvement of peripheral proliferation itself can explain the observed CD4$^+$ T cell dynamics:

$$\begin{cases} \tilde{\pi} = \tilde{\pi}_0 + \beta_1 \mathbb{1}_{trt} + \beta_2 d & t \leq 16 \\ \tilde{\pi} = \tilde{\pi}_0 & t > 16 \end{cases} \tag{4.8}$$

The alternative hypothesis was that other additional mechanisms (as an improvement of production rate and/or of survival rate of quiescent cells) are required:

$$\begin{cases} \tilde{\mu}_Q = \tilde{\mu}_{Q_0} + \beta_3 \mathbb{1}_{trt} + \beta_4 d & t > 16 \\ \tilde{\mu}_Q = \tilde{\mu}_{Q_0} & t \leq 16 \end{cases} \tag{4.9}$$

$$\begin{cases} \tilde{\lambda} = \tilde{\lambda}_0 + \beta_5 \mathbb{1}_{trt} + \beta_6 d & t \leq 16 \\ \tilde{\lambda} = \tilde{\lambda}_0 & t > 16 \end{cases} \tag{4.10}$$

Here, $\mathbb{1}_{trt}$ indicates whether placebo ($\mathbb{1}_{trt} = 0$) or IL-7 ($\mathbb{1}_{trt} = 1$) injections have been received; and d is the quantity of the dose received. As we can see in the equations, the original model considers two possible covariates: the IL-7 treatment and a possible dose-related effect (assumed to be linear). The time of IL-7 effect on proliferation rate ($t = 16$ days) was found by profile likelihood.

In all cases, random effects were supposed on λ and ρ:

$$\begin{cases} \tilde{\lambda}^i(t) &= \tilde{\lambda}_0 + b^i_\lambda \\ \tilde{\rho}^i(t) &= \tilde{\rho}_0 + b^i_\rho \end{cases} \tag{4.11}$$

4.5.2 Results for the original model

The results obtained with the simplest statistical model showed a significant linear increase of estimated proliferation rate according to the dose group. Interestingly, this increased peripheral proliferation alone could not explain the long-term changes in CD4 count, and the fact of adding a supplementary effect on the mortality rate μ_Q and/or the production rate λ improved the results from a statistical point of view. Both models (fixed effects on π and μ_Q, or on π and λ) described correctly the CD4 count, and fits of the two model were not easily distinguishable (see Figure 4.2).

Statistical model considering an effect on π and μ_Q provided slightly better results from a statistical point of view (LCVa and likelihood results) where proliferation rate improved from 0.027 cells/day to 0.107-0.156 cells/day and
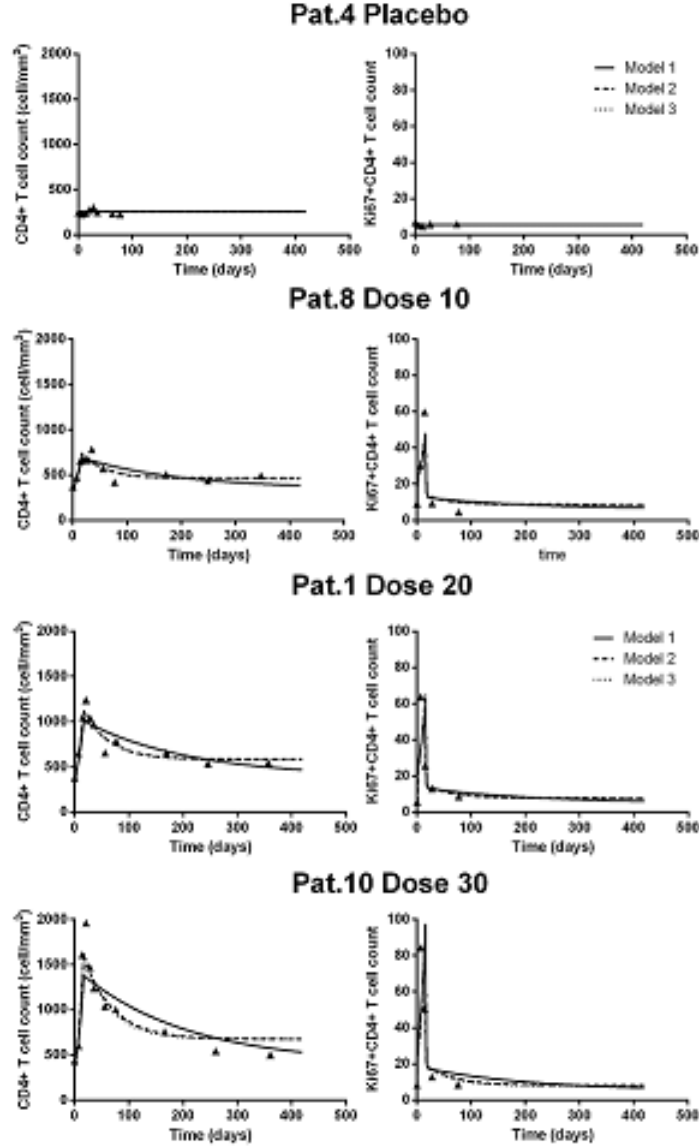
Figure 4.2: Goodness of fit of CD4 count for a random patient in each dose group from INSPIRE (1) when considering only an effect on π (Model 1), on π and μ_Q (Model 2) or on π and λ (Model 3)

mortality rate of quiescent cells decreased from 0.061 per day to 0.044-0.049 per day, corresponding to an improvement of the life span from 16.4 days to 20.4-22.7 days (Thiébaut et al., 2014).

As a conclusion, an increase of the survival of Q cells and/or of the production rate also contributes to T-cell homeostasis during IL-7 therapy, even if these parameters could not be perfectly differentiated.

Chapter 5

Modeling a single cycle of r-hIL-7

5.1 Introduction: basic model

In this first part, we have modeled a single cycle of IL-7. We have used data from the INSPIRE (1) study ([Levy et al., 2012](#)), where a r-hIL-7 cycle (3 weekly injections) was administered to 21 patients at different weight-dependent doses: 10, 20 and 30 μg/kg. Also, there were 6 control patients who only received antiretroviral therapy. All treated patients received complete cycles (3 injections), and we have CD4 count measurements at weeks 1, 2, 3 (at the moment of the injections), weeks 4, 5, 6, 9, 12, and afterward, one measurement every three months with a one-year follow up. Also, the number of $CD4^+$ T cells expressing the Ki67 proliferation marker (Ki67 count) was measured at weeks 1, 2, 3, 5 and 12.

5.1.1 Building our basic model

As our "basic model", we have taken the original model explained in the precedent Chapter with a slight modification: instead of two explanatory variables for the effect of the IL-7 on every parameter, we have just kept a power of the dose received: $\eta_1 = \eta_2 = 0.25$. This exponential function was found by profile likelihood (the first step is detailed on Table [5.1](#)).

The statistical model can be written:

$$\begin{cases} \tilde{\pi} = \tilde{\pi}_0 + \beta_\pi d^{\eta_1} & t \leq 16 \\ \tilde{\pi} = \tilde{\pi}_0 & t > 16 \end{cases} \tag{5.1}$$

and

$$\begin{cases} \tilde{\mu}_Q = \tilde{\mu}_{Q_0} + \beta_{\mu_Q} d^{\eta_2} & t > 16 \\ \tilde{\mu}_Q = \tilde{\mu}_{Q_0} & t \leq 16 \end{cases} \tag{5.2}$$

5.1.2 Results for the basic model

In Table [5.2](#) we present the results when applying this model to the INSPIRE data set (N=27 patients receiving 3 weekly injections of glycosylated r-hIL-7 at

33

Table 5.1: Obtained log-likelihood for every model with values for η_1 at the top and values for η_2 on the left

	0.1	0.2	0.3	0.4	0.5	0.6	0.7	0.8	0.9	1
0.1	-19.6	-19.8	-20.8	-22.4	-24.5	-26.9	-29.6	-32	-34.6	-36.9
0.2	-14.6	-13.3	-12.8	-13.2	-14.3	-16	-18.1	-20.3	-22.7	-25.2
0.3	-17.2	-14.7	-13.1	-12.6	-12.3	-13	-14.1	-15.7	-17.4	-19.4
0.4	-24.4	-21.6	-19.3	-17.6	-16.7	-16.3	-16.5	-17.3	-18.4	-19.7
0.5	-33.7	-30.1	-28.4	-26.2	-24.6	-23.6	-23.1	-23.1	-23.6	-24.3
0.6	-43.3	-40.1	-38.6	-36.3	-34.4	-32.9	-31.9	-31.4	-31.2	-31.5
0.7	-52.4	-50.8	-48.7	-46.6	-44.7	-43	-41.7	-40.7	-40.2	-40
0.8	-60.6	-60	-58.3	-56.6	-54.8	-53.1	-51.6	-50.4	-49.6	-49
0.9	-68.2	-67.7	-66.9	-65.8	-64.3	-62.7	-61.2	-60	-58.9	-58.1
1	-75.2	-74.9	-74.5	-73.8	-72.9	-71.7	-70.3	-69	-67.9	-67

doses 10, 20 and 30 μg/kg).

Estimated values of biological parameters are found to be close to those of Thiébaut et al. (2014). Priors, means and standard deviations (in natural and logarithmic scale) of all parameters are shown.

Table 5.2: Priors and estimated mean and standard deviation (sd) of all parameters (in logarithmic and natural scales) for the "basic model" when considering IL-7 effects on π and μ_Q.

	PRIOR (log-scale)		POSTERIOR (log-scale)		POSTERIOR (natural-scale)	
	mean	sd	mean	sd	mean	sd
λ	1.000	1.000	2.041	0.152	**7.700**	*1.174*
ρ	0.000	0.250	0.253	0.130	**1.289**	*0.167*
π	-4.000	1.000	-3.527	0.108	**0.029**	*0.003*
μ_Q	-3.600	0.500	-2.903	0.131	**0.055**	*0.007*
μ_P	-2.500	0.500	-2.653	0.424	**0.070**	*0.030*
β_π	-	-	-	-	**1.233**	*0.039*
β_{μ_Q}	-	-	-	-	**-0.178**	*0.037*
σ_λ	-	-	-	-	**0.213**	*0.062*
σ_ρ	-	-	-	-	**0.387**	*0.138*
σ_{CD4}	-	-	-	-	**0.205**	*0.011*
σ_P	-	-	-	-	**0.228**	*0.026*

Penalized Log-Likelihood : -1.269
NON-Penalized Log-Likelihood :0.918
LCVa :-0.033

Importantly, for every patient we normally have 11 CD4 count measurements, obtained at W1, W2, W3, W4, W5, W6, W9, W12, M6, M9 and M12 while we only have 5 Ki67 count measurements, at weeks W1, W2, W3, W5 and W12 (W=week, M=month).

In Figure 5.1, fits for the basic model are shown, comparing the previous model (with an IL-7 effect on both π and μ_Q) with a simpler model, where

only an effect on π is considered. Fits are shown for two representative enough patients, as patient 16 and Patient 17.
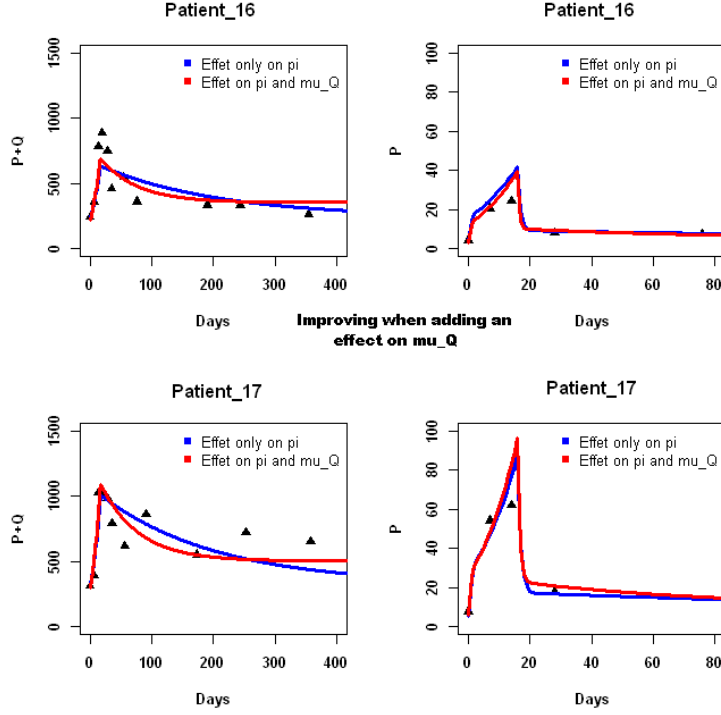
Figure 5.1: Fits of basic model for two representative patients, patient 16 and patient 17, for appreciating the effect of a supplementary IL-7 effect on μ_Q with respect to only an effect on π

Fits of total CD4$^+$ T cells are quite satisfying in the long term, although they are not able to reach the higher observations of the day 21. By contrast, fits of P cells must be improved, because this model does not capture the essential of their dynamics. Next Sections describe our attempts to improve this basic model.

Before starting with the development of different models, a brief study of the coefficient of the reversion rate can be found in Appendix C.

5.2 Incorporating a feedback model

5.2.1 Original feedback term

Feedback is a common mechanism in biological processes. The equilibrium found in biological organisms is generally represented in dynamic systems (even if they are linear) provided that an equilibrium point exists. (A brief study of the equilibrium point can be found in Appendix B). This expression of the equilibrium, that is called homeostasis in biology, is found in a natural way without requiring an explicit feedback term. In spite of this, we tried to incorporate a feedback process into the rate of proliferation in order to mathematically ensure that cells level stays in a credible range. The idea is that, when the number of $CD4^+$ T cells become bigger than reasonable, this factor is going to slow down the growth rate.

One possibility for the feedback factor is: $\frac{1}{(P+Q)^\nu}$ and model is written as follows:

$$\begin{cases} \frac{dQ_i}{dt} = \lambda_i + 2\rho_i P_{ij} - \mu_{Q_i} Q_{ij} - \pi_i Q_{ij} \left[\frac{1}{P+Q} \right]^{\nu_i} \\ \frac{dP_i}{dt} = \pi_i Q_{ij} \left[\frac{1}{P+Q} \right]^{\nu_i} - \rho_i P_{ij} - \mu_{P_i} P_{ij} \end{cases} \quad (5.3)$$

Statistical model for the effect of IL-7 is then considered as previously. Results for this "feedback model" are shown in Table 5.3. Penalized and non-penalized log-likelihoods have improved from -1.269 and 0.918 to 5.793 and 8.926, respectively. Also, LCVa criterium moves from -0.033 to -0.326, even if this enhancement is not evident in descriptive ability of the model.

In Figure 5.2, we present fits for the two-compartment model (with an effect of IL-7 on π and μ_Q) by comparing models with (yellow lines) and without (green lines) feedback.

5.2.2 Other considered possibilities for the feedback term

Possibilities for the way of adding a feedback effect are almost endless. See for instance Lévine and Müllhaupt (2010) for a complete review about control systems engineering. We have tested different "feedback factors", in order to improve the likelihood function and above all to get better fits of proliferating cells. For instance, some of the alternatives considered to modify the feedback term are:

First modification:

To control the proliferation term by means of the total CD4 count through the exponential function, as:

$$\begin{cases} \frac{dQ_i}{dt} = \lambda_i + 2\rho_i P_{ij} - \mu_{Q_i} Q_{ij} - \pi_i Q_{ij} \left[e^{-(P+Q)} \right]^{\nu_i} \\ \frac{dP_i}{dt} = \pi_i Q_{ij} \left[e^{-(P+Q)} \right]^{\nu_i} - \rho_i P_{ij} - \mu_P P_{ij} \end{cases} \quad (5.4)$$

Second modification:

Table 5.3: Priors and estimated mean and standard deviation (sd) of all parameters (in logarithmic and natural scales) for the "basic feedback model" when considering IL-7 effects on π and μ_Q. Penalized (P) and Non Penalized (NP) likelihood and LCVa criteria

	PRIOR (log-scale)		POSTERIOR (log-scale)		POSTERIOR (natural-scale)	
	mean	sd	mean	sd	mean	sd
λ	1.000	1.000	1.653	0.371	**5.220**	*1.936*
ρ	0.000	0.250	0.173	0.139	**1.189**	*0.165*
π	-4.000	1.000	-2.048	0.574	**0.129**	*0.074*
μ_Q	-3.600	0.500	-3.059	0.176	**0.047**	*0.008*
μ_P	-2.500	0.500	-2.614	0.429	**0.073**	*0.031*
ν	-2.500	2.000	-1.355	0.361	**0.258**	*0.093*
β_π	-	-	-	-	**1.354**	*0.073*
β_{μ_Q}	-	-	-	-	**-0.234**	*0.056*
σ_λ	-	-	-	-	**-0.266**	*0.113*
σ_ρ	-	-	-	-	**-0.367**	*0.132*
σ_π	-	-	-	-	**0.078**	*0.040*
σ_{CD4}	-	-	-	-	**0.205**	*0.011*
σ_P	-	-	-	-	**0.208**	*0.025*

Penalized Log-Likelihood :5.793
NON-Penalized Log-Likelihood :8.926
LCVa :-0.326

To add a feedback term on the mortality rate of Q cells μ_Q, in addition to the feedback term on proliferation rate π:

$$\begin{cases} \frac{dQ_i}{dt} = & \lambda_i + 2\rho_i P_{ij} - \mu_{Q_i} Q_{ij} e^{\epsilon_i(P+Q)} - \pi_i Q_{ij} e^{-\nu_i(P+Q)} \\ \frac{dP_i}{dt} = & \pi_i Q_{ij} e^{-\nu_i(P+Q)} - \rho_i P_{ij} - \mu_P P_{ij} \end{cases}$$

<u>Third modification:</u>

Finally, another attempt was to keep both feedback terms when letting the mortality rate of P cells depending on P^2, instead of P:

$$\begin{cases} \frac{dQ_i}{dt} = & \lambda_i + 2\rho_i P_{ij} - \mu_{Q_i} Q_{ij} e^{\epsilon_i(P+Q)} - \pi_i Q_{ij} e^{-\nu_i(P+Q)} \\ \frac{dP_i}{dt} = & \pi_i Q_{ij} e^{-\nu_i(P+Q)} - \rho_i P_{ij} - \mu_P P_{ij}^2 \end{cases}$$

None of these modifications allowed us to improve the LCVa or the individual fits, so we have kept as "feedback model" the original one shown in Equation 5.3.
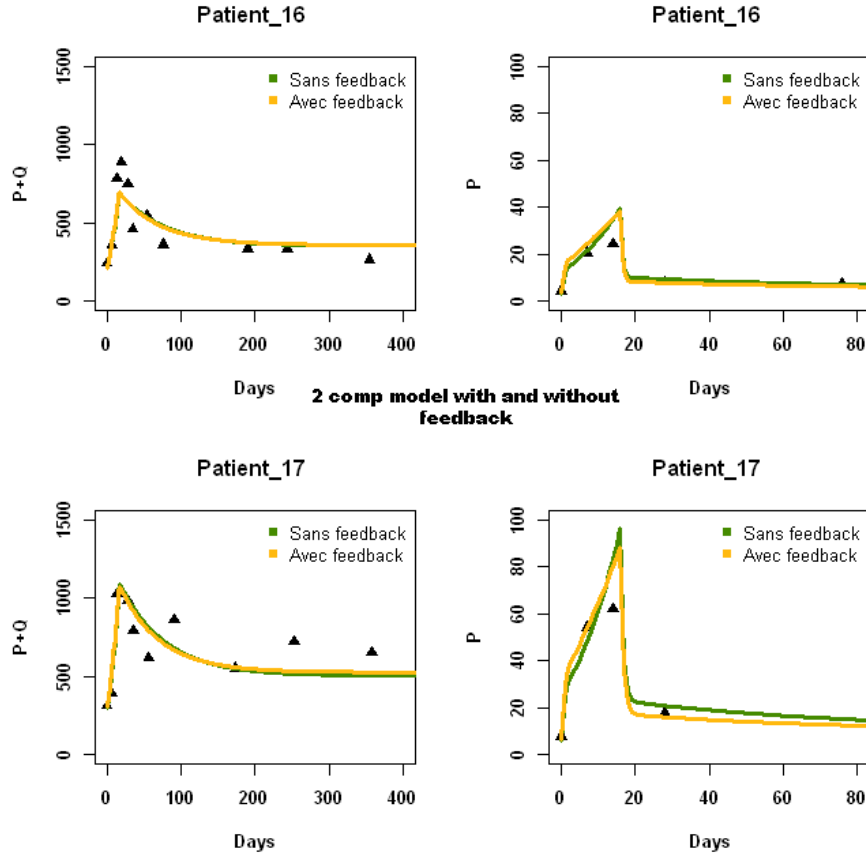
Figure 5.2: Comparison of fits of "basic model" with and without feedback, when considering an effect of IL-7 on π and μ_Q

5.2.3 Conclusion

The model with feedback keeps the same behavior than the model without feedback. This is definitely not the reason for the lack of accuracy of the fits of P cells. Then we changed the approach and we decided to test a model based on the concentration of the drug for each patient at each moment, instead of the dose received. Even if we have few data about the concentration of r-hIL-7 on patients, we have tried to build a satisfactory pharmacokinetic model to precisely estimate this concentration at each time and to use these estimations within a pharmacodynamic model where the IL-7 effect can be considered in a continuous form.

5.3 Pharmacokinetic/pharmacodynamic (PK/PD) model

5.3.1 Introduction

Knowledge of the pharmacokinetics of drugs is essential for defining the treatment protocols, and the study of the pharmacokinetics of antiretroviral drugs has been particularly useful for the HIV infection care (Danner et al., 1995; Hendrix et al., 2004; Bazzoli et al., 2010). We have used data from the first INSPIRE study to characterize the pharmacokinetics of r-hIL-7.

Pharmacokinetics are the process of drugs in the body when they are administered by any route (Gerber, 2000). Main steps in pharmacokinetics of a subcutaneous administered drug as r-hIL-7, are absorption, distribution and elimination. Essentially, after administration the drug reaches the systemic circulation, and is distributed into tissues.

Here, we have tried to use a pharmacokinetic/pharmacodynamic (PK/PD) model to describe the relationship between exogenous Interleukin 7 and CD4 response. (See Prague et al. (2013b); Wang et al. (2014) for examples of PK/PD modeling in HIV field.)

5.3.2 Data

We used information from all the 27 patients of the INSPIRE study. Available blood samples for PK sampling were as follows: at pre-1st injection, 2h post-1st injection, 4h post-1st injection, 6h post-1st injection, 24h post-1st injection, 96h post-1st injection, pre-2nd injection, pre-3rd injection, and 7 days after the third injection.

Four days after receiving an injection, there was no longer r-hIL-7 concentration in the blood for most patients; so in practice, the significant measurements were those at 2h, 4h, 6h, 24h and 96h after the first injection. In Figure 5.3 we can observe the mean IL-7 plasma concentration by group during 7 days after the first injection.

5.3.3 Description of the PK model

We used a mathematical model developed by Mélanie Prague, where three compartments are considered: the first one called "Local compartment" (C_L), that references the administration site (in our case, the subcutaneous tissue), the "Plasma compartment" (C_P) and the "Tissue compartment" (C_T). R-hIL-7 is absorbed at a rate k_a, and it is eliminated at a cl rate. Also, redistribution from the plasma to the tissue compartment (and vice versa) take place at rates k_{pt} and k_{tp}, respectively. A brief description of parameters for the pharmacokinetic model can be found in Table 5.4.

After that, if we are able to estimate tissue and plasma concentration of r-hIL-7 at every time, we would like to use them within the statistical model of lymphocytes. Up to now, we have only used the dose received for every patient, a fixed value (10, 20 or 30 μg/kg) which did not let us to study the IL-7 effect in a continuous form. Theoretical advantages of the use of tissue or plasma concentration are obvious: for instance we would be able to consider a

r-hIL-7 plasma concentration (pg/mL)
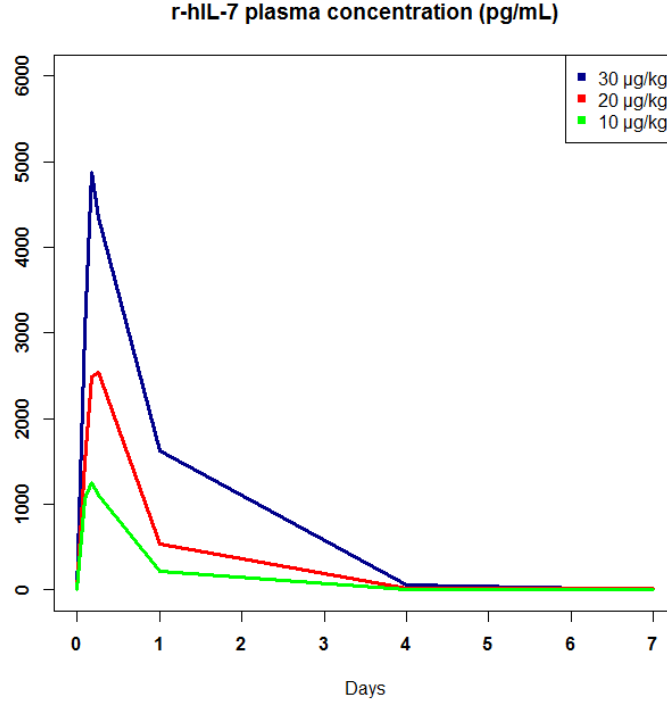
Figure 5.3: Mean IL-7 plasma concentration for patients from INSPIRE study by group during 7 days after the first injection

statistical model without being forced to establish an artificial life for the IL-7 effect:

$$\tilde{\pi} = \tilde{\pi}_0 + \beta \mathrm{conc}^\eta \quad \forall \mathrm{t} > 0$$

instead of

$$\begin{cases} \tilde{\pi} = \tilde{\pi}_0 + \beta_\pi d^{0.25} & \mathrm{t} \in (0, 16] \\[2mm] \tilde{\pi} = \tilde{\pi}_0 & \mathrm{else} \end{cases}$$

With parameter's meaning according to Table 5.4, the mathematical model can be written as follows:

$$\begin{cases} \frac{dC_L}{dt} = -k_a C_L & C_L(0) = \mathrm{dose}_0 \\[3mm] \frac{dC_P}{dt} = \frac{k_a C_L}{V_0} + \frac{k_{tp} V_T C_T}{V_0} - k_{pt} C_P - \mathrm{cl} C_P & C_P(0) = 0 \\[3mm] \frac{dC_T}{dt} = \frac{k_{pt} V_0 C_P}{V_T} - k_{tp} C_T & C_T(0) = 0 \end{cases}$$

As for the statistical model, we have considered no additional fixed effects, and random effects on k_a, cl and V_0. As for the model for the observation, only the plasma compartment C_P can be observed.

Table 5.4: Biological meaning of pharmacokinetic parameters

k_a	Uptake rate (h^{-1})
cl	Clearance rate (h^{-1})
V_0	Volume of distribution in plasma compartment (m^3)
V_T	Volume of distribution in tissue compartment (m^3)
k_{pt}	Absorption from plasma to tissue (h^{-1})
k_{tp}	Absorption from tissue to plasma (h^{-1})

5.3.4 Results of the PK model

Identifiability problems prevented us from estimating all parameters at the same time; so in practice, we considered $k_{tp} = k_{pt}$ (absorption from tissue to plasma equals to absorption from plasma to tissue). With this constraint, we fitted the pharmacokinetic data with the previously described model. Thanks to NIMROD, pharmacokinetic parameters were estimated (in logarithmic scale) at $(ka, cl, V_0, V_t, k_{tp} = k_{pt}) = (-2.67, -1.01, -2.55, -3.10, -4.22)$.

As the next step, we want to use the calculated trajectories of the plasma and/or tissue concentration for improving results of our "basic model", where the mathematical model is the two-compartment model with feedback, and the statistical model would be:

$$\tilde{\pi} = \tilde{\pi}_0 + \beta \mathrm{conc}^{\nu}$$

While doing this, we had to make some decisions, as:

Dose-weight question

Should we consider the PK process according only to the quantity of dose received, or according to the ratio dose-weight? As we have said, the study INSPIRE has provided us information about 21 patients, who have received 3 weekly subcutaneous injections of r-hIL-7 in doses 10, 20 or 30 μg/kg, plus two patients by dose level who were randomized to receive placebo. Thus, the quantity of r-hIL-7 that has been administered for every patient can be seen as having two levels:

- First, the patient has been allocated within one of the three treatment groups.

- Second, the quantity of IL-7 that he is going to receive will depend on his weight.

It is precisely this last "level" which we would like to make disappear. How can we get this? We are going to keep in mind only the group of treatment (10 μg/kg, 20 μg/kg or 30 μg/kg), and we do not take care of the weight of the patients. We supposed that all of them have the same weight (the average of all subjects).

Tissue or Plasma Concentration

By taking into account the fact that we have two estimated concentrations, we have had to decide which one is the most appropriate. After some tests, we have kept the tissu concentration, with an exponent $\nu = 0.40$, that has been estimated by profile likelihood (see Table 5.5). It should be noted, however, that the model with the dose is far better than all other PK models.

Table 5.5: Estimated means of all parameters in logarithmic scale for the "pharmacokinetic model" for different exponential functions of tissue (Ti) and plasma (Pl) concentration. Penalized log-likelihood (PLL) and LCVa criteria.

	$d^{0.25}$	$Ti^{0.30}$	$Pl^{0.30}$	$Ti^{0.40}$	$Pl^{0.40}$	$Ti^{0.50}$	$Pl^{0.50}$	$Ti^{0.60}$	$Pl^{0.60}$
$\tilde{\lambda}$	-0.62	-0.26	-0.35	-0.29	0.10	-0.17	0.24	-0.08	0.20
$\tilde{\rho}$	-0.13	-0.66	-0.95	-0.73	-1.13	-0.78	-1.20	-0.84	-1.20
$\tilde{\pi}$	-3.07	-0.20	-1.20	-0.59	-1.68	-0.57	-2.13	-0.60	-1.76
$\tilde{\mu}_Q$	-3.92	-4.55	-4.53	-4.54	-4.85	-4.50	-4.84	-4.50	-4.83
$\tilde{\mu}_P$	-3.26	-2.23	-3.10	-2.53	-1.82	-2.66	-1.86	-2.67	-1.85
$\tilde{\nu}$	-1.88	-0.32	-0.56	-0.40	-0.76	-0.40	-0.90	-0.40	-0.78
$\beta\pi$	1.40	2.17	2.50	2.11	3.45	2.02	3.46	1.98	3.35
σ_λ	0.57	0.32	0.52	0.41	0.32	0.43	0.27	0.53	0.23
σ_ρ	0.36	0.28	0.27	0.28	0.12	0.27	0.12	0.25	0.13
σ_π	0.02	0.19	0.16	0.18	0.13	0.20	0.19	0.23	0.22
PLL	-20.6	-59.1	-106.0	-57.2	-121.7	-60.8	-126.8	-68.6	-130.6
LCVa	0.65	2.20	3.96	2.13	4.51	2.26	4.71	2.55	4.84

No random effects

Continuing with the idea of the dose-weight question, we decided to consider no random effects (random effects equal to zero) within the PK model, in order to have values in the concentration curves that are proportional to the

dose received. Considering that our intention is to extrapolate this model in subsequent studies with a much more bigger number of patients, this option is going to let us to reduce a sizable amount of calculation time.

5.3.5 Pharmacodynamic model

Then we have calculated the trajectories for INSPIRE patients, we have simulated all the three peaks, and after that we have obtained the average for every dose. We have the estimated concentration available for every patient, according to his treatment group. So, in the end we have defined the statistical model as follows:

$$\tilde{\pi} = \tilde{\pi}_0 + \beta\pi C_T^{0.40} \tag{5.5}$$

So the concentration model is defined by the basic mathematical model for two compartments (Equation 4.6) and this statistical model. This is a pattern that is very close to the dose model; in fact, we have just substituted the dose by the concentration. But this difference converts it into a more complex model from a computational point of view and much more "realistic" from a biological point of view. We expected that this concentration model allows us to improve the results we have obtained, by keeping in mind its continuity and softness with respect to the previous dose model. Howver, with this model, best results were found as likelihood function equals to -54.5 and LCVa equals to 2.03. So, despite all different possibilities that have been tested, we have not reached our aim: to improve the obtained results for the Dose model. Thus, we have embarked in the search of an appropriate function with the aim of getting close to results achieved with the Dose model.

5.3.6 Sigmoid function as the pharmaco-dynamic function

In order to make the most of our PK model, we are going to become milder the step from dose models to concentration models.

- Dose models had a disadvantage by their huge discontinuity with respect to time (effect only below day 16...)

- Concentration models allow us not to abruptly interrupt the effect

That is the reason why we have started to search a function allowing us a flexibility in the step/no effect of the treatment. We thought of a sigmoid function, in order to take advantage to his "S" shape. Function we though were functions as follows:

$$f(x) = \frac{1}{1 + e^{-\alpha(x-\gamma)}} \tag{5.6}$$

By adding terms for having f(0) = 0 and $\lim_{x\to\infty} f(x) = 1$, and estimating γ, we obtain a final equation that can be written as follows:

$$\tilde{\pi} = \tilde{\pi}_0 + \beta \frac{1 - e^{-\alpha C_T(t)}}{1 + e^{-\alpha(C_T(t)-1.69)}} \tag{5.7}$$

We have fixed several values for α, in order to estimate only one extra parameter. In Table 5.6, we show the results achieved for this "sigmoid concentration

model", for α = 0.5, 1, 2 and 5. We are going to compare these results with the "basic model" under identical conditions (in both models random effects are supposed on λ and ρ).

Table 5.6: Estimated means of all parameters in logarithmic scale for the "sigmoid model" with $C_T^{0.40}$ for α = 0.5, 1, 2 and 5 when considering only an IL-7 effect on proliferation rate π. Penalized log-likelihood (PLL) and LCVa criteria.

	$\mathbf{d}^{0.25}$	$\alpha = \mathbf{0.5}$	$\alpha = \mathbf{1}$	$\alpha = \mathbf{2}$	$\alpha = \mathbf{5}$
$\tilde{\lambda}$	-0.55	-0.10	-0.24	-0.10	0.22
$\tilde{\rho}$	-0.14	0.31	0.27	0.27	0.23
$\tilde{\pi}$	-3.10	-2.47	-2.54	-2.53	-2.54
$\tilde{\mu}_Q$	-3.93	-3.22	-3.20	-3.19	-3.24
$\tilde{\mu}_P$	-3.23	-3.12	-3.19	-3.08	-3.06
$\tilde{\nu}$	-1.90	-2.04	-2.18	-2.18	-2.12
$\beta\pi$	1.41	3.66	2.53	2.05	1.87
σ_λ	0.58	0.71	0.69	0.68	0.69
σ_ρ	0.35	0.51	0.45	0.42	0.45
σ_{CD4}	0.22	0.26	0.26	0.27	0.29
σ_P	0.21	0.47	0.49	0.50	0.51
PLL	-17.8	-147.5	-153.7	-170.4	-192.8
LCVa	0.67	5.48	5.70	6.32	7.16

5.3.7 Conclusion of the concentration model

All information contained in concentration data seems to be captured with data from the dose received. Furthermore, in spite of different efforts to include the estimated concentration in the statistical model we have not achieved as good results as those obtained with the dose, not even approximately. This fact has led us back to the previous "Dose model". Nevertheless, we can keep in mind the possibility of using estimated concentrations in the future, perhaps when we had more information about drug distribution and/or more available data.

5.4 Four-compartment model

5.4.1 Introduction

Our next goal was to develop a more complex model, that allows us to adequately model the trajectories of CD4 count, and, especially, of Ki67 count. Here, our aim was to divide both quiescent and proliferating compartments into naive and memory cells. The most accepted way to differentiate these populations seems to be the expressed isoform of a surface molecule called CD45. The isoform contained in most naive T cells has a segment encoded by an exon designated A, that can be called CD45RA$^+$ (CD45 "restricted A"). Most memory cells, on the other hand, express an isoform without the A exon RNA, and can be called CD45R0$^+$. However, this way of distinguishing naive from memory T cells is not perfect, and interconversion between CD45RA$^+$ and CD45RO$^+$ populations has been documented (Abbas et al., 2011). We know that Interleukin 7 modulates the homeostasis in both naive and memory T cells subsets (Jaleco et al., 2003). However, the proliferation rates can differ between cell populations (Fry and Mackall, 2005; Surh et al., 2006)

5.4.2 Description of the four-compartment model

For the sake of simplicity, the notation here has been slightly changed. In this section, we have worked with the following populations:

- Naive non-proliferating cells (Q)

- Naive proliferating cells (P)

- Memory non-proliferating cells (Q')

- Memory proliferating cells (P')

As for the mathematical model, we are going to consider:

$$
\begin{cases}
\frac{dQ}{dt} = & \lambda + 2\rho P - \mu_Q Q - \pi Q \\[2mm]
\frac{dP}{dt} = & \pi Q - \rho P - \mu_P P - \tau P \\[2mm]
\frac{dQ'}{dt} = & 2\rho' P' - \mu'_Q Q' - \pi' Q' + \tau P \\[2mm]
\frac{dP'}{dt} = & \pi' Q' - \rho' P' - \mu'_P P'
\end{cases}
$$

A visual description of this model can be seen in Figure 5.4. The equilibrium point for the usual values of the parameters can be found in Appendix B.

We are going to start with the simplest model: without feedback effect. As for the statistical model, we start by considering an IL-7 effect on naive and memory proliferation rate, as follows:

$$
\begin{cases}
\tilde{\pi} = & \tilde{\pi}_0 + & \beta_\pi d^{0.25} \\
\tilde{\pi}' = & \tilde{\pi}'_0 + & \beta_{\pi'} d^{0.25}
\end{cases}
$$

and eventually we can consider supplementary effects on mortality rates μ_Q and μ'_Q, and on production rate λ or τ.
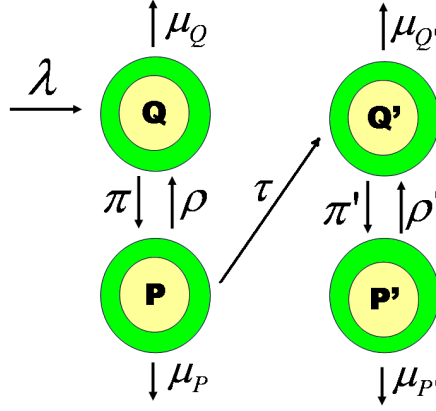
Figure 5.4: Mathematical representation of the original 4 compartments model, where proliferating naive cells become quiescent memory cells at rate τ

$$\begin{cases} \tilde{\mu}_Q = & \tilde{\mu}_{Q_0} + & \beta_{\mu_Q} d^{0.25} \\ \tilde{\mu}'_Q = & \tilde{\mu}_{Q'_0} + & \beta_{\mu'_Q} d^{0.25} \\ \tilde{\lambda} = & \tilde{\lambda}_0 + & \beta_\lambda d^{0.25} \\ \tilde{\tau} = & \tilde{\tau}_0 + & \beta_\tau d^{0.25} \end{cases}$$

We have tried to use as information as possible from the two compartments model, as the prior information. For example, for λ, (rate of production of the non-proliferating cells), there was no reason to think it is going to change, so we used for the prior an average of posterior values previously obtained. For the conversion rate τ, we had no previously idea, so we have put a non-informative prior, in order to have no influence in posterior results. In a first approximation, we have kept the same parameters as being affected by random effects (λ and ρ).

Observed compartments: We have observed, for 27 patients, the total cell population ($Q + Q' + P + P'$) as before, and the total proliferating cells ($P + P'$), total naive cells ($Q + Q'$) and proliferating naive cells. We must keep in mind that more than 60 percent of the time we only have one of the four possible "observed compartments" (the other three have not been measured). As before, we had 11 CD4 count measurements for every patient, obtained at W1, W2, W3, W4, W5, W6, W9, W12, M6, M9 and M12 and only 5 measurements for Ki67 count, naive cells count, and proliferating naive cells count (at weeks W1, W2, W3, W5 and W12).

The model for the observations is as follows:

$$\begin{cases} Y_{j1}^i = \sqrt[4]{(P + P' + Q + Q')(t_{j1}^i, \tilde{\xi}^i)} + \epsilon_{j1}^i \\ Y_{k2}^i = \sqrt[4]{P + P'(t_{k2}^i, \tilde{\xi}^i)} + \epsilon_{k2}^i \\ Y_{k3}^i = \sqrt[4]{P + Q(t_{k3}^i, \tilde{\xi}^i)} + \epsilon_{k3}^i \\ Y_{k4}^i = \sqrt[4]{P(t_{k4}^i, \tilde{\xi}^i)} + \epsilon_{k4}^i \end{cases} \qquad (5.8)$$

46

5.4.3 Results of the four-compartment model

In Table 5.7 the mean (in logarithmic scale) and standard deviation for all estimated parameters are presented, with non-identifiable parameters in gray. We have compared the four-compartment model previously exposed, and another one with a slightly modification (see Figure 5.5), where proliferating naive cells directly become proliferating memory cells at rate τ.
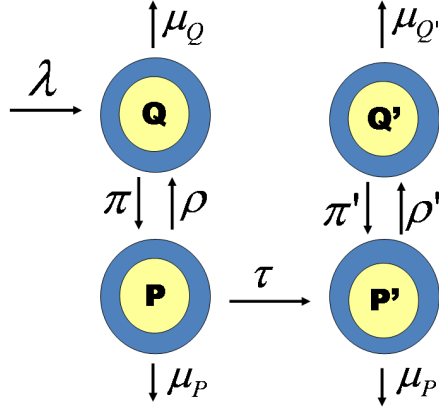
Figure 5.5: Mathematical representation of the modified 4 compartments model, where proliferating naive cells become proliferating memory cells at rate τ

When regarding obtained values for τ and ρ' we perceive some identifiability problems, owing to insufficient information. Some fits for patients 16 and 17 are shown in Figures 5.6 and 5.7 (for both patterns with only an effect on π and π').
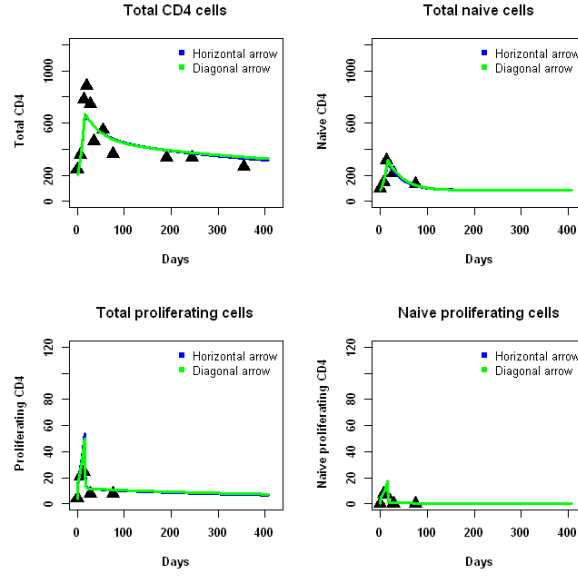
Figure 5.6: Fits of four-compartment model with an effect of IL-7 on π and π' for patient 16. Horizontal arrow stands for a switch from naive proliferating cells to memory proliferating cells. Diagonal arrow stands for a switch from naive proliferating cells to memory quiescent cells.
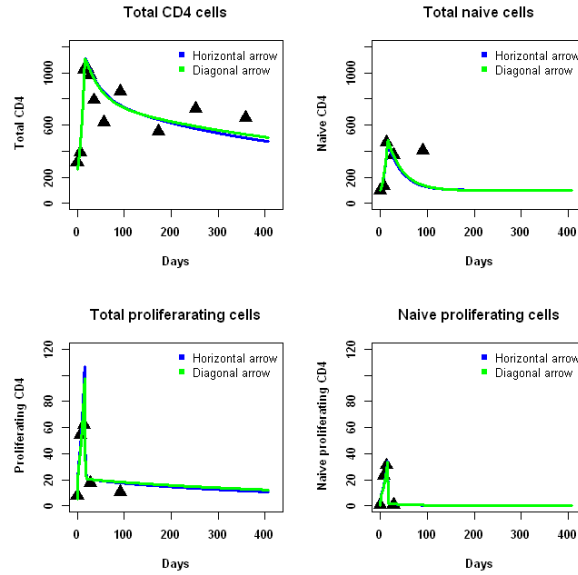
Figure 5.7: Fits of four-compartment model with an effect of IL-7 on π and π' for patient 17. Horizontal arrow stands for a switch from naive proliferating cells to memory proliferating cells. Diagonal arrow stands for a switch from naive proliferating cells to memory quiescent cells.

Table 5.7: Estimated parameters mean for different several four-compartment model. Non identifiable parameters are shown in gray. Non Penalized likelihood (NPLL) and LCVa criteria.

	HORIZONTAL ARROW				DIAGONAL ARROW			
	Effect $\pi\ \pi'$	Effect $\pi\ \pi'$ λ	Effect $\pi\ \pi'$ τ	Effect $\pi\ \pi'$ $\mu_Q\ \mu_{Q'}$	Effect $\pi\ \pi'$	Effect $\pi\ \pi'$ λ	Effect $\pi\ \pi'$ τ	Effect $\pi\ \pi'$ $\mu_Q\ \mu_{Q'}$
$\tilde{\lambda}$	1.118	1.066	0.808	1.046	1.064	0.987	0.852	0.976
$\tilde{\tau}$	-0.341	-0.339	0.140	-0.325	-0.048	0.039	0.531	-0.050
$\tilde{\mu}_P$	-2.416	-2.390	-2.344	-2.318	-2.334	-2.163	-2.175	-2.262
$\tilde{\mu}_{P'}$	-2.229	-2.233	-2.188	-2.229	-2.163	-2.017	-2.151	-1.806
$\tilde{\rho}$	0.783	0.785	0.586	0.788	0.950	0.837	0.679	0.963
$\tilde{\rho}'$	-0.271	-0.262	-0.212	-0.256	-0.347	-0.376	-0.256	-0.386
$\tilde{\pi}$	-4.442	-4.464	-4.603	-4.467	-4.235	-4.304	-4.367	-4.237
$\tilde{\pi}'$	-3.728	-3.727	-3.722	-3.732	-3.705	-3.721	-3.694	-3.704
μ_Q	-3.252	-3.303	-3.561	-3.335	-3.280	-3.360	-3.559	-3.364
$\mu_{Q'}$	-3.878	-3.877	-3.853	-3.874	-3.924	-3.993	-3.867	-4.072
β_π	2.281	2.299	2.205	2.301	2.219	2.235	2.080	2.225
$\beta_{\pi'}$	1.031	1.014	1.216	1.016	1.128	1.135	1.246	1.193
β_λ	-	-0.042	-	-	-	0.641	-	-
β_τ	-	-	-1.203	-	-	-	-1.345	-
β_{μ_Q}	-	-	-	0.018	-	-	-	0.036
$\beta_{\mu_{Q'}}$	-	-	-	-0.005	-	-	-	-0.05
σ_λ	0.218	0.219	0.230	0.220	0.216	0.213	0.214	0.213
σ_τ	0.419	0.425	0.544	0.432	0.405	0.445	0.557	0.411
σ_{CD4}	0.211	0.212	0.214	0.213	0.213	0.213	0.212	0.213
σ_P	0.304	0.300	0.293	0.298	0.298	0.296	0.291	0.293
σ_{CD4_N}	0.369	0.364	0.334	0.361	0.363	0.365	0.347	0.357
σ_{P_N}	0.218	0.217	0.220	0.218	0.224	0.220	0.221	0.226
NPLL	-81.036	-80.810	-74.699	-80.643	-84.177	-83.505	-75.161	-83.356
LCVa	3.345	3.691	3.202	3.142	3.295	3.205	2.882	3.132

5.5 Three β's model

Here, we rededicated ourselves to the "basic model", where two sub-populations of CD4$^+$ T cells, CD4$^+$Ki67$^-$ (Q) and CD4$^+$Ki67$^+$ (P) are considered. As we have found in Section 4.5, there is undoubtedly an strong effect of exogenous IL-7 on proliferation of the so-called quiescent cells. Our main problem, however, is that we have not managed to adequately fit the cell response in terms of the trajectory of the proliferating cells.

We are going to focus on a major question: Have all the three injections the same quantitative effect on proliferation of CD4$^+$ T cells? Or, more accurately, what is the role of every single injection in the whole effect of a cycle? To allow a different proliferation effect between injections, the statistical model is modified to let π to vary as follows:

$$\begin{cases} \tilde{\pi} = \tilde{\pi}_0 + \beta_1 d^{0.25} & \text{for } t \text{ days after the first injection} \\ \tilde{\pi} = \tilde{\pi}_0 + \beta_2 d^{0.25} & \text{for } t \text{ days after the second injection} \\ \tilde{\pi} = \tilde{\pi}_0 + \beta_3 d^{0.25} & \text{for } t \text{ days after the third injection} \end{cases} \qquad (5.9)$$

What first needs to be clarified is how long every injection can produce its effect. Up to now, we specified 16 days as the period for the whole cycle effect; but here we have to deal with every injection as a whole. This is important because later in this work we are going to analyze data from the INSPIRE 2 and INSPIRE 3 studies. There, patients have not necessarily received complete cycles, but sometimes they have received 2-injection cycles or even cycles with a single injection.

In Table 5.8, likelihood functions and LCVa for $t \in [2,7]$.

Table 5.8: Likelihood functions and LCVa when considering a r-hIL-7 effect on π through a single β_π for 16 days and different β's for t days. The effect on μ_Q has been considered as previously (see Equation 4.9). Random effects are applied on λ and ρ. Penalized log-likelihood (PLL), Non-Penalized log-likelihood (NPLL) and LCVa criteria

	PLL	NPLL	LCVa
Same β (t=16)	-1.269	0.918	-0.033
$t = 2$	-15.474	-3.061	0.136
$t = 3$	-10.854	-0.453	0.029
$t = 4$	-5.847	2.375	-0.073
$t = 5$	0.998	7.177	-0.260
$t = 6$	8.309	11.978	-0.431
$t = 7$	**20.981**	**18.361**	**-0.775**

Best results have been obtained when considering an effect for 7 days following each injection. We improved 22 points of likelihood with respect to the "basic model", and is in fact the model that offers us the best results in terms of likelihood and LCVa.

To recapitulate, this model is built with the original mathematical model with feedback, and fixed effects on π during 7 days after each injection, and on μ_Q as usual. Let d_i the dose received for patient i, and let N_t^i the number of injections that patient i has received until time t. The statistical description for the proliferation effect remains as follows:

$$\tilde{\pi}^i(t) = \tilde{\pi}_0 + \sum_{k=1}^{3} \mathbb{1}_{\{N_t^i = k\}} \, \beta_{\pi_k} \, d_i^{0.25} \, \mathbb{1}_{\{N_t^i - N_{t-7}^i = 1\}}$$

As already mentioned, random effects are added on the production rate λ and the reversion rate ρ. In Table 5.9 we have complete results for this model.

Table 5.9: Priors and estimated mean and standard deviation (sd) of all parameters (in logarithmic and natural scales) for the "3 β's model" with an effect on π for 7 days when considering patients from INSPIRE (1)

	PRIOR (log-scale)		POSTERIOR (log-scale)		POSTERIOR (natural-scale)	
	mean	sd	mean	sd	mean	sd
λ	1.000	1.000	2.129	0.289	**8.405**	*2.433*
ρ	0.000	0.250	0.115	0.144	**1.122**	*0.161*
π	-4.000	1.000	-2.802	0.638	**0.061**	*0.039*
μ_Q	-3.600	0.500	-2.883	0.196	**0.056**	*0.011*
μ_P	-2.500	0.500	-2.727	0.384	**0.065**	*0.025*
ν	-2.500	2.000	-2.022	0.813	**0.132**	*0.108*
$\beta_{\pi 1}$	-	-	-	-	**1.453**	*0.072*
$\beta_{\pi 2}$	-	-	-	-	**1.154**	*0.070*
$\beta_{\pi 3}$	-	-	-	-	**0.838**	*0.195*
β_{μ_Q}	-	-	-	-	**-0.260**	*0.079*
σ_λ	-	-	-	-	**-0.257**	*0.086*
σ_ρ	-	-	-	-	**0.391**	*0.133*
σ_{CD4}	-	-	-	-	**0.210**	*0.011*
σ_P	-	-	-	-	**0.171**	*0.018*

Penalized Log-Likelihood :18.361
NON-Penalized Log-Likelihood :20.981
LCVa :-0.775

The major improvement obtained with the "three-β's model" is not in terms of likelihood, but in terms of the descriptive capacity of the proliferating compartment. For the first time, an adequate fit of Ki67 count is achieved, as can be verified in Figure 5.8.
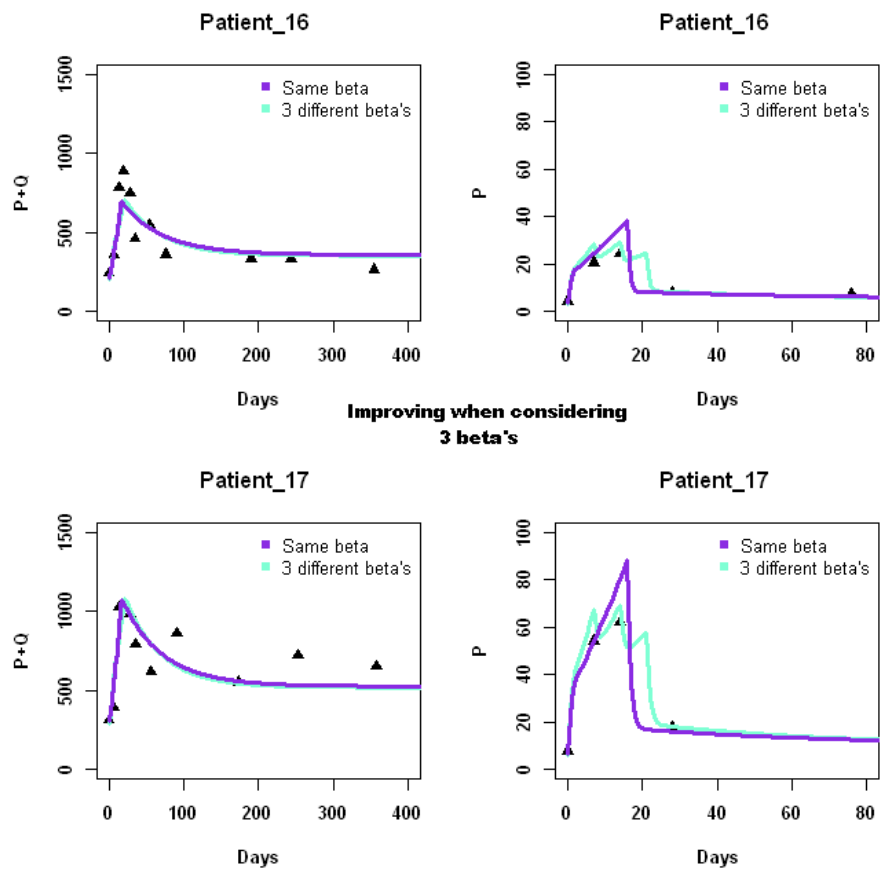
Figure 5.8: Fits for the "three-β's model

5.6 Three-compartment model

5.6.1 Basis of the three-compartment model

In this section, we have tried to build a mathematical model enabling different injection effects in a mechanistic way. Let Q* being a third intermediate compartment, where cells are ready to proliferate as in Figure 5.12.
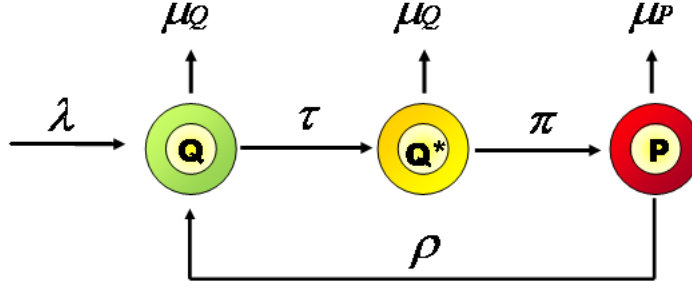
Figure 5.9: Graphical representation for the 3 compartments model

As before, we consider that Q cells are produced at a constant rate λ, and die at a rate μ_Q. But now, these Q cells become Q* cells at a rate τ. Q* cells can proliferate to P cells at a rate π, and for reasons of simplicity, we consider they die at a rate $\mu_{Q*} = \mu_Q$. As for the "basic model", μ_P is the mortality rate of P cells that, in turn, will become Q cells at a rate ρ (see Equation 5.10).

$$
\begin{cases}
\frac{dQ}{dt} = & \lambda + 2\rho P - \mu_Q Q - \tau Q \\[2mm]
\frac{dQ^*}{dt} = & \tau Q - \mu_Q Q^* - \pi Q^* \\[2mm]
\frac{dP}{dt} = & \pi Q^* - \rho P - \mu_P P
\end{cases}
\tag{5.10}
$$

Several hypotheses can support such a behavior. As a first idea, we can consider that there are some cells with a week density of CD127 (the Interleukin-7 receptor), that will not immediately react to the immunotherapy, and on the other hand there are some other cells with a strong density of CD127, that will respond fast to the IL-7 and will start to proliferate without delay. Antibodies against r-hIL-7 could take part of another hypothesis, and their presence would have a direct effect on the response to injections.

This three-compartment model allows cells to have a "step by step" response when τ is small enough. However, when τ tends to infinity we are in the case of the 2 compartments model, and results will be the same. To start, we have considered the "three-compartment model" without feedback, and best results in terms of likelihood and LCVa have been found when the supplementary IL-7 effect was considered on λ, instead of μ_Q (see Equation 5.11).

$$\begin{cases} \tilde{\pi} = \tilde{\pi}_0 + \beta_\pi d^{0.25} & d \le 16 \\ \tilde{\pi} = \tilde{\pi}_0 & t > 16 \\ \\ \tilde{\lambda} = \tilde{\lambda}_0 + \beta_\lambda d^{0.25} & d \le 16 \\ \tilde{\lambda} = \tilde{\lambda}_0 & t > 16 \end{cases} \tag{5.11}$$

As previously, we observe only data from CD4 count and Ki67 count (to note that there are only two observable compartments for three "real" compartments), so the model of the observations is the same as for the "basic model":

$$\begin{cases} Y_{j1}^i = \sqrt[4]{(P + Q + Q*)(t_{j1}^i, \tilde{\xi}^i)} + \epsilon_{j1}^i \\ Y_{k2}^i = \sqrt[4]{P(t_{k2}^i, \tilde{\xi}^i)} + \epsilon_{k2}^i \end{cases} \tag{5.12}$$

In Table 5.10 we have numerical results for this "three-compartment model", that have been improved compared with the "basic model" (from -1.269 to 9.484 for the likelihood and from -0.033 to -0.377 for the LCVa. However, it has failed to reach the level of the "three-β's model". Some modifications have been therefore considered, that are explained in next Section.

Table 5.10: Results for the "three-compartment model" without feedback. Fixed effects on π and λ. Non Penalized and Penalized likelihoods and LCVa critieria.

	PRIOR (log-scale)		POSTERIOR (log-scale)		POSTERIOR (natural-scale)	
	mean	sd	mean	sd	mean	sd
λ	1.000	4.000	-0.081	0.133	**0.922**	*0.123*
ρ	0.000	4.000	-2.265	0.221	**0.104**	*0.023*
π	-4.000	4.000	-4.857	0.092	**0.008**	*0.001*
μ_Q	-3.600	4.000	-5.111	0.095	**0.006**	*0.001*
μ_P	-2.500	4.000	-6.490	3.707	**0.002**	*0.006*
τ	-2.500	4.000	-4.990	0.279	**0.007**	*0.002*
β_π	-	-	-	-	**3.204**	*0.484*
β_λ	-	-	-	-	**2.880**	*0.129*
σ_λ	-	-	-	-	**0.223**	*0.055*
σ_ρ	-	-	-	-	**0.309**	*0.110*
σ_{CD4}	-	-	-	-	**0.229**	*0.011*
σ_P	-	-	-	-	**0.163**	*0.016*

Penalized Log-Likelihood :9.484
NON-Penalized Log-Likelihood :10.467
LCVa :-0.377

5.6.2 Three-compartment model with a thymic compartment

With the aim of still improving statistical results and fits, we have looked at some possible variations of the "three-compartment model". One possibility could be to let immature CD4* T cells to incorporate to the system more progressively. The generation of mature CD4$^+$ T lymphocytes in the thymus can be represented in the model described in Figure 5.10, incorporating a "thymic compartment".
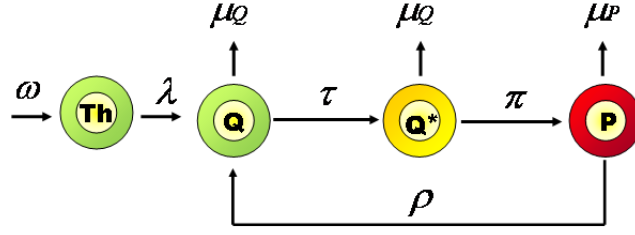
Figure 5.10: Fits for the three-compartment model

In this case, mathematical model could be written as follows, where T_h is the new thymic compartment, and ω is the rate of entry of lymphoid progenitor cells into the thymus. Results for this model will be shown in Section 5.6.4.

$$
\begin{cases}
\frac{dT_h}{dt} = & \omega - \lambda T_h \\[2mm]
\frac{dQ}{dt} = & \lambda T_h + 2\rho P - \mu_Q Q - \tau Q \\[2mm]
\frac{dQ^*}{dt} = & \tau Q - \mu_Q Q^* - \pi Q^* \\[2mm]
\frac{dP}{dt} = & \pi Q^* - \rho P - \mu_P P
\end{cases}
\tag{5.13}
$$

5.6.3 Three-compartment model with a Q$^+$ compartment

We have also interrogated us about the possibility that not all cells expressing the ki67 marker are really proliferating cells. Before explaining this second variation of the "three-compartment model" we expose a little background about the Ki67 bio-marker. Ki67 is a nuclear protein associated with cellular proliferation, a biological process essential to all living organisms for maintaining homeostasis (Bologna-Molina et al., 2013). It was firstly identified in 1983 by Gerdes et al. (1983), and it is known to be expressed in all active phases of the cell cycle (G(1), S, G(2) and mitosis) while it is undetectable in resting cells (G0). There is a bio-marker that has been largely used in cancer research, because the fraction of Ki67$^+$ tumor cells is often correlated with the clinical course of the disease (Scholzen et al., 2000; Verhoven et al., 2013). But also it is

the most widely used in HIV studies for measuring cellular proliferation (Douek et al., 2001; Mohri et al., 2001; Chomont et al., 2009). However, we can consider that $Ki67^+$ is not lost immediately after mitosis, and then a small percentage of $CD4^+$ T cells expressing this bio-marker are no longer proliferating.

This is the theory besides the "Q^+ compartment model", graphically portrayed in Figure 5.11.
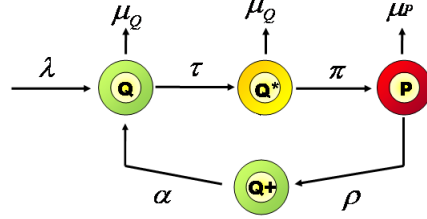
Figure 5.11: Graphical representation for the "three-compartment model" with a Q^+ compartment

The corresponding mathematical model being:

$$\begin{cases} \frac{dQ}{dt} = & \lambda + \alpha Q^+ - \mu_Q Q - \tau Q \\[2mm] \frac{dQ^*}{dt} = & \tau Q - \mu_Q Q^* - \pi Q^* \\[2mm] \frac{dP}{dt} = & \pi Q^* - \rho P - \mu_P P \\[2mm] \frac{dQ^+}{dt} = & 2\rho P - \alpha Q^+ \end{cases} \qquad (5.14)$$

In spite of our efforts, we have not been able to find a response for the percentage of $CD4^+Ki67^+$ cells that are not really proliferating. Regardless, we wanted to be in a position to allow $CD4^+$ T cells to keep this marker for a few time later but, unfortunately, this model did not lead us to significant improvements, either in terms of likelihood values or fits (results not shown).

5.6.4 Three-compartment model with feedback

Here too, we have considered the fact of adding a feedback process. Nevertheless, this "three-compartment model" offers us several possibilities. The feedback term can be applied as usual on proliferation rate (Q^* cells that are proliferating) or on τ, Q cells that are converting into Q^* cells, ready to proliferate.

Mathematical model with an hypothetical feedback term on both terms would be as follows:

$$\begin{cases} \frac{dQ}{dt} = & \lambda + 2\rho P - \mu_Q Q - \tau Q \left[\frac{1}{P+Q+Q^*} \right]^{\eta} \\[2mm] \frac{dQ^*}{dt} = & \tau Q \left[\frac{1}{P+Q+Q^*} \right]^{\eta} - \mu_Q Q^* - \pi Q^* \left[\frac{1}{P+Q+Q^*} \right]^{\nu} \\[2mm] \frac{dP}{dt} = & \pi Q^* \left[\frac{1}{P+Q+Q^*} \right]^{\nu} - \rho P - \mu_P P \end{cases} \qquad (5.15)$$

In terms of likelihood and LCVa, the model expressing a feedback effect on proliferation rate provides us better results, with no major differences in parameters estimation (see Table 5.11).

Table 5.11: Summary for the "three-compartment model" with and without feedback. Fixed effects are considered on π and λ. Non Penalized likelihood and LCVa criteria.

	Without Feedback	Feedback on π	Feedback on τ
$\tilde{\lambda}$	-0.081	-0.514	-0.417
$\tilde{\rho}$	-2.265	-2.223	-2.208
$\tilde{\pi}$	-4.857	-2.301	-4.810
$\tilde{\mu}_Q$	-5.111	-5.223	-5.202
$\tilde{\mu}_P$	-6.490	-6.934	-6.830
$\tilde{\tau}$	-4.990	-4.886	-3.263
$\tilde{\nu}$	-	-0.836	-
$\tilde{\eta}$	-	-	-1.255
β_π	3.204	3.221	2.948
β_λ	2.880	3.234	3.151
σ_λ	0.223	0.261	0.250
σ_ρ	0.309	0.293	0.292
σ_{CD4}	0.229	0.225	0.225
σ_P	0.163	0.158	0.164
NPLL	10.467	15.750	13.133
LCVa	-0.377	-0.568	-0.470

Nevertheless, differences found in likelihood between the "three-compartment model" with and without feedback are not observed in the descriptive capacity of these two models (see 5.12).

5.6.5 Conclusion of the three-compartment model

The fact that the Q^* compartment could not be identified discouraged us from going ahead with this "three-compartment model": despite our attempts we did not found a satisfactory biological explanation for the Q^* compartment. One of the possibilities we regarded was that it could be related to the number of $CD4^+$ T cells expressing the Inteleukin-7 receptor CD127, but no clear connection exists between the estimated curve of the Q^* compartment and absolute observed $CD4^+CD127^{high}$ cells number. The fact that we did not have a convincing hypothesis to explain this Q^* compartment made us reconsider the "three-β's model", that will be recovered in the next Chapter to model repeated cycles.
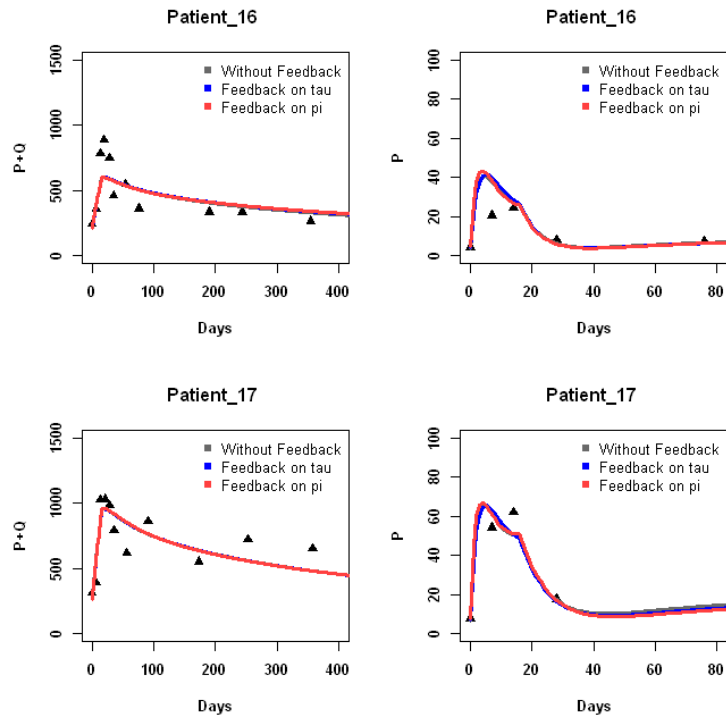
Figure 5.12: Comparison of the "three-compartment model" with and without feedback (on π or on τ). No differences are observed.

Chapter 6

Modeling repeated cycles of IL-7

6.1 Incorporating data from INSPIRE 2 and IN-SPIRE 3 studies

As it has been said in Section 3.3, INSPIRE 2 and INSPIRE 3 are, to our knowledge, the first and only clinical trials where repeated cycles of exogenous Interleukin 7 have been administrated to HIV-infected patients. When adding data from the 23 and 84 treated patients from INSPIRE 2 and INSPIRE 3, respectively, we count on N=128 patients receiving at least one cycle of r-hIL-7. Data have been included from the time of the first injection. Overall, 197 r-hIL-7 cycles were administered, 41 of them incomplete cycles consisting of 1 or 2 injections.

First of all, we applied the "three-β's model" to first cycles of all 128 IN-SPIRE patients. For the first twelve patients of INSPIRE 2, clinic visits were scheduled as for the INSPIRE patients: at weeks 1, 2 and 3 (at the moment of the injections), weeks 4, 5, 6, 9 and 12, and after that all three months until the next cycle (if CD4 count < 550 cells/μL). For the remaining eleven patients of INSPIRE 2, and for patients of INSPIRE 3, visits at week 9 were not performed. Measurements of CD4 count were made within all visits for all patients, while Ki67 count are available only for the first 12 treated patients of INSPIRE 2 at weeks 1, 2, 3, 5 and 12 within the first cycle. For the rest of them, no Ki67 count measurements are available.

Here, we have changed the statistical model of the r-hIL-7 effect on μ_Q. Instead of considering that the effect begins at day 16 (two days after the third injection), we have considered it to begin two days after the first one. This allows us to homogenize complete cycles with cycles of one or two injections. Also, it was difficult to accept a permanent mortality effect, since here we deal with patients followed up for a long time. This is why, from now on, the effect on the mortality rate μ_Q is considered to be constant since two days after the first injection for twelve months, followed by a linear decrease during other twelve months, without significantly modifying the results obtained with previous models. The fixed effect on μ_Q can be written as $\tilde{\mu}_Q = \tilde{\mu}_{Q_0} + \beta_{\mu_Q} d^{0.25} f(t)$

with

$$f(t) = \begin{cases} 1 & if \quad 2 < t \leq 360 \\ 1 - (t - 360)/360 & if \quad 360 < t \leq 720 \\ 0 & if \quad 720 < t \end{cases} \qquad \text{(t in days)}$$

When incorporating data from all patients, with the indicated statistical model, we obtain the results displayed on Table 6.1.

Table 6.1: Priors and estimated mean and standard deviation (sd) of all parameters (in logarithmic and natural scales) for the "3 β's model" when considering all the 128 patients (only data from the first cycle).

	PRIOR (log-scale)		POSTERIOR (log-scale)		POSTERIOR (natural-scale)	
	mean	sd	mean	sd	mean	sd
λ	1.000	1.000	2.355	0.087	**10.541**	*0.920*
ρ	0.000	0.250	0.635	0.102	**1.887**	*0.192*
π	-4.000	1.000	-3.306	0.125	**0.037**	*0.005*
μ_Q	-3.600	0.500	-2.617	0.080	**0.073**	*0 .006*
μ_P	-2.500	0.500	-2.187	0.258	**0.112**	*0.029*
$\beta_{\pi 1}$	-	-			**1.155**	*0.079*
$\beta_{\pi 2}$	-	-			**1.120**	*0.081*
$\beta_{\pi 3}$	-	-			**0.622**	*0.073*
β_{μ_Q}	-	-			**-0.239**	*0.022*
σ_λ	-	-			**0.267**	*0.025*
σ_ρ	-	-			**0.575**	*0.108*
σ_{CD4}	-	-			**0.241**	*0.003*
σ_P	-	-			**0.305**	*0.025*

Penalized Log-Likelihood :-279.8
NON-Penalized Log-Likelihood :-273.3
LCVa :2.136

There are some differences with respect to the values found when analyzing only the INSPIRE (1) patients. Production rate and mortality rates have been found to be is slightly bigger, contrary to proliferation rate. However, main results are fully maintained. The quantitative effects of the successive injections are not equal. They are all significantly different from zero; the first and second ones are similar but the effect of the third one is considerably weaker. Here, when considering data from all patients, we can also observe a noticeable improvement with respect to the model with same β's, since LCVa is equal to 2.136 vs 2.558 (results not shown).

6.2 Cycle effect model: Effect of successive cycles

In order to model the long-term effect of a r-hIL-7 cure, we must incorporate information from repeated cycles to the data set. During a median follow-up of 23 months, there were 33 patients receiving only one cycle, 60 patients receiving two cycles, 13 patients receiving 3 cycles and an only patient received 4 cycles. There was no clear difference between the $CD4^+$ T cells responses after the first and the second cycle in patients receiving complete cycles. Median months between cycles was 12 for INSPIRE 2 (because per protocol half of the patients were followed for a year before administration of a new cycle) and 6 for INSPIRE 3. 95 of the 107 initial cycles were completed, while 10 of them were 2-injection cycles and 2 were 1-injection cycles. As for the 90 repeated cycles, there were 60 completed cycles, 15 2-injection cycles and 15 1-injection cycles. The median number of injections received par patient over the follow-up was 5. In this Section we care about the effect of repeated cycles, and a key question is: Have repeated cycles the same quantitative effect than initial ones? Or, more precisely, can the great increase in $CD4^+$ proliferation be maintained through repeated cycles in the long term?

Let β_C be a new fixed effect to estimate: the so-called "cycle effect", that can be incorporated into the statistical model as follows:

$$\tilde{\pi}^i(t) = \tilde{\pi}_0 + \left[\beta_C \mathbb{1}_{\{C(t)>1\}} + \sum_{k=1}^{3} \mathbb{1}_{\{N_t^i=k\}} \ \beta_{\pi_k} \ d_i^{0.25}\right] \mathbb{1}_{\{N_t^i - N_{t-7}^i = 1\}}$$

where $\mathbb{1}_{C(t)>1}$ equals to 1 if a cycle has been received before time t and 0 otherwise. As previously, we consider a constant effect on μ_Q for twelve months, followed by a linear decrease for another twelve months if a new cycle is not received.

Results for this "cycle effect model" are shown in Table 6.2. We found that the "cycle effect" is distributed as $\beta_C \sim \mathcal{N}(-0.163, 0.015)$; that is, it is significantly negative. In natural scale, we found $e^{-0.163} = 0.85$. The effect on proliferation rate within successive cycles is found to be 0.85 times the effect of the first one. Several explanations could justify this fact, as the presence of antibodies anti r-hIL-7 after the first cycle. Also we must consider the homeostatic regulation of $CD4^+$ T cells, that naturally depends on the starting point. There are significant differences in mean CD4 count before the initial and repeated cycles: the mean CD4 count at baseline was 266 cells/μL whereas it was 456 cells/μL before repeated cycles.

Figures 6.1 and 6.2 show some fits of real data from INSPIRE 2 and 3 patients obtained with the "cycle effect model".

Table 6.2: Priors and estimated mean and standard deviation (sd) of all parameters (in logarithmic and natural scales) for the "cycle effect model" when considering all cycles for each patient; Penalized and Non Penalized likelihoods, and LCVa criteria

	PRIOR (log-scale)		POSTERIOR (log-scale)		POSTERIOR (natural-scale)	
	mean	sd	mean	sd	mean	sd
λ	1.000	1.000	1.672	0.061	**5.323**	*0.326*
ρ	0.000	0.250	0.892	0.093	**2.440**	*0.226*
π	-4.000	1.000	-2.853	0.074	**0.058**	*0.004*
μ_Q	-3.600	0.500	-2.610	0.068	**0.074**	*0.005*
μ_P	-2.500	0.500	-2.567	0.200	**0.077**	*0.015*
$\beta_{\pi 1}$					**0.931**	*0.042*
$\beta_{\pi 2}$					**0.707**	*0.043*
$\beta_{\pi 3}$					**0.229**	*0.042*
β_{μ_Q}					**-0.082**	*0.006*
β_C					**-0.163**	*0.015*
σ_λ					**0.243**	*0.026*
σ_ρ					**0.515**	*0.084*
σ_{CD4}					**0.289**	*0.003*
σ_P					**0.281**	*0.019*

Penalized Log-Likelihood :-618.6
NON-Penalized Log-Likelihood :-609.4
LCVa :4.762
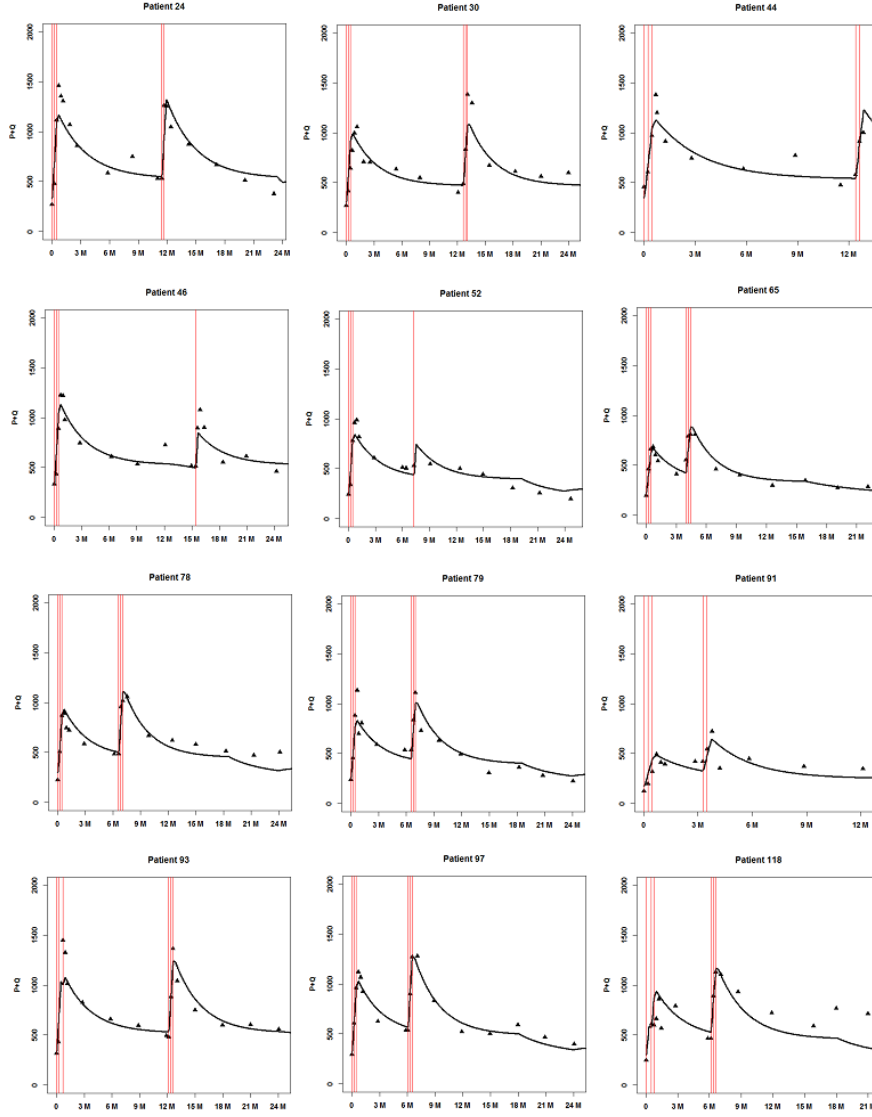
Figure 6.1: Fits for the "cycle effect model" of total CD4 count for 12 patients from INSPIRE 2 and 3 chosen randomly among those who received more than a cycle.
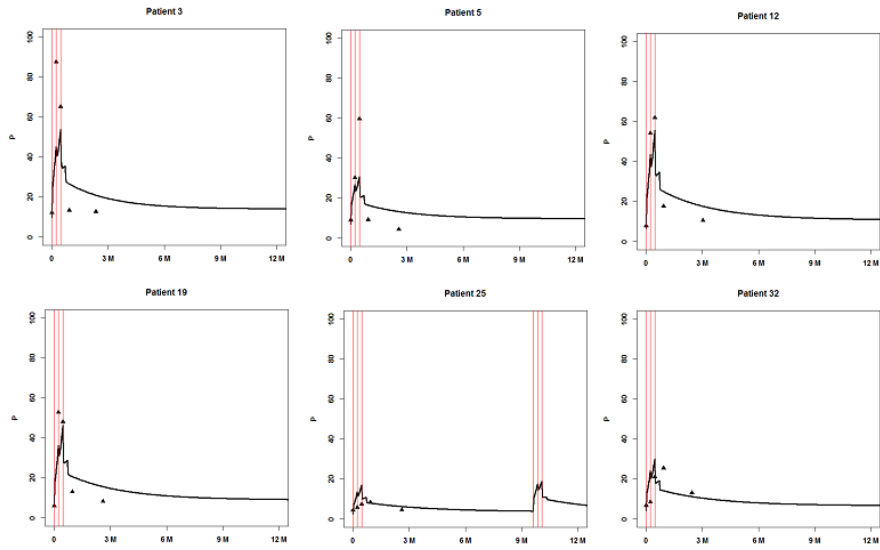
Figure 6.2: Fits for the "cycle effect model" of Ki67 count for 6 patients from INSPIRE and INSPIRE 2 chosen randomly among those who had measurements for this biomarker (only during the first cycle).

We have investigated if the feedback term could explain this apparent "cycle effect". As CD4 count is significantly higher before repeated cycles, a feedback mechanism could intervene by preventing CD4 count from surpassing a physiological level of 1200-1300 cells/μL, through the already explained homeostatic regulation. We have added a simple feedback term as previously:

$$\begin{cases} \frac{dQ}{dt} = \lambda + 2\rho P - \mu_Q Q - \pi Q \frac{1}{(P+Q)^\nu} \\[2mm] \frac{dP}{dt} = \pi Q \frac{1}{(P+Q)^\nu} - \rho P - \mu_P P \end{cases}$$

Numerical and identifiability problems when dealing with such a complex model applied to this large data set prevented us from directly estimate the feedback coefficient ν. Computing the likelihood for $\nu = 0.05$, 0.1, 0.15, 0.2, 0.25, 0.30 we found best results when ν=0.1. Results for the "cycle model with feedback" are shown in Table 6.3.

Table 6.3: Priors and estimated mean and standard deviation (sd) of all parameters (in logarithmic and natural scales) for the "cycle effect model" when considering all cycles for each patient **including a feedback term with ν=0.1**. Penalized and Non Penalized likelihood, and LCVa criteria

	PRIOR (log-scale)		POSTERIOR (log-scale)		POSTERIOR (natural-scale)	
	mean	sd	mean	sd	mean	sd
λ	1.000	1.000	0.275	0.157	1.316	0.207
ρ	0.000	0.250	1.052	0.083	2.863	0.238
π	-4.000	1.000	-1.975	0.068	0.139	0.009
μ_Q	-3.600	0.500	-2.538	0.067	0.079	0.005
μ_P	-2.500	0.500	-2.212	0.138	0.109	0.015
$\beta_{\pi 1}$					0.806	0.038
$\beta_{\pi 2}$					0.626	0.037
$\beta_{\pi 3}$					0.212	0.035
β_{μ_Q}					-0.063	0.005
β_C					-0.153	0.015
σ_λ					-0.608	0.097
σ_ρ					-0.440	0.071
σ_{CD4}					0.286	0.004
σ_P					0.301	0.021

Penalized Log-Likelihood :-598.0
NON-Penalized Log-Likelihood :-584.5
LCVa :4.567

We can observe that, despite the significantly feedback term this model does not modify the cycle effect, which is still highly significant.

6.3 Repeated cycles maintaining adequate CD4 count

We want to compare some different protocols of r-hIL-7 cycles administration for an average patient (having both random effects equal to zero), in order to study the long term efficacy of the treatment in some different scenarios. As for INSPIRE 2 and INSPIRE 3 studies, we consider that CD4 count are measured every three months, and a new cycle is administered when CD4 count<500 cells/μL. We have compared four protocols that can be described as follows:

- Protocol A: All repeated cycles

- Protocol B: An initial complete cycle followed by 2-injection cycles

- Protocol C: An initial complete cycle followed by 1-injection cycles

- Protocol D: All 2-injection cycles

Expected trajectories for every protocol can be found in Figure 6.3.
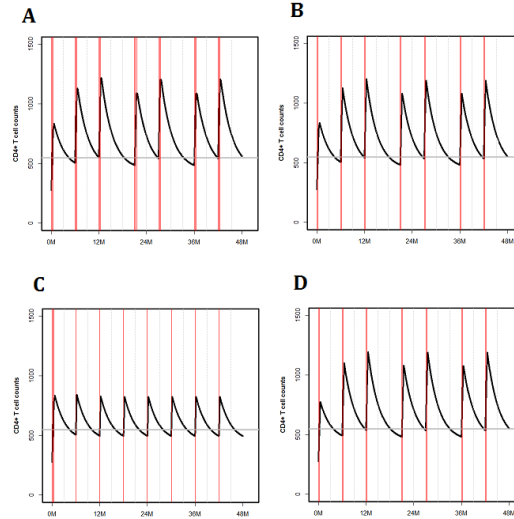
Figure 6.3: CD4 count (cells/μL) predictions for 4 years for a patient having $b^i_\rho = b^i_\lambda = 0$. Protocols A, B and C include a first complete cycle followed by: complete cycles (A), two-injection cycles (B) and one-injection cycles (C). Protocol D includes only 2-injection cycles. Vertical dotted lines are CD4 count (every three months) and vertical solid lines are injections. Horizontal line marks the CD4 threshold of 550 cells/μL.

These protocols were compared over a four-year period in terms of: number of cycles and injections received, median CD4 count over the follow-up and time (in days) spent below 500 cells/μL.

As can be observed in Table 6.4 we found no major differences regarding median CD4 count or time under 500 cells/μL between Protocol A and Protocol B (all complete cycles vs an initial complete cycle followed by 2-injection cycles).

However Protocol B requires 15 injections instead of 21. As for the Protocol C (initial complete cycle followed by 1-injection cycles) time spent under 500 CD4/μL is identical than in Protocol A with only 10 injections, but it achieves a lower median CD4 count and it requires one more cycle. Protocol D is slightly worse in terms of time below 500 cells/μL.

Table 6.4: Comparison of the number of injections and cycles received, time under 500 CD4 count and median CD4 count for a patient with random effects equal to zero for the four protocols through four years. In protocol A, the patient always receives complete cycles; in protocol B, the patient receives a first complete cycle followed by repeated cycles composed of two injections; in protocol C the patient receives a first complete cycle followed by repeated cycles of one single injection; in protocol D the patient always receives 2-injection cycles (including the initial one)

	A	B	C	D
Number of injections received	21	15	10	14
Number of cycles received	7	7	8	7
Time under 500 CD4/μL (days)	60	73	60	87
Median CD4 count	678	663	588	654

6.4 Adaptive protocols

In this Section, we are going to apply these simulations to real patients from INSPIRE 2 and INSPIRE 3. We have taken two patients and we collect CD4 count measurements during the first received cycle in order to calculate their random effects values. We have used this information to compute expected trajectories and determine which would be the best protocol for each one.

Patient A had a good response in terms of CD4 count. Parameters with random effect have been estimated by Parametric Empirical Bayes as being λ = 6.586 and $\rho = 4.797$ (all the other parameters are the population parameters obtained in the "cycle effect model").

In Figure 6.4 we display the expected trajectories for this patient.

Table 6.5 shows results for the four criteria. According to our model, the four protocols lead to minor differences for the four criteria. Protocol B would spare 2 injections with respect to Protocol A where having little impact on the CD4 count, and even Protocol C and D would be admissible.

Patient B had a poor response in terms of CD4 count. The value of the parameters with random effect for him have been estimated to λ = 3.284 and $\rho = 1.956$ (all the other parameters are the population parameters obtained in the "cycle effect model").
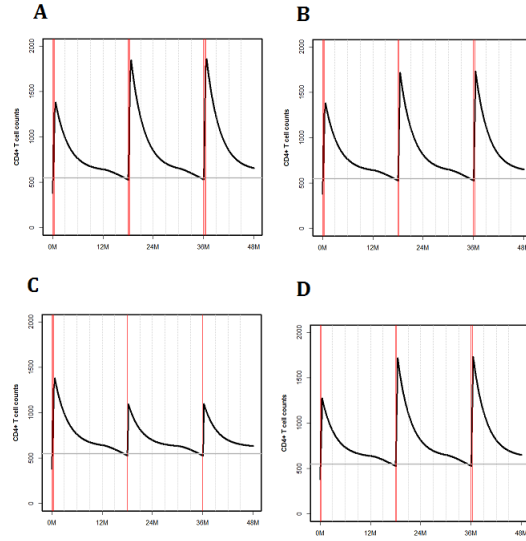
Figure 6.4: CD4 count (cells/μL) predictions for 4 years for a particularly good responder patient. Protocols A, B and C include a first complete cycle followed by: complete cycles (A), two-injection cycles (B) and one-injection cycles (C). Protocol D includes only 2-injection cycles. Vertical dotted lines are CD4 count (every three months) and vertical solid lines are injections. Horizontal line marks the CD4 threshold of 550 cells/μL.

Table 6.5: Comparison of the number of injections and cycles received, time under 500 CD4 count and median CD4 count for a "good responder" patient for the four protocols through four years. In protocol A, the patient always receives complete cycles; in protocol B, the patient receives a first complete cycle followed by repeated cycles composed of two injections; in protocol C the patient receives a first complete cycle followed by repeated cycles of one single injection; in protocol D the patient always receives 2-injection cycles (including the initial one)

	A	B	C	D
Number of injections received	9	7	5	6
Number of cycles received	3	3	3	3
Time under 500 CD4/μL (days)	3	3	3	3
Median CD4 count	721	709	669	703

In Figure 6.5 we display the expected trajectories for this patient. Table 6.6 shows results for the four criteria for this patient. Our model predicts that
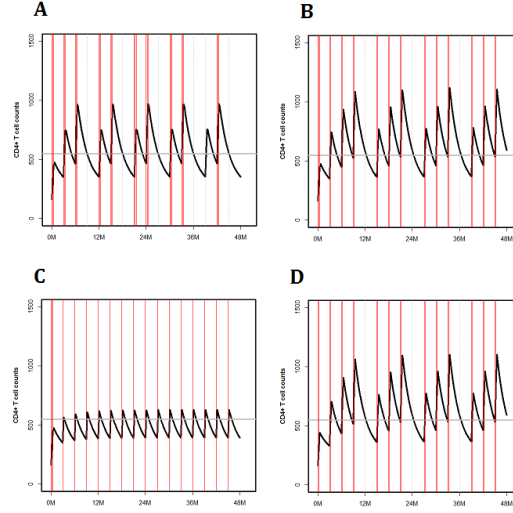
Figure 6.5: CD4 count (cells/μL) predictions for 4 years for a patient with a particularly poor response. Protocols A, B and C include a first complete cycle followed by: complete cycles (A), two-injection cycles (B) and one-injection cycles (C). Protocol D includes only 2-injection cycles. Vertical dotted lines are CD4 count (every three months) and vertical solid lines are injections. Horizontal line marks the CD4 threshold of 550 cells/μL.

this patient could benefit from 2-injection cycles (protocol B) without loss of efficiency in terms of CD4 count or time over 500 cells/μL (the improvement supposed in the table seems to be due to chance). In this case, 1-injection cycles could not be considered since time spent below 500 cells/μL is much higher than for 2-injection cycles and the patient would receive three more cycles. Also, the median CD4 count is worse than for the rest of protocols. Protocol D could also be considered.

As we said before, Parametric Empirical Bayes estimators allows us to estimate prior distributions for random effects. *A posteriori* of the PEB estimator asymptotically converges to the true values of patient's parameters.

Table 6.6: Comparison of the number of injections and cycles received, time under 500 CD4 count and median CD4 count for a "bad responder" patient for the four protocols through four years. In protocol A, the patient always receives complete cycles; in protocol B, the patient receives a first complete cycle followed by repeated cycles composed of two injections; in protocol C the patient receives a first complete cycle followed by repeated cycles of one single injection; in protocol D the patient always receives 2-injection cycles (including the initial one)

	A	**B**	**C**	**D**
Number of injections received	30	27	18	26
Number of cycles received	10	13	16	13
Time under 500 CD4/μL (days)	561	366	893	381
Median CD4 count	549	617	470	611

6.5 Conclusion

This Chapter can be found as an article in Appendix E, and it is projected to be submitted to *Annals of Applied Statistics* in November 2015. It provides, as main conclusions, the decreasing effect of successive injections on proliferation rate and the weak but significant "cycle effect". The introduction of the feedback term has not significantly changed the fact that the effect of repeated cycles on proliferation rate is slightly weaker than the effect of the initial one. Other possibilities, as the presence of r-hIL-7 antibodies after the first cycle could be considered.

Also, simulations show how these repeated cycles are able to maintain adequate CD4 count for a long time. Despite the fact that the most appropriate model depends on every individual, our results agree with the survival analysis presented in Section 3.3.5. where no differences are found when comparing the time spent over 500 cells/μL after a complete cycle or a 2-injection cycle.

Also, some other questions regarding the interaction between the r-hIL-7 and the immune system could be modeled with additional data, for instance, preferential effects on specific T cell subsets as recent thymic emigrants (RTEs) and naive non-RTE T cell populations (Mackall et al., 2011).

Finally, when talking about predictions and individual expected trajectories, it has been said that Parametric Bayes Estimator allows us to estimate prior distributions for random effects. The PEB estimators asymptotically converges to the true values of patient's parameters. Our results would, however, be more accurate if "real" values for random effects could be computed.

Chapter 7

Conclusion

In this thesis work we have focused on the effects of exogenous Interleukin 7 (IL-7) on $CD4^+$ T lymphocytes from a statistical point of view. We have worked with an existing mathematical model based on a system of ordinary differential equations involving two cell compartments: quiescent Q and proliferating P $CD4^+$ T cells. This system naturally includes five biological parameters: production rate λ of quiescent cells (cells entering the system, including thymic production), proliferation rate π (from quiescent to proliferating), reversion rate ρ (every P cell is divided and produces two Q cells) and mortality rates of both sub-populations μ_Q and μ_P. The effect on proliferation rate was found to be highly significant, as well as effects on mortality rate of quiescent cells and production rate depending on the model. We have made some variations to the original model with the aim of searching an improvement in terms of the "goodness" of the model.

We have used a complex method for the estimation of the parameters that was created in the team several years ago. A mixed effect model applied on the biological parameters and a model for the observations, together with the previously cited mathematical model constitute the backbone of this approach. Over it, an algorithm based on a maximum likelihood estimation is used, where the presence of random effects implies a hierarchical approach. This method, that integrates the individual likelihoods over the random effects via the adaptive Gaussian quadrature, was subsequently adapted to compute the maximum *a posteriori* of the assumed normal distributions. By using an approximated variance matrix, and based on the Robust Variance Scoring (RVS) algorithm, this approach was implemented in a Fortran program called NIMROD, which has been used during this thesis work.

When modeling a single cycle of IL-7 injections, we did an unsuccessful attempt to link a pharmacokinetic and a pharmacodynamic model (using the plasma or the tissue concentration of exogenous IL-7) in order to study its effect in a continuous form. This did not provide us satisfying results and we focused on doing modifications in the mathematical and the statistical model with the dose received. The first modification we tried within the mathematical model was to add a "feedback effect" on proliferation rate, in order to boost the natural tendency of the ODE system to return to the equilibrium point. A small but significant improvement in likelihood functions and LCVa criteria was unfortunately not followed by an improvement of fits of real data. We turned

into more sophisticated mathematical model as the "four-compartment model", where quiescent and proliferating $CD4^+$ T cells were in turn divided into naive and memory cells. Data we had at our disposal were not sufficient to determine if every one of these compartments was correctly fitted.

An important result was obtained when the statistical model was changed in order to let every injection have a quantitative different effect within a cycle. This "three-β's model" has provided us the best results so far when modeling a single cycle. The declining trend in the effect of successive injections leads us to consider a "three-compartment model", where we could assume a gradual response of the quiescent cells, but it did not let us express this declining response adequately. However, this descending trend (concretely the fact that the third injection seems to have a weak effect) is probably the most important result underlined by this thesis work.

This result was confirmed when analyzing data from INSPIRE 2 and INSPIRE 3 studies, where repeated cycles of exogenous IL-7 were administrated for the first time to HIV-infected patients that did not reach to improve immune system to adequate levels after combined antiretroviral therapy (cART). A Shared Gamma Frailty model studying the probability of dropping under 550 cells/μL showed that the Hazard Ratio when receiving 1-injection cycles was equal to 4.29 (1.32,13.90) with regard to complete cycles. However, the fact of receiving 2-injection cycles was not significant. The strongest predictor of dropping below 550 $CD4^+$ T cells was CD4 count at baseline (p < 0.001) while other considered variables as age, sex, type of cycle (initial/maintenance), HIV DNA levels at baseline... were not significant. As other important results, INSPIRE 2 and INSPIRE 3 studies confirmed the main increase among naive and central memory sub-populations with no relative rise of Tregs. When analyzing the time spent over 500 cells/μL in patients with a follow-up of 21-24 months, the median time spent above 500 CD4 count was 13.7 months (8.4,20.1).

When modeling data from repeated cycles, two major questions have been highlighted: the decreasing effect of successive injections was confirmed when including initial and repeated cycles from all INSPIRE patients. Also a "cycle-effect" was identified, that may mean that repeated cycles could have a slightly weaker effect than the initial ones. We tried to explain this apparent "cycle effect" with the introduction of a feedback term, that could collect the natural homeostatic regulation of the $CD4^+$ cells. This term was not enough to explain the "cycle effect", and the doubt remains: is this apparent difference due to the natural homeostasis process (that we have failed to capture with the "feedback model") or there are another factors that could explain this (as the presence of antibodies after the first cycle)? And what is more important, has this apparent difference an impact on CD4 count in the long term?

Our predictions suggest that the effect of r-hIL-7 can be maintained through repeated cycles in the long term. When considering a regular patient (having both random effects equal to zero) we found that, after a first complete cycle, 2-injection cycles could be administered instead of complete cycles without having a negative impact on CD4 count or time spent over 500 cells/μL. This result is confirmed when applying predictions of different protocols of administration to real patients. The inclusion of random effects (that are found to be significant) allows us to consider this dynamic model as an assistance for personalized treatment decisions. However, exact values for random effects could be necessary to accurately predict the behavior of every protocol.

To finish, some results are shown about an update of the local HIV epidemic obtained during a 3 months internship in Navarra (Spain). A descriptive analysis of data was followed by an analysis of the variables related with the diagnostic delay. IDUs as the way of transmission and old age were the variables that appeared to have the most important influence on the fact of having a late diagnosis. Survival analysis offered some interesting results as the comparison between the survival time regarding the CD4 count at diagnosis. Some parametrical models were adjusted, as the Weibull model, and finally, we tried to estimate the number of people living with HIV without diagnosis. Software provided by UNAIDS (Spectrum and EPP package) allows us to estimate that approximately 2000 people could be infected with the HIV virus right now in Navarra, while only half of them are diagnosed. These results should be confirmed with more accurate data about the different population risk sizes and prevalences.

Chapter 8

Résumé détaillé en français

Cette thèse a été entièrement financée par l'Institut de Recherche Vaccinale (VRI). Le VRI a été labellisé en 2011 dans le cadre de la création des laboratoires d'excellence (Labex) par le Ministère de l'Enseignement Supérieur et de la Recherche, dont il a été un des lauréats. Son projet prolonge le programme vaccinal de l'ANRS, l'organisme public chargé de coordiner et financer la recherche sur le VIH/SIDA et les hépatites virales. Le VRI est dirigé par le Pr Yves Levy, et il a pour mission de répondre aux défis scientifiques et aux obstacles que représente le développement de vaccins efficaces contre le VIH et l'hépatite C. Ce travail de thèse s'inscrit dans la division Biostatistique et bioinformatique, dirigée par le Pr Rodolphe Thiébaut.

8.1 Introduction

8.1.1 Contexte épidémiologique

Un des huit Objectifs du Millénaire pour le Développement (OMD) établis par l'ONU comprenait la lutte contre le VIH/SIDA. Ces objectifs avaient comme date d'expiration l'année 2015, et à cette occasion, ONUSIDA a présenté un rapport pour décrire la situation actuelle. Dans ce rapport il a été estimé que pendant l'année 2013 environ 2,1 millions de personnes ont été infectées (ce qui représente une chute du 38% depuis 2001) et 1,5 millions de personnes sont décédées pour des causes liées au SIDA. En ce moment, il est estimé que 35 millions de personnes vivent avec le VIH dans le monde (et la tendance est à la hausse), dont 19 millions ne connaissent pas leur statut. Depuis le début de la pandémie, environ 40 millions de personnes sont mortes. Malgré les progrès accomplis pendant ces 30 ans, la problématique liée au VIH/SIDA constitue une catastrophe humaine aux proportions énormes et implique un défi majeur aux progrès et la stabilité des sociétés d'aujourd'hui.

8.1.2 Contexte biologique

En 1981 et 1982, plusieurs cas de pneumonie, candidose, sarcome de Kaposi et diverses infections virales furent constatées aux Etats-Unis parmi de jeunes hommes homosexuels. Assez tôt, un nouveau *syndrome d'immunodéficience humaine* fut défini, mais l'agent étiologique restait inconnu. En 1983, le virus

VIH fut isolé et identifié comme la cause de ce nouveau syndrome. Le VIH est un rétrovirus appartenant à la famille des lentivirus. Il est capable de transcrire son génome (codé sous forme d'ARN) en ADN, qui va s'intégrer dans le génome des cellules hôtes. Deux types principaux peuvent être distingués: VIH-1 et VIH-2, comprenant de nombreux groupes et sous-types. Le VIH-2, beaucoup moins répandu, est moins virulent que le VIH-1 et présente une progression plus lente vers le SIDA. Dans ce travail, nous ferons toujours référence au VIH-1, même si nous utiliserons le terme VIH pour une question de clarté.

Peu de temps après la découverte du VIH, les molécules CD4 (situées à la surface des lymphocytes T CD4$^+$) furent identifiées comme les récepteurs cellulaires utilisés pour le virus. Actuellement, nous savons que ce récepteur est insuffisant pour la pénétration du virus, et que le cycle de réplication commence quand la protéine virale gp120 rencontre le récepteur CD4 et un corécepteur (CXCR4 ou CCR5) dans la surface cellulaire. Une fois que le virus pénètre dans la cellule, l'enzyme transcriptase inverse permet la synthèse d'ADN à partir d'ARN du virus. Cet ADN va être incorporé à la charge chromosomique de la cellule (grâce à l'enzyme intégrase), et de nouvelles particules virales vont être produites et libérées dans le milieu extracellulaire où elles chercheront d'autres lymphocytes susceptibles d'être infectés. Cela se traduit par une prolifération virale extrêmement importante au début de l'infection (pendant les premières semaines ou mois), accompagnée d'une chute du niveau de lymphocytes CD4$^+$. Après nous trouvons la phase asymptomatique, qui peut prendre plusieurs années, pendant laquelle nous observons un état de "faux équilibre" où la charge virale est à peu près stable et le nombre de CD4$^+$ diminue très légèrement. Cette phase va aboutir (à défaut d'un traitement efficace) à un état d'immunodéficience sévère qui annonce la phase finale de la maladie (phase SIDA). Le système immunitaire est épuisé et le patient meurt d'une maladie opportuniste.

L'apparition de la thérapie antirétrovirale transforma le scénario de la pandémie du VIH. Le groupe des NRTI (inhibiteurs nucléotidiques de la transcriptase inverse) fut le premier à apparaître. La Zidovudine (AZT) fut la première molécule autorisée pour des patients atteints de SIDA, mais bientôt les résistances apparurent (leur apparition a été estimée à environ 90% pour les personnes en phase SIDA et 31% des personnes dans la phase initiale au bout de 12 mois). Une deuxième molécule appartenant aux NRTI, Didanosine, fut employée pour les personnes ayant développé une résistance à l'AZT, mais peu de temps après on put observer que le problème des résistances était commun à toutes les monothérapies (dû principalement à l'extraordinaire capacité de mutation du virus). Ensuite, d'autres antirétroviraux apparurent, comme les PI (inhibiteurs de la protéase) ou les NNRTI (inhibiteurs non-nucléotidiques de la transcriptase inverse).

L'utilisation combinée de trois ou plus de ces antirétroviraux parvint à maintenir sur le long terme la réduction de la réplication virale et l'augmentation du nombre de CD4$^+$, ce qui représente une vraie révolution dans la prise en charge de ces patients. De nos jours, l'espérance de vie des patients vivant avec le VIH peut être comparée à celle de la population générale lorsque le nombre de CD4$^+$ peut être maintenu au-dessus de 500 cellules/μL. Dans la pratique, les deux principaux critères pour évaluer l'effectivité de la thérapie antirétrovirale sont la charge virale, qui devrait être aussi petite que possible, et le nombre de lymphocytes T CD4$^+$ par microlitre. En effet, même si la charge virale a été

supprimée (elle n'est pas détectable), le nombre de CD4$^+$ a une très grande influence dans la progression clinique des patients sous thérapie antirétrovirale. Il a été montré dans de nombreuses études que plus le nombre de CD4$^+$ est élevé, moins important sera le risque de morbidité et de mortalité pour ces patients, et cette différence est particulièrement remarquable lorsqu'on parle de faibles niveaux de CD4$^+$. C'est la raison pour laquelle il est si important de définir le concept de *Immunological Low Responder* (des patients ayant une réponse faible d'un point de vue immunologique bien qu'ils aient une bonne réponse virologique). Mais comme nous allons le voir, il y a des difficultés qui ont empêché un accord universel pour cette terminologie.

8.1.3 Patients à faible réponse immunitaire

Une fois que le traitement antirétroviral est commencé, il faut s'attendre à une diminution majeure de la charge virale jusqu'à des niveaux indétectables, et une augmentation du nombre de CD4$^+$ jusqu'à des niveaux considérés suffisants. Néanmoins pour un petit pourcentage des patients le traitement va échouer et la charge virale ne va pas devenir indétectable. Et aussi, pour un pourcentage non négligeable de patients, la réussite d'un point de vue virologique ne s'accompagnera pas d'une réussite d'un point de vue immunologique. Ces patients peuvent être appelés *Immunological Low Responders* (qui ont une réponse immunologique faible) mais ils ont aussi été appelés *Immunological Non Responders* ou *Inadequate Immunological Responders*. Mais plus important que la dénomination c'est le fait de discerner qui sont les patients qui peuvent être considérés comme des "mauvais répondeurs". Y a-t-il un seuil qu'on peut fixer, comme 500 cellules/μL? Doit-il s'agir d'un rapport entre les niveaux pré traitement et post traitement, comme un pourcentage (d'au moins 25%) ou un chiffre (une récupération d'au moins 100 CD4$^+$)? Toutes ces possibilités ont été utilisées dans la littérature scientifique, ce qui montre qu'il n'y a pas une seule définition pour ces *Immunological Low Responders*. Aussi, une autre question majeure est de déterminer combien de temps doit-on attendre après le début du traitement pour déterminer si un patient a bien répondu ou pas. Le fait que la thérapie antirétrovirale d'un patient soit modifiée assez régulièrement (dû à l'apparition de nouveaux traitements, ou à cause des résistances...) implique que l'effet d'une thérapie particulière sur le nombre de CD4$^+$ à long terme n'est pas facile à étudier. Deux théories s'opposent: celle qui suppose une augmentation faible mais continue du nombre de CD4$^+$, même après plusieurs années de thérapie, et celle qui mise sur un *effet plateau*, par lequel il existerait un nombre maximal de CD4$^+$ qu'on ne peut pas franchir, même en continuant la thérapie.

S'il est difficile de définir qui sont les patients considérés comme *Immunological Low Responders*, il est aussi également difficile d'estimer leur nombre. Plusieurs auteurs ont donné des chiffres approximatifs pour ce pourcentage, qui peuvent varier de 5 à 45%, en sachant que la réponse immunologique sera d'autant plus satisfaisante que le nombre initial de CD4$^+$ sera haut. Effectivement le nombre de CD4$^+$ au moment de commencer le traitement a été identifié comme un facteur fortement associé avec le nombre de CD4$^+$ au cours du traitement, mais ce n'est pas le seul paramètre qui a une influence sur la réponse immunitaire. La phase de l'infection pendant laquelle le traitement est commencé (le plus tôt sera le mieux) et l'âge (peut être dû à son effet sur la réponse thymique) vont aussi avoir une influence significative. Récemment,

d'autres facteurs comme le niveau de cellules T régulatrices (Treg) ou le niveau de la protéine inflammatoire 1β ont été proposés. Quelques travaux ont étudié l'effet supplémentaire de certains antirétroviraux, comme le Maraviroc, sur des *Immunological Low Responders* sans obtenir de réponses concluantes.

8.1.4   Immunothérapie

Les approches basées sur les antirétroviraux ne sont pas les seuls enjeux de la recherche actuelle sur le VIH. L'immunothérapie (visant à obtenir une réponse immunitaire effective capable de développer des défenses) est une des questions majeures dans la scène actuelle de la recherche d'un traitement contre le VIH. Nous allons nous focaliser sur cette première composante, l'immunothérapie. Mise à part la problématique des patients *Immunological Low Responders*, l'étude des effets de ces interventions visant à booster le système immunitaire est d'une grande importance pour l'ensemble des personnes vivant avec le VIH. Dès le moment où il a été réalisé que, malgré l'efficacité de la thérapie antirétroviral combinée, elle n'arriverait pas à éradiquer l'infection (en tout cas dans un délai de temps raisonnable), ces interventions supplémentaires ont été regardées avec espoir.

Lorsqu'on parle de réponse immunitaire, il est naturel de considérer les Interleukines comme une des possibilités thérapeutiques. Les Interleukines appartiennent à la famille des cytokines, qui agissent comme outils de communication parmi les lymphocytes. Elles vont permettre d'établir et contrôler une réponse immunitaire adéquate. Les cellules immunitaires pourront de cette façon transmettre des informations sur un processus infectieux qui seront reçues par d'autres cellules ayant les récepteurs nécessaires. C'est un processus extrêmement complexe; les signaux envoyés peuvent concerner autant l'activation, production ou prolifération des lymphocytes $CD4^+$ que le ralentissement de l'activité cellulaire lorsque l'infection est surmontée. Ce processus est gravement perturbé lors de l'infection par VIH, car la population de lymphocytes $CD4^+$ est modifiée quantitativement et qualitativement. Aussi, les signaux sont incorrectement envoyés et reçus, ce qui conduit à une impossibilité du système immunitaire de préserver l'équilibre, et par conséquent à une destruction progressive.

Une des cytokines connues pour son influence sur le système immunitaire est l'Interleukine 2 (IL-2). Sa capacité de stimuler la réponse immunitaire étant connue avant la découverte du VIH, elle a été longtemps considérée comme le candidat le plus prometteur pour l'immunothérapie contre ce virus. Depuis les années 90, plusieurs études ont montré la capacité de l'IL-2 exogène (administré de façon intermittente comme un complément de la thérapie antirétroviral combinée) à augmenter considérablement le nombre de lymphocytes $CD4^+$. Elle fut longtemps considérée comme une thérapie prometteuse, mais les espoirs disparaissent avec l'apparition de deux études indépendantes, comprenant plus de 5800 patients et présentés au même temps (lors du congrès *CROI 2009: 16th Conference on Retroviruses and Opportunistic Infections*). Ces études ne réussissent pas à montrer une vraie différence dans les risque de décès ou d'apparition de maladies opportunistes parmi les patients traités et les non traités, malgré une incontestable augmentation du nombre total de lymphocytes $CD4^+$. Peu de temps après on a attribué cette apparente contradiction au fait que l'augmentation du nombre de $CD4^+$ est due en partie à une expansion importante des cellules T régulatrices, chargées d'inhiber l'activation, la

prolifération et la production des cellules T effectrices.

8.1.5 Interleukine 7

Une autre cytokine identifiée comme ayant un rôle majeur dans la réponse immunitaire est l'Interleukine 7 (IL-7), elle sera la molécule clé dans ce travail. L'Interleukine 7 fut identifiée pour la première fois en 1988 sous la forme d'un facteur de prolifération des lymphocytes B. Peu de temps après on a découvert qu'elle a, de la même façon, une importance capitale dans le développement des lymphocytes T. L'IL-7 est sécrétée par la moelle osseuse et le thymus. L'ensemble des mécanismes exacts par lesquels cette cytokine intervient dans le contrôle immunitaire sont encore en train d'être étudiés. On connait déjà son importance pour stimuler la régénération des cellules $CD4^+$, par exemple à travers la production thymique, ainsi que pour aider la prolifération et la survie des cellules matures. La possibilité d'une thérapie utilisant de l'IL-7 exogène a aussi été envisagée dans d'autres maladies comme le cancer ou la septicémie. En 2009, les deux premiers études (à notre connaissance) évaluant l'administration de *Recombinant Human Interleukin 7* (r-hIl-7) aux personnes vivant avec le VIH furent présentées. Une premier étude fut focalisée sur l'administration d'une seule injection de r-hIL-7 non glycosylée, et une deuxième étudiait l'administration de huit injections de r-hIL-7 tous les deux jours (pendant 16 jours). Selon les résultats de ces deux études une dose acceptable pourrait osciller entre 3 et 30 μg/kg. Une augmentation importante du nombre de cellules fut observée dans quasiment toutes les sous-populations (avec un maximum vers 21 jours après la première injection), sans observer une augmentation de la proportion des cellules T régulatrices. De la même façon, il fut observé que presque toutes les cellules se mirent à proliférer d'avantage sous l'effet de l'IL-7. Ces études ont été le point de départ des trois études INSPIRE, qui ont été réalisées avec de l'Interleukine 7 glycosylée (ayant une demie vie plus longue) et qui sont l'axe de ce travail.

8.2 Les études INSPIRE

8.2.1 Background: INSPIRE (1)

L'étude INSPIRE (1) a été présentée en 2012 et elle comprend 27 participants vivant avec le VIH. Ces patients ont un nombre de $CD4^+$ entre 101-400 cellules/μL malgré une charge virale indétectable après au moins un an sous thérapie antirétrovirale. Les patients ont été répartis dans trois groupes, recevant trois injections hebdomadaires de r-hIL-7 (de 10, 20 ou 30 μg/kg) plus un groupe témoin de 6 patients (tous les patients ont continué à recevoir la thérapie antirétrovirale). Les résultats ont été encourageants: une augmentation importante du nombre de cellules CD4 (dépendant de la dose) a été observée, spécialement parmi les cellules naives et les mémoires centrales. Les cellules prolifératives (mesurées par le marqueur Ki67) ont aussi connu une augmentation, et ce sans augmentation significative du nombre de Treg. De ce fait, l'Interleukine 7 est considérée comme une possibilité réelle et puissante pour favoriser une bonne réponse immunitaire chez les *Immunological Low Responders*. Cela a conduit au lancement de deux études (INSPIRE 2 et INSPIRE

3) envisageant la possibilité d'appliquer des cycles répétés d'Interleukine 7. Ces cycles répétés ont comme objectif de maintenir le nombre de lymphocytes CD4$^+$ au-dessus d'un seuil préfixé et considéré comme adéquat (en l'occurrence 500 cellules/μL). Au cours de cette thèse, nous avons contribué à analyser les données brutes provenant de ces deux études, et nous allons les décrire.

8.2.2 Analyse descriptive d'INSPIRE 2 et 3

INSIPIRE 2 et INSPIRE 3 ont également été menées avec des patients vivant avec le VIH, sous thérapie antirétrovirale et ayant une réponse immune insuffisante (CD4$^+$ $\in$]100,400] pour INSPIRE 2 et CD4$^+$ $\in$]100,350] pour INSPIRE 3) malgré une charge virale indétectable. INSPIRE 2 a été conduit avec 23 participants (des Etats Unis et du Canada), qui ont reçu d'abord un premier cycle (3 injections hebdomadaires) de r-hIL-7 à une dose de 20 μg/kg. Les douze premiers patients ont attendu un an avant d'être à nouveau traités lorsque leur nombre de CD4$^+$ était inférieur à 550 cellules/μL. Le reste des patients ont été contrôlés tous les trois mois et lorsque leur nombre de CD4$^+$ était inférieur à 550 cellules/μL ils ont également reçu un nouveau cycle. INSPIRE 3 comprend 88 patients de l'Europe (Milano et Zurich) et l'Afrique du Sud (Johannesburg et Bloemfontein). Les patients d'INSPIRE 3 ont été divisés en deux groupes, le groupe dit "CYT107" (en référence au nom de la molécule utilisée) et le groupe "Control". Le premier groupe a reçu un premier cycle suivi de cycles répétés quand le nombre de CD4$^+$ (mesuré aussi tous les trois mois) était inférieur à 550 cellules/μL. Les patients du groupe "Control" ont été suivis pendant 12 mois sans recevoir d'intervention (autre que continuer avec la thérapie antirétrovirale). Après ces 12 mois s'ils étaient encore au-dessous de 550 cellules/μL ils ont commencé avec un premier cycle suivi des cycles répétés si nécessaire comme pour le groupe "CYT107". Sur un total de 107 patients qui ont reçu au moins un cycle, 74 ont reçu un deuxième cycle, 15 ont reçu un troisième cycle et uniquement un patient a reçu quatre cycles. Le nombre total de cycles reçus a donc été de 197, dont 42 étaient incomplets (composés d'uniquement une ou deux injections, au lieu de trois). Il est important de signaler que le nombre moyen de CD4$^+$ avant les cycles initiaux était de 266 cellules/μL, avec 473 cellules/μL avant le deuxième cycle et 373 cellules/μL avant le troisième cycle. Quelques résultats provenant du premier cycle des patients d'INSPIRE 2 ont déjà été présentés par Irini Sereti en 2012 (notamment les résultats concernant l'intégrité de la barrière intestinale à travers une biopsie rectale).

Pour le reste des données, elles ont été présentées dans l'article Thiébaut et al. (2015 in revision) et parmi les conclusions principales nous trouvons:

- Quant aux effets adverses, la r-hIL-7 a globalement été bien tolérée. Les effets secondaires indésirables étaient de grade $\leq$ 1 (77,6%), de grade 2 (20,7%) et de grade > 3 (1,7%)

- Nous avons analysé le temps passé au-dessus de 500 CD4 parmi les patients qui avaient un suivi complet de 21 à 24 mois. Il a été trouvé que la moitié de ces patients ont passé plus de 63% du temps de suivi au-dessus de 500 cellules/μL. Le temps moyen au-dessus de ce seuil a été de 13,7 mois.

- Un modèle de Weibull (modèle paramétrique de survie réalisé grâce au

package R "Frailtypack") a été utilisé pour identifier quelles sont les variables ayant une influence significative sur l'évènement "passage en dessous de 550 CD4 cellules/μL". Il a été trouvé que le facteur le plus influent est le niveau de CD4$^+$ avant le traitement (p-value < 0,001, rapport de risques = 11,1). Un des résultats principaux de ces études concerne l'efficacité des cycles incomplets (composés de 1 ou 2 injections) par rapport aux cycles complets (3 injections). Il a été trouvé que les cycles de deux injections ne semblent pas avoir un effet différent des cycles complets, tandis que le fait de recevoir un cycle composé d'une seule injection est significatif (rapport de risques 4,29, intervalle de confiance (1,32, 13,90) à 95%). Un autre résultat extrêmement important fait référence à l'effet des cycles répétés par rapport aux cycles initiaux. Avec ce modèle, nous n'avons pas trouvé des différences significatives (rapport de risques 0,86, intervalle de confiance (0,51, 1,46) à 95%). Les autres variables étudiées (l'âge, le sexe, l'origine ethnique, le temps depuis le diagnostic de VIH, la durée de la thérapie antirétrovirale, la phase de l'infection lors du diagnostic ou le niveau de charge virale avant le traitement avec r-hIL-7) étaient non significatives.

- Une augmentation dans quasiment tous les sous-types cellulaires a été observée, notamment parmi les cellules naïves et les cellules mémoires centrales, ainsi qu'une augmentation du pourcentage des cellules qui prolifèrent (mesurées par le biomarqueur Ki67). Et cela sans augmentation de la proportion des cellules T régulatrices.

- Environ la moitié des patients ont eu des pics transitoires de charge virale au-dessus de 50 cp/mL. 13% des patients d'INSPIRE 2 et 17% des patients d'INSPIRE 3 ont eu des pics au-dessus de 200 cp/mL.

- En conclusion, les études INSPIRE 2 et INSPIRE 3 ont montré que les cycles répétés de r-hIL-7 peuvent promouvoir et maintenir une restauration du nombre de lymphocytes CD4$^+$ chez des patients sous thérapie antirétrovirale combinée.

8.3 Modélisation mathématique

8.3.1 Contexte

Dans la recherche médicale, les modèles mathématiques basés sur des équations différentielles ont été largement utilisés, en particulier les systèmes biologiques qui décrivent l'interaction entre différentes populations cellulaires. Nous avons travaillé avec des modèles dits mécanistes, qui expriment nos connaissances biologiques à travers des équations (dans notre cas, il s'agit d'un système d'équations différentielles ordinaires : EDOs). Ces modèles peuvent être appelés des modèles dynamiques, les équations cherchant à représenter les caractéristiques les plus importantes des mécanismes biologiques sous-jacents.

Nos connaissances sur la dynamique virale du HIV ont augmenté significativement grâce à ces modèles dynamiques. En 1995 et 1996, Ho, Wei et Perelson ont présenté les travaux qui peuvent être considérés comme le point de départ de l'histoire de la modélisation du virus HIV. Ces premiers travaux nous ont

permis d'avoir quelques estimations qui ont bouleversé les connaissances sur l'interaction du système immunitaire et le virus. Il a été estimé que la demie vie du virus dans le sang était de seulement 6 heures, tandis que le taux de production pouvait atteindre les 10^{10} particules virales par jour. Grâce à ces découvertes, il a été compris que l'équilibre apparent pendant la phase asymptomatique de l'infection par VIH était la conséquence des dynamiques virale et lymphocytaire très importantes. Ces modèles sont devenus progressivement plus complexes au fur et à mesure que nos connaissances biologiques augmentaient.

8.3.2   Approche utilisée

Nous avons utilisé pour ce travail une approche mécaniste basée sur un système d'EDOs qui est particulièrement intéressante pour sa partie statistique. Depuis l'année 2007, l'équipe utilise une approche basée sur trois points principaux : le modèle mathématique, le modèle dit "statistique" ou de variabilité des paramètres et le modèle des observations, qui vont être décrits. Une approximation fréquentiste du maximum de vraisemblance basée sur une adaptation des méthodes de type Newton fut proposée en 2007. La présence dans nos modèles d'effets aléatoires et la possible non-linéarité du système d'équations complexifient cette méthode. Les effets aléatoires obligent à l'utilisation d'une approche hiérarchique, où les vraisemblances individuelles vont être calculées conditionnellement aux effets aléatoires. Après, une intégration pourra être faite sur ces effets aléatoires. Cette approche a été ultérieurement adaptée pour le calcul d'une approximation normale de la distribution *a posteriori* (justifiée par le théorème de Bernstein-von Mises). Une approximation de la matrice hessienne est utilisée, et l'approximation normale *a posteriori* peut être calculée en maximisant la vraisemblance pénalisée. Cet approche semi-bayésienne nous permet de pouvoir prendre en compte certaines informations connues *a priori* sur la valeur de nos paramètres.

   Le critère qui a été utilisé pour comparer les vraisemblances pénalisées a été LCVa (une extension du critère d'Akaike qui permet de corriger pour le nombre de paramètres et la pénalisation). Toute cette approche a été implémentée dans le programme NIMROD. La procédure d'optimisation est basée sur l'algorithme RVS (*Robust Variance Scoring*). Une fois que les scores individuels ont été calculés grâce à l'aide de la formule de Louis, la vraisemblance observée et les scores sont calculés comme la somme sur tous les individus. Finalement, ces scores seront utilisés pour approximer la matrice hessienne. Cependant, NIMROD est implémenté avec une option de passage à un algorithme classique de Levenberg-Marquardt lorsque l'algorithme est bloqué. Cet algorithme est robuste loin du maximum, lorsque la vraisemblance pénalisée n'est pas très proche d'une forme quadratique. NIMROD a trois critères d'arrêt : deux classiques (un seuil pour le déplacement dans l'espace des paramètres et un seuil pour la variation de la vraisemblance) plus un critère nommé RDM (*Relative Distance to Maximum*). Ce critère peut être interprété comme un rapport entre l'erreur numérique et l'erreur statistique. Une fois que l'algorithme a convergé, les trajectoires individuelles peuvent être calculées grâce aux estimateurs *Parameteric Empirical Bayes (PEB)*.

8.3.3 Modèle original

Ce travail de thèse est basé sur un modèle déjà existant (Thiébaut et al., 2014), qui a été appliqué à des patients qui ont reçu un premier cycle de r-hIL-7. Ce modèle comprend deux populations de lymphocytes CD4$^+$: quiescentes (Q) et prolifératifs (P). Les cellules Q sont produites à un taux λ, elles deviennent des cellules P à un taux π et vont mourir à un taux μ_Q. Les cellules P vont diviser et produire deux cellules Q à un taux ρ et elles vont mourir à un taux μ_P. Le système mathématique peut être écrit ainsi:

$$\begin{cases} \frac{dQ}{dt} = \lambda + 2\rho P - \mu_Q Q - \pi Q \\ \frac{dP}{dt} = \pi Q - \rho P - \mu_P P \end{cases}$$

Avec $\xi^i = (\lambda^i, \rho^i, \pi^i, \mu_Q^i, \mu_P^i)$ le vecteur des paramètres biologiques pour l'individu i. Une transformation logarithmique est appliquée sur ces paramètres biologiques pour assurer la positivité : $\tilde{\xi}^i = \log(\xi^i)$. Un modèle à effets aléatoires est appliqué sur les paramètres biologiques pour permettre une certaine variabilité interindividuelle. Il a été considéré que les injections de r-hIL-7 ont un effet sur la prolifération pendant 16 jours après la première injection (chiffre trouvé par profil de vraisemblance). Cet effet va dépendre du fait d'avoir reçu le traitement ($\mathbb{1}_{trt}$), et aussi de la quantité de dose reçue (d).

$$\begin{cases} \tilde{\pi} = \tilde{\pi}_0 + \beta_1 \mathbb{1}_{trt} + \beta_2 d & d \leq 16 \\ \tilde{\pi} = \tilde{\pi}_0 & t > 16 \end{cases}$$

De la même façon, des effets supplémentaires peuvent être considérés sur le taux de mortalité des cellules Q (dans ce cas-là l'effet est considéré après 16 jours jusqu'au moins la fin du suivi) ou sur le taux de production :

$$\begin{cases} \tilde{\mu}_Q = \tilde{\mu}_{Q_0} + \beta_3 \mathbb{1}_{trt} + \beta_4 d & t > 16 \\ \tilde{\mu}_Q = \tilde{\mu}_{Q_0} & t \leq 16 \end{cases}$$

$$\begin{cases} \tilde{\lambda} = \tilde{\lambda}_0 + \beta_5 \mathbb{1}_{trt} + \beta_6 d & t \leq 16 \\ \tilde{\lambda} = \tilde{\lambda}_0 & t > 16 \end{cases}$$

Deux effets aléatoires ont été considérés sur λ et ρ :

$$\begin{cases} \tilde{\lambda}^i = \tilde{\lambda} + b_\lambda^i \\ \tilde{\rho}^i = \tilde{\rho} + b_\rho^i \end{cases}$$

Avec b_λ et b_ρ étant des effets aléatoires Gaussiens, indépendants, de moyenne zéro et variance σ_λ et σ_ρ respectivement.

Le modèle des observations est basé sur plusieurs observations du nombre de cellules CD4$^+$ aux temps discrets t_{j1} et le nombre de cellules CD4$^+$Ki67$^+$ aux temps discrets t_{k2}. Les mesures « réelles » seront considérées comme la somme des mesures « observées » plus une erreur de mesure ϵ (Gaussiens, indépendants, de moyenne zéro et variance σ_{CD4} et σ_P) :

$$\begin{cases} Y_{j1}^i = \sqrt[4]{(P+Q)(t_{j1}^i, \tilde{\xi}^i)} + \epsilon_{j1}^i \\ Y_{k2}^i = \sqrt[4]{P(t_{k2}^i, \tilde{\xi}^i)} + \epsilon_{k2}^i \end{cases}$$

Le résultat obtenue par Thiébaut et al. (2014) est que l'effet sur la prolifération cellulaire est très important, mais il n'est pas suffisant pour expliquer la variation dans le nombre de cellules CD4$^+$. Le modèle est amélioré d'un point de vue statistique lorsqu'on rajoute un effet sur μ_Q ou sur λ. Par contre, les prédictios des deux modèles ne peuvent pas être distingués à l'œil, et aucun modèle n'arrive à bien modéliser le comportement des cellules P.

8.3.4 Notre modèle de base

Nous avons construit notre modèle de base en partant du modèle expliqué précédemment. Le modèle mathématique est le même, et le modèle statistique change légèrement. Au lieu de considérer l'effet des injections de r-hIL-7 comme dépendant de deux variables : le fait d'être traité et la quantité de dose reçue, on a juste considéré un effet dépendant de la dose reçue à une certaine puissance.

$$\begin{cases} \tilde{\pi} = \tilde{\pi}_0 + \beta_\pi d^{\eta_1} & d \le 16 \\ \tilde{\pi} = \tilde{\pi}_0 & t > 16 \end{cases}$$

et

$$\begin{cases} \tilde{\mu}_Q = \tilde{\mu}_{Q_0} + \beta_{\mu_Q} d^{\eta_2} & t > 16 \\ \tilde{\mu}_Q = \tilde{\mu}_{Q_0} & t \le 16 \end{cases}$$

Les valeurs des exposants ont été trouvées par profil de vraisemblance comme $\eta_1 = \eta_2 = 0{,}25$. Quand on applique ce modèle aux données d'INSPIRE 1 (N=27 patients qui ont reçu un cycle de r-hIL-7 selon les doses 10, 20 ou 30 μg/kg), nous avons trouvé les moyennes du vecteur des paramètres (λ,ρ,π,μ_Q,μ_P,β_π,β_{μ_Q}, σ_λ,σ_{rho},σ_{CD4},σ_P) = (7,700, 1,289, 0,029, 0,055, 0,070, 1,233, -0,178, 0,213, 0,387, 0,205, 0,228). La valeur de la vraisemblance pénalisé est de -1,269 et le LCVa = -0,033. Les courbes obtenues avec ce modèle peuvent être trouvées en rouge dans la Figure 5.1. Elles ont été comparées avec les courbes obtenues lorsqu'on considère un seul effet sur le taux de prolifération. Nous avons cherché à améliorer les prédictios des cellules P en introduisant un terme de rétroaction (*feedback*). Ce terme sera appliqué sur le taux de prolifération, pour empêcher le nombre de cellules d'augmenter au-delà de ce qui est raisonnable. Plusieurs termes ont été considérés, comme $\left[\frac{1}{P+Q}\right]^\nu$, $\left[e^{-(P+Q)}\right]^\nu$, $e^{\epsilon(P+Q)}$. Aucune de ces modifications ne nous a pas permis d'obtenir d'améliorations majeures. Les résultats les plus convaincants d'un point de vue statistique ont été trouvés avec le premier terme pour le feedback. Le modèle peut être écrit comme :

$$\begin{cases} \frac{dQ}{dt} = \lambda + 2\rho P - \mu_Q Q - \pi Q \left[\frac{1}{P+Q}\right]^\nu \\ \frac{dP}{dt} = \pi Q \left[\frac{1}{P+Q}\right]^\nu - \rho P - \mu_P P \end{cases}$$

L'exposant ν étant significatif, il a été estimé à environ 0,26. Malheureusement, ce modèle a le même comportement que le modèle sans feedback (et les mêmes prédictios), et il demande un temps de calcul beaucoup plus important. Nous reviendrons sur ce modèle mais d'abord nous étudierons quelques modifications sur le modèle de base, ayant comme premier objectif l'amélioration des prédictios des cellules P.

8.3.5 Modèle pharmacocinétique

Nous avons quelques observations de la concentration de la r-hIL-7 au moment de la première injection, ainsi que 2h, 4h, 6h, 24h et 96h après. Nous avons utilisé ces informations pour travailler avec un modèle pharmacocinétique existent dans l'équipe pour décrire l'absorption, la distribution et l'élimination de la r-hIL-7. Nous distinguons trois compartiments : le compartiment local (C_L), le compartiment plasmatique (C_P) et le compartiment tissulaire (C_T). Si nous appelons k_a le taux d'assimilation, cl le taux d'élimination, V_P et V_t le volume de distribution dans le compartiments plasmatique et tissulaire, et k_{pt} et k_{tp} les taux d'absorption du plasma au tissue et du tissue au plasma, respectivement, le modèle peut être écrit :

$$\begin{cases} \frac{dC_L}{dt} = -k_a C_L & C_L(0) = \text{dose}_0 \\\\ \frac{dC_P}{dt} = \frac{k_a C_L}{V_0} + \frac{k_{tp} V_T C_T}{V_0} - k_{pt} C_P - \text{cl} C_P & C_P(0) = 0 \\\\ \frac{dC_T}{dt} = \frac{k_{pt} V_0 C_P}{V_T} - k_{tp} C_T & C_T(0) = 0 \end{cases}$$

Les paramètres ont été estimés à (ka, cl, V_0, V_t, $k_{tp} = k_{pt}$) = (-2,67, -1,01, -2,55, -3,10, -4,22), avec la contrainte $k_{tp} = k_{pt}$ à cause de problèmes d'identifiabilité. Ce modèle pharmacocinétique va nous servir de base pour un modèle pharmaco-dynamique, où nous pourrons nous baser sur la concentration à tous les temps au lieu de la dose reçue, ce qui va nous permettre d'avoir un modèle d'une apparence plus "continue". Quelques hypothèses ont été faites pour implémenter ce modèle pharmacodynamique. Par exemple, la dose reçue a été considérée comme étant indépendant du poids, la concentration utilisée a été la concentration tissulaire à la puissance 0,40 (trouvé par profil de vraisemblance. Aussi, nous avons décidé de ne pas inclure des effets aléatoires, dans le but d'obtenir courbes moyennes qui seront proportionnelles à la dose reçue. Cela nous permet aussi d'économiser un temps de calcul considérable. Le modèle statistique pour l'effet de la r-hIL-7 sur la prolifération peut alors s'écrire :

$$\tilde{\pi} = \tilde{\pi}_0 + \beta \pi C_T^{0,40}$$

Contrairement à ce que pouvait être attendu, tous les résultats avec la concentration étaient moins satisfaisants que le résultat du modèle avec la dose. Néanmoins, nous avons fait un dernier essai en considérant une fonction sigmoïde comme fonction pharmacodynamique, sans succès.

8.3.6 Modèle à 4 compartiments

Lors de l'étape suivante nous avons utilisé un nouveau modèle mathématique: le modèle à 4 compartiments. Ce modèle comprend quatre sous-populations lymphocytaires, les cellules naives non prolifératives (Q), les naives prolifératives (P), les mémoires non-prolifératives (Q') et les mémoires prolifératives (P'). Ce modèle va nous permettre de prendre en compte les différences existantes parmi ces populations, comme la différence dans la prolifération. Les cellules naives et mémoires vont être distinguées par les marqueurs CD45RA$^+$ (naives) ou

CD45RO$^+$ (mémoire). Le modèle mathématique peut être écrit comme :

$$\begin{cases} \frac{dQ}{dt} = & \lambda + 2\rho P - \mu_Q Q - \pi Q \\[2mm] \frac{dP}{dt} = & \pi Q - \rho P - \mu_P P - \tau P \\[2mm] \frac{dQ'}{dt} = & 2\rho' P' - \mu'_Q Q' - \pi' Q' \\[2mm] \frac{dP'}{dt} = & \pi' Q' - \rho' P' - \mu'_P P' + \tau P \end{cases}$$

Ou avec une petite modification, comme :

$$\begin{cases} \frac{dQ}{dt} = & \lambda + 2\rho P - \mu_Q Q - \pi Q \\[2mm] \frac{dP}{dt} = & \pi Q - \rho P - \mu_P P - \tau P \\[2mm] \frac{dQ'}{dt} = & 2\rho' P' - \mu'_Q Q' - \pi' Q' + \tau P \\[2mm] \frac{dP'}{dt} = & \pi' Q' - \rho' P' - \mu'_P P' \end{cases}$$

Le modèle des observations peut être écrit:

$$\begin{cases} Y^i_{j1} = \sqrt[4]{(P + P' + Q + Q')(t^i_{j1}, \tilde{\xi}^i)} + \epsilon^i_{j1} \\[2mm] Y^i_{k2} = \sqrt[4]{P + P'(t^i_{k2}, \tilde{\xi}^i)} + \epsilon^i_{k2} \\[2mm] Y^i_{k3} = \sqrt[4]{P + Q(t^i_{k3}, \tilde{\xi}^i)} + \epsilon^i_{k3} \\[2mm] Y^i_{k4} = \sqrt[4]{P(t^i_{k4}, \tilde{\xi}^i)} + \epsilon^i_{k4} \end{cases}$$

Différents modèles statistiques ont été appliqués, comme un effet de la r-hIL-7 sur le taux de prolifération des cellules naives et/ou mémoires, des effets additionnels sur les taux de mortalité ou de production. Nous avons toujours gardé la même structure : un effet de la dose à travers la racine quatrième. Malgré les nombreuses tentatives, les résultats obtenus étaient moins prometteurs que ceux obtenus avec le modèle à deux compartiments.

8.3.7 Modèle à 3 β's

Maintenant nous allons étudier le meilleur modèle obtenu avec les données d'un seul cycle: le modèle à 3 β's . Nous sommes donc retournés au modèle de base, avec un changement majeur dans le modèle statistique. On va permettre aux différentes injections d'avoir des effets quantitativement différents sur le taux de prolifération. Si on considère que chaque injection a un effet indépendant (pendant 7 jours) le modèle statistique peut s'écrire comme :

$$\begin{cases} \tilde{\pi} = \tilde{\pi}_0 + \beta_1 d^{0.25} & t \in \ ]0, 7] \\ \tilde{\pi} = \tilde{\pi}_0 + \beta_2 d^{0.25} & t \in \ ]7, 14] \\ \tilde{\pi} = \tilde{\pi}_0 + \beta_3 d^{0.25} & t \in \ ]14, 21] \end{cases}$$

Avec ce modèle, on a pu observer une amélioration très importante au niveau des prédictios des cellules P, comme nous pouvons le vérifier dans la Figure 5.8. L'enjeu est alors d'essayer d'intégrer cet échelonnement des effets des injections dans le modèle mathématique.

8.3.8 Modèle à 3 compartiments

Nous avons considéré un troisième compartiment, dans l'occurrence nommé Q*, où les cellules non-prolifératives pourront rester dans un premier temps lorsqu'elles seront prêtes à proliférer. Si on appelle τ au taux de passage de Q à Q*, le modèle peut s'écrire :

$$\begin{cases} \frac{dQ}{dt} = & \lambda + 2\rho P - \mu_Q Q - \tau Q \\\\ \frac{dQ^*}{dt} = & \tau Q - \mu_Q Q^* - \pi Q^* \\\\ \frac{dP}{dt} = & \pi Q^* - \rho P - \mu_P P \end{cases}$$

Avec le même modèle statistique que pour le modèle à deux compartiments, et un modèle des observations qui peut s'exprimer :

$$\begin{cases} Y_{j1}^i = \sqrt[4]{(P + Q + Q*)(t_{j1}^i, \tilde{\xi}^i)} + \epsilon_{j1}^i \\\\ Y_{k2}^i = \sqrt[4]{P(t_{k2}^i, \tilde{\xi}^i)} + \epsilon_{k2}^i \end{cases}$$

Quelques modifications mineures ont été faites sur ce modèle, comme le fait d'introduire un compartiment thymique pour pouvoir représenter la génération de cellules immatures (qui vont s'incorporer plus lentement au système). Aussi, nous avons créé un nouveau compartiment pour mettre en évidence le fait qu'il pourrait avoir des cellules qui venaient juste de proliférer, mais qui n'avaient pas encore perdu leur marqueur Ki67. Ces modèles ont été explorés avec et sans feedback, avec différentes possibilités pour le modèle statistique, sans jamais obtenir les résultats du modèle "à 3 β's".

8.3.9 Modélisation des données d'INSPIRE 2 et 3

Modélisation des premiers cycles

Le modèle "à 3 β's" a été ensuite appliqué à l'ensemble des données provenant des premiers cycles de l'ensemble des patients provenants des études INSPIRE (1), INSPIRE 2 et INSPIRE 3, avec une légère modification. Pendant ces deux études, les patients ont été suivis pendant longtemps (environ 2 ans) et l'idée de considérer l'effet de la r-hIL-7 sur la mortalité des cellules Q comme étant permanent est plus difficilement justifiée. Cela nous a décidé à étudier un effet sur μ_Q en deux étapes : un effet constant pendant une année après un cycle avec une décroissance linéaire pendant la deuxième année, si un nouveau cycle n'a pas été reçu, comme :

$$f(t) = \begin{cases} 1 & if \quad 2 < t \le 360 \\ 1 - (t - 360)/360 & if \quad 360 < t \le 720 \qquad \text{(t en jours)} \\ 0 & if \quad 720 < t \end{cases}$$

Lorsqu'on a appliqué ce modèle à l'ensemble des données d'INSPIRE 1, INSPIRE 2 et INSPIRE 3, les valeurs obtenues des paramètres ont été (λ, ρ, π, μ_Q, μ_P, $\boldsymbol{\beta_{\pi_1}}$, $\boldsymbol{\beta_{\pi_2}}$, $\boldsymbol{\beta_{\pi_3}}$, β_{μ_Q}, σ_λ, σ_{rho}, σ_{CD4}, σ_P) = (10,541; 1,887; 0,037; 0,073; 0,112; **1,155**; **1,120**; **0,622**; -0,239; 0,267; 0,575; 0,241; 0,305). La valeur de la vraisemblance pénalisée était égale à -279,8 et le LCVa égal à 2,136.

Effet cycle

Le dernier grand résultat est l'introduction d'un "effet cycle" dans le modèle statistique. Nous allons inclure les données de tous les patients et tous les cycles (initiaux et répétés). Lorsqu'on veut permettre aux cycles répétés d'avoir un effet légèrement différent que les cycles initiaux, un nouveaux paramètre dois s'ajouter au modèle statistique: que nous allons appeler β_C. Si N_t^i est le nombre d'injections reçues par le patient i au temps t, et $C(t)$ le nombre de cycles reçus par le patient i au temps t, le modèle peut s'écrire comme :

$$\tilde{\pi}^i(\mathrm{t}) = \tilde{\pi}_0 + \left[\beta_C \mathbb{1}_{\{C(t)>1\}} + \sum_{k=1}^{3} \mathbb{1}_{\{N_t^i=k\}} \; \beta_{\pi_k} \; d_i^{0.25}\right] \mathbb{1}_{\{N_t^i - N_{t-7}^i = 1\}}$$

Avec ce modèle, l'effet cycle est significatif (moyenne -0,163, écart type 0,015). Dans l'échelle naturelle, cela revient à dire qu'un cycle répété a un effet de 0,85 fois l'effet d'un cycle initial. Pourtant, lors de l'analyse statistique des données d'INSPIRE 2 et INSPIRE 3 nous n'avions trouvé aucune différence. Pour analyser si ceci peut être due à un mécanisme d'autorégulation (du fait que le nombre de cellules CD4$^+$ avant un cycle répété et normalement bien plus élevé qu'avant un cycle initial) nous avons réintroduit l'effet *feedback* dans le modèle mathématique. Nous avons estimé le coefficient *feedback* par profil de vraisemblance et nous avons trouvé $\nu = 0,1$. Malgré l'amélioration de la vraisemblance pénalisée (de 20 points) et le LCVa (de 0,2 points), cet effet *feedback* n'a pas neutralisé l'effet cycle. Une autre explication pourrait être la présence d'anticorps après un premier cycle, qui va faire que la réponse aux cycles suivants sera un peu moins faible. Ce sont des suppositions qui pourraient faire l'objet de recherches dans le futur.

Protocoles d'administration

Pour en finir avec la modélisation des cycles répétés, nous avons comparé différents protocoles possibles d'administration des injections de r-hIL-7. Les protocoles suivants ont été comparés pendant 4 ans: Protocole A (tous les cycles complets), Protocole B (un premier cycle complet, suivi de cycles de deux injections), Protocole C (un premier cycle complet, suivi de cycles d'une seule injection) et Protocole D (tous les cycles de deux injections). Nous avons comparés ces protocoles en termes de nombre de cycles et d'injections reçus, temps passé au-dessous de 550 CD4$^+$ et nombre moyen de cellules CD4$^+$ pendant les 4 ans. Nous avons trouvé que, pour un patient moyen (ayant les effets aléatoires égaux à zéro) le Protocol B peut offrir un nombre moyen de CD4$^+$ et un temps passé au-dessus de 550 cellules/μL très similaire au Protocol A, avec 15 injections au lieu de 21. Les prédictions peuvent être trouvés dans la Figure 6.3. Nous avons également comparé ces 4 scénarios pour deux patients réels d'INSPIRE 2 et INSPIRE 3, ayant eu une réponse particulièrement bonne et mauvaise aux injections de r-hIL-7. Dans les deux cas le Protocol B (un premier cycle complet suivi de cycles composés de deux injections) semble être suffisant pour maintenir un niveau acceptable de CD4$^+$ la plupart du temps (Figures 6.4 et 6.5).

8.4 L'épidémiologie du VIH à Pamplona

Pour conclure, j'ai eu l'opportunité de faire un stage de 3 mois à l'*Universidad Pública de Navarra* (Espagne) dans le cadre du projet Mérimée (qui cherche à favoriser la coopération parmi les écoles doctorales françaises et espagnoles). Le projet prévoyait une actualisation d'une étude populationnelle basée sur la pandémie de VIH et SIDA à Navarra. Actuellement, 640.000 personnes habitent dans cette région, dont la pyramide démographique corresponde à une population âgée (Figure F.1). Le diagnostic et le traitement de l'infection par VIH a lieu dans un petit nombre d'hôpitaux, ce qui permet d'avoir un registre très précis des infections depuis que le premier cas fut signalé en 1985. Depuis ce jour, 1861 personnes ont été diagnostiquées de VIH.

Nous avons premièrement actualisé une analyse descriptive de l'épidémiologie du VIH et du SIDA. Dans la Table F.1 nous pouvons trouver la distribution des nouvelles infections dans le temps. Dans les Figures F.2 et F.3 la distribution de l'âge au moment du diagnostic est présenté séparément pour les hommes et les femmes. Concernant la nationalité, les étrangers (les personnes nées en dehors de l'Espagne) représentent environ le 35% des infections. En termes de retard dans le diagnostic, l'âge semble avoir un effet significatif (les tranches d'âge les plus élevées présentent un risque plus important de retard dans le diagnostic). Aussi, pendant les années 1994-1997 (quand la voie sexuelle s'est imposé comme la principale voie de transmission) le pourcentage de diagnostiques tardifs est plus important que pendant les années 1990-1993. La voie de transmission semble aussi avoir une influence (moins de retard dans le diagnostic parmi les consommateurs de drogues injectables). Ceci est possiblement dû au fait que presque toutes ces infections ont été diagnostiquées au début de la pandémie, quand une grande sensibilisation est apparue parmi les personnes ayant des comportements à risque. Lorsque le retard dans le diagnostic est défini comme un nombre de cellules $CD4^+$ inférieur à 200 cellules/μL ou inférieur à 350 cellules/μL au moment du diagnostic, il n'y a pas de différences majeures (Table F.3). Une étude de survie a aussi été réalisée pour le temps libre de SIDA (temps passé entre le diagnostic de VIH et le diagnostic de SIDA). La courbe de Kaplan-Meier en fonction de l'âge peut être trouvée dans la Figure F.5. Les courbes sont significativement différentes lorsqu'on divise les patients selon leur nombre de $CD4^+$ au moment du diagnostic. Des modèles paramétriques ont aussi été appliqués, comme le modèle de Weibull, dont les résultats peuvent être trouvés dans la Table F.6. Nous avons finalement utilisé un logiciel nommé *Spectrum* pour estimer le nombre de personnes qui vivent avec le VIH à Navarra et qui ne sont pas diagnostiquées. Ce logiciel a été développé par ONUSIDA, et il permet de faire ce type d'estimations à partir des données qui sont envoyées périodiquement par les différents états. Nous avons utilisé ce logiciel pour calculer le nombre de personnes infectées sans diagnostiquer en Espagne, et ce chiffre a été adapté proportionnellement à la population de Navarra. Il a était obtenu que 2045 personnes pourrait être infectées de VIH (le double de ceux qui sont diagnostiqués actuellement). Ce résultat doit être mis en perspective car d'autres informations sont nécessaires pour établir plus précisément le chiffre d'infections, comme la taille et la prévalence parmi les populations à risque.

Appendix A

Appendix A: Computing NIMROD calculation time

In order to try to minimize, as much as possible, the level of computational complexity in NIMROD, we did several tests for comparing the calculation time for the "basic model".

We are placed on the original mathematical model:

$$\begin{cases} \frac{dQ}{dt} = \lambda + 2\rho P - \mu_Q Q - \pi Q \\[2mm] \frac{dP}{dt} = \pi Q - \rho P - \mu_P P \end{cases}$$

considering only a r-hIL-7 effect on proliferation rate π through the fourth rate of the dose:

$$\begin{cases} \tilde{\pi} = \tilde{\pi}_0 + \beta_\pi d^{0.25} & t \leq 16 \\ \tilde{\pi} = \tilde{\pi}_0 & t > 16 \end{cases}$$

and a single random effect on lambda:

$$\tilde{\lambda} = \tilde{\lambda}_0 + b_\lambda, \quad b_\lambda \sim \mathcal{N}(0, \sigma_\lambda)$$

We will use the GNU profiler, *gprof*, to study which parts of the program are taking most of the execution time, and how we can to intervene with the aim of reducing the calculation time.

Importance of the number of patients

We compare changes in computation time through two iterations (time expressed in seconds) when comparing the same model for a different number of patients. A clear correlation was established between the number of patients and the calculation time, that after our tests, could grow slightly faster than a linear form. In NIMROD, values for the global variable ABSERR can be provided (this variable is used in the subroutine *optimization.f90* while it is defined in *module.f90*). ABSERR is supposed to give us the absolute error we are willing to accept when computing the derivatives. Value by default is equal to $\frac{1}{N_p}$ with N_p is the number of patients. We tested results when the value of ABSERR was fixed (for instance at ABSERR $= \frac{1}{30}$) and when it was depending

to the number of patients, without founding significant changes (see Table A.1 for a comparison for 6, 12 and 100 patients).

Table A.1: Computational time (expressed in seconds) for two iterations of the "basic model" when changing the number of patients

	6 patients	12 patients	100 patients
ABSERR $= \frac{1}{N_p}$	28.8	90.4	814.7
ABSERR $= \frac{1}{30}$	28.8	90.9	815.0

Analytic vs numerical solution

Sometimes, we are able to compute analytic solutions for the ODE system so-called "mathematical model". This is particularly true when we deal with a linear system, as the "basic model". In that case, we interrogated us about the convenience of looking for and facilitating the analytic solution, instead of let NIMROD to search a numerical solution. We compared the time taking for computing trajectories of 6, 12 and 100 patients if the analytic solution is delivery directly by the user and if it must be computed numerically (see Table A.2).

Table A.2: Computational time (expressed in seconds) for computing trajectories of 6, 12 and 100 patients when the analytic solution is delivery and when it must be computed numerically

	6 patients	12 patients	100 patients
Analytic solution	0.034	0.069	0.603
Numerical solution	0.045	0.099	0.886

As expected, the analytic solution should be provided in order to minimize the calculation time as much as possible (because computing trajectories can be done thousands of times within every launched model); even if differences are not as important as it may seem.

Appendix B

Appendix B: Equilibrium points

We have wondered about the stability of the equilibrium points of this EDO system. An equilibrium point of a dynamical system generated by a system of ordinary differential equations is a solution that does not change with time.

In this case, equilibrium points have been obtained (with Maple) as being:

$$Q_0 = \frac{(\rho + \mu_P) * \lambda}{\pi * (\mu_P - \rho) + \mu_Q * (\rho + \mu_P)}$$

$$P_0 = \frac{\pi * \lambda}{\pi * (\mu_P - \rho) + \mu_Q * (\rho + \mu_P)}$$

Equilibrium points can be stable or unstable.

Classification of the equilibrium points depending on parameter's value

$$\begin{pmatrix} \frac{dQ}{dt} \\ \frac{dP}{dt} \end{pmatrix} = \begin{pmatrix} -\mu_Q - \pi & 2\rho \\ \pi & -\rho - \mu_P \end{pmatrix} \begin{pmatrix} Q \\ P \end{pmatrix} + \begin{pmatrix} \lambda \\ 0 \end{pmatrix} \tag{B.1}$$

$$\text{So } A = \begin{pmatrix} -\mu_Q - \pi & 2\rho \\ \pi & -\rho - \mu_P \end{pmatrix} \tag{B.2}$$

If real parts of all eigenvalues are negative, then the equilibrium is asymptotically stable.

$$*|A - \eta I| = \begin{vmatrix} -\mu_Q - \pi - \eta & 2\rho \\ \pi & -\rho - \mu_P - \eta \end{vmatrix} = (-\mu_Q - \pi - \eta)(-\rho - \mu_P - \eta) - 2\rho\pi =$$

$$\eta = \frac{-\mu_Q - \pi - \rho - \mu_P \pm \sqrt{(\mu_Q + \pi + \rho + \mu_P)^2 - 4[\rho\mu_Q + \mu_Q\mu_P + \pi\mu_P - \rho\pi]}}{2}$$
$$\tag{B.3}$$

So, condition for asymptotic stability:

$$\rho\mu_Q + \mu_Q\mu_P + \pi\mu_P - \rho\pi > 0 \longrightarrow \rho\mu_Q + \mu_Q\mu_P + \pi\mu_P > \rho\pi \tag{B.4}$$

As a result, this division of the parameters space produces two complementary regions: a region R_S where equilibrium points are asymptotically stable, and a region R_{NS} where equilibrium points are non-stable.

- R_S $\rho\mu_Q + \mu_Q\mu_P + \pi\mu_P > \rho\pi$

- R_{NS} $\rho\mu_Q + \mu_Q\mu_P + \pi\mu_P < \rho\pi$

For parameter's value in R_{ns}, we are going to obtain P < 0, Q < 0. However, this R_{ns} region is not a problem for us because usual values we take for priors and obtained estimations of parameters always belong to R_S.

Equilibrium for the four compartments model

As for the four compartment models (described in 5.4), there is one only equilibrium point if we adjust for the regular values of the parameters:

$$
\begin{cases}
Q = \dfrac{\lambda(\rho+\tau+\mu_P)}{-\rho\pi+\rho\mu_Q+\mu_P\pi+\mu_P\mu_Q+\tau\pi+\tau\mu_Q} \\[3mm]
P = \dfrac{\lambda\pi}{-\rho\pi+\rho\mu_Q+\mu_P\pi+\mu_P\mu_Q+\tau\pi+\tau\mu_Q} \\[3mm]
Q' = \dfrac{N_{Q'}}{D_{Q'}} \\[3mm]
P' = \dfrac{N_{P'}}{D_{P'}}
\end{cases}
$$

where

$N_{Q'} = 2\pi\rho'\tau\lambda$

$N_{P'} = (\pi' + \mu'_Q)\pi\tau\lambda$

$D_{Q'} = (\mu_P\pi\rho'\mu'_Q+\mu_P\pi\mu'_P\pi'+\mu_P\pi\mu'_P\mu'_Q+\mu_P\mu_Q\rho'\mu'_Q+\tau\pi\rho'\mu'_Q+\mu_P\mu_Q\mu'_P\pi'-\mu_P\mu_Q\rho'\pi'-\tau\pi_N\rho'\pi'+\tau\mu_Q\rho'\mu'_Q+\tau\pi\mu'_P\pi'+\mu_P\mu_Q\mu'_P\mu'_Q-\tau\mu_Q\ \rho'\pi'-\mu_P\pi\rho'\pi'+\tau\mu_Q\mu'_P\pi'+\tau\mu_Q\mu'_P\mu'_Q-\rho\pi\rho'\mu'_Q-\rho\pi\mu'_P\mu'_Q-\rho\mu'_Q\rho'\pi'-\rho\pi\mu'_P\pi'\rho\mu_Q\mu'_P\pi'+\rho\mu_Q\mu'_P\mu'_Q+\rho\pi\rho'\pi'+\rho\mu_Q\rho'\mu'_Q+\tau\pi\mu'_P\mu'_Q)$

$D_{P'} = (\mu_P\pi\rho'\mu'_Q+\mu_P\pi\mu'_P\pi'+\mu_P\pi\mu'_P\mu'_Q+\mu_P\mu_Q\rho'\mu'_Q+\tau\pi\rho'\mu'_Q+\mu_P\mu_Q\mu'_P\pi'-\mu_P\mu_Q\rho'\pi'-\tau\pi\rho'\pi'+\tau\mu_Q\rho'\mu'_Q+\tau\pi\mu'_P\pi'+\mu_P\mu_Q\mu'_P\mu'_Q-\tau\mu_Q\ \rho'\pi'-\mu_P\pi\rho'\pi'+\tau\mu_Q\mu'_P\pi'+\tau\mu_Q\mu'_P\mu'_Q-\rho\pi\rho'\mu'_Q-\rho\pi\mu'_P\mu'_Q-\rho\mu_Q\rho'\pi'-\rho\pi\mu'_P\pi'+\rho\mu_Q\mu'_P\pi'+\rho\mu_Q\mu'_P\mu'_Q+\rho\pi\rho'\pi'+\rho\mu_Q\rho'\mu'_Q+\tau\pi\mu'_P\mu'_Q)$

Appendix C

Appendix C: Coefficient of the reversion rate

Sometimes, when this "basic model" has been presented at scientific meetings, people have interrogated us about the coefficient of the reversion rate ρ in the mathematical model (here expressed in a general form N):

$$\begin{cases} \frac{dQ}{dt} = \lambda + \boldsymbol{N\rho}\,P - \mu_Q Q - \pi Q \\[2mm] \frac{dP}{dt} = \pi Q - \boldsymbol{\rho}\,P - \mu_P P \end{cases}$$

Even if the biological background maintains the idea that N=2 (we say that "every P cell divides and produces two Q cells"), we wanted to further explore this decision. The loss of P cells is conditioned by the reversion rate ρ and the mortality rate μ_P. We can put 3ρ, 4ρ or $n\rho$ and this will not have a real impact (only the value of μ_P will be modify to keep the behavior of the second equation). There is only one possibility that is not included in this analysis: the case where the coefficient is equals to one:

$$\begin{cases} \frac{dQ}{dt} = \lambda + \boldsymbol{\rho P} - \mu_Q Q - \pi Q \\[2mm] \frac{dP}{dt} = \pi Q - \rho P - \mu_P P \end{cases}$$

In this case there is not proliferation, and μ_P must be negative in order to reach the same likelihood as with the previous model. But a constraint is applied on biological parameters to prevent them from being negatives (the logarithmic transformation). While keeping this constraint, we found that log-likelihood and LCVa when N=1 are much worse (-177.5 and 5.74, respectively) than the original model with 2ρ (-1.27 and -0.03).

Appendix D

Appendix D: CID's paper

Repeated Cycles of Recombinant Human Interleukin 7 in HIV-Infected Patients with low CD4 T cell Reconstitution on Antiretroviral Therapy: Results of two Phase II Multicentre Studies.

Rodolphe Thiébaut, INSERM U897, INRIA SISTM, Bordeaux University, Bordeaux, France,

Ana Jarne, INSERM U897, INRIA SISTM, Bordeaux University, Bordeaux, France,

Jean-Pierre Routy, McGill University, Montreal, Quebec, Canada,

Irini Sereti, NIAID NIH, Bethesda, MD USA,

Margaret Fischl, School of Medicine, Miami, FL, USA,

Prudence Ive, Clinical HIV Research Unit, Johannesburg, South Africa,

Roberto F. Speck, Division of Infectious Diseases, University of Zurich, University Hospital of Zurich, Switzerland,

Gianpiero D'Offizi, Institute for Infectious Diseases Lazzaro Spallanzani, Rome, Italy,

Salvatore Casari, Infectious and Tropical Diseases Unit, Brescia, Italy,

Daniel Commenges, INSERM U897, INRIA SISTM, Bordeaux University, Bordeaux, France,

Sharne Foulkes, JOSHA Research, Bloemfontein, South Africa,

Ven Natarajan, Leidos Biomedical Research Inc, Frederick National Laboratory for Cancer Research, Frederick, MD 21702

Thérèse Croughs, INSERM/ANRS, Paris, France,

Jean-François Delfraissy, INSERM/ANRS, Paris, France,

Guiseppe Tambussi, San Raffaele Scientific Institute, Milano, Italy,

Yves Levy, Inserm, U955, Université Paris Est, Faculté de médecine, Créteil, Vaccine Research Institute (VRI), Créteil, AP-HP, Hôpital H. Mondor - A. Chenevier, Service d'immunologie clinique et maladies infectieuses, Créteil, France,

Michael M. Lederman, Case Western Reserve University, Cleveland, OH USA

Keywords: Interleukin-7, HIV, immune restoration, T cell recovery, CD4

Short title: R-hIL-7 repeated cycles in HIV infection

Corresponding authors:

Pr Rodolphe Thiébaut   INSERM U897, INRIA SISTM, Université Bordeaux

146 Rue Leo Saignat 33076 Bordeaux Cedex Tel: +33 5 57 57 45 21 Fax: +33 5 56 24 00 81

Email: rodolphe.thiebaut@u-bordeaux.fr

Pr Yves Levy, Service d'immunologie clinique, Hôpital Henri Mondor,

51 Av du Maréchal de Lattre de Tassigny, 94019 Créteil, France Email: yves.levy@hmn.aphp.fr

Summary: In this pooled analysis of two phase II trials, repeated cycles of Recombinant Human Interleukin-7 administration were safe and led to a sustained increase of CD4 T cell count in HIV individuals with low CD4 T cell reconstitution on antiretroviral therapy.

Abstract

Background: Phase I/II studies in HIV-infected patients receiving ART have shown that one cycle of 3 weekly subcutaneous (s/c) injections of Recombinant Human Interleukin 7 (r-hIL-7) is safe and improves immune CD4 T cell restoration. Herein, we report data from two phase II trials evaluating the effect of repeated cycles of r-hIL-7 (20 μg/kg) with the objective of restoring a sustained CD4 T cell count over 500 cells/μL.

Methods: INSPIRE 2 was a single arm trial conducted in the US and Canada. INSPIRE 3 was a two arm trial with 3:1 randomization to r-hIL-7 vs. control conducted in Europe and South Africa. Participants with plasma HIV-RNA<50 copies/mL while on ART and with CD4 T cell counts between 101-400 cells/μL were eligible. A repeat cycle was administered when CD4 T cells fell below 550 /μL.

Results: A total of 107 patients were treated and received one (n=107), two (n=74), three (n=14) or four (n=1) r-hIL-7 cycles over a median follow-up of 23 months. R-hIL-7 was well tolerated. Four grade 4 events were observed including one asymptomatic ALT elevation. After the second cycle, anti-r-hIL-7 binding antibodies developed in 82% and 77% (neutralizing in 38% and 37%) in INSPIRE 2 and 3, without impact on the CD4 T cell response. Half the patients spent more than 63% of their follow-up time with more than 500 CD4 T cells/μL.

Conclusion: Repeated cycles of r-hIL-7 were well tolerated and achieved sustained CD4 T cell restoration to over 500 cells/μL in the majority of study participants.

Introduction

Antiretroviral therapy (ART) has led to a profound improvement in morbidity and mortality in HIV infection [1–5]. In some patients suppressing plasma viremia below detection levels is not associated with a significant increase of CD4 T cell counts [6,7]. This failure of CD4 T cell restoration is associated with increased morbidity [2,4] and those who present late in disease course are less likely to normalize CD4 T cell counts over time. These patients may therefore benefit from strategies to rapidly enhance CD4 T cell recovery [8,9].

Early phase I/II trials evaluating the effect of Recombinant Human Interleukin 7 (r-hIL-7) have shown T cell count increases, reasonable tolerance, and no increase in T regulatory cells but occasional instances of transitory plasma viral load rebound ("blips") [10–12]. The administration of r-hIL-7 led to an increase in naïve and central memory CD4 T cells related to increased cell proliferation and possibly to an increased thymic output and/or cell survival [12,13]. In a substudy three months after the first injection an improvement in gut barrier integrity was observed as well as a decrease of inflammatory markers measured in the blood. [14]. As CD4 T cell counts exceeding 500/µL have been associated with better clinical outcomes [3], we thought to examine the effect of repeated cycles of r-hIL-7 therapy on reaching and sustaining CD4 T cell count above this threshold. A simulation based on the mathematical modelling of the response to the initial treatment cycle suggested that repeated r-hIL-7 cycles might be helpful for this purpose [13]. Here we report on the effect of repeated cycles of r-hIL-7 in two Phase II multicentre studies on maintaining CD4 T cell counts above 500 cells/µL.

Methods

Intervention: Recombinant Human IL-7

Recombinant Human Interleukin-7 (r-hIL-7, product code number CYT107 by the Cytheris company at the time of the trials) is a glycosylated 152 amino acid r-hIL-7 expressed in a Chinese hamster ovary (CHO) cell line. A first "induction" cycle of 3 weekly subcutaneous (SC) injections of r-hIL-7 20µg/kg was given on days 0, 7, 14. Subjects were eligible to receive new "maintenance" cycles of r-hIL-7 if the CD4 T cell counts fell below 550 cells/µL at quarterly monitoring.

Study Designs

The designs of the two studies are summarized in Figure 1 (A and B).

INSPIRE 2 (CLI-107-13) was a single arm clinical trial conducted in the USA (Case Western Reserve, NIH/intramural NIAID, University of Miami) and in Canada (McGill University Health Centre). The study was approved by the ethics committees of the participating institutions (University Hospitals/Case Medical Centre, NIAID, University of Miami and McGill Health Centre), and all subjects provided written informed consent at screening. The study was registered in clinicaltrials.gov, NCT01190111. Eligible participants had to be receiving ART for a minimum of one year with plasma HIV-RNA < 50 copies/mL and with CD4 T cell counts between 101-400 cells/µL. Patients received a cycle of 3 weekly subcutaneous injections of r-hIL-7 20µg/kg [12]. The study was amended 12 months after its initiation to repeat cycles of CYT107 administration to maintain CD4 T cell counts > 500 cells/µL.

INSPIRE 3 (CLI-107-14) was an open-label, controlled, randomized trial of r-hIL-7 treatment to restore and maintain CD4 T cell counts above 500 cells/µL. This trial was conducted in Italy (Milano, Brescia, Roma), Switzerland (Zurich) and South Africa (Johannesburg and Bloemfontein) and was approved by the ethics committees of the participating institutions; all subjects provided written informed consent at screening. The study was registered in EudraCT, #2010-019773-15 and clinicaltrials.gov, NCT01241643. Eligible participants had to be receiving ART for at least 2 years with plasma HIV-RNA < 50 copies/mL for at least 18 months and with CD4 T cell counts between 101-350 cells/µL.

While treated by ART, patients were randomized in two (2) arms "CYT107 Arm" and "Control Arm" with a ratio 3:1 (3 CYT107: 1 control). Patient randomized to the "CYT107 Arm" received induction treatment within 2 weeks and then were followed quarterly. r-hIL-7 was administered at the dose of 20 µg/kg for 3 weekly administrations. A new cycle of r-hIL-7 (3 weekly doses) was administered if at any quarterly evaluation the CD4 T cell count fell below 550 cells/µL. A maximum of four cycles was administered over 21 months and 3 over the first 12 months. Patients randomized to the "Control Arm" were followed without receiving study treatment for one year. If CD4 T cell counts were still below 500 cells/µL, an induction cycle of r-hIL-7 of 3 weekly doses was administered and then, repeated maintenance cycles of r-hIL-7 were given if quarterly evaluations showed CD4 counts below 550 cells/µL.

In both trials, patients with chronic hepatitis B or C or who were seropositive for HIV-2 or HTLV 1 or 2 were excluded.

End Points

Here we report the restoration and maintenance of CD4 T cell counts above 500 cells/μL in HIV-infected patients who had failed to recover adequate immunological status (based on CD4 T cells count) despite virological control. Routine safety assessments included measurement of plasma HIV RNA levels, proviral DNA in circulating PBMC and assays of anti-CYT107 antibodies. Occurrence of adverse events was monitored during each cycle of CYT107 as well as at each quarterly visit. Markers of coagulation and inflammation (D-Dimer, sCD14, 16sDNA) were also monitored in some subjects as reported elsewhere [14].

Circumstances of premature study termination

INSPIRE 3 was prematurely terminated as the Cytheris company was liquidated on June 18th 2013. All patients were however followed for at least 3 months after the last study drug administration as per protocol.

Immunogenicity analyses

Anti-CYT107 antibodies in heparinized plasma were measured by ELISA (MSD® technology) at d0, d28 and d35 of the first cycle, and d0 and d28 of later cycles. Measurement was also performed at 3 months, and repeated every three months if positive. Neutralizing antibodies against CYT107 were detected in heparinized plasma using a cell-based bioassay. Briefly, plasma samples and controls were prepared in 4% plasma and 2x concentration of IL-7, and incubated for 1 hour at 37°C in 5% CO_2 to allow neutralizing antibodies to bind the IL-7. Next, an equal volume suspension of a

murine IL-7 dependent B cell line (PB-1, 4 x.10^6 cells/mL) was added to each well. The plate was incubated 44-48 hours at 37°C, in 5% CO2. CellTiter 96® AQueous One Solution (-MTS, Promega) was added to all wells and the plate was incubated for approximately 4 hours at 37°C/5%CO2. Absorbance at 490nm was then read on a plate reader to measure cell proliferation.

HIV-DNA quantification

HIV1-DNA quantification was performed at d0, d28, d90 and at the end of study for INSPIRE 2 on whole blood samples using a quantitative real-time PCR method. DNA was extracted from whole blood samples and HIV load quantified by nested qPCR, using a technique allowing detection of 2 copy of HIV DNA per reaction [15].

Statistical methods

The analyses were performed with R Version 3.0.2 or later (2013 The R Foundation for Statistical Computing).

For studying the percentage of time spent with CD4 T cell count exceeding 500 CD4 T cells/µL, patients from INSPIRE 2 and the CYT107 arm of INSPIRE 3 with a follow-up of 21-24 months were included. The analysis was adjusted for baseline CD4 T cell count classified in two strata: [101-200] and (200-350]. To study the factors associated with a drop of CD4 T cell count below 550 cells/µL, only patients with CD4 T cell count > 550 cells/µL two weeks after the last injection were included. The time spent above 550 CD4 T cells/µL was imputed by linear interpolation when a measure below 550 cells/µL was observed; otherwise, the observation was right-censored (no drop observed until this date). A proportional hazard model was used for studying the effects of covariates

(initial CD4 count, age, gender). Since most patients had repeated cycles of injections, they could fall below 550 cells/μL several times; therefore, the correlation between times observed in the same patient had to be taken into account (precluding the use of an ordinary Cox model). For this purpose, a shared gamma frailty model was used. The R package Frailtypack allowed us to fit the hazard function using a parametric model (assuming a Weibull hazard function) [16].

Results

Study population

Eligibility for INSPIRE 2 and 3 is presented in Figure 2. Among the 111 patients included in the two trials (23 in INSPIRE 2 and 88 in INSPIRE 3), the median (IQR) CD4 T cell count at baseline was 263 (191; 320) in INSPIRE 2 and 266 (215; 326) cells/µL in INSPIRE 3. Patient characteristics are described in Table 1. During a follow-up of 23 (22; 24) and 22 (20; 23) months respectively, most patients started two treatment cycles but some cycles were incomplete with receipt of one or two injections rather than three (Figure 3). The median number of total injections received was 5 (3; 6). Treatments received by the 107 treated patients are summarized in Table 2.

CD4 T cell response

CD4 T cell and CD4 T cell subpopulation responses (supplementary Figure 1) were similar to published data in the 23 INSPIRE 2 patients [11,12,14]. Briefly, the CD4 cell increase was mainly among naïve and central memory cells following r-hIL-7 injections with a transient increase of Ki67+ (cycling) CD4 T cells and without any relative increase of markers associated with T regulatory cells. Total CD4 T cell dynamics were similar in INSPIRE 2 and INSPIRE 3, therefore the data were merged (Figure 4 A and B) for further analyses. There was no clear difference between the CD4 T cell responses after the first and the second cycle in the 95 and 49 patients who received complete (3 injections) first and second cycles respectively (Figure 4 C). During the maintenance cycles (second and later cycles), the CD4 T cell responses are presented according to the number of injections received (Figure 4 D).

Among the 23 and 86 patients exposed to r-hIL-7 in INSPIRE 2 and INSPIRE 3, 26% (6) and 16% (14) developed anti drug binding antibodies (ADA) to CYT107 at the end of the first cycle. After the second cycle, these proportions increased to 82% and 77% in the 14 and 44 patients exposed, respectively. Neutralizing antibodies developed in none of 23 patients in INSPIRE 2 and in one of 86 patients in INSPIRE 3 after the first cycle and 6 (38%) and 21 (37%) patients after the second cycle in INSPIRE 2 and 3 respectively. There was no impact of the presence of antibodies on the CD4 T cell dynamics (supplementary Figure 2).

The median time spent above 500 CD4 T cells/μL for the 76 patients with a follow-up of 21–24 months after the first injection was 13.7 months (8.4, 20.1). Half of these patients spent more than 63% of their follow-up (that ranged between 21-24 months) with more than 500 CD4 T cells/μL. To look at the factors associated with the probability of dropping below 550 CD4 T cells/μL (the threshold to start a new cycle of r-hIL-7) in the 95 patients who achieved a CD4 T cell count above 550 cells/μL two weeks after a cycle, a Shared Gamma Frailty model was adjusted for the baseline CD4 T cell count, the number of injections in each cycle and the type of cycle (initial or maintenance). In this model (Table 3), fewer injections had a higher probability of dropping below 550 CD4 T cells/μL (p=0.023). This probability was greater after one injection (HR=4.3, CI=1.3; 13.9) than after three injections whatever the cycle. The difference between two and three injections was not significant (HR=2.2, CI=0.79; 6.6). Lower baseline CD4 T cell count was the stronger predictor (p<.0001) of dropping below 550 CD4 T cells/μL, with risk increasing dramatically in persons with fewer than 200 CD4 T cells/μL at baseline (HR=11.1, CI=4.0; 30.7). The type of cycle (initial vs. maintenance) was not associated with the probability of dropping below 550 CD4 T cells/μL (p=0.57). Other variables:

age, sex, ethnic origin, time since HIV diagnosis, duration of cART, stage at diagnosis and proviral HIV DNA levels at baseline were not found to be predictive for CD4 T cell drop (data not shown).

Safety and tolerability

A total of 198 cycles were administered to 113 patients (including two participants who withdrew) and r-hIL-7 was overall well tolerated. A total of 1300 drug Related Adverse Events (RAEs) were reported, most (77.6%) were grade ≤1, 20.7% grade 2 and 1.7% grade ≥3. The mean number of RAEs reported at each cycle did not vary. The most common r-hIL-7-related AEs (RAEs) were injection-related reactions of grade 1 or 2, primarily local erythema (53.8%), grade 1 lymphadenopathy (7.5%), grade 1 fever (2.5%), rash of grade 1 or 2 (2.4%) and fatigue of grade 1 (3.6%). No deaths related to r-hIL-7 were reported. Three serious adverse events related to r-hIL-7 were reported: two grade 3 rashes and one grade 1 rash associated with a hospitalization. Two patients were treated with oral corticosteroids for apparent hypersensitivity reactions. Five patients developed an anaphylactic/allergic reaction, one grade 2 and four grade 3. These comprised of diffuse, pruritic rashes associated in one patient with swelling of the tongue. No pulmonary symptoms or alterations in pulse or blood pressure were reported. No immune reconstitution inflammatory syndrome was reported neither. In four patients, treatment included antihistamines and corticosteroids for one day that led to resolution of all symptoms. One patient was treated with antihistamines only and recovered in three days. AST/ALT elevations were reported in 10 patients (9.2%), most were grade 1 or 2 (88%). One patient developed an asymptomatic grade 4 AST/ALT

elevation that was considered a probably RAE. Ten patients developed grade ≥ 3 AE of hypophosphataemia, three were considered possibly RAEs.

The HIV RNA and DNA changes

Nearly half of the patients had HIV RNA blips exceeding 50 copies/mL and 13% in INSPIRE 2 and 17% in INSPIRE 3 exceeded 200 copies/mL (Table 4). Injection of r-hIL-7 was postpone in four patients because of these blips. In 18 patients of INSPIRE 2, there was an increase of the HIV DNA concentration from a median of 1.97 $\log_{10}$ copies/mL (1.39, 2.48) to 2.58 (2.00, 2.96) at day 28 (p<0.0001) and 2.27 (1.65, 2.85) at 3 months (p<0.0001) after the first cycle (supplementary Figure 3).

Plasma coagulation and Inflammatory markers

D-dimer, measured in INSPIRE 3, did not change significantly from baseline with a mean level of 0.274 mg/L (std ±0.179) at baseline and 0.323 mg/L (±0.507) at M12 and 0.224 mg/L (±0.113) at M21. Likewise, CRP levels in INSPIRE 2 and 3 remained the same during the course of the study: 6.1 (±9.4 mg/L) at baseline, 4.2 (±6.0 mg/L) at M12 and 6.1 (±17.9 mg/L) at M21 (supplementary figures 4, 5).

Discussion

We report the results of the first two studies evaluating the effect of repeated administration of cycles of r-hIL-7 on immune restoration. The first treatment cycle increased naïve and central memory CD4 T cells as reported previously [11,12]. We found that repeated r-hIL-7 cycles led to even greater increases in CD4 T cell counts resulting in a longer time spent above 500 cells/μL for those who received at least two injections per cycle. Although repeated doses of r-hIL-7 led to the development of both binding and neutralizing antibodies against the product, this was not associated with any blunting of the CD4 T cell increases induced by r-hIL-7 administration.

As shown in an INSPIRE 2 substudy, administration of r-hIL-7 was associated with improvement of gut barrier integrity and a decrease at 3 months in inflammatory/coagulation markers sCD14 and D dimers [14]. In this larger study however, D-dimer decreases were not observed at three months nor did we see a decrease in CRP levels. We found here that repeated cycles of r-hIL-7 led to a longer time spent with CD4 cells above 500 cells/μL. The clinical impact of this CD4 T cell increase is unknown and needs to be explored through a larger scale randomized clinical trial focusing on the occurrence of clinical endpoints.

r-hIL-7 appears to have a reasonable safety profile even with repeated cycles of administration. The study product was tolerated well and the incidence of serious adverse events was low enough to allow consideration of further development with the goal of asking if CD4 T cell increases result in clinical benefit. At the same time as we observed r-hIL-7 induced proliferation and expansion of memory CD4 T cells, treated patients experienced "blips" in plasma HIV RNA levels and an apparent increase in numbers of circulating cells containing proviral DNA. The significance of these virologic

effects is uncertain. While homeostatic responses to IL-7 have been implicated in maintaining the latent HIV reservoir in CD4 T cells [17], occurrence of viral blips seen in r-hIL-7 recipients in this and other studies [10–12], suggests that the cellular proliferation induced by r-hIL-7 also can activate or enhance HIV expression. Thus, the net effects of r-hIL-7 administration on the infectious viral reservoir merit further study. Further studies are also warranted to explore the clinical impact of r-hIL-7 administration as well as the long term impact of this therapy on immune function. As shown previously, the CD4 T cell increase after administration of r-hIL-7 is likely due to increased CD4 T cell proliferation but also may relate to additional mechanisms such as improvement of cell survival and thymic output [13]. Repeated r-hIL-7 cycles might lead to an even more durable effect such as might be the consequence of improvement of lymphoid tissue architecture as reported in the gut [14] reversing abnormalities seen in advanced HIV infection [18].

In conclusion, repeated cycles of r-hIL-7 can improve and sustain CD4 restoration with increases of predominantly naïve and central memory CD4 T cells. This intervention could help persons who present for care late in disease course or who does not respond well to antiretroviral therapy achieve higher CD4 T cell counts sooner, possibly preventing morbidities and mortality [3,19].

References

1   Bonnet F, Chene G, Thiebaut R, Dupon M, Lawson Ayayi S, Pellegrin JL, *et al.* Trends and determinants of severe morbidity in HIV-infected patients: The ANRS CO3 Aquitaine Cohort, 2000-2004. *HIV Med* 2007; **8**:547–554.

2   Mocroft A, Furrer HJ, Miro JM, Reiss P, Mussini C, Kirk O, *et al.* The incidence of AIDS-defining illnesses at a current CD4 count ≥ 200 cells/μL in the post-combination antiretroviral therapy era. *Clin Infect Dis* 2013; **57**:1038–47.

3   Lewden C, Chene G, Morlat P, Raffi F, Dupon M, Dellamonica P, *et al.* HIV-infected adults with a CD4 cell count greater than 500 cells/mm3 on long-term combination antiretroviral therapy reach same mortality rates as the general population. *J Acquir Immune Defic Syndr* 2007; **46**:72–77.

4   Young J, Psichogiou M, Meyer L, Ayayi S, Grabar S, Raffi F, *et al.* CD4 cell count and the risk of AIDS or death in HIV-Infected adults on combination antiretroviral therapy with a suppressed viral load: a longitudinal cohort study from COHERE. *Plos Med* 2012; **9**:e1001194.

5   May MT, Gompels M, Delpech V, Porter K, Orkin C, Kegg S, *et al.* Impact on life expectancy of HIV-1 positive individuals of CD4+ cell count and viral load response to antiretroviral therapy: UK cohort study. *AIDS* 2014; :1193–1202.

6   Gilson RJC, Man S-L, Copas A, Rider A, Forsyth S, Hill T, *et al.* Discordant responses on starting highly active antiretroviral therapy: suboptimal CD4 increases despite early viral suppression in the UK Collaborative HIV Cohort (UK CHIC) Study. *HIV Med* 2010; **11**:152–60.

7   O'Connor JL, Smith CJ, Lampe FC, Hill T, Gompels M, Hay P, *et al.* Failure to achieve a CD4+ cell count response on combination antiretroviral therapy despite consistent viral load suppression. *AIDS* 2014; **28**:919–24.

8   Mocroft A, Lundgren JD, Sabin ML, Monforte A d'Arminio, Brockmeyer N, Casabona J, *et al.* Risk factors and outcomes for late presentation for HIV-positive persons in europe: results from the

collaboration of observational HIV epidemiological research europe study (COHERE). *PLoS Med* 2013; **10**:e1001510.

9   Pantaleo G, Lévy Y. Vaccine and immunotherapeutic interventions. *Curr Opin HIV AIDS* 2013; **8**:236–42.

10   Sereti I, Dunham RM, Spritzler J, Aga E, Proschan MA, Medvik K, *et al.* IL-7 administration drives T cell-cycle entry and expansion in HIV-1 infection. *Blood* 2009; **113**:6304–6314.

11   Levy Y, Lacabaratz C, Weiss L, Viard JP, Goujard C, Lelievre JD, *et al.* Enhanced T cell recovery in HIV-1-infected adults through IL-7 treatment. *J Clin Invest* 2009; **119**:997–1007.

12   Levy Y, Sereti I, Tambussi G, Routy J-P, Lelievre JD, Delfraissy J-F, *et al.* Effects of r-hIL-7 on T Cell Recovery and Thymic Output in HIV-infected Patients receiving antiretroviral therapy: results of a Phase I/IIa Randomized, Placebo Controlled, Multicenter Study. *Clin Infect Dis* 2012; **55**:291–300.

13   Thiebaut R, Drylewicz J, Lacabaratz C, Sekaly R, Lederman MM. Quantifying and Predicting the Effect of Exogenous Interleukin-7 on CD4 + T Cells in HIV-1 Infection. 2014; **10**. doi:10.1371/journal.pcbi.1003630

14   Sereti I, Estes JD, Thompson WL, Morcock DR, Fischl MA, Micheaux SL De, *et al.* Decreases in Colonic and Systemic Inflammation in Chronic HIV Infection after IL-7 Administration. *Plos Pathog* 2014; **10**:e1003890.

15   Avettand-Fènoël V, Chaix M-L, Blanche S, Burgard M, Floch C, Toure K, *et al.* LTR real-time PCR for HIV-1 DNA quantitation in blood cells for early diagnosis in infants born to seropositive mothers treated in HAART area (ANRS CO 01). *J Med Virol* 2009; **81**:217–23.

16   Rondeau V, Mazroui Y, Gonzalez JR. FRAILTYPACK: An R package for the analysis of correlated survival data with frailty models using the penalized likelihood estimation. *J Stat Softw* 2011; **VV**:1–26.

17   Chomont N, El-Far M, Ancuta P, Trautmann L, Procopio FA, Yassine-Diab B, *et al.* HIV reservoir size and persistence are driven by T cell survival and homeostatic proliferation. *Nat Med* 2009; **15**:893–U92.

18   Zeng M, Smith AJ, Wietgrefe SW, Southern PJ, Schacker TW, Reilly CS, *et al.* Cumulative mechanisms

of lymphoid tissue fibrosis and T cell depletion in HIV-1 and SIV infections. *J Clin Invest* 2011;

121:998–1008.

19   Engsig FN, Zangerle R, Katsarou O, Dabis F, Reiss P, Gill J, *et al.* Long-term mortality in HIV-positive

individuals virally suppressed for >3 years with incomplete CD4 recovery. *Clin Infect Dis* 2014;

58:1312–21.

Table 1. Participant characteristics in INSPIRE 2 and INSPIRE 3 studies.

Characteristics	INSPIRE 2 (N=23)	INSPIRE 3 (N=88)
Number of treated and analysed patients	23	84
Median age, years (Q1,Q3)	47 (42,51)	43 (37,51)
Female, %	13.1%	34.1%
Ethnic origin (Caucasian/African/Other)	(16/3/4)	(39/46/3)
Median time since HIV diagnosis, years (Q1,Q3)	8 (4,20)	6 (3,13)
Median duration of ARV, years (Q1,Q3)	5 (4,16)	4 (3,6)
Clinical stage at diagnosis (A/B/C)	(12/2/9)	(38/11/39)
Median CD4 T-cell count, cells/µL (Q1,Q3)	263 (191,320)	266 (215,326)
Median CD8 T-cell count, cells/µL (Q1,Q3)	604 (405,867)	633 (457,843)
Median CD4 T-cell count nadir, cells/µL (Q1,Q3)	41 (19,163)	54 (19,126)
Median CD4/CD8 ratio	0.48 (0.27,0.59)	0.42 (0.29,0.56)
Median of months of follow up (Q1,Q3)	23 (22,24)	22 (20,23)
Median months between cycles (Q1,Q3)	[a]12 (6,12)	6 (6,9)
Median number of injections received (Q1,Q3)	5 (3,6)	5 (3,6)
Median number of started cycles (Q1,Q3)	2 (1.5,2)	2 (1,2)
Median number of completed cycles (Q1,Q3)	1 (1,2)	1 (1,2)

[a]First 12 patients in INSPIRE2 were followed for a year before administration of a new cycle.

Table 2. Description of the treatment received in INSPIRE 2 (N=23) and INSPIRE 3 (N=84) studies.

	Characteristics	INSPIRE 2	INSPIRE 3	TOTAL
Cycle 1	Initial CD4 cell count/µL	263	267	266
	Starting cycle	23	84	107
	Completed cycle	20	75	95
	1 injection	-	2	2
	2 injections	3	7	10
Cycle 2	Initial CD4 cell count/µL	473	478	473
	Starting cycle	17	57	74
	Completed cycle	10	39	49
	1 injection	2	10	12
	2 injections	5	8	13
Cycle 3	Initial CD4 cell count	316	474	373
	Starting cycle	3	12	15
	Completed cycle	2	8	10
	1 injection	-	3	3
	2 injections	1	1	2
Cycle 4	Initial CD4 cell count	-	475	475
	Starting cycle	-	1	1
	Complete cycle	-	1	1
	1 injection	-	-	-
	2 injections	-	-	-

Table 3. Factors associated with dropping to < 550 CD4 cells/μl

Shared Gamma Frailty model using a Weibull hazard function. Data are based on 95 patients with a CD4 T cell count > 550 cells/μL two weeks after the last injection of r-hIL-7 that represent a total of 151 cycles. After adjustment, there was still unexplained inter-individual variability in the probability of dropping below 550 cells/μL as the variance of the frailty parameter (0.822) was significantly different from 0 (p=0.006).

Factor	Hazard Ratio	95% CI	P-value
Baseline CD4 T cell count			**< 0.001**
CD4 > 200 cells/μL	1		
CD4 ≤ 200 cells/μL	11.10	(4.02, 30.66)	
Type of IL-7 cycle			0.57
Initial cycle	1		
Maintenance cycle	0.86	(0.51, 1.46)	
Number of injections in a given cycle			**0.023**
Three injections	1		
Two injections	2.27	(0.79, 6.55)	
One injection	4.29	(1.32, 13.90)	

Table 4. **Plasma HIV RNA dynamics during the follow-up after the first injection of r-hIL-7 in INSPIRE 2 and 3.**

Trial	Total measurements	% of RNA >50	% of RNA >200	% of treated patients with at least one HIV RNA>50	% of treated patients with at least one HIV RNA>200
INSPIRE 2	364	8.8	1.1	52.2	13.0
INSPIRE 3	1374	6.8	2.3	44.0	17.1

Figure 1a. INSPIRE 2 design

Figure 1b. INSPIRE 3 design

Figure 2. Flow chart of INSPIRE 2 & INSPIRE 3

Figure 3. Individual changes in CD4 T cells over time following injections of r-hIL-7.

Figure 4. CD4 T cell dynamics after r-hIL-7 injections. A) INSPIRE 2, B) INSPIRE 3, C) according to the first or second cycle (time 0 is the beginning of the first or second cycle), D) according to the number of injections performed in cycles following the initial one

Figure 1A
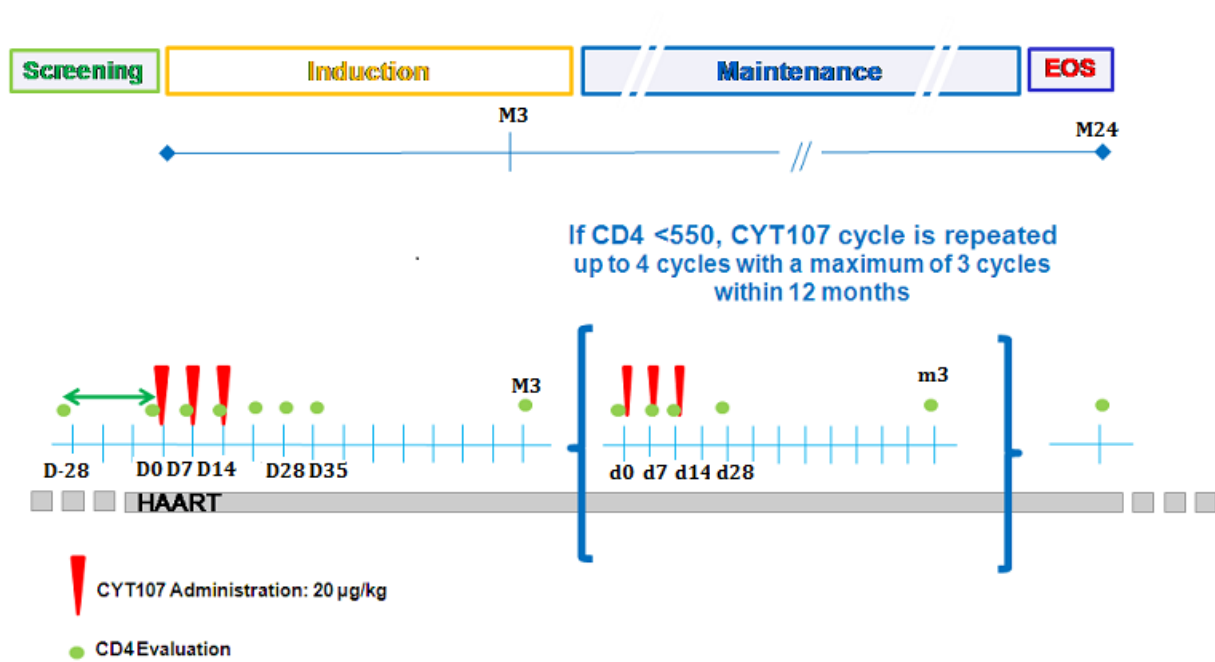
Figure 1B

Figure 2

INSPIRE 2

36 patients screened

13 patients not included

23 included patients

23 analyzed patients

INSPIRE 3

135 patients screened

43 patients not randomized

92 patients randomized

2 patients withdrew

CYT107 arm
N = 66

Control arm
N = 24

2 patients withdrew

64 analyzed patients

24 analyzed patients
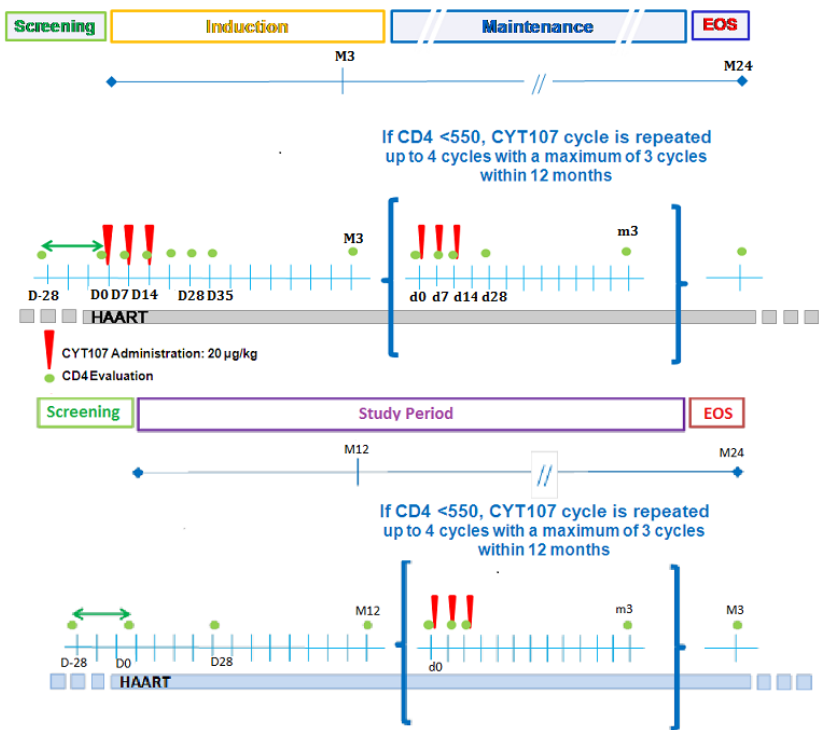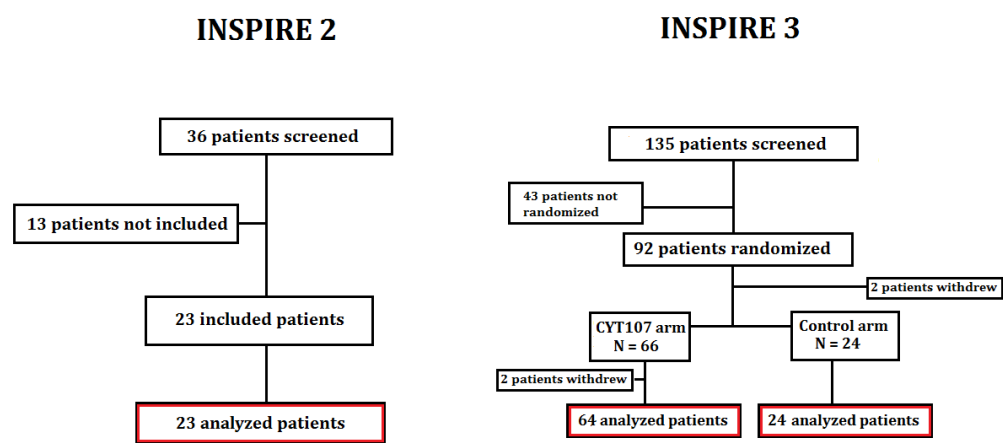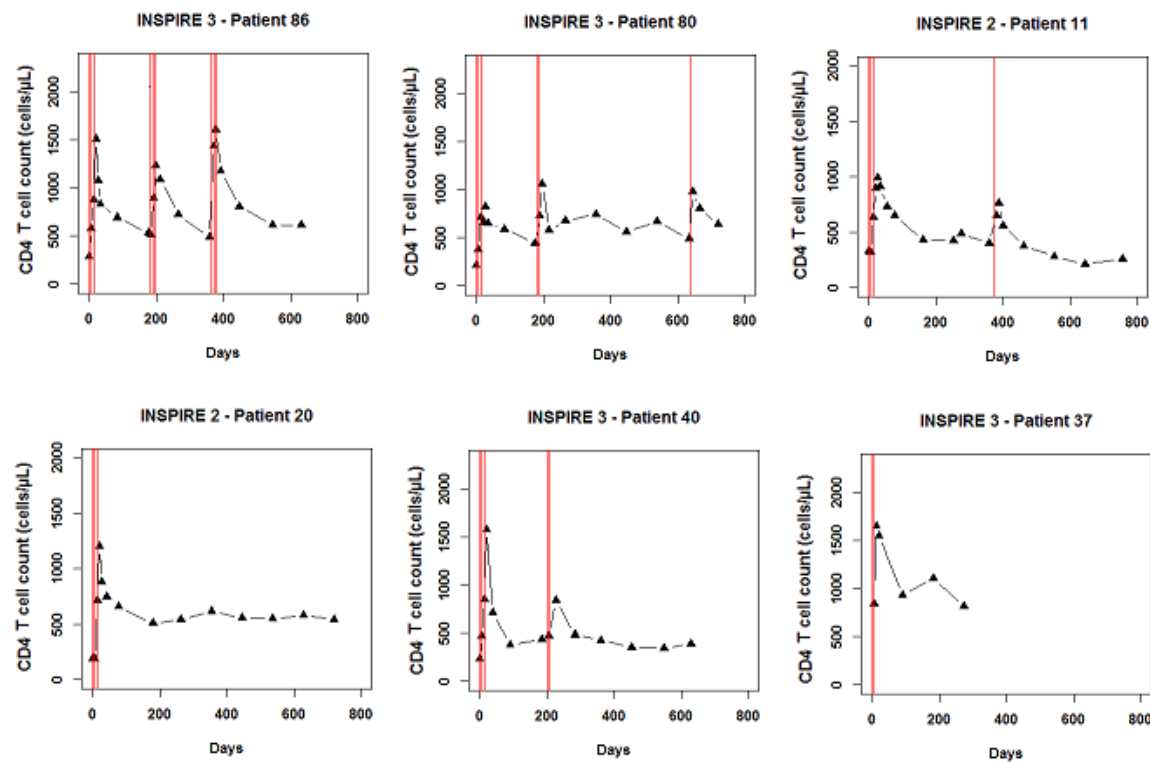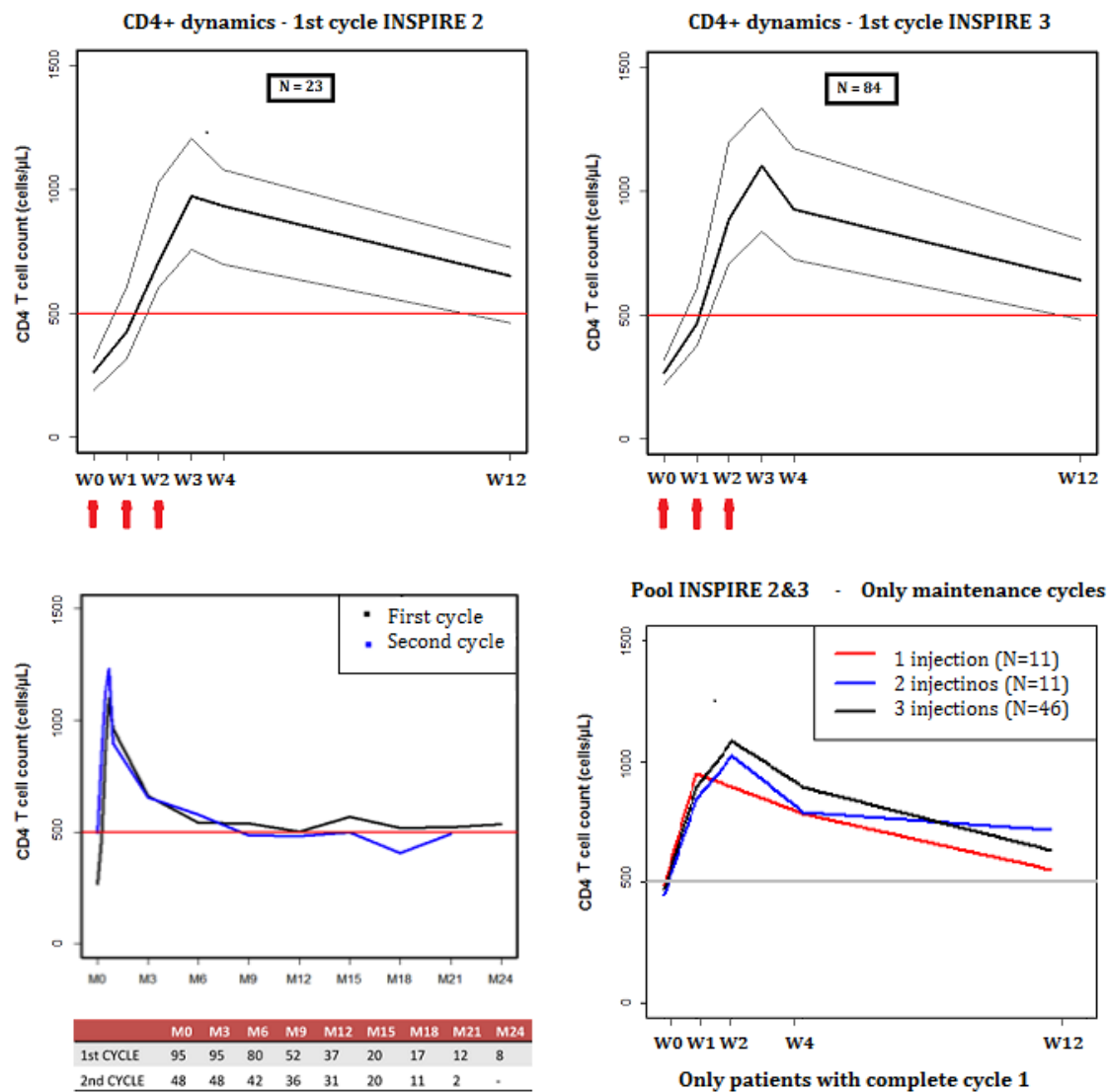
Figure 3

Figure 4

Suppementary Figure 1A. Detailed immune response in INSPIRE 2 patients for total CD4, Tregs, CD31+, CD4 naïve, central memory (TCM) and effector memory (TEM) at baseline to week 12 (W12).
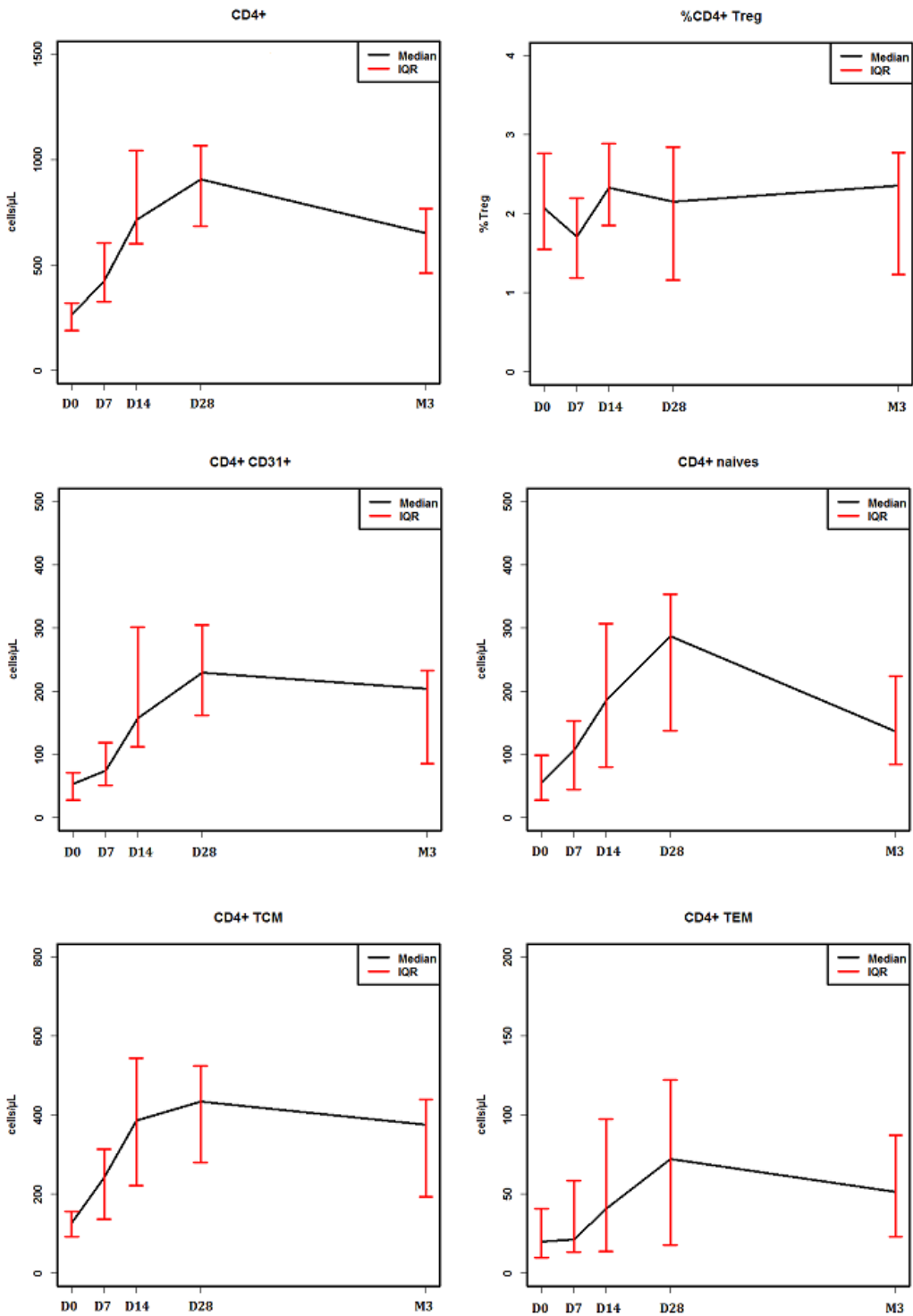
Supplementary Figure 1B. Detailed immune response in the subsample of the first 12 patients included in INSPIRE 2 for Ki67, CTLA4, LFA1, Tbet, Tim3 and PD1 markers at baseline to week 12 (W12).
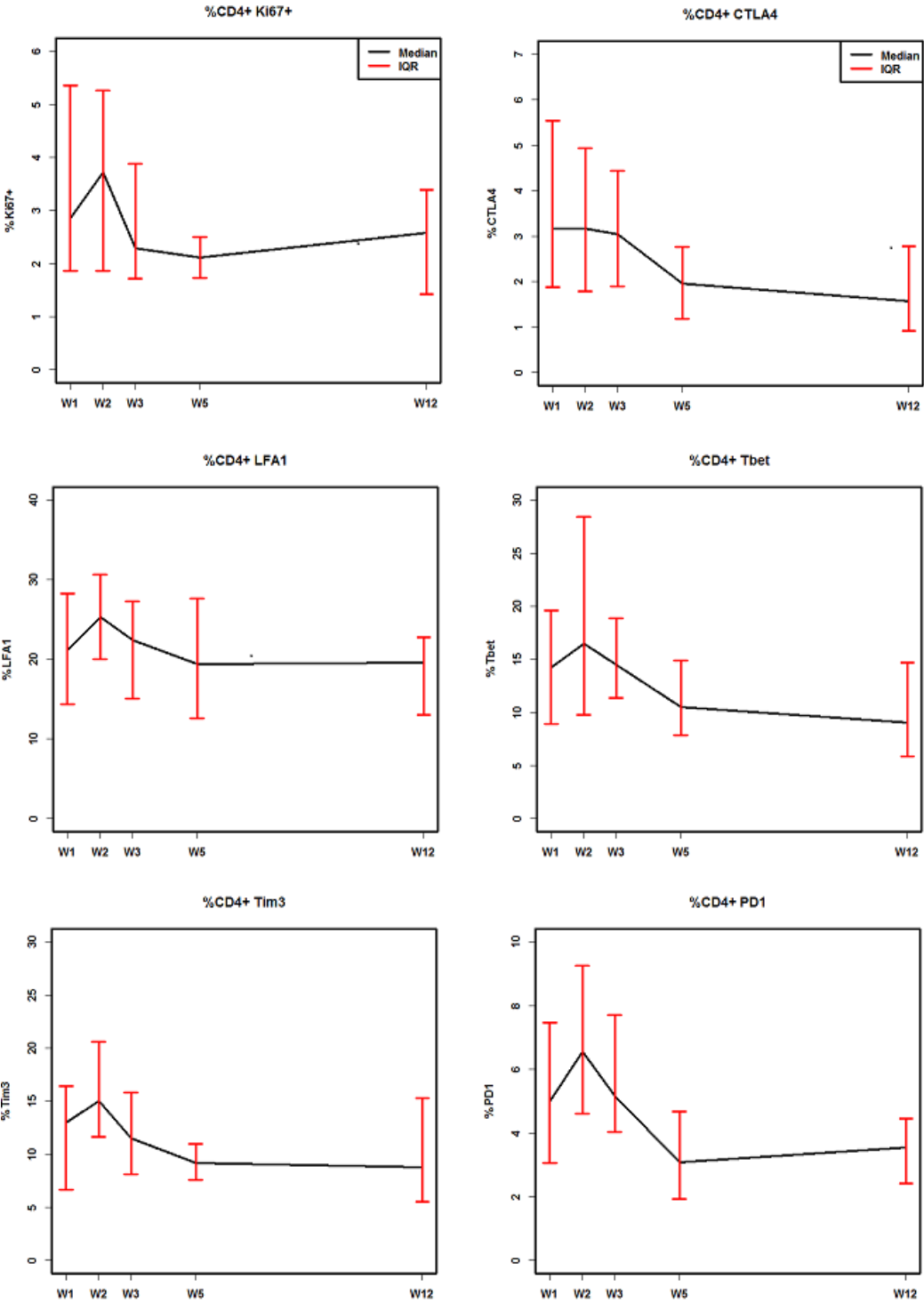
Supplementary Figure 2. CD4 T cell dynamics (median and IQR) according to the presence of binding antibodies against IL-7 (ADA) A) After the first cycle and B) After the second cycle.
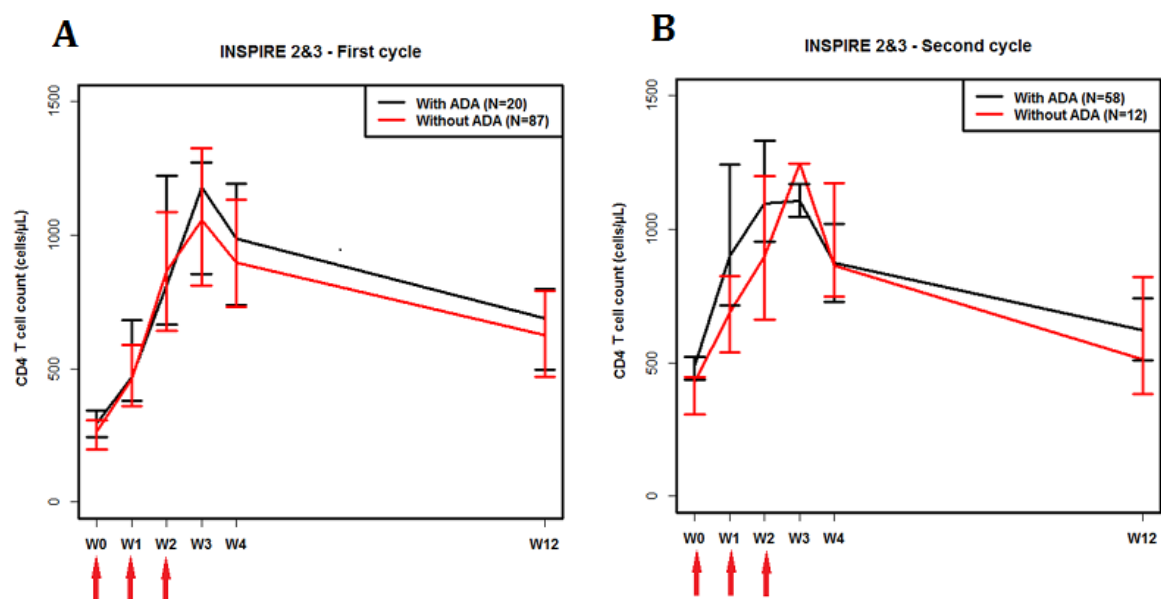
Supplementary Figure 3. Median (IQR) of HIV DNA concentration by million of PBMC in INSPIRE 2 (N=22): 1.97 log10 copies/mL (1.39, 2.48) at day 0 (baseline), 2.58 (2.00, 2.96) at day 28 and 2.27 (1.65, 2.85) at week 12. Wilcoxon matched paired tests.

Log(HIVDNA copies) / mL
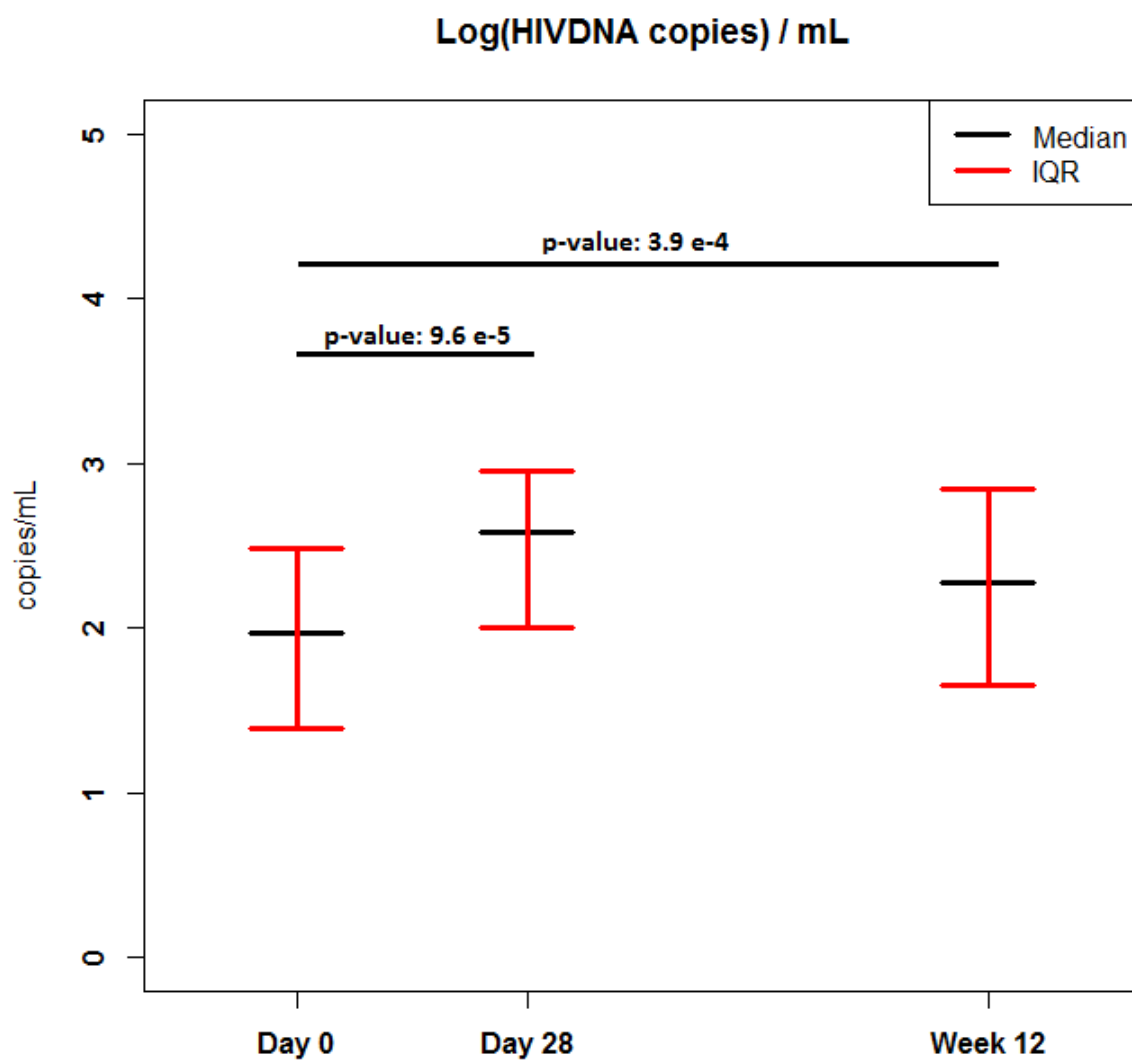
Supplementary Figure 4. Median and first and third quartiles of CRP in INSPIRE 2 and 3 from day 0

(D0) to month 21 (M21) (excluding center 15). Wilcoxon matched pairs tests.
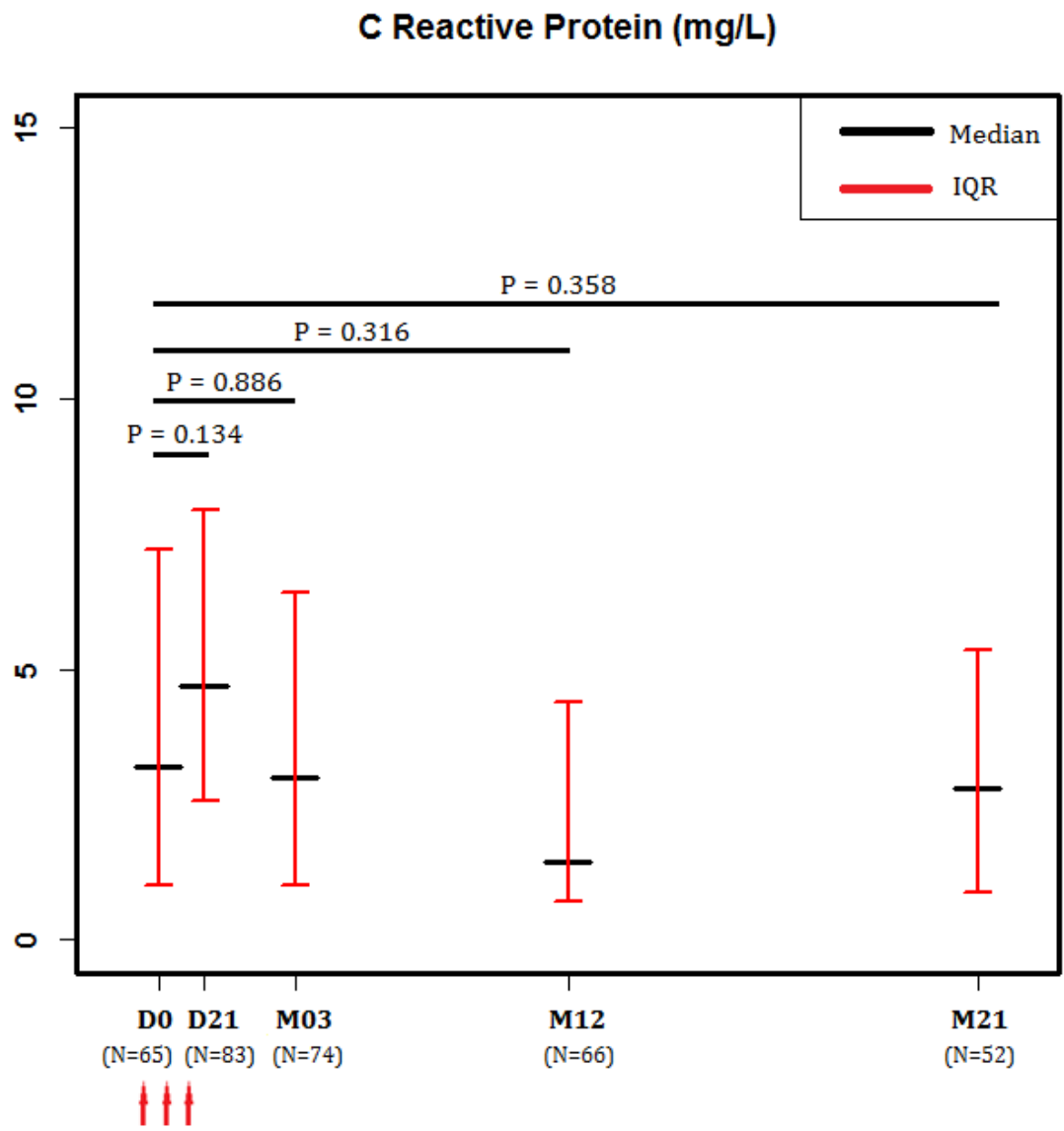
Supplementary Figure 5. Median and first and third quartile of D-dimer in INSPIRE 3 from day 0 (D0) to month 21 (M21) (excluding centers 42 and 43). Wilcoxon matched pairs tests.
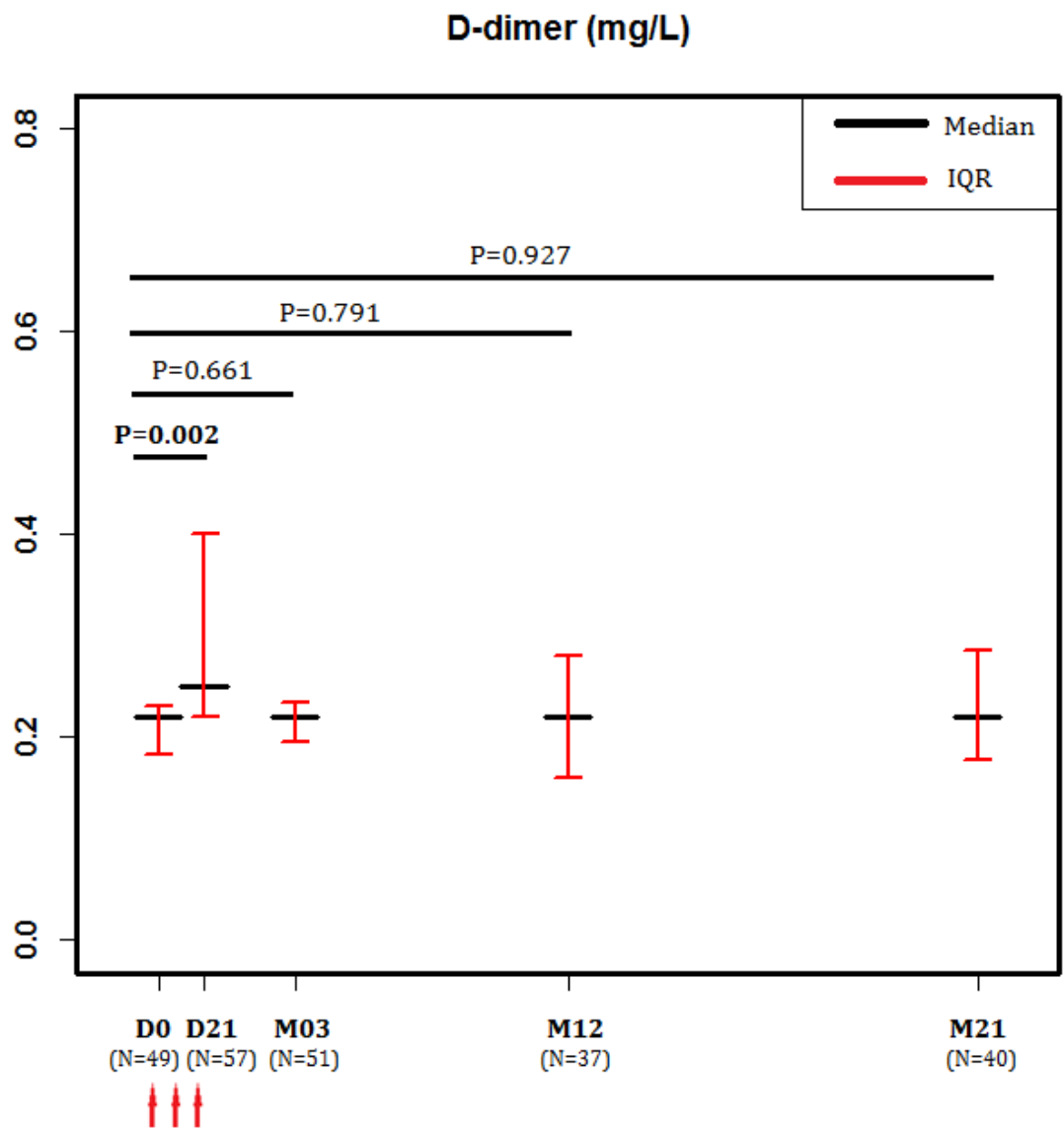
Appendix E

Appendix E: AOAS's paper

MODELING CD4$^+$ T CELLS DYNAMICS IN HIV-INFECTED PATIENTS RECEIVING REPEATED CYCLES OF EXOGENOUS INTERLEUKIN 7

By Ana Jarne[*], Daniel Commenges[*], Mélanie Prague[*,§], Yves Lévy[†,‡] and Rodolphe Thiébaut[*,‡] for inspire 2&3 study group

INSERM-INRIA SISTM team[*], INSERM U955[†], VRI Paris[‡], Harvard T.H. Chan School of Public Health[§]

Combination Antiretroviral Therapy (cART) succeeds to control viral replication in most HIV infected patients. This is normally followed by a reconstitution of the CD4$^+$ T cells pool; however, this does not happen for a substantial proportion of patients. For these patients, an immunotherapy based on injections of Interleukin 7 (IL-7) has been recently proposed as a co-adjutant treatment in the hope of obtaining long-term reconstitution of the T cells pool. Several questions arise as to the long-term efficiency of this treatment and the best protocol to apply. Mathematical and statistical models can help answering these questions.

We develop a model based on a system of ordinary differential equations and a statistical model of variability and measurement. We can estimate key parameters of this model using the data from the main studies for this treatment, the INSPIRE, INSPIRE 2 & INSPIRE 3 trials. In all three studies, cycles of three injections have been administered; in the last two studies, for the first time, repeated cycles of exogenous IL-7 have been administered. Repeated measures of total CD4$^+$ T cells count in 128 patients as well as CD4$^+$Ki67$^+$ T cells count (the number of cells expressing the proliferation marker Ki67) in some of them were available. Our aim was to estimate the possible different effects of successive injections in a cycle, to estimate the effect of repeated cycles and to assess different protocols.

The use of dynamical models together with our complex statistical approach allow us to analyze major biological questions. We found a strong effect of IL-7 injections on the proliferation rate; however, the effect of the third injection of the cycle appears to be much weaker than the first ones. Also, despite a slightly weaker effect of repeated cycles with respect to the initial one, our simulations show the ability of this treatment of maintaining adequate CD4$^+$ T cells count for years. We were also able to compare different protocols, showing that cycles of two injections should be sufficient in most cases.

1. Introduction. Infection by the Human Immunodeficiency Virus (HIV) leads to severe lymphopenia and general immune dysfunction. Combination

---

Antiretroviral Therapy (cART) allows controlling viral load in most patients and often leads to an adequate immune restoration. However, not all patients get a satisfactory immune reconstitution despite undetectable viral load. Sereti et al. (2014) called these patients "immunological non responders"; we prefer to call them "immunological low responders" because these patients can still experience an increase of $CD4^+$ T cells count under cART, albeit insufficient.

A treatment based on injections of exogenous Interleukin-7 (IL-7) has been recently proposed, and is for the moment the only promising approach in this context (Sereti et al., 2009; Levy et al., 2009, 2012). Endogenous IL-7 is a cytokine produced by non-marrow-derived stromal and epithelial cells, and since it was discovered in 1988 (Namen et al., 1988), it has been found to play an important role in peripheral maintenance of T cells (Fry and Mackall, 2002; Mackall, Fry and Gress, 2011). In HIV-infected patients, a correlation between plasma levels of endogenous IL-7 and $CD4^+$ T cell counts has already been reported (Beq et al., 2004), and different mechanisms of action of IL-7 regarding regulation of T lymphocytes number and behavior have been uncovered, as enhancing thymopoiesis (Mackall et al., 2001; Okamoto et al., 2002), proliferation (Vieira et al., 1998; Sportès et al., 2008) and survival (Seddon, Tomlinson and Zamoyska, 2003; Kondrack et al., 2003) of $CD4^+$ T cells.

Mathematical representations of the behavior of the immune system in the context of HIV infection have been useful to describe and quantify biological processes that are not directly observed; the interaction between HIV virions and $CD4^+$ T cells was firstly modeled by Ho et al. (1995) and Perelson et al. (1996). For modeling the effect of exogenous IL-7 administration, it is not useful to model virus concentration (because viral load is undetectable under cART), but it is necessary to distinguish between quiescent and proliferating cells. In this context, Thiébaut et al. (2014) have quantified the contribution of several biological mechanisms in $CD4^+$ T cells homeostasis. They have studied the effect of a single cycle of exogenous IL-7. Here, we extend this approach with a modified statistical model for analyzing repeated cycles, based on data from 3 clinical studies, INSPIRE, INSPIRE 2 and INSPIRE 3. We focus on several major clinical questions. What is the effect of the different injections in a cycle? What is the effect of repeated cycles? What is the long-term efficacy of this therapy in maintaining $CD4^+$ T cells count at a satisfactory level (over 500 cells/μL)? What is the best protocol of injections?

This paper is divided into 7 sections. Section 2 gives an overview of the INSPIRE studies and the available data. Section 3 describes the main struc-

ture of the mathematical and statistical models. Section 4 presents and compares different statistical models: the "basic model" studying the effect of exogenous IL-7 over a cycle as a whole, the "3 β's model" allowing the successive injections of a cycle to have different effects, and the "cycle effect model" investigating the long term effect when administering repeated cycles. Section 5 compares results of four possible protocols (varying the number of injections of a cycle) and predicts their impact on the maintenance of CD4$^+$ T cells count > 500 cells/μL for an average patient. Section 6 explores the possibility of optimizing the protocol by investigating in simulation the trajectories of CD4$^+$ T cells count in good and bad responders. Section 7 concludes.

2. Data and materials.

2.1. *Data source and subjects.* The data have been compiled from three phase I/II multicenter studies: INSPIRE (Levy et al., 2012), INSPIRE 2 and INSPIRE 3 (Thiébaut et al., 2015 in revision). These studies investigated the effect of a *purified glycosylated recombinant human Interleukin 7* (r-hIL-7) treatment on immune restoration in immunological low responder patients. All participants were aged ≥ 18 years, were under stable cART for at least 2 years, presenting CD4$^+$ T cells count between 100-350 cells/μL (100-400 cells/μL for INSPIRE 2), and undetectable viral load for at least 6 months prior to screening.

In the first study, INSPIRE, 21 patients received three weekly injections (a "complete cycle") of r-hIL-7 at different weight-dependent doses: 10, 20 and 30 μg/kg and the main objective was to evaluate the safety of this treatment. INSPIRE 2 and INSPIRE 3 (with 23 and 84 treated patients, respectively) further studied the biological activity (as well as the safety) of repeated cycles of r-hIL-7 at 20 μg/kg. In this paper, data for all treated patients from the three studies (N=128) have been included from the time of the first injection. Overall, 197 r-hIL-7 cycles were administered (41 of them were incomplete cycles consisting of 1 or 2 injections). More details are provided in a previous publication (Thiébaut et al., 2015 in revision).

2.2. *Study design and observations.* Within the first INSPIRE study, all patients received complete cycles. They had clinic visits at weeks 1, 2 and 3 (at the moment of the injections), weeks 4, 5, 6, 9 and 12, and after, one visit every 3 months; see Levy et al. (2012) for more information. Among many measured biomarkers, our model uses total CD4$^+$ T cells count and the number of CD4$^+$ T cells expressing the Ki67 proliferation marker, hereafter called "CD4 count" and "Ki67 count", respectively. Measurements of CD4

counts were made at each visit, while Ki67 counts were only measured at weeks 1, 2, 3, 5 and 12.

For the first twelve patients of INSPIRE 2, clinic visits within the initial cycles were scheduled as for the INSPIRE study (for the rest of them, visits at week 9 were not performed). After, if CD4 counts were found to be below 550 cells/μL in one of the quarterly visits, a new r-hIL-7 cycle was administered (with the exception of the first 12 patients, who wait a year before receiving a new cycle). Within these repeated cycles, clinic visits were scheduled at weeks 1, 2 and 3 (at the moment of the injections), weeks 5 and 12, and once again quarterly visits are made to check the CD4 count. A maximum of 4 cycles within 21 months and a maximum of 3 cycles within 12 months were established, and all patients have been followed up at least 3 months after the last cycle. CD4 counts were measured at all visits for all patients, while Ki67 counts were measured only for the first cycles of the first 12 patients at weeks 1, 2, 3, 5 and 12.

For INSPIRE 3, patients were randomized into two arms: "r-hIL-7 arm" and "Control arm" with a ratio 3:1 (3 r-hIL-7 : 1 Control). Patients of the "r-hIL-7 arm" received the same treatment scheme as patients from INSPIRE 2. Patients of the "Control arm" were first followed up without receiving the r-hIL-7 for one year, and if CD4 count was still below 500 cells/μL, r-hIL-7 treatment was started as for the other group (Thiébaut et al., 2015 in revision). CD4 counts were measured at all visits. No Ki67 counts measurements were available.

The total duration of the studies was 12, 24 and 21 months for INSPIRE, INSPIRE 2 and INSPIRE 3, respectively.

3. Mathematical and statistical structure.

3.1. *Mathematical and statistical models.* Our theoretical framework to describe the dynamics of CD4 and Ki67 counts is based on the same system of ordinary differential equations (ODE) as proposed by Thiébaut et al. (2014). For patient i this model can be written as:

$$\begin{cases} \frac{dQ^i}{dt} &= \lambda^i + 2\rho^i P^i - \pi^i Q^i - \mu_Q^i Q^i \\ \frac{dP^i}{dt} &= \pi^i Q^i - \rho^i P^i - \mu_P^i P^i \end{cases}$$

The initial condition is assumed to be the equilibrium point (specified by $\frac{dQ^i}{dt}(0) = 0$, $\frac{dP^i}{dt}(0) = 0$).

A graphical representation of the system can be found in Figure 1. This model includes two state variables: P, the concentration of proliferating cells

expressing the Ki67 proliferation marker (CD4$^+$Ki67$^+$) and Q, the concentration of quiescent cells (CD4$^+$Ki67$^-$). We have also investigated a model with a feedback term, obtained by multiplying the basic proliferation rate by $\frac{1}{(P^i+Q^i)^\nu}$, where ν is a parameter to be estimated. We did not retain this feedback term because it did not lead to major improvement of the fit while requiring much more computation time (see Appendix A).

The vector of parameters of the ODE system is $\boldsymbol{\xi^i} = [\lambda^i, \rho^i, \pi^i, \mu_Q^i, \mu_P^i]$. These parameters have a biological interpretation: λ is the production rate, ρ is the reversion rate, π is the proliferation rate and μ_Q and μ_P are the mortality rates of Q and P cells, respectively. The logarithmic transformation ensures positivity of these biological parameters: $\tilde{\boldsymbol{\xi}}^i = \log(\boldsymbol{\xi}^i)$.
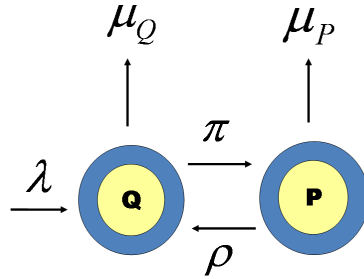
Fig 1: Graphical representation of the mathematical model

Modeling the variability of the parameters is a crucial ingredient in our model because it allows to have a joint estimation of parameters across the population instead of fitting the model patient-by-patient. A mixed-effect model can be assumed for each transformed parameter l, $l = 1,...,p$ (here $p = 5$):

$$\tilde{\xi}_l^i(t) = \phi_l + \beta_l^\top z_l^i(t) + u_l^i$$

where ϕ_l is the intercept, β_l is a vector of regression coefficients, $\boldsymbol{z_l^i}$ is a vector of explanatory variables, and u_l^i are random effects assumed to be independently and identically normally distributed. Thus, the parameters can vary between subjects, but also with time through the time-dependent explanatory variables. In practice, for parsimony, random effects and explanatory variables are included for a subset of the parameters.

In this paper, we present and discuss several of these variability models. The random effects have been applied on λ and ρ: $u_\lambda^i \sim \mathcal{N}(0, \sigma_\lambda^2)$, $u_\rho^i \sim \mathcal{N}(0, \sigma_\rho^2)$ for all the models. The explanatory variables used are functions of the dose and of the timing of the r-hIL-7 injections and are used to model the

proliferation rate (π) and the mortality rate (μ_Q). These choices are based on many trials and on previous results of the literature (as in Thiébaut et al. (2014)).

We also need a model for the observations. The state variables $(P^i(t), Q^i(t))$ are not directly observable; we only have discrete-time observations of some functions of the components of this vector. Let Y^i_{1j} and Y^i_{2k} be the CD4 count and the Ki67 count for patient i at time t_{ij} and t_{ik}, respectively. The following observation scheme is assumed:

$$\begin{cases} (Y^i_{1j})^{0.25} & = & (P^i(t_{ij}) + Q^i(t_{ij}))^{0.25} & + & \epsilon_{i1j} \\ (Y^i_{2k})^{0.25} & = & P^i(t_{ik})^{0.25} & + & \epsilon_{i2k} \end{cases}$$

with independently normally distributed measurement errors: $\epsilon_{i1j} \sim \mathcal{N}(0, \sigma^2_{CD4})$, $\epsilon_{i2k} \sim \mathcal{N}(0, \sigma^2_P)$. Note that the times of observations may be different for the two observed components; indeed there were less observations of Ki67 counts than of CD4 counts.

3.2. *Inference.* The vector θ to be estimated includes the intercepts of the biological parameters $(\phi_\lambda, \phi_\rho, \phi_\pi, \phi_{\mu_Q}, \phi_{\mu_P})$, the regression coefficients $(\beta_\pi, \beta_{\mu_Q})$, the variances of the random effects $(\sigma_\lambda, \sigma_\rho)$ and the variances of the measurement errors (σ_{CD4}, σ_P). As in Guedj, Thiébaut and Commenges (2007a), first the individual likelihoods given the random effects can be computed; then, the individual likelihoods are computed by integrating over the random effects via the adaptive Gaussian quadrature (Genz and Keister, 1996; Pinheiro and Bates, 2000); the global log-likelihood is the sum of the individual log-likelihoods. The parameters can then in principle be estimated by maximum likelihood. However, due to identifiability problems, it is useful to adopt an approximate Bayesian approach, as in Drylewicz, Commenges and Thiebaut (2012). The prior distribution $\pi(\theta)$ allows incorporating prior knowledge taken from the literature. In such very complex models MCMC algorithm generally fail, so we use an approximate Bayesian inference, simpler than the INLA approach of Rue, Martino and Chopin (2009) which is also difficult to apply here. Bayes theorem gives

$$\log[P(\theta \mid Y)]) = L(\theta) + \log[\pi(\theta)] + C,$$

where $P(\theta \mid Y)$ is the posterior distribution, $L(\theta)$ is the log-likelihood and C is the normalization constant. The Bernstein-Von Mises theorem (Van der Vaart, 2000) justifies a normal approximation of the posterior (NAP). The NAP can be computed by maximizing the penalized log-likelihood $L^P(\theta) = L(\theta) + log[\pi(\theta)]$ and computing the inverse of the Hessian of $-L^P(\theta)$, $H^{-1}_{L^P}$. Thus, the NAP is $\mathcal{N}(\tilde{\theta}, H^{-1}_{L^P}(\tilde{\theta}))$.

This computation can be achieved with the NIMROD program (Prague et al., 2013) which uses the so-called RVS algorithm (Commenges et al., 2006); parallel computing is implemented to achieve acceptable computation times. Other approaches have been proposed for fitting ODE-based models: Ramsay et al. (2007) proposed a penalized likelihood approach for the trajectories of the state variables circumventing the need of solving the ODE system, but this approach has also numerical issues in presence of random effects; Kuhn and Lavielle (2005) have proposed the stochastic approximation expectation maximisation (SAEM) algorithm which can also be used for maximising a log-likelihood or a penalized log-likelihood. One advantage of the RVS algorithm is the possibility of computing a stringent stopping criterion. See Appendix B for details.

3.3. *Comparison of different models.* Here, we present more than one possible statistical model to describe the effect of r-hIL-7 on biological parameters. To compare them, apart direct likelihood comparison and individual fits, we use an approximate cross-validation criterion, LCVa, proposed by Commenges et al. (2007). LCVa is an extension of Akaike criterion (AIC), similar to the General Information Criterion (GIC) (Konishi and Kitagawa, 2008) that corrects not only for the number of parameters but also for the penalization; LCVa is normalized on the number of observations (see Commenges et al. (2008) and Commenges et al. (2015) for further developments). This criterion is:

$$\text{LCVa} = -\,\text{n}^{-1}[\,\text{L}(\tilde{\theta}) - \text{Trace}(\text{H}_{L^P}^{-1}(\tilde{\theta})\text{H}_L(\tilde{\theta}))],$$

where H_L is the Hessian of minus the log-likelihood. Since LCVa estimates a "risk" (cross-entropy or Kullback-Leibler risk equivalently), the smaller the better. Differences in criteria values between two models can be considered as "large" beyond 0.1 when the response is univariate. However, when the response is multivariate, the threshold for considering a difference as "large" should be higher, because LCVa, as defined here, is normalized on the number of subjects and does not take into account the number of observations per subject.

4. Main results.

4.1. *Basic model: A cycle as a whole entity.* Firstly, we are interested in estimating the global effect of the first cycle of r-hIL-7. To begin with, only first received cycles for each patient have been considered. As in Thiébaut et al. (2014) the effect of r-hIL-7 is considered to be dose-dependent. In our

case, we have chosen a to consider a power of the dose (as is common in pharmacology), that was fixed as 0.25 par profile likelihood (that is, the fourth root of the dose).

The effect on proliferation π is taken into account during 7 days (this time was also fixed by profile likelihood) after each injection. Besides, the effect on the mortality rate μ_Q is considered to be constant from two days after the first injection during twelve months, followed by a linear decrease during another twelve months. As already mentioned, random effects are added on the production rate λ and the reversion rate ρ. Let d_i the dose received for patient i, and let N_t^i the number of injections that patient i has received until time t. The statistical description for this first model is as follows:

$$\begin{cases} \tilde{\pi}^i(t) & = & \tilde{\pi}_0 & & + & \beta_\pi & d_i^{0.25} & \mathbb{1}_{\{N_t^i - N_{t-7}^i = 1\}} \\ \tilde{\lambda}^i(t) & = & \tilde{\lambda}_0 & + & u_\lambda^i \\ \tilde{\mu}_Q^i(t) & = & \tilde{\mu}_{Q_0} & & + & \beta_{\mu_Q} & d_i^{0.25} & f(t) \\ \tilde{\rho}^i(t) & = & \tilde{\rho}_0 & + & u_\rho^i \\ \tilde{\mu}_P^i(t) & = & \tilde{\mu}_{P_0} \end{cases}$$

where $\mathbb{1}_{\{N_t^i - N_{t-7}^i = 1\}}$ is an indicator function taking value 1 if an injection has been administrated in the last 7 days, and

$$(1) \qquad f(t) = \begin{cases} 1 & if & 2 < t \le 360 \\ 1 - (t - 360)/360 & if & 360 < t \le 720 \\ 0 & if & 720 < t \end{cases}$$

Taking the same priors as Thiébaut et al. (2014), we ran the analysis with the NIMROD program. The results are displayed in Table 1; r-hIL-7 injections increase the proliferation rate (π) from 0.041 per day at baseline to 0.135 per day during 7 days after each injection (for the dose equal to 20 μg/kg). Also the estimated mortality rate of Q cells decreases from 0.104 per day at baseline to 0.072 during the first year after the treatment.

4.2. *3 β's model: A cycle as three different injections.*   Here we focus on a major question: Have all the three injections the same quantitative effect on proliferation of CD4$^+$ T cells? Or, more accurately, what is the role of every single injection in the whole effect of a cycle? For this model too, we only consider the first received cycle for each patient. The statistical model for π was:

$$\tilde{\pi}^i(t) = \tilde{\pi}_0 + \sum_{k=1}^{3} \mathbb{1}_{\{N_t^i = k\}} \beta_{\pi_k} d_i^{0.25} \mathbb{1}_{\{N_t^i - N_{t-7}^i = 1\}}$$

TABLE 1
Priors and estimated mean and standard deviation (sd) of all parameters (in logarithmic and natural scales) for the "basic" model when considering only the first cycle for all patients from INSPIRE 1, 2 & 3; Penalized (P) and Non Penalized (NP) likelihoods, and LCVa criteria

	PRIOR (log-scale)		POSTERIOR (log-scale)		POSTERIOR (natural-scale)	
	mean	sd	mean	sd	mean	sd
λ	1.000	1.000	2.967	0.062	**19.440**	*1.196*
ρ	0.000	0.250	0.680	0.095	**1.973**	*0.187*
π	-4.000	1.000	-3.185	0.115	**0.041**	*0.005*
μ_Q	-3.600	0.500	-2.264	0.073	**0.104**	*0.008*
μ_P	-2.500	0.500	-1.550	0.202	**0.212**	*0.043*
β_π					**0.997**	*0.058*
β_{μ_Q}					**-0.305**	*0.020*
σ_λ					**0.254**	*0.025*
σ_ρ					**0.534**	*0.096*
σ_{CD4}					**0.254**	*0.003*
σ_P					**0.299**	*0.023*
P likelihood			**-338.7**			
NP likelihood			**-327.4**			
LCVa			**2.558**			

The results are displayed in Table 2. The quantitative effects of the successive injections are not equal. They are all significantly different from zero; the first and second one are similar but the effect of the third one is considerably weaker. With this model there is a noticeable improvement with respect to the previous one (LCVa is equal to 2.136 vs 2.558).

4.3. *Cycle effect model: Effect of successive cycles.*   Among the 128 treated patients from all the three studies, 74 have received more than one cycle. A key question is: Have these repeated cycles the same quantitative effect with respect to initial ones? CD4 counts are higher before starting repeated cycles. Also, antibodies anti-r-hIL-7 could appear after an initial cycle, modifying the effect of r-hIL-7 when cycles are repeated. The second goal of this paper is to estimate possible quantitative differences in repeated versus initial cycles. To make this possible, we included data from all received cycles and we estimated a new fixed effect: the "cycle effect" β_C. We keep the notation t_{i1} for the time when patient i receives the first injection of a cycle. If $C(t)$ counts the number of cycles received at time t, let $\mathbb{1}_{C(t)>1}$ be 1 if a cycle has been received before time t, 0 otherwise. The cycle effect is incorporated into the statistical model of proliferation rate as follows:

TABLE 2

Priors and estimated mean and standard deviation (sd) of all parameters (in logarithmic and natural scales) for the "3 β's" model when considering only the first cycle for all patients from INSPIRE 1, 2 & 3; Penalized (P) and Non Penalized (NP) likelihoods, and LCVa criteria

	PRIOR (log-scale)		POSTERIOR (log-scale)		POSTERIOR (natural-scale)	
	mean	sd	mean	sd	mean	sd
λ	1.000	1.000	2.355	0.087	**10.541**	*0.920*
ρ	0.000	0.250	0.635	0.102	**1.887**	*0.192*
π	-4.000	1.000	-3.306	0.125	**0.037**	*0.005*
μ_Q	-3.600	0.500	-2.617	0.080	**0.073**	*0.006*
μ_P	-2.500	0.500	-2.187	0.258	**0.112**	*0.029*
$\beta_{\pi1}$					**1.155**	*0.079*
$\beta_{\pi2}$					**1.120**	*0.081*
$\beta_{\pi3}$					**0.622**	*0.073*
β_{μ_Q}					**-0.239**	*0.022*
σ_λ					**0.267**	*0.025*
σ_ρ					**0.575**	*0.108*
σ_{CD4}					**0.241**	*0.003*
σ_P					**0.305**	*0.025*
P likelihood			**-279.8**			
NP likelihood			**-273.3**			
LCVa			**2.136**			

$$\tilde{\pi}^i(\mathrm{t}) = \tilde{\pi}_0 + \left[\beta_C \mathbb{1}_{\{C(t)>1\}} + \sum_{k=1}^{3} \mathbb{1}_{\{N_t^i=k\}} \; \beta_{\pi_k} \; d_i^{0.25} \right] \mathbb{1}_{\{N_t^i - N_{t-7}^i = 1\}}$$

The results are displayed in Table 3. The posterior distribution of the cycle effect β_C has mean equal to -0.163 and standard deviation equal to 0.015. In other words, the cycle effect is found to be significantly negative. In natural scale, the effect on proliferation rate for successive cycles is found to be $\mathrm{e}^{-0.163} = 0.85$ times the effect of the first cycle. The biological interpretation of the cycle effect is not yet clearly explained. One explanation may be that the first cycle has modified the reaction of the immune system to further injections; one possibility is that antibodies against IL-7 decrease the efficient concentration of IL-7 obtained at the target. However, we must take into consideration differences in mean CD4 count before the initial and repeated cycles. The mean CD4 count at baseline was 266 cells/μL whereas it was 456 cells/μL before repeated cycles. Considering the homeostatic regulation of the population of CD4$^+$ cells, that prevents CD4 counts from exceeding 1200-1300 cells/μL, a feedback mechanism may explain an apparent cycle effect. With the aim to deeper study this phenomenon, we have incorporated

a feedback term (see Appendix A). We found that a feedback effect could indeed be detected, but this had no major influence on the estimate of the cycle effect.

TABLE 3

Priors and estimated mean and standard deviation (sd) of all parameters (in logarithmic and natural scales) for the "cycle effect" model when considering all cycles for all patients from INSPIRE 1, 2 & 3; Penalized (P) and Non Penalized (NP) likelihoods, and LCVa criteria

	PRIOR (log-scale)		POSTERIOR (log-scale)		POSTERIOR (natural-scale)	
	mean	sd	mean	sd	mean	sd
λ	1.000	1.000	1.672	0.061	**5.323**	*0.326*
ρ	0.000	0.250	0.892	0.093	**2.440**	*0.226*
π	-4.000	1.000	-2.853	0.074	**0.058**	*0.004*
μ_Q	-3.600	0.500	-2.610	0.068	**0.074**	*0.005*
μ_P	-2.500	0.500	-2.567	0.200	**0.077**	*0.015*
$\beta_{\pi 1}$					**0.931**	*0.042*
$\beta_{\pi 2}$					**0.707**	*0.043*
$\beta_{\pi 3}$					**0.229**	*0.042*
β_{μ_Q}					**-0.082**	*0.006*
β_C					**-0.163**	*0.015*
σ_λ					**0.243**	*0.026*
σ_ρ					**0.515**	*0.084*
σ_{CD4}					**0.289**	*0.003*
σ_P					**0.281**	*0.019*
P likelihood			**-618.6**			
NP likelihood			**-609.4**			
LCVa			**4.762**			

Appendix C and D show some fits of real data from INSPIRE 2 and 3 obtained with this model. Individual predicted trajectories were computed using the Parametric Empirical Bayes (PEB) for the parameters having a random effect (λ and ρ). Several protocols have been compared in the next Section by means of this model.

5. Comparing different protocols for an average patient. We have used the "cycle effect model" to compare different administration protocols of r-hIL-7 containing complete and incomplete cycles. We always assumed that CD4 counts are measured every three months, and a new cycle is administered when CD4 count < 550 cells/μL for 4 years. We examined four possibilities: in protocol A, the patient always receives complete cycles; in protocol B, the patient receives a first complete cycle followed by repeated cycles composed of two injections; in protocol C the patient receives a first complete cycle followed by repeated cycles of one single injection; in protocol D the patient always receives 2-injection cycles (including the initial one).

The protocols were compared according to three criteria computed over a four-year period: number of injections and cycles received, median CD4 count over the follow-up and time spent below 500 cells/μL. The criteria were computed for an average patient having both random effects equal to zero (equilibrium values of 272 and 6.3 for CD4 and Ki67 counts, respectively).

The results are displayed in Table 4, and we can observe the expected trajectories in Figure 2.

A complete cycle followed by 2-injection cycles (Protocol B) could lead to similar results than Protocol A in terms of median CD4 count, with the non negligible advantage that Protocol B requires 15 injections instead of 21. Protocol C ensures and identical time spent under 500 cells/μL with only 10 injections, but achieves a median CD4 count lower than Protocol A. Protocol D is also slightly worse than Protocol A in terms of time below 500 cells/μL.

TABLE 4

Comparison of the number of injections and cycles received, time under 500 CD4 count and median CD4 count for a patient with RE equal to zero for the four protocols through four years. In protocol A, the patient always receives complete cycles; in protocol B, the patient receives a first complete cycle followed by repeated cycles composed of two injections; in protocol C the patient receives a first complete cycle followed by repeated cycles of one single injection; in protocol D the patient always receives 2-injection cycles (including the initial one)

	A	B	C	D
Number of injections received	21	15	10	14
Number of cycles received	7	7	8	7
Time under 500 CD4/μL (days)	60	73	60	87
Median CD4 count	678	663	588	654

6. Adaptive protocols: towards a personalized medicine. Let a patient beginning the r-hIL-7 treatment with a first cycle during which we collect several CD4 count measurements in order to know the value of his random effects. This information can be used to calculate the expected trajectories of this patient when applying the 4 previous protocols. We have taken individual information for two real patients from INSPIRE 2 and INSPIRE 3 studies and we want to compare what would be the best protocol
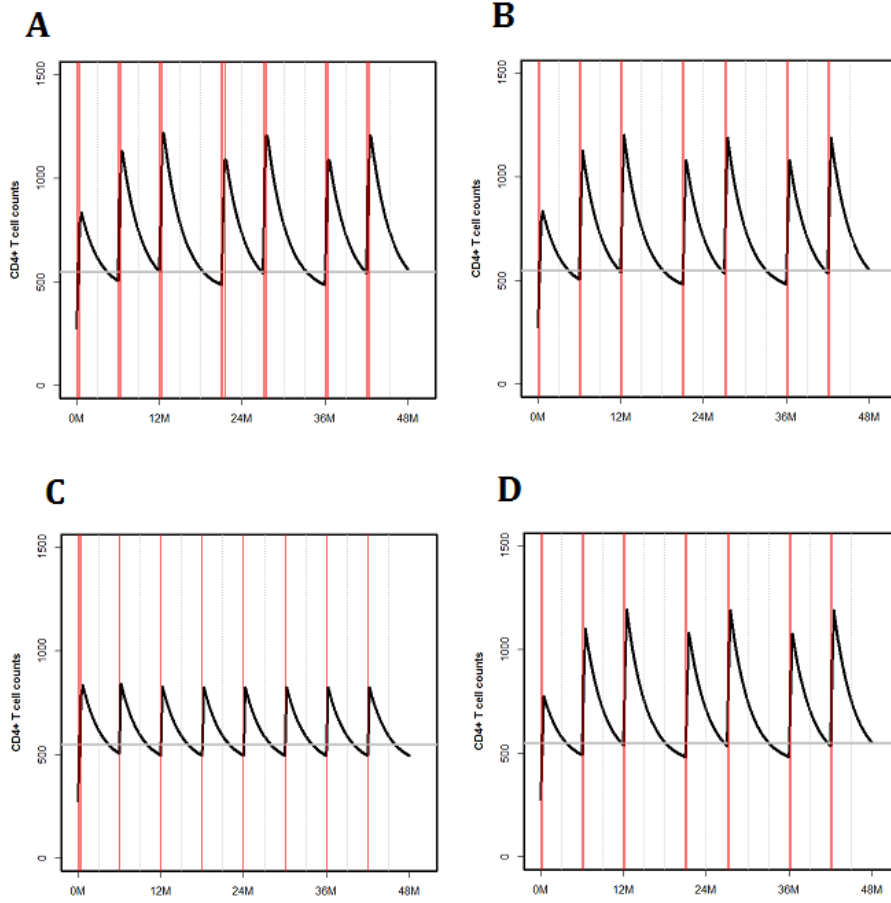
Fig 2: CD4 count (cells/μL) predictions for 4 years for a patient having b^i_ρ = b^i_λ = 0. Protocols A, B and C include a first complete cycle followed by: complete cycles (A), two-injection cycles (B) and one-injection cycles (C). Protocol D includes only 2-injection cycles. Vertical dotted lines are CD4 count assessments (every three months) and vertical solid lines are injections. Horizontal line marks the CD4 threshold of 550 cells/μL.

for them.

Firstly, we have chosen a patient having a very good response in terms of CD4 count. For this patient, the value of the parameters including random effects are equal to $\lambda = 6.586$ and $\rho = 4.797$ (all the other parameters are the population parameters obtained in the "cycle effect" model).

In Figure 3 we predict the expected trajectories and Table 5 displays the

four criteria for this patient. According to our model, there are only minor differences between the four protocols for this patient for the four criteria. Protocol B would spare 2 injections with little impact on the CD4 count and even Protocol C would be admissible.
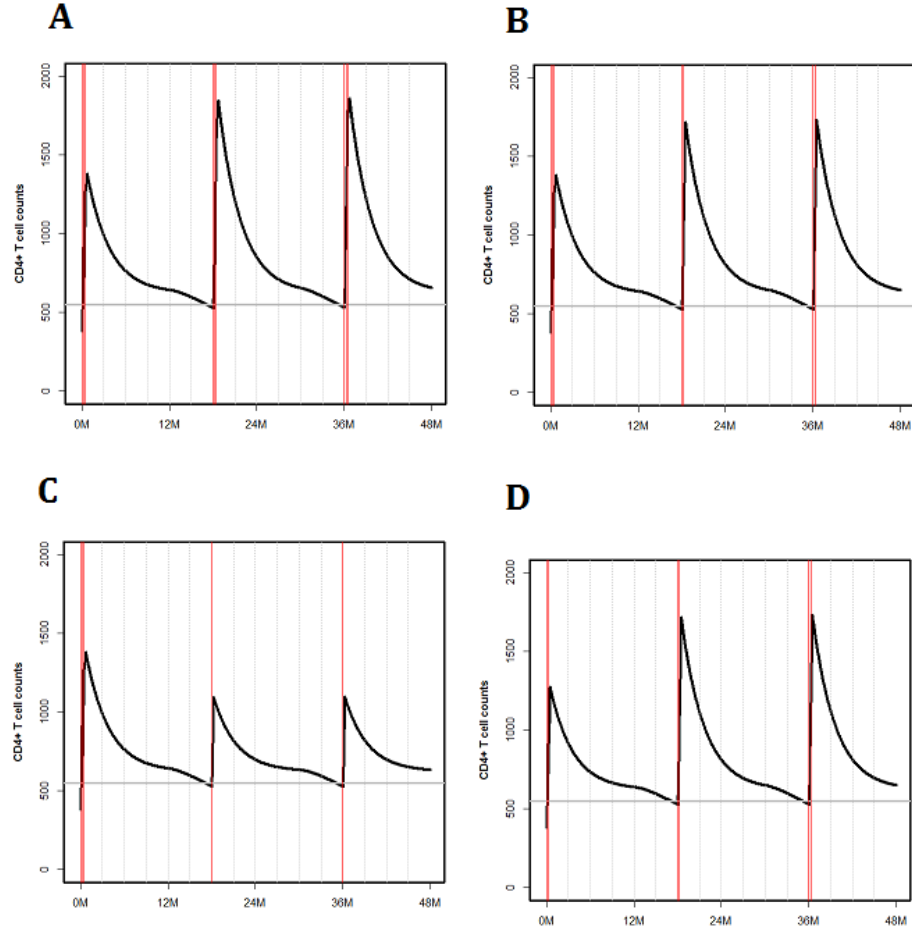
Fig 3: CD4 count (cells/μL) predictions for 4 years for a particularly good responder patient. Protocols A, B and C include a first complete cycle followed by: complete cycles (A), two-injection cycles (B) and one-injection cycles (C). Protocol D includes only 2-injection cycles. Vertical dotted lines are CD4 count assessments (every three months) and vertical solid lines are injections. Horizontal line marks the CD4 threshold of 550 cells/μL.

We have chosen another patient having a particularly poor response to

Comparison of the number of injections and cycles received, time under 500 CD4 count and median CD4 count for a "good responder" patient for the four protocols through four years. In protocol A, the patient always receives complete cycles; in protocol B, the patient receives a first complete cycle followed by repeated cycles composed of two injections; in protocol C the patient receives a first complete cycle followed by repeated cycles of one single injection; in protocol D the patient always receives 2-injection cycles (including the initial one)

	A	**B**	**C**	**D**
Number of injections received	9	7	5	6
Number of cycles received	3	3	3	3
Time under 500 CD4/μL (days)	3	3	3	g 3
Median CD4 count	721	709	669	703

the r-hIL-7 treatment. In this case, the value of the parameters including random effects is equal to $\lambda = 3.284$ and $\rho = 1.956$.

Figure 4 displays the expected trajectories for the different protocols and Table 6 gives the four criteria for this patient. Our model predicts that this patient could benefit from 2-injection cycles (protocol B) without loss of efficiency in terms of CD4 count or time over 500 cells/μL. However, 1-injection cycles (Protocol C) would not be enough.

7. Discussion. INSPIRE 2 and INSPIRE 3 are the first studies where repeated cycles of r-hIL-7 were administrated to test the long-term restoration of the immune system in low immunological responders. Here we have used a simple mathematical model with complex statistical approaches to model the effect of these repeated cycles on $CD4^+$ T cells concentration. We worked with two $CD4^+$ T cells populations: quiescent and proliferating (presenting the Ki67$^+$ marker).

When considering every injection separately, the first important result of this paper is that our model predicts a decreasing effect of successive injections on proliferation rate; the third injection seems to have a weaker effect. We also found that the effect of repeated cycles on proliferation rate was slightly weaker than the effect of the initial one; the order of magnitude, however, is the same. This can be due to the natural homeostatic regulation of $CD4^+$ T cells, since repeated cycles start at a higher CD4 count. In order

A

B

C

D
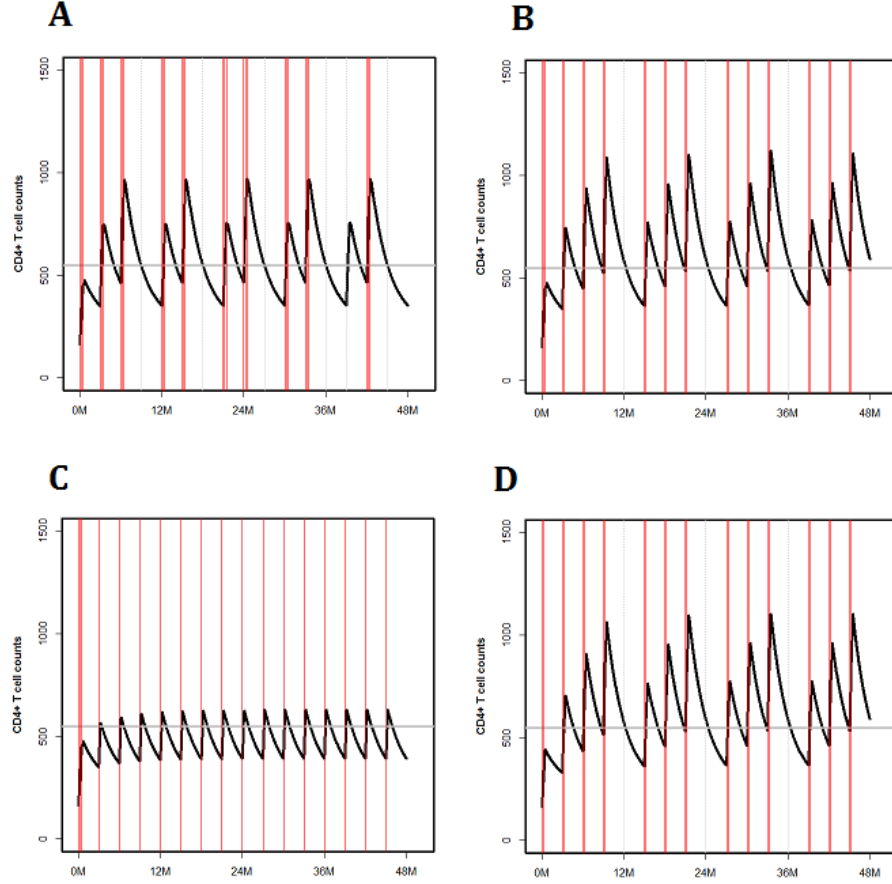
Fig 4: CD4 count (cells/μL) predictions for 4 years for a patient with a particularly poor response. Protocols A, B and C include a first complete cycle followed by: complete cycles (A), two-injection cycles (B) and one-injection cycles (C). Protocol D includes only 2-injection cycles. Vertical dotted lines are CD4 count assessments (every three months) and vertical solid lines are injections. Horizontal line marks the CD4 threshold of 550 cells/μL.

to investigate this question, we have introduced a feedback term; in this case the feedback term slightly improved the fit but the estimate of the "cycle effect" did not change much. Thus although a feedback mechanism is plausible, there may be other reason, such as the presence of antibodies,

TABLE 6

Comparison of the number of injections and cycles received, time under 500 CD4 count and median CD4 count for a "bad responder" patient for the four protocols through four years. In protocol A, the patient always receives complete cycles; in protocol B, the patient receives a first complete cycle followed by repeated cycles composed of two injections; in protocol C the patient receives a first complete cycle followed by repeated cycles of one single injection; in protocol D the patient always receives 2-injection cycles (including the initial one)

	A	B	C	D
Number of injections received	30	27	18	26
Number of cycles received	10	13	16	13
Time under 500 CD4/μL (days)	561	366	893	381
Median CD4 count	549	617	470	611

for a slightly weaker effect of repeated cycles.

Simulations show how these repeated cycles are able to maintain adequate CD4 counts for a long time. We have compared four protocols and shown that cycles of two injections should be sufficient, sparing a certain number of injections without detrimental effect on CD4 count. Our results agree with a survival analysis presented in Thiébaut et al. (2015 in revision) who compared the time spent over 500 cells/μL after a 3-injection cycle and a 2-injection cycle.

Also, the inclusion of random effects is a key ingredient when considering dynamic models as assistance for treatment personalized decisions. Inter-individual differences in parameters imply inter-individual differences in expected trajectories that can be used for devising adaptive treatment strategies (Prague et al., 2012). We could use this mechanistic model for guiding the treatment, with the aim of minimizing the number of administered injections within repeated cycles ensuring the expected response. Predictions could also easily be made for different time lapses between cycles or thresholds for receiving a new cycle.

Some other questions regarding the interaction between the r-hIL-7 and the immune system could be modeled with additional data. For instance, preferential effects on specific T cell subsets as recent thymic emigrants (RTEs) and naive non-RTE T cell populations (Mackall, Fry and Gress, 2011) could be analyzed.

APPENDIX A: MODEL WITH A FEEDBACK TERM

Trajectories satisfying an ODE system have an intrinsic tendency to return to the equilibrium point, when it exists, which is the case for the systems proposed in this paper. In this sense, a feedback term is not necessary to ensure homeostasis, a key concept in physiology. We have, however, considered adding a feedback term in the mathematical model in order to examine the cycle effect β_C in depth. This term will explicitly avoid CD4$^+$ T cells to proliferate without control and possibly ensure a faster return to an equilibrium point. The simplest feedback term is $[\frac{1}{P+Q}]^\nu$, and can be added in both equations to the proliferation term. The system with feedback is as follows:

$$
\begin{cases}
\frac{dQ^i}{dt} = \lambda^i + 2\rho^i P^i - \mu_Q^i Q^i - \pi^i Q^i \frac{1}{(P^i + Q^i)^\nu} \\[2mm]
\frac{dP^i}{dt} = \pi^i Q^i \frac{1}{(P^i + Q^i)^\nu} - \rho^i P^i - \mu_P^i P^i
\end{cases}
$$

Models with feedback were fitted using the 39 patients of INSPIRE who had Ki67 count measurements. The feedback coefficient was estimated at $\nu = 0.119$. In Table 7 we compare some models with and without feedback term.

TABLE 7

Comparison of loglikelihoods and LCVa criteria of models with and without feedback for all INSPIRE patients with CD4 and Ki67 count measurements (N=39)

	WITHOUT FEEDBACK		WITH FEEDBACK	
	Basic model	3 β's model	Basic model	3 β's model
NP loglike	-44.643	-36.549	-41.735	-36.419
P loglike	-49.393	-41.306	-46.965	-41.015
LCVa	1.146	0.940	1.073	0.963

The feedback term does not lead to a great improvement of the LCVa criterion, especially for the 3 β's model.

The detection of a cycle effect raises anew the issue of a possible feedback. It may be that the feedback could not be detected when starting with very low CD4 count, but could be more visible when starting at higher CD4 count; this feedback might explain the apparent cycle effect. To answer this question we ran the model for repeated cycles with feedback. With this more complicated model and larger data set, we could not directly estimate the parameter ν, so we resort to profile likelihood. Computing the likelihood for $\nu = 0.05, 0.1, 0.15, 0.20, 0.25, 0.30$ we found that the best likelihood was obtained for $\nu = 0.1$, a value close to what was estimated in the small data set ($\nu = 0.119$). The results are shown in Table 8.

TABLE 8

Priors and estimated mean and standard deviation (sd) of all parameters (in logarithmic and natural scales) for the "cycle effect" model when considering all cycles for each patient including a feedback term with $\nu = 0.1$; Penalized (P) and Non Penalized (NP) likelihood and LCVa criteria

	PRIOR (log-scale)		POSTERIOR (log-scale)		POSTERIOR (natural-scale)	
	mean	sd	mean	sd	mean	sd
λ	1.000	1.000	0.275	0.157	1.316	0.207
ρ	0.000	0.250	1.052	0.083	2.863	0.238
π	-4.000	1.000	-1.975	0.068	0.139	0.009
μ_Q	-3.600	0.500	-2.538	0.067	0.079	0.005
μ_P	-2.500	0.500	-2.212	0.138	0.109	0.015
$\beta_{\pi 1}$					0.806	0.038
$\beta_{\pi 2}$					0.626	0.037
$\beta_{\pi 3}$					0.212	0.035
β_{μ_Q}					-0.063	0.005
β_C					-0.153	0.015
σ_λ					-0.608	0.097
σ_ρ					-0.440	0.071
σ_{CD4}					0.286	0.004
σ_P					0.301	0.021
P likelihood			**-598.0**			
NP likelihood			**-584.5**			
LCVa			**4.567**			

For the repeated cycles data set, the feedback term leads to an improvement of the LCVa criterion. This may reflect a biological feedback mechanism. However, this does not modify the cycle effect β_C.

APPENDIX B: IDENTIFIABILITY AND CONVERGENCE

As can be easily verified, both models with and without the feedback term, present no problems regarding the "theoretical" identifiability (that depends on the model structure) but even so, they could present "practical" identifiability problems as explained in Guedj, Thiébaut and Commenges (2007b). In fact, practical identifiability problems are a mix of statistical and numerical problems which are difficult to disentangle; with scarce information, the variances of the estimators are large, but it comes also with a flat shape of the log-likelihood, making it difficult to maximize. The difficulty is enhanced by the fact that there are several layers of numerical computation needed to compute the likelihood, leading to an accumulation of numerical errors.

A crucial point in an iterative algorithm is the stopping criteria. Besides the displacement in the parameter space and the variation of the likelihood function, another convergence criterion proposed by Commenges et al. (2006) has been implemented in NIMROD. It is the Relative Distance to Maximum (RDM) defined as

$$\mathrm{RDM}(\theta^{(k)}) = \frac{U^P(\theta^{(k)})^T G^{-1}(\theta^{(k)}) U^P(\theta^{(k)})}{p}$$

where $U^P(\cdot)$ is the penalized score and $G(\cdot)$ is an approximation of the Hessian of minus the penalized likelihood. This criterion can be interpreted as the ratio of the numerical error over the statistical error, and is asymptotically invariant near the maximum to any one-to-one transformation of the parameters. Prague et al. (2013) propose 0.1 as a good default value.

APPENDIX C: SOME FITS OF TOTAL CD4$^+$ T CELL COUNTS
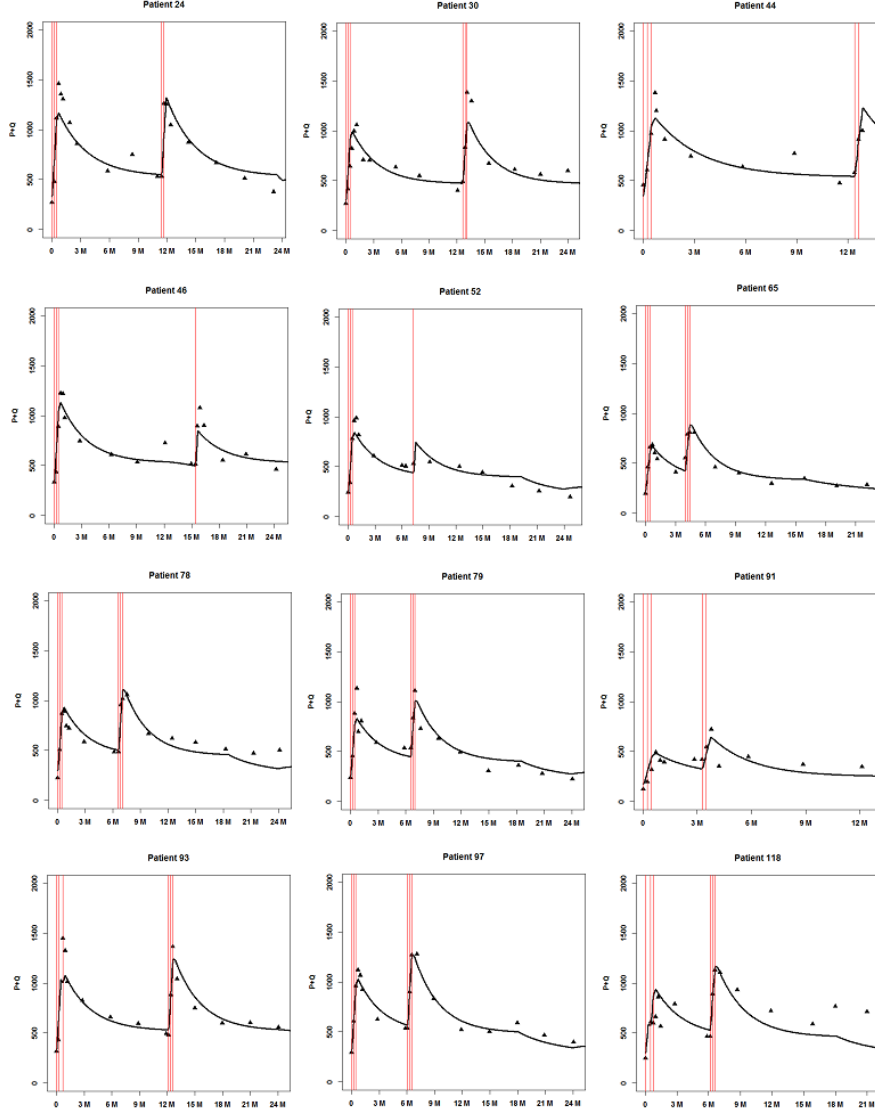
Fig 5: *Cycle effect model*: Fits of total CD4 count for 12 patients from INSPIRE 2 and 3 chosen randomly among those who received more than a cycle.

APPENDIX D: SOME FITS OF CD4$^+$KI67$^+$ T CELLS

Fig 6: *Cycle effect model*: Fits of Ki67 count for 6 patients from INSPIRE and INSPIRE 2 chosen randomly among those who had measurements for this biomarker (only during the first cycle).

ACKNOWLEDGEMENTS

REFERENCES

BEQ, S., RANNOU, M.-T., FONTANET, A., DELFRAISSY, J.-F., THÈZE, J. and COLLE, J.-H. (2004). HIV infection: pre-highly active antiretroviral therapy IL-7 plasma levels correlate with long-term CD4 cell count increase after treatment. *Aids* **18** 563–565.

COMMENGES, D., JACQMIN-GADDA, H., PROUST, C. and GUEDJ, J. (2006). A newton-like algorithm for likelihood maximization: The robust-variance scoring algorithm. *arXiv preprint math/0610402*.

COMMENGES, D., JOLY, P., ANNE, G.-P. and LIQUET, B. (2007). Choice between Semiparametric Estimators of Markov and Non-Markov Multi-state Models from Coarsened Observations. *Scandinavian Journal of Statistics* **34** 33–52.

COMMENGES, D., SAYYAREH, A., LETENNEUR, L., GUEDJ, J., BAR-HEN, A. et al. (2008). Estimating a difference of Kullback–Leibler risks using a normalized difference of AIC. *The Annals of Applied Statistics* **2** 1123–1142.

COMMENGES, D., PROUST-LIMA, C., SAMIERI, C. and LIQUET, B. (2015). A universal approximate cross-validation criterion for regular risk functions. *The international journal of biostatistics* **11** 51–67.

DRYLEWICZ, J., COMMENGES, D. and THIEBAUT, R. (2012). Maximum a Posteriori estimation in dynamical models of primary HIV infection. *Statistical Communications in Infectious Diseases* **4**.

FRY, T. J. and MACKALL, C. L. (2002). Interleukin-7: from bench to clinic. *Blood* **99** 3892–3904.

GENZ, A. and KEISTER, B. (1996). Fully symmetric interpolatory rules for multiple integrals over infinite regions with Gaussian weight. *Journal of Computational and Applied Mathematics* **71** 299–309.

GUEDJ, J., THIÉBAUT, R. and COMMENGES, D. (2007a). Maximum likelihood estimation in dynamical models of HIV. *Biometrics* **63** 1198–1206.

GUEDJ, J., THIÉBAUT, R. and COMMENGES, D. (2007b). Practical identifiability of HIV dynamics models. *Bulletin of mathematical biology* **69** 2493–2513.

HO, D. D., NEUMANN, A. U., PERELSON, A. S., CHEN, W., LEONARD, J. M., MARKOWITZ, M. et al. (1995). Rapid turnover of plasma virions and CD4 lymphocytes in HIV-1 infection. *Nature* **373** 123–126.

KONDRACK, R. M., HARBERTSON, J., TAN, J. T., MCBREEN, M. E., SURH, C. D. and BRADLEY, L. M. (2003). Interleukin 7 regulates the survival and generation of memory CD4 cells. *The Journal of experimental medicine* **198** 1797–1806.

KONISHI, S. and KITAGAWA, G. (2008). *Information criteria and statistical modeling.* Springer Science & Business Media.

KUHN, E. and LAVIELLE, M. (2005). Maximum likelihood estimation in nonlinear mixed effects models. *Computational Statistics & Data Analysis* **49** 1020–1038.

LEVY, Y., LACABARATZ, C., WEISS, L., VIARD, J.-P., GOUJARD, C., LELIÈVRE, J.-D., BOUÉ, F., MOLINA, J.-M., ROUZIOUX, C., AVETTAND-FÉNOÊL, V. et al. (2009). Enhanced T cell recovery in HIV-1–infected adults through IL-7 treatment. *The Journal of clinical investigation* **119** 997.

LEVY, Y., SERETI, I., TAMBUSSI, G., ROUTY, J., LELIEVRE, J., DELFRAISSY, J., MOLINA, J., FISCHL, M., GOUJARD, C., RODRIGUEZ, B. et al. (2012). Effects of recombinant human interleukin 7 on T-cell recovery and thymic output in HIV-infected patients receiving antiretroviral therapy: results of a phase I/IIa randomized, placebo-controlled, multicenter study. *Clinical infectious diseases* **55** 291–300.

MACKALL, C. L., FRY, T. J. and GRESS, R. E. (2011). Harnessing the biology of IL-7 for therapeutic application. *Nature Reviews Immunology* **11** 330–342.

MACKALL, C. L., FRY, T. J., BARE, C., MORGAN, P., GALBRAITH, A. and GRESS, R. E. (2001). IL-7 increases both thymic-dependent and thymic-independent T-cell regeneration after bone marrow transplantation. *Blood* **97** 1491–1497.

NAMEN, A., SCHMIERER, A., MARCH, C., OVERELL, R., PARK, L., URDAL, D. and MOCHIZUKI, D. (1988). B cell precursor growth-promoting activity. Purification and characterization of a growth factor active on lymphocyte precursors. *The Journal of experimental medicine* **167** 988–1002.

OKAMOTO, Y., DOUEK, D. C., MCFARLAND, R. D. and KOUP, R. A. (2002). Effects of exogenous interleukin-7 on human thymus function. *Blood* **99** 2851–2858.

PERELSON, A. S., NEUMANN, A. U., MARKOWITZ, M., LEONARD, J. M. and HO, D. D. (1996). HIV-1 dynamics in vivo: virion clearance rate, infected cell life-span, and viral generation time. *Science* **271** 1582–1586.

PINHEIRO, J. C. and BATES, D. M. (2000). *Mixed-effects models in S and S-PLUS.* Springer.

PRAGUE, M., COMMENGES, D., DRYLEWICZ, J. and THIÉBAUT, R. (2012). Treatment Monitoring of HIV-Infected Patients based on Mechanistic Models. *Biometrics* **68** 902–911.

PRAGUE, M., COMMENGES, D., GUEDJ, J., DRYLEWICZ, J. and THIÉBAUT, R. (2013). NIMROD: A program for inference via a normal approximation of the posterior in models with random effects based on ordinary differential equations. *Computer methods and programs in biomedicine* **111** 447-458.

RAMSAY, J. O., HOOKER, G., CAMPBELL, D. and CAO, J. (2007). Parameter estimation for differential equations: a generalized smoothing approach. *Journal of the Royal Statistical Society: Series B (Statistical Methodology)* **69** 741–796.

RUE, H., MARTINO, S. and CHOPIN, N. (2009). Approximate Bayesian inference for latent Gaussian models by using integrated nested Laplace approximations. *Journal of the royal statistical society: Series b (statistical methodology)* **71** 319–392.

SEDDON, B., TOMLINSON, P. and ZAMOYSKA, R. (2003). Interleukin 7 and T cell receptor signals regulate homeostasis of CD4 memory cells. *Nature immunology* **4** 680–686.

SERETI, I., DUNHAM, R. M., SPRITZLER, J., AGA, E., PROSCHAN, M. A., MEDVIK, K., BATTAGLIA, C. A., LANDAY, A. L., PAHWA, S., FISCHL, M. A. et al. (2009). IL-7 administration drives T cell–cycle entry and expansion in HIV-1 infection. *Blood* **113**

6304-6314.

Sereti, I., Estes, J. D., Thompson, W. L., Morcock, D. R., Fischl, M. A., Croughs, T., Beq, S., de Micheaux, S. L., Yao, M. D., Ober, A. et al. (2014). Decreases in colonic and systemic inflammation in chronic HIV infection after IL-7 administration. *PLoS Pathog* **10** e1003890.

Sportès, C., Hakim, F. T., Memon, S. A., Zhang, H., Chua, K. S., Brown, M. R., Fleisher, T. A., Krumlauf, M. C., Babb, R. R., Chow, C. K. et al. (2008). Administration of rhIL-7 in humans increases in vivo TCR repertoire diversity by preferential expansion of naive T cell subsets. *The Journal of experimental medicine* **205** 1701–1714.

Thiébaut, R., Drylewicz, J., Prague, M., Lacabaratz, C., Beq, S., Jarne, A., Croughs, T., Sekaly, R.-P., Lederman, M. M., Sereti, I. et al. (2014). Quantifying and Predicting the Effect of Exogenous Interleukin-7 on CD4+ T Cells in HIV-1 Infection. *PLoS computational biology* **10** e1003630.

Thiébaut, R., Jarne, A., Routy, J.-P., Sereti, I., Fischl, M., Ive, P., Speck, R. et al. (2015 in revision). Repeated Cycles of Recombinant Human Interleukin 7 in HIV-Infected Patients with low CD4 T cell reconstitution on Antiretroviral Therapy: Results of two Phase II Multicenter Studies.

Van der Vaart, A. W. (2000). *Asymptotic statistics* **3**. Cambridge university press.

Vieira, M., Soares, D., Borthwick, N. J., Maini, M. K., Janossy, G., Salmon, M. and Akbar, A. N. (1998). IL-7-dependent extrathymic expansion of CD45RA+ T cells enables preservation of a naive repertoire. *The Journal of Immunology* **161** 5909–5917.

E-mail: rodolphe.thiebaut@isped.u-bordeaux2.fr

Appendix F

HIV epidemy figures in Navarra (Spain)

F.1 Introduction

During this period I have had the opportunity to participate into the **Merimée 2014 program: International Ph Degree**, a program searching to encourage a structured and sustainable cooperation between French doctoral schools and Spanish partners. It is a shared scientific project including the reception of doctoral students in French and Spanish doctoral programs. In my case, I did a 3 months internship at the *Universidad Pública de Navarra* (Spain), under the supervision of Pr Francisco Guillén, Aurelio Barricarte and Jesús Castilla. The original purpose (that was subsequently extended as we will see) was to update a previous work presented in the thesis work of Dr Pablo Aldaz: a population based study of the HIV and AIDS epidemic in the region of Navarra.

According to the census, there were 640.356 people living in Navarra on January 1st, 2014; of which 50.3% were women. Many of these people (90.7%) were born in Spain, and among the foreign nationals, Europeans represent a majority, followed by Africans and Americans. We can observe in Figure F.1 the demographic pyramid corresponding to an aging population, where the birth rate is dropping and life expectancy is rising.
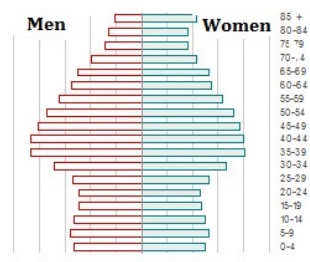
Figure F.1: Population pyramid in Navarra (Spain). Obtained from http:// www.navarra.es/home_es/Navarra/Asi+es+Navarra/Navarra+en +cifras/Demografia/poblacion.htm at October, 1st 2015

Characteristics of the region of Navarra (with a relatively low population density), where diagnosis and treatment of HIV infections are centralized in few hospitals, let an early data collection and follow up. Since 1985 Navarra has had an official registration of all the detected cases of HIV infection, AIDS diagnosis and deaths of people living with HIV. This database offers a global and realistic vision of the epidemic by including individuals that are normally under-represented in these clinical cohorts, as people who are not regularly provided attention through the health system or those who die due to causes beyond the HIV infection.

Since the first case in 1985, there have been 1861 HIV diagnosis, and the epidemic has not shown a homogeneous trend through time. Some important events as the development of tests for early detection and, specially, the emergence of cART therapy have been turning points in life expectancy and quality of life. For instance, new infections have decreased in 33% since 2001. Here, we want to review the epidemic since the first cases were diagnosed until January 1st, 2014. With the aim to have an adjusted and precise view of the impact of this infection in Navarra, we have focused our work on four main axis:

F.2   Descriptive analysis of data

At the beginning, the idea was essentially to do an update of the work realized by Dr Pablo Aldaz for his PhD degree: to do a descriptive analysis of HIV infection from 1985 to 2013, both included. To begin with, in Table F.1 we can observe the trend of the number of HIV diagnosis.

Table F.1: Number of HIV diagnosis in Navarra by period from 1985 to 2013

Period	Number of cases	Percentage
1985-1989	569	30,6
1990-1993	465	25,0
1994-1997	250	13,4
1998-2001	174	9,3
2002-2005	135	7,3
2006-2009	131	7,0
2010-2013	137	7,4

The incidence appears to have stalled since the year 2000. However, if we consider annual data, we can observe a slight upturn in the last years (data not shown). Regarding the mode of transmission, in our days a large majority of new infections are contracted via the sexual pathway.

In Figure F.2 and F.3 we have represented the mean age at diagnosis of HIV by sex, where we can observe an upward trend for both men and women.

The proportion of foreign nationals among the new diagnosis has shown an increasing trend, and in the last years this proportion has been of about 35% (data not shown).
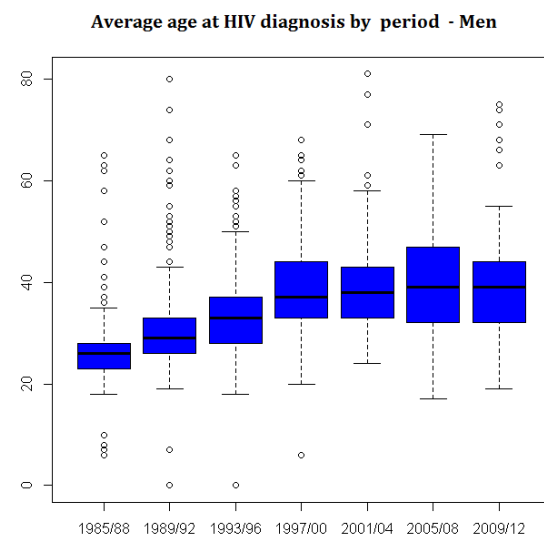
Figure F.2: Mean age at HIV diagnosis among men
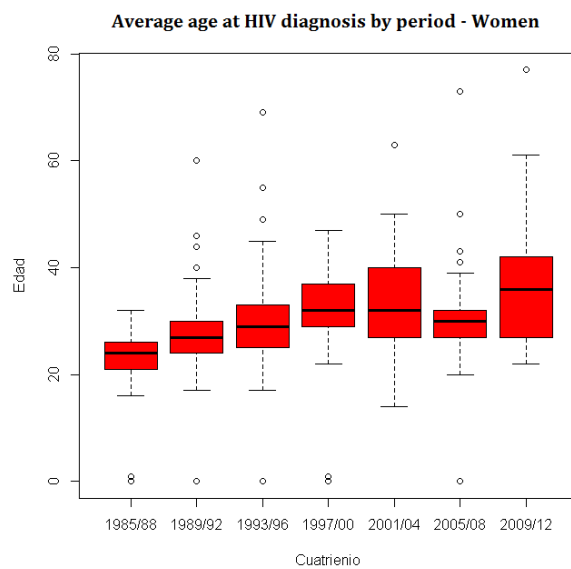
Figure F.3: Mean age at HIV diagnosis among women

Table F.2: Multivariate descriptive analysis of the dependance of the late diagnosis on age, sex, period of diagnosis, origin or way of transmission

	Coefficient	Pr($> |z|$)	Confidence interval
Age by group			
0 - 19	0.891	0.856	(0.256,3.099)
20 - 29	1		
30 - 39	1.576	0.037	(1.027,2.417)
40 - 49	3.882	< 0.01	(2.350,6.415)
≥ 50	4.959	< 0.01	(2.818,8.728)
Sex			
Men	1		
Women	0.935	0.723	(0.645,1.355)
Period			
1985-1989	0.613	0.088	(0.349,1.077)
1990-1993	1		
1994-1997	1.818	0.013	(1.132,2.922)
1998-2001	1.280	0.369	(0.747,2.195)
2002-2005	1.202	0.556	(0.651,2.220)
2006-2009	0.963	0.909	(0.508,1.827)
2010-2013	0.523	0.068	(0.261,1.050)
Nationality			
Spanish	1		
Other	0.989	0.965	(0.602,1.625)
Way of transmission			
Sexual	1		
IDUs	0.490	< 0.001	(0.326,0.735)
Other	0.806	0.475	(0.446,1.458)

F.3 Diagnostic delay

In the second part we deal with one of today's main obstacles for effective control of HIV infection, both at individual and epidemic levels: the late diagnosis, here defined as a simultaneous diagnosis of HIV and AIDS (within the same month or over two consecutive months).

We will use a multivariate analysis carried out through a logistic regression, in order to study the dependence of the response variable (late diagnosis) on some factors such as age, sex, way of transmission, CD4 baseline or origin. We must consider that it was not until 2002 that CD4 count baseline was systematically referred. Specifically, this information is available for 459 of 1861 patients (25%). Age was stratified and the reference group was chosen to be people aged 20-29 (see Table F.2).

The following key conclusions can be drawn: Older age groups are significantly more likely to have a late diagnosis, while sex does not appear to be relevant. With respect to the period of diagnosis, there is only the segment of 1994-1997 where the percentage of late diagnosis was significantly higher than the reference segment of 1990-1993. We have found no effect of the origin in late diagnosis. Sexual way appears as having a more important probability of being diagnosed with CD4 count < 350 cells/μL.

Table F.3: Comparison of the dependance of diagnostic delay according to the definition on age, sex, period, origin and way of transmission

	SIMULTANEOUS DIAGNOSIS	LATE DIAGNOSIS	ADVANCED DISEASE
Age by group			
	0 - 19	0 - 19	0 - 19
	20 - 29	**20 - 29**	**20 - 29**
	30 - 39	30 - 39 aos	30 - 39
	40 - 49	40 - 49	40 - 49
	≥ 50	≥ 50	≥ 50
Sex			
	Men	**Men**	**Men**
	Women	Women	Women
Period			
	2002-2005	**2002-2005**	**2002-2005**
	2006-2009	2006-2009	2006-2009
	2010-2013	2010-2013	2010-2013
Nationality			
	Spanish	**Spanish**	**Spanish**
	Other	Other	Other
Way of transmission			
	Sexual	**Sexual**	**Sexual**
	IDUs	IDUs	IDUs
	Other	Other	Other

Now, we will study the relationship between CD4 count and late diagnosis. We will use three different ways to refer to diagnostic delay based on CD4 count, that will be evaluated and compared.

- Late diagnosis : CD4 count < 350 cells/mm^3 at HIV diagnosis

- Advanced disease : CD4 count < 200 cells/mm^3 at HIV diagnosis

In order to evaluate and compare these two markers, we will rely on data from 2002 up to now, because as it has been said, available CD4 measurements before 2002 were incomplete. We have once again made a multivariate analysis, only for these last years (Table F.3).

As it can be verified, no major differences have been found with these three definitions. Only the fact of being infected through IDUs way appears no more as a "protective" factor.

F.4 Survival analysis : Cox model and Kaplan-Meier curves

In this third part we focus on a survival study of two events of interest: analyzing two survival times: the AIDS-free time (time since HIV diagnosis to first AIDS-defining event) and the time since HIV diagnosis to death. As in any survival study, data we count on present some characteristics that prevent us

from applying usual methods of data analysis. It must be taken into account that we have a great quantity of censured observations: people with a diagnosis of HIV infection that have not developed AIDS and/or are still alive.

F.4.1   Analysis of the AIDS-free time

To get an idea of how the AIDS-free time is distributed globally, we can find the Kaplan-Meier survival curves for the event "diagnosis of AIDS" in relation to the sex (Figure F.4) and also to the age group (Figure F.5).
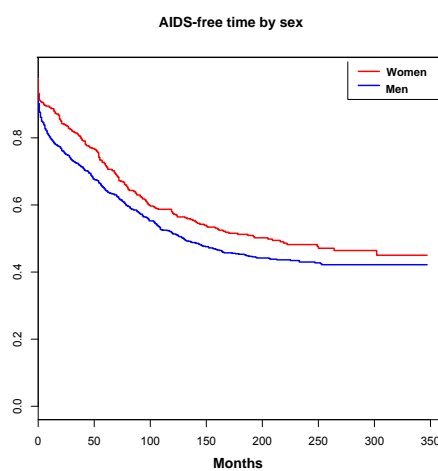
Figure F.4:   Kaplan-Meier survival curve when the event is the diagnosis of AIDS with respect to the sex
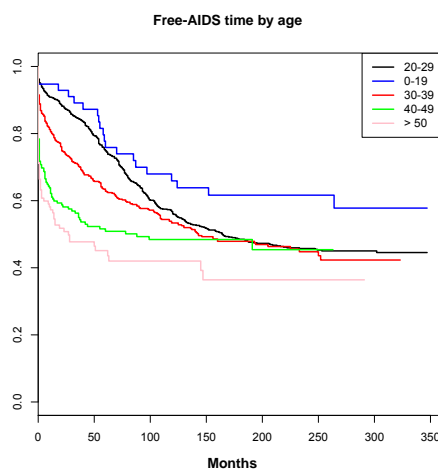
Figure F.5:   Kaplan-Meier survival curve when the event is the diagnosis of AIDS with respect to the age group

In Figure F.6 survival curves for the entire population distinguishing between the existence or not of a diagnosis delay (defined by CD4 < 200 cells/μL):

AIDS-free time by CD4 count
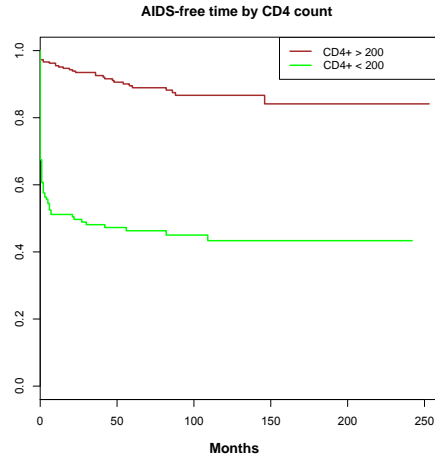
Figure F.6: Kaplan-Meier survival curve when the event is the diagnosis of AIDS by distinguishing by CD4 count bigger or lower than 200 cells/μL

The log-rank test (also called Mantel-Haenszel test) tells us that in both cases curves are significantly different (p-value < 0.001). Logically a CD4 count below 200 cells/μL at diagnosis augurs a worse survival than a CD4 count below 350 cells/μL.

F.4.2 Analysis of survival time: from HIV diagnosis to death

If we apply a Cox model for the survival time from HIV diagnosis to death, we find similar results (see Table F.4).

In view of the results achieved, you might think that being a foreigner is a protective factor. However, the large-scale immigration is a recent phenomenon in Navarra that has coincided in time with the development of cART, and the resulting improvement in life expectancy.

F.5 Survival study: Parametric models

Although the Cox model is the most widely used in this type of analysis, parametric models are considered as being more precise for estimating the probability of survival. Furthermore, this type of models is essential if we want to obtain the risk function in an explicit form, for instance if we want to compute the absolute value of survival function for a specific value of a covariate.

After the appearance of cART, the use of these parametric models has considerably expanded when studying the survival of people living with HIV. Data from the "ART Cohort Collaboration", collecting 13 trials from Europe and North America, have been used for several studies which have shown the relevance of using parametric models, and especially Weibull based models (Egger

Table F.4: Survival analysis for the time from HIV diagnosis to death

	Coefficient	Pr($> |z|$)
Sex		
Men	1	
Women	0.736	< 0.01
Age		
0-19	0.751	0.190
20 - 29	1	
30 - 39	1.637	< 0.01
40 - 49	3.191	< 0.01
≥ 50	4.288	< 0.01
Period		
1985-1989	1.229	0.015
1990-1993	1	
1994-1997	0.457	< 0.01
1998-2001	0.305	< 0.01
2002-2005	0.179	< 0.01
2006-2009	0.142	< 0.01
2010-2013	0.388	< 0.01
Nationality		
Spanish	1	
Other	0.317	< 0.01

et al., 2002; May et al., 2004). Also, an Australian cohort of HIV patients was used to compare the relevance of four parametric survival models: exponential, Weibull, log-normal and log-logistic. Results can be found in Nakhaee and Law (2011).

Here, we wanted to apply six parametric models to our data, in order to evaluate differences among them, as well as comparing survival functions from these models with the one obtained with Kaplan-Meier (see Table F.5).

Table F.5: Comparing likelihood function for each one of the parametric models

PARAMETRIC MODEL	Likelihood	p-value
Exponential	-5557.2	< 0.01
Gaussian	-6010.1	< 0.01
Logistic	-6044.2	< 0.01
Weibull	-5521.5	< 0.01
Log-normal	-5544.2	< 0.01
Log-logistic	-5515.4	< 0.01

We will only develop the Weibull model, because it is the most extended (Table F.6):

When comparing both survival curves (the one obtained with Kaplan-Meier and the one obtained with the parameteric Weibull model) they are overlapping.

Table F.6: Weibull model applied to our data

	Coefficient	$\Pr(> \|z\|)$
Sex		
Men	1	
Women	0.764	< 0.001
Age by group		
0-19	0.743	0.176
20-29	1	
30-39	1.655	< 0.01
40-49	3.201	< 0.01
> 50	4.319	< 0.01
Nationality		
Spanish	1	
Other	0.318	< 0.01
Period		
1985-1989	1.216	0.021
1990-1993	1	
1994-1997	0.467	< 0.01
1998-2001	0.318	< 0.01
2002-2005	0.189	< 0.01
2006-2009	0.152	< 0.01
2010-2013	0.376	0.04

Comparing survey functions
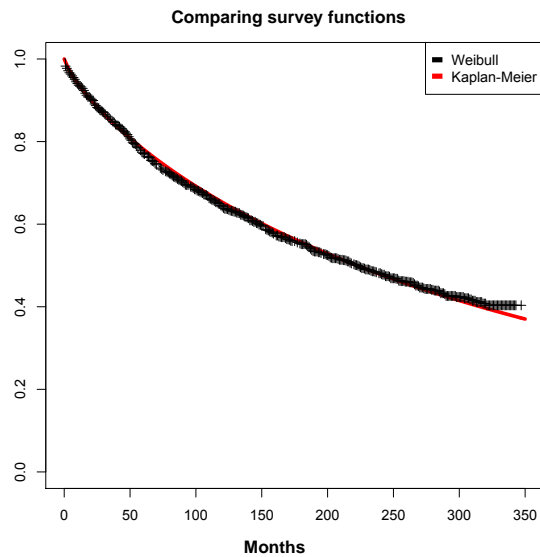
F.6 Estimating the number of people living with HIV infection without diagnosis in Navarra

To know the number of people infected with HIV, estimation models are necessary. Alternatively, for knowing this data exactly, we should test everybody regularly, which is logistically impossible and ethically problematical. UNAIDS facilitates a software for estimating this figure for all countries. To create the original files that will be used by this program, there is in every country a team of epidemiologists, demographists and other specialists. Once data are collected, each country sends their files, that will be revised by UNAIDS and validated in collaboration with WHO and UNICEF. UNAIDS is responsible for ensuring that results are presented in a homogeneous way and can be compared across countries and through time.

Software used for these estimations is called Spectrum and EPP (Estimates and Projections Package), and it was developed by the *Institute Futures*. In Mars 2013, the group *Reference Group on Estimates, Modeling and Projections* published the most recent guide for the utilization of Spectrum. Spectrum is formed by different projects, and the project we are interested in is called *AIM: AIDS impact model*. It can be used to make national and regional estimation as the number of people living with HIV or the number of new infections. Also since 2013, Spectrum has contained the package EPP (Estimates and Projection Package) that can be used to design epidemic curves.

For countries considered of "concentrated epidemic", like Spain, demographic and epidemiological data must be provided (as the number of persons under cART) to adequately use the program Spectrum. The information required concerns, on the one hand, the sub-populations that are at increased risk of acquiring HIV (sex workers, IDUs) and, on the other hand, the general population. When estimating prevalence, data from reported HIV cases and supervision of pregnant women are necessary for the general population, and repeated prevalence studies will be required for sub-populations at increased risk. As for the estimation of the incidence in general population, prevalence curves and information about the number of people under cART will be necessary, while incidence estimations among risk populations will be based on prevalence and death rates, as well as on hypotheses of HIV transmission and progression based on literature revision and analysis of raw data of experts.

Every country will send estimations every two years. In 2012, 186 countries sent these data, that will be used by Spectrum for computing estimations and make them public. Data from 155 of these countries were shared in 2013 (this is not the case for Spain). In 2013, some improvements in estimation method were applied, as calculating incidence based on people under cART from 15 to 49, instead of everybody over 15, revised of mortality by AIDS-non-related causes among IDUs.

Based on this program, we have estimated general rates for Spanish people and they have been prorated to the number of people living in Navarra. When considering that Spanish people are 46.727.890 while Navarra people are 644.566, we have divided the estimations by $644.566/46.727.890 = 0.0138$.

We obtained that the number of estimated AIDS-related deaths in Navarra in 2012 could be 10.99 (9.79,12.14), while data tells us that there were 11 persons who died in this period. Similarly, the number of new HIV diagnosis in 2013

is estimated to be 45.00 (29.86,59.73) where 43 real diagnosis were found in Navarra in this period.

Finally, the number of people living with HIV is estimated by Spectrum as being equal to 2045 (1830,2243). If we consider that 1013 persons are diagnosed in Navarra at this moment, we could conclude that approximately half of the people living nowadays with HIV are not diagnosed. However, this data must be treated very carefully, and estimations about size and HIV prevalence among risk categories should be provided to increase the accuracy.

Bibliography

Abul K Abbas, Andrew HH Lichtman, and Shiv Pillai. *Cellular and molecular immunology: with STUDENT CONSULT Online Access*. Elsevier Health Sciences, 2011.

D Abrams, Y Lévy, M Losso, A Babiker, G Collins, D Cooper, J Darbyshire, S Emery, L Fox, F Gordin, et al. Interleukin-2 therapy in patients with hiv infection. *The New England journal of medicine*, 361(16):1548–59, 2009.

Laith J Abu-Raddad. Role of acute hiv infection in driving hiv transmission: Implications for hiv treatment as prevention. *PLoS medicine*, 12(3):e1001803–e1001803, 2015.

Kahtonna Allen, Octavio Mesner, Anuradha Ganesan, Thomas A OBryan, Robert G Deiss, Brian K Agan, and Jason F Okulicz. Association between hepatitis b vaccine antibody response and cd4 reconstitution after initiation of combination antiretroviral therapy in hiv-infected persons. *BMC infectious diseases*, 15(1):203, 2015.

Brigitte Autran, Guislaine Carcelain, Tao Sheng Li, Catherine Blanc, Dominique Mathez, Roland Tubiana, Christine Katlama, Patrice Debre, and Jacques Leibowitch. Positive effects of combined antiretroviral therapy on cd4+ t cell homeostasis and function in advanced hiv disease. *Science*, 277 (5322):112–116, 1997.

Valérie Badot, Remco KMAC Luijten, Joel A van Roon, Geneviève Depresseux, Selda Aydin, Benoît J Van den Eynde, Frédéric A Houssiau, and Bernard R Lauwerys. Serum soluble interleukin 7 receptor is strongly associated with lupus nephritis in patients with systemic lupus erythematosus. *Annals of the rheumatic diseases*, pages annrheumdis–2012, 2012.

Françoise Barré-Sinoussi, Jean-Claude Chermann, Fetal Rey, Marie Therese Nugeyre, Sophie Chamaret, Jacqueline Gruest, Charles Dauguet, Charles Axler-Blin, Françoise Vézinet-Brun, Christine Rouzioux, et al. Isolation of a t-lymphotropic retrovirus from a patient at risk for acquired immune deficiency syndrome (aids). *Science*, 220(4599):868–871, 1983.

Françoise Barré-Sinoussi, Anna Laura Ross, and Jean-François Delfraissy. Past, present and future: 30 years of hiv research. *Nature Reviews Microbiology*, 11 (12):877–883, 2013.

Manuel Battegay, Reto Nüesch, Bernard Hirschel, and Gilbert R Kaufmann. Immunological recovery and antiretroviral therapy in hiv-1 infection. *The Lancet infectious diseases*, 6(5):280–287, 2006.

Caroline Bazzoli, Vincent Jullien, Clotilde Le Tiec, Elisabeth Rey, France Mentré, and Anne-Marie Taburet. Intracellular pharmacokinetics of antiretroviral drugs in hiv-infected patients, and their correlation with drug action. *Clinical pharmacokinetics*, 49(1):17–45, 2010.

Stéphanie Beq, Jean-François Delfraissy, and Jacques Theze. Interleukin-7 (il-7): immune function, involvement in the pathogenesis of hiv infection and therapeutic potential. *European cytokine network*, 15(4):279–289, 2004.

Marion Berard and David F Tough. Qualitative differences between naive and memory t cells. *Immunology*, 106(2):127–138, 2002.

Ronell Bologna-Molina, Adalberto Mosqueda-Taylor, Nelly Molina-Frechero, Ana D Mori-Estevez, and Guillermo Sánchez-Acuña. Comparison of the value of pcna and ki-67 as markers of cell proliferation in ameloblastic tumor. *Medicina oral, patologia oral y cirugia bucal*, 18(2):e174, 2013.

W John Boscardin, Jeremy MG Taylor, and Ngayee Law. Longitudinal models for aids marker data. *Statistical Methods in Medical Research*, 7(1):13–27, 1998.

Onur Boyman and Jonathan Sprent. The role of interleukin-2 during homeostasis and activation of the immune system. *Nature Reviews Immunology*, 12(3): 180–190, 2012.

Itzhak Brook. Approval of zidovudine (azt) for acquired immunodeficiency syndrome: A challenge to the medical and pharmaceutical communities. *JAMA*, 258(11):1517–1517, 1987.

Omobolaji T Campbell Yesufu and Rajesh T Gandhi. Update on human immunodeficiency virus (hiv)-2 infection. *Clinical infectious diseases*, 52(6):780–787, 2011.

Andrew Carr, Stefano Vella, Menno D de Jong, Franco Sorice, Allison Imrie, Charles A Boucher, David A Cooper, Dutch-Italian-Australian Nevirapine Study Group, et al. A controlled trial of nevirapine plus zidovudine versus zidovudine alone in p24 antigenaemic hiv-infected patients. *Aids*, 10(6):635–642, 1996.

G Chêne et al. Prognostic importance of initial response in hiv-1 infected patients starting potent antiretroviral therapy: analysis of prospective studies. *The Lancet*, 362(9385):679–686, 2003.

Nicolas Chomont, Mohamed El-Far, Petronela Ancuta, Lydie Trautmann, Francesco A Procopio, Bader Yassine-Diab, Genevieve Boucher, Mohamed-Rachid Boulassel, Georges Ghattas, Jason M Brenchley, et al. Hiv reservoir size and persistence are driven by t cell survival and homeostatic proliferation. *Nature medicine*, 15(8):893–900, 2009.

Tae-Wook Chun, Delphine Engel, Stephanie B Mizell, Claire W Hallahan, Maria Fischette, Sohee Park, Richard T Davey, Mark Dybul, Joseph A Kovacs, Julia A Metcalf, et al. Effect of interleukin-2 on the pool of latently infected, resting cd4+ t cells in hiv-1-infected patients receiving highly active antiretroviral therapy. *Nature medicine*, 5(6):651–655, 1999.

Myron S Cohen, Ying Q Chen, Marybeth McCauley, Theresa Gamble, Mina C Hosseinipour, Nagalingeswaran Kumarasamy, James G Hakim, Johnstone Kumwenda, Beatriz Grinsztejn, Jose HS Pilotto, et al. Prevention of hiv-1 infection with early antiretroviral therapy. *New England journal of medicine*, 365(6):493–505, 2011.

Ann C Collier, Robert W Coombs, David A Schoenfeld, Roland L Bassett, Joseph Timpone, Alice Baruch, Michelle Jones, Karen Facey, Caroline Whitacre, Vincent J McAuliffe, et al. Treatment of human immunodeficiency virus infection with saquinavir, zidovudine, and zalcitabine. *New England Journal of Medicine*, 334(16):1011–1018, 1996.

Daniel Commenges, Hélene Jacqmin-Gadda, Cécile Proust, and Jérémie Guedj. A newton-like algorithm for likelihood maximization: The robust-variance scoring algorithm. *arXiv preprint math/0610402*, 2006.

Daniel Commenges, Pierre Joly, Gégout-Petit Anne, and Benoit Liquet. Choice between semi-parametric estimators of markov and non-markov multi-state models from coarsened observations. *Scandinavian Journal of Statistics*, 34 (1):33–52, 2007.

Daniel Commenges, A Sayyareh, Luc Letenneur, Jeremie Guedj, Avner Bar-Hen, et al. Estimating a difference of kullback–leibler risks using a normalized difference of aic. *The Annals of Applied Statistics*, 2(3):1123–1142, 2008.

Daniel Commenges, Cécile Proust-Lima, Cécilia Samieri, and Benoit Liquet. A universal approximate cross-validation criterion for regular risk functions. *The international journal of biostatistics*, 11(1):51–67, 2015.

David A Cooper, Jose M Gatell, Susanne Kroon, Nathan Clumeck, Judith Millard, Frank-D Goebel, Johan N Bruun, Georg Stingl, Rex L Melville, Juan Gonzalez-Lahoz, et al. Zidovudine in persons with asymptomatic hiv infection and cd4+ cell counts greater than 400 per cubic millimeter. *New England Journal of Medicine*, 329(5):297–303, 1993.

Angus G Dalgleish, Peter CL Beverley, Paul R Clapham, Dorothy H Crawford, Melvyn F Greaves, and Robin A Weiss. The cd4 (t4) antigen is an essential component of the receptor for the aids retrovirus. *Nature*, 1984.

Sven A Danner, Andrew Carr, John M Leonard, Leah M Lehman, Francesc Gudiol, Juan Gonzales, Antonio Raventos, Rafael Rubio, Emilio Bouza, Vicente Pintado, et al. A short-term study of the safety, pharmacokinetics, and efficacy of ritonavir, an inhibitor of hiv-1 protease. *New England Journal of Medicine*, 333(23):1528–1534, 1995.

Richard T D'Aquila, Michael D Hughes, Victoria A Johnson, Margaret A Fischl, Jean-Pierre Sommadossi, SH Liou, Joseph Timpone, Maureen Myers, Nesli

Basgoz, Manette Niu, et al. Nevirapine, zidovudine, and didanosine compared with zidovudine and didanosine in patients with hiv-1 infection. a randomized, double-blind, placebo-controlled trial. national institute of allergy and infectious diseases aids clinical trials group protocol 241 investigators. *Annals of internal medicine*, 124(12):1019–1030, 1996.

JH Darbyshire, Delta Coordinating Committee, et al. Delta: a randomised double-blind controlled trial comparing combinations of zidovudine plus didanosine or zalcitabine with zidovudine alone in hiv-infected individuals. *The Lancet*, 348(9023):283–291, 1996.

Sander de Kivit, Ludwijn JR Lempsink, Jill Plants, Jeffrey Martinson, Ali Keshavarzian, and Alan L Landay. Modulation of tim-3 expression on nk and t cell subsets in hiv immunological non-responders. *Clinical Immunology*, 156 (1):28–35, 2015.

Blandine de Saint-Vis, Isabelle Fugier-Vivier, Catherine Massacrier, Claude Gaillard, Béatrice Vanbervliet, Smina Aït-Yahia, Jacques Banchereau, Yong-Jun Liu, Serge Lebecque, and Christophe Caux. The cytokine profile expressed by human dendritic cells is dependent on cell subtype and mode of activation. *The Journal of Immunology*, 160(4):1666–1676, 1998.

A Adam Ding and Hulin Wu. Assessing antiviral potency of anti-hiv therapies in vivo by comparing viral decay rates in viral dynamic models. *Biostatistics*, 2(1):13–29, 2001.

Hans Dooms. Interleukin-7: fuel for the autoimmune attack. *Journal of autoimmunity*, 45:40–48, 2013.

Daniel C Douek, Michael R Betts, Brenna J Hill, Susan J Little, Richard Lempicki, Julia A Metcalf, Joseph Casazza, Christian Yoder, Joseph W Adelsberger, Randy A Stevens, et al. Evidence for increased t cell turnover and decreased thymic output in hiv infection. *The Journal of Immunology*, 167 (11):6663–6668, 2001.

Julia Drylewicz, Daniel Commenges, and Rodolphe Thiebaut. Maximum a posteriori estimation in dynamical models of primary hiv infection. *Statistical Communications in Infectious Diseases*, 4(1), 2012.

Matthias Egger, Margaret May, Geneviève Chêne, Andrew N Phillips, Bruno Ledergerber, François Dabis, Dominique Costagliola, Antonella D'Arminio Monforte, Frank de Wolf, Peter Reiss, et al. Prognosis of hiv-1-infected patients starting highly active antiretroviral therapy: a collaborative analysis of prospective studies. *The Lancet*, 360(9327):119–129, 2002.

Diana Finzi, Joel Blankson, Janet D Siliciano, Joseph B Margolick, Karen Chadwick, Theodore Pierson, Kendall Smith, Julianna Lisziewicz, Franco Lori, Charles Flexner, et al. Latent infection of cd4+ t cells provides a mechanism for lifelong persistence of hiv-1, even in patients on effective combination therapy. *Nature medicine*, 5(5):512–517, 1999.

Margaret A Fischl, Douglas D Richman, Michael H Grieco, Michael S Gottlieb, Paul A Volberding, Oscar L Laskin, John M Leedom, Jerome E Groopman,

Donna Mildvan, Robert T Schooley, et al. The efficacy of azidothymidine (azt) in the treatment of patients with aids and aids-related complex. *New England Journal of Medicine*, 317(4):185–191, 1987.

Nathan Ford, Kathryn Stinson, Howard Gale, Edward J Mills, Wendy Stevens, Mercedes P González, Jessica Markby, and Andrew Hill. Cd4 changes among virologically suppressed patients on antiretroviral therapy: a systematic review and meta-analysis. *Journal of the International AIDS Society*, 18(1), 2015.

Sara Fritzell, Sofia Eberstål, Emma Sandén, Edward Visse, Anna Darabi, and Peter Siesjö. Ifnγ in combination with il-7 enhances immunotherapy in two rat glioma models. *Journal of neuroimmunology*, 258(1):91–95, 2013.

Terry J Fry and Crystal L Mackall. Interleukin-7: from bench to clinic. *Blood*, 99(11):3892–3904, 2002.

Terry J Fry and Crystal L Mackall. The many faces of il-7: from lymphopoiesis to peripheral t cell maintenance. *The Journal of Immunology*, 174(11):6571–6576, 2005.

Terry J Fry, Elizabeth Connick, Judith Falloon, Michael M Lederman, David J Liewehr, John Spritzler, Seth M Steinberg, Lauren V Wood, Robert Yarchoan, Judy Zuckerman, et al. A potential role for interleukin-7 in t-cell homeostasis. *Blood*, 97(10):2983–2990, 2001.

Julie C Gaardbo, Hans J Hartling, Andreas Ronit, Karoline Springborg, Lise MR Gjerdrum, Elisabeth Ralfkiær, Kristina Thorsteinsson, Henrik Ullum, Åse B Andersen, and Susanne D Nielsen. Regulatory t cells in hiv-infected immunological nonresponders are increased in blood but depleted in lymphoid tissue and predict immunological reconstitution. *JAIDS Journal of Acquired Immune Deficiency Syndromes*, 66(4):349–357, 2014.

Robert C Gallo. The early years of hiv/aids. *Science*, 298(5599):1728–1730, 2002.

Alan Genz and BD Keister. Fully symmetric interpolatory rules for multiple integrals over infinite regions with gaussian weight. *Journal of Computational and Applied Mathematics*, 71(2):299–309, 1996.

John G Gerber. Using pharmacokinetics to optimize antiretroviral drug-drug interactions in the treatment of human immunodeficiency virus infection. *Clinical infectious diseases*, 30(Supplement 2):S123–S129, 2000.

Johannes Gerdes, Ulrich Schwab, Hilmar Lemke, and Harald Stein. Production of a mouse monoclonal antibody reactive with a human nuclear antigen associated with cell proliferation. *International journal of cancer*, 31(1):13–20, 1983.

Pierre-Marie Girard, Christine Katlama, and Gilles Pialoux. *VIH. Edition 2007*. Wolters Kluwer France, 2007.

Michael S Gottlieb, Robert Schroff, Howard M Schanker, Joel D Weisman, Peng Thim Fan, Robert A Wolf, and Andrew Saxon. Pneumocystis carinii pneumonia and mucosal candidiasis in previously healthy homosexual men: evidence of a new acquired cellular immunodeficiency. *New England Journal of Medicine*, 305(24):1425–1431, 1981.

Sophie Grabar, Vincent Le Moing, Cecile Goujard, Catherine Leport, Michel D Kazatchkine, Dominique Costagliola, and Laurence Weiss. Clinical outcome of patients with hiv-1 infection according to immunologic and virologic response after 6 months of highly active antiretroviral therapy. *Annals of internal medicine*, 133(6):401–410, 2000.

Simon G Gregory, Silke Schmidt, Puneet Seth, Jorge R Oksenberg, John Hart, Angela Prokop, Stacy J Caillier, Maria Ban, An Goris, Lisa F Barcellos, et al. Interleukin 7 receptor α chain (il7r) shows allelic and functional association with multiple sclerosis. *Nature genetics*, 39(9):1083–1091, 2007.

Jérémie Guedj, Rodolphe Thiébaut, and Daniel Commenges. Maximum likelihood estimation in dynamical models of hiv. *Biometrics*, 63(4):1198–1206, 2007.

Sudhir Gupta. *Immunology of HIV infection*. Springer US, 1996.

Scott M Hammer, David A Katzenstein, Michael D Hughes, Holly Gundacker, Robert T Schooley, Richard H Haubrich, W Keith Henry, Michael M Lederman, John P Phair, Manette Niu, et al. A trial comparing nucleoside monotherapy with combination therapy in hiv-infected adults with cd4 cell counts from 200 to 500 per cubic millimeter. *New England Journal of Medicine*, 335(15):1081–1090, 1996.

Charlotte Harrison. Autoimmune disease: targeting il-7 reverses type 1 diabetes. *Nature Reviews Drug Discovery*, 11(8):599–599, 2012.

Craig W Hendrix, Ann C Collier, Michael M Lederman, Dominique Schols, Richard B Pollard, Stephen Brown, J Brooks Jackson, Robert W Coombs, Marshall J Glesby, Charles W Flexner, et al. Safety, pharmacokinetics, and antiviral activity of amd3100, a selective cxcr4 receptor inhibitor, in hiv-1 infection. *JAIDS Journal of Acquired Immune Deficiency Syndromes*, 37(2): 1253–1262, 2004.

Alan C Hindmarsh. Odepack, a systematized collection of ode solvers, rs stepleman et al.(eds.), north-holland, amsterdam,(vol. 1 of), pp. 55-64. *IMACS transactions on scientific computation*, 1:55–64, 1983.

David D Ho, Avidan U Neumann, Alan S Perelson, Wen Chen, John M Leonard, Martin Markowitz, et al. Rapid turnover of plasma virions and cd4 lymphocytes in hiv-1 infection. *Nature*, 373(6510):123–126, 1995.

Jessica N Hodge, Sharat Srinivasula, Zonghui Hu, Sarah W Read, Brian O Porter, Insook Kim, JoAnn M Mican, Chang Paik, Paula DeGrange, Michele Di Mascio, et al. Decreases in il-7 levels during antiretroviral treatment of hiv infection suggest a primary mechanism of receptor-mediated clearance. *Blood*, 118(12):3244–3253, 2011.

R Hofmeister, AR Khaled, N Benbernou, E Rajnavolgyi, K Muegge, and SK Durum. Interleukin-7: physiological roles and mechanisms of action. *Cytokine & growth factor reviews*, 10(1):41–60, 1999.

Yangxin Huang, Dacheng Liu, and Hulin Wu. Hierarchical bayesian methods for estimation of parameters in a longitudinal hiv dynamic system. *Biometrics*, 62(2):413–423, 2006.

Sara Jaleco, Louise Swainson, Valérie Dardalhon, Maryam Burjanadze, Sandrina Kinet, and Naomi Taylor. Homeostasis of naive and memory cd4+ t cells: Il-2 and il-7 differentially regulate the balance between proliferation and fas-mediated apoptosis. *The Journal of Immunology*, 171(1):61–68, 2003.

Inma Jarrin, Nikos Pantazis, Judith Dalmau, Andrew N Phillips, Ashley Olson, Cristina Mussini, Faroudy Boufassa, Dominique Costagliola, Kholoud Porter, Julià Blanco, et al. Does rapid hiv disease progression prior to combination antiretroviral therapy hinder optimal cd4 r t-cell recovery once hiv-1 suppression is achieved? *AIDS*, 500:15–00467, 2015.

PJ Kanki, K USMB Travers, RG Marlink, ME Essex, S MBoup, A Gueye-Ndiaye, T Siby, I Thior, JL Sankale, CC Hsieh, et al. Slower heterosexual spread of hiv-2 than hiv-1. *The Lancet*, 343(8903):943–946, 1994.

Rami Kantor, Lameck Diero, Allison DeLong, Lydia Kamle, Sarah Muyonga, Fidelis Mambo, Eunice Walumbe, Wilfred Emonyi, Philip Chan, E Jane Carter, et al. Misclassification of first-line antiretroviral treatment failure based on immunological monitoring of hiv infection in resource-limited settings. *Clinical Infectious Diseases*, 49(3):454–462, 2009.

Urs Karrer, Bruno Ledergerber, Hansjakob Furrer, Luigia Elzi, Manuel Battegay, Matthias Cavassini, Angele Gayet-Ageron, Bernard Hirschel, Patrick Schmid, Marina Russotti, et al. Dose-dependent influence of didanosine on immune recovery in hiv-infected patients treated with tenofovir. *Aids*, 19(17): 1987–1994, 2005.

Robert E Kass and Duane Steffey. Approximate bayesian inference in conditionally independent hierarchical models (parametric empirical bayes models). *Journal of the American Statistical Association*, 84(407):717–726, 1989.

Gilbert R Kaufmann, Hansjakob Furrer, Bruno Ledergerber, Luc Perrin, Milos Opravil, Pietro Vernazza, Matthias Cavassini, Enos Bernasconi, Martin Rickenbach, Bernard Hirschel, et al. Characteristics, determinants, and clinical relevance of cd4 t cell recovery to¡ 500 cells/μl in hiv type 1infected individuals receiving potent antiretroviral therapy. *Clinical infectious diseases*, 41(3): 361–372, 2005.

Colleen F Kelley, Christina MR Kitchen, Peter W Hunt, Benigno Rodriguez, Frederick M Hecht, Mari Kitahata, Heide M Crane, James Willig, Michael Mugavero, Michael Saag, et al. Incomplete peripheral cd4+ cell count restoration in hiv-infected patients receiving long-term antiretroviral treatment. *Clinical Infectious Diseases*, 48(6):787–794, 2009.

Sherrie L Kelly and David P Wilson. Hiv cascade monitoring and simple modelling reveals potential for reductions in hiv incidence. *Journal of acquired immune deficiency syndromes (1999)*, 2015.

Mari M Kitahata, Stephen J Gange, Alison G Abraham, Barry Merriman, Michael S Saag, Amy C Justice, Robert S Hogg, Steven G Deeks, Joseph J Eron, John T Brooks, et al. Effect of early versus deferred antiretroviral therapy for hiv on survival. *New England Journal of Medicine*, 360(18):1815–1826, 2009.

David Klatzmann and Abul K Abbas. The promise of low-dose interleukin-2 therapy for autoimmune and inflammatory diseases. *Nature Reviews Immunology*, 2015.

David Klatzmann, Eric Champagne, Sophie Chamaret, Jacqueline Gruest, Denise Guetard, Thierry Hercend, Jean-Claude Gluckman, and Luc Montagnier. T-lymphocyte t4 molecule behaves as the receptor for human retrovirus lav. 1984.

Joseph A Kovacs, Michael Baseler, Robin J Dewar, Susan Vogel, Richard T Davey Jr, Judith Falloon, Michael A Polis, Robert E Walker, Randy Stevens, Norman P Salzman, et al. Increases in cd4 t lymphocytes with intermittent courses of interleukin-2 in patients with human immunodeficiency virus infectiona preliminary study. *New England Journal of Medicine*, 332(9):567–575, 1995.

Joseph A Kovacs, Susan Vogel, Jeffrey M Albert, Judith Falloon, Richard T Davey Jr, Robert E Walker, Michael A Polis, Katherine Spooner, Julia A Metcalf, Michael Baseler, et al. Controlled trial of interleukin-2 infusions in patients infected with the human immunodeficiency virus. *New England Journal of Medicine*, 335(18):1350–1356, 1996.

Michael J Kozal, Kenda Kroodsma, Mark A Winters, Robert W Shafer, Brad Efron, David A Katzenstein, and Thomas C Merigan. Didanosine resistance in hiv-infected patients switched from zidovudine to didanosine monotherapy. *Annals of internal medicine*, 121(4):263–268, 1994.

Reinhard Kurth and Norbert Bannert. *Retroviruses: molecular biology, genomics and pathogenesis*. Horizon Scientific Press, 2010.

Christoph G Lange and Michael M Lederman. Immune reconstitution with antiretroviral therapies in chronic hiv-1 infection. *Journal of Antimicrobial Chemotherapy*, 51(1):1–4, 2003.

Brendan A Larder, Graham Darby, and Douglas D Richman. Hiv with reduced sensitivity to zidovudine (azt) isolated during prolonged therapy. *Science*, 243 (4899):1731–1734, 1989.

Jean Lévine and Philippe Müllhaupt. *Advances in the Theory of Control, Signals and Systems with Physical Modeling*, volume 407. Springer, 2010.

Y Levy, C Capitant, S Houhou, I Carriere, JP Viard, C Goujard, JA Gastaut, E Oksenhendler, L Boumsell, E Gomard, et al. Comparison of subcutaneous and intravenous interleukin-2 in asymptomatic hiv-1 infection: a randomised controlled trial. *The Lancet*, 353(9168):1923–1929, 1999.

Y Levy, I Sereti, G Tambussi, JP Routy, JD Lelievre, JF Delfraissy, JM Molina, M Fischl, C Goujard, B Rodriguez, et al. Effects of recombinant human interleukin 7 on t-cell recovery and thymic output in hiv-infected patients receiving antiretroviral therapy: results of a phase i/iia randomized, placebo-controlled, multicenter study. *Clinical Infectious Diseases*, 55(2):291–300, 2012.

Yves Levy, Christine Lacabaratz, Laurence Weiss, Jean-Paul Viard, Cecile Goujard, Jean-Daniel Lelièvre, François Boué, Jean-Michel Molina, Christine Rouzioux, Véronique Avettand-Fénoêl, et al. Enhanced t cell recovery in hiv-1–infected adults through il-7 treatment. *The Journal of clinical investigation*, 119(4):997, 2009a.

Yves Levy et al. Effect of interleukin-2 on clinical outcomes in patients with cd4+ cell count 50 to 299/mm3: primary results of the silcaat study. In *16th Conference on Retroviruses and Opportunistic Infections*, pages 8–11, 2009b.

Charlotte Lewden, Genevieve Chêne, Philippe Morlat, Francois Raffi, Michel Dupon, Pierre Dellamonica, Jean-Luc Pellegrin, Christine Katlama, Francois Dabis, Catherine Leport, et al. Hiv-infected adults with a cd4 cell count greater than 500 cells/mm3 on long-term combination antiretroviral therapy reach same mortality rates as the general population. *JAIDS Journal of Acquired Immune Deficiency Syndromes*, 46(1):72–77, 2007.

Charlotte Lewden, Vincent Bouteloup, Stéphane De Wit, Caroline Sabin, Amanda Mocroft, Jan Christian Wasmuth, Ard van Sighem, Ole Kirk, Niels Obel, George Panos, et al. All-cause mortality in treated hiv-infected adults with cd4 500/mm3 compared with the general population: evidence from a large european observational cohort collaboration. *International Journal of Epidemiology*, page dyr164, 2011.

Tao Sheng Li, Roland Tubiana, Christine Katlama, Vincent Calvez, H Ait Mohand, and Brigitte Autran. Long-lasting recovery in cd4 t-cell function and viral-load reduction after highly active antiretroviral therapy in advanced hiv-1 disease. *The Lancet*, 351(9117):1682–1686, 1998.

M Losso and D Abrams. Effect of interleukin-2 on clinical outcomes in patients with a cd4+ cell count of 300/mm3: primary results of the esprit study. In *16th Conference on Retroviruses and Opportunistic Infections*, pages 8–11, 2009.

Thomas A Louis. Finding the observed information matrix when using the em algorithm. *Journal of the Royal Statistical Society. Series B (Methodological)*, pages 226–233, 1982.

Wangko Lundström, Natasha M Fewkes, and Crystal L Mackall. Il-7 in human health and disease. In *Seminars in immunology*, volume 24, pages 218–224. Elsevier, 2012.

Gary Maartens, Connie Celum, and Sharon R Lewin. Hiv infection: epidemiology, pathogenesis, treatment, and prevention. *The Lancet*, 384(9939):258–271, 2014.

Crystal L Mackall, Terry J Fry, and Ronald E Gress. Harnessing the biology of il-7 for therapeutic application. *Nature Reviews Immunology*, 11(5):330–342, 2011.

David K Male and Jonathan Brostoff. *Immunologie*. Elsevier Masson, 2007.

Giulia Marchetti, Giusi M Bellistrì, Elisa Borghi, Camilla Tincati, Stefania Ferramosca, Maria La Francesca, Giulia Morace, Andrea Gori, and Antonella d'Arminio Monforte. Microbial translocation is associated with sustained failure in cd4+ t-cell reconstitution in hiv-infected patients on long-term highly active antiretroviral therapy. *Aids*, 22(15):2035–2038, 2008.

Donald W Marquardt. An algorithm for least-squares estimation of nonlinear parameters. *Journal of the Society for Industrial & Applied Mathematics*, 11 (2):431–441, 1963.

Claudio M Mastroianni, Gabriele Forcina, Gabriella dEttorre, Miriam Lichtner, Fabio Mengoni, Claudia DAgostino, and Vincenzo Vullo. Circulating levels of interleukin-7 in antiretroviral-naive and highly active antiretroviral therapy-treated hiv-infected patients. *HIV clinical trials*, 2(2):108–112, 2001.

Margaret May, Patrick Royston, Matthias Egger, Amy C Justice, and Jonathan AC Sterne. Development and validation of a prognostic model for survival time data: application to prognosis of hiv positive patients treated with antiretroviral therapy. *Statistics in medicine*, 23(15):2375–2398, 2004.

Margaret T May, Mark Gompels, Valerie Delpech, Kholoud Porter, Chloe Orkin, Stephen Kegg, Phillip Hay, Margaret Johnson, Adrian Palfreeman, Richard Gilson, et al. Impact on life expectancy of hiv-1 positive individuals of cd4+ cell count and viral load response to antiretroviral therapy. *AIDS (London, England)*, 28(8):1193, 2014.

Hiroaki Mitsuya, Kent J Weinhold, Phillip A Furman, Marty H St Clair, S Nusinoff Lehrman, Robert C Gallo, Dani Bolognesi, David W Barry, and Samuel Broder. 3'-azido-3'-deoxythymidine (bw a509u): an antiviral agent that inhibits the infectivity and cytopathic effect of human t-lymphotropic virus type iii/lymphadenopathy-associated virus in vitro. *Proceedings of the National Academy of Sciences*, 82(20):7096–7100, 1985.

Amanda Mocroft, Andrew N Phillips, Jose Gatell, Bruno Ledergerber, Martin Fisher, Nathan Clumeck, Marcello Losso, Adriano Lazzarin, G Fatkenheuer, JD Lundgren, et al. Normalisation of cd4 counts in patients with hiv-1 infection and maximum virological suppression who are taking combination antiretroviral therapy: an observational cohort study. *The Lancet*, 370(9585): 407–413, 2007.

Hiroshi Mohri, Alan S Perelson, Keith Tung, Ruy M Ribeiro, Bharat Ramratnam, Martin Markowitz, Rhonda Kost, Leor Weinberger, Denise Cesar, Marc K Hellerstein, et al. Increased turnover of t lymphocytes in hiv-1 infection and its reduction by antiretroviral therapy. *The Journal of experimental medicine*, 194(9):1277–1288, 2001.

Doris Anne Morgan, Francis W Ruscetti, Robert Gallo, et al. Selective in vitro growth of t lymphocytes from normal human bone marrows. *Science*, 193 (4257):1007–1008, 1976.

Carl N Morris. Parametric empirical bayes inference: theory and applications. *Journal of the American Statistical Association*, 78(381):47–55, 1983.

Santo Motta and Francesco Pappalardo. Mathematical modeling of biological systems. *Briefings in Bioinformatics*, 14(4):411–422, 2013.

Scott N Mueller, Thomas Gebhardt, Francis R Carbone, and William R Heath. Memory t cell subsets, migration patterns, and tissue residence. *Annual review of immunology*, 31:137–161, 2013.

F Nakhaee and M Law. Parametric modelling of survival following hiv and aids in the era of highly active antiretroviral therapy: data from australia. *Eastern Mediterranean Health Journal*, 3(17):231–237, 2011.

Anthony E Namen, Ann E Schmierer, Carl J March, Robert W Overell, Linda S Park, David L Urdal, and Diane Y Mochizuki. B cell precursor growth-promoting activity. purification and characterization of a growth factor active on lymphocyte precursors. *The Journal of experimental medicine*, 167(3):988–1002, 1988.

Martin Nowak and Robert M May. *Virus dynamics: mathematical principles of Immunology and virology*. Oxford university press, 2000.

Afam A Okoye and Louis J Picker. Cd4+ t-cell depletion in hiv infection: mechanisms of immunological failure. *Immunological reviews*, 254(1):54–64, 2013.

Collaboration of Observational HIV Epidemiological Research in Europe in EuroCoord Opportunistic Infections Project Team COHERE et al. Cd4 cell count and the risk of aids or death in hiv-infected adults on combination antiretroviral therapy with a suppressed viral load: a longitudinal cohort study from cohere. *PLoS medicine*, 9(3):e1001194, 2012.

Nadine G Pakker, Eugene DMB Kroon, Marijke TL Roos, Sigrid A Otto, David Hall, Ferdinand WNM Wit, Dörte Hamann, Marina E van der Ende, Frans AP Claessen, Robert H Kauffmann, et al. Immune restoration does not invariably occur following long-term hiv-1 suppression during antiretroviral therapy. *Aids*, 13(2):203–212, 1999.

Frank J Palella Jr, Kathleen M Delaney, Anne C Moorman, Mark O Loveless, Jack Fuhrer, Glen A Satten, Diane J Aschman, and Scott D Holmberg. Declining morbidity and mortality among patients with advanced human immunodeficiency virus infection. *New England Journal of Medicine*, 338(13): 853–860, 1998.

Giuseppe Pantaleo and Yves Lévy. Vaccine and immunotherapeutic interventions. *Current Opinion in HIV and AIDS*, 8(3):236–242, 2013.

Sophie Patterson, Angela Cescon, Hasina Samji, Keith Chan, Wendy Zhang, Janet Raboud, Ann N Burchell, Curtis Cooper, Marina B Klein, Sean B Rourke, et al. Life expectancy of hiv-positive individuals on combination antiretroviral therapy in canada. *BMC infectious diseases*, 15(1):274, 2015.

Miguel-Angel Perales, Jenna D Goldberg, Jianda Yuan, Guenther Koehne, Lauren Lechner, Esperanza B Papadopoulos, James W Young, Ann A Jakubowski, Bushra Zaidi, Humilidad Gallardo, et al. Recombinant human interleukin-7 (cyt107) promotes t-cell recovery after allogeneic stem cell transplantation. *Blood*, 120(24):4882–4891, 2012.

Alan S Perelson. Modelling viral and immune system dynamics. *Nature Reviews Immunology*, 2(1):28–36, 2002.

Alan S Perelson, Avidan U Neumann, Martin Markowitz, John M Leonard, and David D Ho. Hiv-1 dynamics in vivo: virion clearance rate, infected cell life-span, and viral generation time. *Science*, 271(5255):1582–1586, 1996.

Theodore Pierson, Justin McArthur, and Robert F Siliciano. Reservoirs for hiv-1: mechanisms for viral persistence in the presence of antiviral immune responses and antiretroviral therapy. *Annual review of immunology*, 18(1): 665–708, 2000.

José C Pinheiro and Douglas M Bates. Approximations to the log-likelihood function in the nonlinear mixed-effects model. *Journal of computational and Graphical Statistics*, 4(1):12–35, 1995.

José C Pinheiro and Douglas M Bates. *Mixed-effects models in S and S-PLUS*. Springer, 2000.

Mélanie Prague, Daniel Commenges, Jérémie Guedj, Julia Drylewicz, and Rodolphe Thiébaut. Nimrod: A program for inference via a normal approximation of the posterior in models with random effects based on ordinary differential equations. *Computer methods and programs in biomedicine*, 111 (2):447–458, 2013a.

Mélanie Prague, Daniel Commenges, and Rodolphe Thiébaut. Dynamical models of biomarkers and clinical progression for personalized medicine: The hiv context. *Advanced drug delivery reviews*, 65(7):954–965, 2013b.

Christian Prebensen, Thor Ueland, Annika E Michelsen, Andreas Lind, Frank O Pettersen, Tom Eirik Mollnes, Pål Aukrust, Anne Ma Dyrhol-Riise, and Dag Kvale. High mip-1 [beta] levels in plasma predict long-term immunological non-response to suppressive antiretroviral therapy in hiv infection. *JAIDS Journal of Acquired Immune Deficiency Syndromes*, 2015.

Hein Putter, SH Heisterkamp, JMA Lange, and F De Wolf. A bayesian approach to parameter estimation in hiv dynamical models. *Statistics in medicine*, 21 (15):2199–2214, 2002.

Krishnan Radhakrishnan and Alan C Hindmarsh. *Description and use of LSODE, the Livermore solver for ordinary differential equations*. National Aeronautics and Space Administration, Office of Management, Scientific and Technical Information Program, 1993.

Douglas D Richman, Janet M Grimes, and Stephen W Lagakos. Effect of stage of disease and drug dose on zidovudine susceptibilities of isolates of human immunodeficiency virus. *JAIDS Journal of Acquired Immune Deficiency Syndromes*, 3(8):743–746, 1990.

Virginie Rondeau, Yassin Mazroui, and Juan R Gonzalez. frailtypack: an r package for the analysis of correlated survival data with frailty models using penalized likelihood estimation or parametrical estimation. *Journal of Statistical Software*, 47(4):1–28, 2012.

Michelle Rosenzwajg, Guillaume Churlaud, Roberto Mallone, Adrien Six, Nicolas Dérian, Wahiba Chaara, Roberta Lorenzon, S Alice Long, Jane H Buckner, Georgia Afonso, et al. Low-dose interleukin-2 fosters a dose-dependent regulatory t cell tuned milieu in t1d patients. *Journal of autoimmunity*, 58:48–58, 2015.

Stefano Rusconi, Paola Vitiello, Fulvio Adorni, Elisa Colella, Emanuele Focà, Amedeo Capetti, Paola Meraviglia, Clara Abeli, Stefano Bonora, Marco DAnnunzio, et al. Maraviroc as intensification strategy in hiv-1 positive patients with deficient immunological response: an italian randomized clinical trial. 2013.

EV Saidakova, LB Korolevskaya, NG Shmagel, KV Shmagel, and VA Chereshnev. The role of interleukin 7 and its cell receptor in a poor recovery of cd4 t cells in hiv-infected patients receiving antiretroviral therapy. In *Doklady Biological Sciences*, volume 1, pages 313–315. Pleiades Publishing, 2014.

J Saison, T Ferry, J Demaret, D Maucort Boulch, F Venet, T Perpoint, F Ader, V Icard, C Chidiac, and G Monneret. Association between discordant immunological response to highly active anti-retroviral therapy, regulatory t cell percentage, immune cell activation and very low-level viraemia in hiv-infected patients. *Clinical & Experimental Immunology*, 176(3):401–409, 2014.

Taheri Sathaliyawala, Masaru Kubota, Naomi Yudanin, Damian Turner, Philip Camp, Joseph JC Thome, Kara L Bickham, Harvey Lerner, Michael Goldstein, Megan Sykes, et al. Distribution and compartmentalization of human circulating and tissue-resident memory t cell subsets. *Immunity*, 38(1):187–197, 2013.

Thomas Scholzen, Johannes Gerdes, et al. The ki-67 protein: from the known and the unknown. *Journal of cellular physiology*, 182(3):311–322, 2000.

Benedict Seddon, Peter Tomlinson, and Rose Zamoyska. Interleukin 7 and t cell receptor signals regulate homeostasis of cd4 memory cells. *Nature immunology*, 4(7):680–686, 2003.

Irini Sereti, Richard M Dunham, John Spritzler, Evgenia Aga, Michael A Proschan, Kathy Medvik, Catherine A Battaglia, Alan L Landay, Savita Pahwa, Margaret A Fischl, et al. Il-7 administration drives t cell–cycle entry and expansion in hiv-1 infection. *Blood*, 113(25):6304–6314, 2009.

Irini Sereti, Jacob D Estes, William L Thompson, David R Morcock, Margaret A Fischl, Therese Croughs, Stephanie Beq, Sylvie Lafaye de Micheaux,

Michael D Yao, Alexander Ober, et al. Decreases in colonic and systemic inflammation in chronic hiv infection after il-7 administration. *PLoS Pathog*, 10(1):e1003890, 2014.

Haina Shin and Akiko Iwasaki. Tissue-resident memory t cells. *Immunological reviews*, 255(1):165–181, 2013.

Yuichiro Shindo, Jacqueline Unsinger, Cary-Ann Burnham, Jonathan M Green, and Richard S Hotchkiss. Interleukin-7 and anti–programmed cell death 1 antibody have differing effects to reverse sepsis-induced immunosuppression. *Shock*, 43(4):334–343, 2015.

Claude Sportès, Rebecca R Babb, Michael C Krumlauf, Frances T Hakim, Seth M Steinberg, Catherine K Chow, Margaret R Brown, Thomas A Fleisher, Pierre Noel, Irina Maric, et al. Phase i study of recombinant human interleukin-7 administration in subjects with refractory malignancy. *Clinical Cancer Research*, 16(2):727–735, 2010.

Rosalyn E Stahl, Alvin Friedman-Kien, Ronald Dubin, Michael Marmor, and Susan Zolla-Pazner. Immunologic abnormalities in homosexual men: relationship to kaposi's sarcoma. *The American journal of medicine*, 73(2):171–178, 1982.

Schlomo Staszewski, Veronica Miller, Sibylle Rehmet, Thomas Stark, Jean De Creé, Marc De Brabander, Monika Peeters, Koen Andries, Marc Moeremans, Marc De Raeymaeker, et al. Virological and immunological analysis of a triple combination pilot study with loviride, lamivudine and zidovudine in hiv-1-infected patients. *Aids*, 10(5):F1–F7, 1996.

Hans-Jürgen Stellbrink, Jan van Lunzen, Michael Westby, Eithne O'Sullivan, Claus Schneider, Axel Adam, Lutwin Weitner, Birger Kuhlmann, Christian Hoffmann, Stefan Fenske, et al. Effects of interleukin-2 plus highly active antiretroviral therapy on hiv-1 replication and proviral dna (cosmic trial). *Aids*, 16(11):1479–1487, 2002.

Charles D Surh, Onur Boyman, Jared F Purton, and Jonathan Sprent. Homeostasis of memory t cells. *Immunological reviews*, 211(1):154–163, 2006.

James E Talmadge, John D Jackson, Linda Kelsey, Claudia D Borgeson, Connie Faltynek, and Greg A Perry. T-cell reconstitution by molecular, phenotypic, and functional analysis in the thymus, bone marrow, spleen, and blood following split-dose polychemotherapy and therapeutic activity for metastatic breast cancer in mice. *Journal of immunotherapy*, 14(4):258–268, 1993.

Rodolphe Thiébaut, Hélène Jacqmin-Gadda, Abdel Babiker, and Daniel Commenges. Joint modelling of bivariate longitudinal data with informative dropout and left-censoring, with application to the evolution of cd4+ cell count and hiv rna viral load in response to treatment of hiv infection. *Statistics in medicine*, 24(1):65–82, 2005.

Rodolphe Thiébaut, Julia Drylewicz, Mélanie Prague, Christine Lacabaratz, Stéphanie Beq, Ana Jarne, Thérèse Croughs, Rafick-Pierre Sekaly, Michael M

Lederman, Irini Sereti, et al. Quantifying and predicting the effect of exogenous interleukin-7 on cd4+ t cells in hiv-1 infection. *PLoS computational biology*, 10(5):e1003630, 2014.

Rodolphe Thiébaut, Ana Jarne, Jean-Pierre Routy, Irini Sereti, Margaret Fischl, Prudence Ive, Roberto Speck, et al. Repeated cycles of recombinant human interleukin 7 in hiv-infected patients with low cd4 t cell reconstitution on antiretroviral therapy: Results of two phase ii multicenter studies. 2015 in revision.

Ronald E Unger, Jorg Kreuter, and Helga Ruubsamen-Waigmann. *Antivirals against AIDS*. Informa Health Care, 2000.

Homer O Valenzona, Satwant Dhanoa, Fred D Finkelman, and Dennis G Osmond. Exogenous interleukin 7 as a proliferative stimulant of early precursor b cells in mouse bone marrow: efficacy of il-7 injection, il-7 infusion and il-7–anti-il-7 antibody complexes. *Cytokine*, 10(6):404–412, 1998.

Aad W Van der Vaart. *Asymptotic statistics*, volume 3. Cambridge university press, 2000.

Joel AG van Roon, Marieke C Verweij, Marion Wenting-van Wijk, Kim MG Jacobs, Johannes WJ Bijlsma, and Floris PJG Lafeber. Increased intraarticular interleukin-7 in rheumatoid arthritis patients stimulates cell contact–dependent activation of cd4+ t cells and macrophages. *Arthritis & Rheumatism*, 52(6):1700–1710, 2005.

Anthony T Vella, Steven Dow, Terry A Potter, John Kappler, and Philippa Marrack. Cytokine-induced survival of activated t cells in vitro and in vivo. *Proceedings of the National Academy of Sciences*, 95(7):3810–3815, 1998.

Bret Verhoven, Yan Yan, Mark Ritter, Li-Yan Khor, Elizabeth Hammond, Christopher Jones, Mahul Amin, Jean-Paul Bahary, Kenneth Zeitzer, and Alan Pollack. Ki-67 is an independent predictor of metastasis and cause-specific mortality for prostate cancer patients treated on radiation therapy oncology group (rtog) 94-08. *International Journal of Radiation Oncology* Biology* Physics*, 86(2):317–323, 2013.

Maria Vieira, D Soares, Nicola J Borthwick, Mala K Maini, George Janossy, Mike Salmon, and Arne N Akbar. Il-7-dependent extrathymic expansion of cd45ra+ t cells enables preservation of a naive repertoire. *The Journal of Immunology*, 161(11):5909–5917, 1998.

Paul A Volberding, Stephen W Lagakos, Matthew A Koch, Carla Pettinelli, Maureen W Myers, David K Booth, Henry H Balfour Jr, Richard C Reichman, John A Bartlett, Martin S Hirsch, et al. Zidovudine in asymptomatic human immunodeficiency virus infection: a controlled trial in persons with fewer than 500 cd4-positive cells per cubic millimeter. *New England Journal of Medicine*, 322(14):941–949, 1990.

Kun Wang, David Z DArgenio, Edward P Acosta, Anandi N Sheth, Cecile Delille, Jeffrey L Lennox, Corenna Kerstner-Wood, and Ighovwerha Ofotokun. Integrated population pharmacokinetic/viral dynamic modelling of

lopinavir/ritonavir in hiv-1 treatment-naïve patients. *Clinical pharmacokinetics*, 53(4):361–371, 2014.

Xiping Wei, Sajal K Ghosh, Maria E Taylor, Victoria A Johnson, Emilio A Emini, Paul Deutsch, Jeffrey D Lifson, Sebastian Bonhoeffer, Martin A Nowak, Beatrice H Hahn, et al. Viral dynamics in human immunodeficiency virus type 1 infection. *Nature*, 373(6510):117–122, 1995.

Laurence Weiss, Fabrice A Letimier, Matthieu Carriere, Sylvie Maiella, Vladimira Donkova-Petrini, Brice Targat, Arndt Benecke, Lars Rogge, and Yves Levy. In vivo expansion of naive and activated cd4+ cd25+ foxp3+ regulatory t cell populations in interleukin-2–treated hiv patients. *Proceedings of the National Academy of Sciences*, 107(23):10632–10637, 2010.

Yanni Xiao, Hongyu Miao, Sanyi Tang, and Hulin Wu. Modeling antiretroviral drug responses for hiv-1 infected patients using differential equation models. *Advanced drug delivery reviews*, 65(7):940–953, 2013.

Robert Yarchoan, Jill A Lietzau, Bach-Yen Nguyen, Otis W Brawley, James M Pluda, M Wayne Saville, Kathleen M Wyvill, Seth M Steinberg, Riad Agbaria, Hiroaki Mitsuya, et al. A randomized pilot study of alternating or simultaneous zidovudine and didanosine therapy in patients with symptomatic human immunodeficiency virus infection. *Journal of Infectious Diseases*, 169 (1):9–17, 1994.

Jinfang Zhu, Hidehiro Yamane, and William E Paul. Differentiation of effector cd4 t cell populations. *Annual review of immunology*, 28:445, 2010.

Abstract: Fight against HIV and AIDS has shown major improvements in life expectancy and quality of life of HIV-infected people since the introduction of the cART. Today, viral load dramatically decreases a few weeks after starting antiretroviral therapy, and it becomes undetectable after 6 months for most of patients. This usually leads to an adequate reconstitution of $CD4^+T$ cells pool, but this is not necessarily always true. This thesis is focalised on these "low immunological responder" patients, who have not reached acceptable levels of $CD4^+$ T cells count despite undetectable viral load 6 months after having started the cART therapy.

Today, Interleukin 7 (a cytokine naturally secreted in the bone marrow and the thymus) is considered as one of the rare potential solution to boost the immune system in this situation. During this thesis work, we have collaborated to analyze data from the INSPIRE 2 & 3 trials, where repeated cycles (3 subcutaneous injections) of recombinant human Interleukin 7 have been administered to a total of 107 of these "low responder patients".

We have used dynamical models based on systems of ordinary differential equations to study the effect of the exogenous Interleukin 7 on $CD4^+$ T cells through the three INSPIRE studies. A mathematical model together with a mixed effects model applied on the biological parameters of the ODE system and a "model for the observations" make up the structure of our work. A maximum likelihood approach based on an adaptation of a Newton-like method is combined with a maximum *a posteriori* estimation in a semi-Bayesian context.

Key words: Biostatistics, $CD4^+$ T cells, clinical trials, differential equations, HIV, Interleukin 7, modeling.

Résumé: Des progrès majeurs dans l'espérance et la qualité de vie ont été enregistrés dans la lutte contre le VIH et le SIDA avec l'introduction des traitements antirétroviraux combinés. De nos jours, cette thérapie réduit nettement la charge virale après quelques semaines de traitement chez la plupart des patients. Ceci conduit généralement à une reconstitution satisfaisante du nombre de cellules $CD4^+$, mais ce n'est pas toujours le cas. Cette thèse est focalisée sur les patients ayant une réponse immunitaire insuffisante malgré une charge virale indetectable, après au moins 6 mois de thérapie antirétrovirale combinée.

À ce moment, l'Interleukine 7 (une cytokine secrétée par la moelle épinière et le thymus) est une thérapie prometteuse pour restaurer le système immunitaire dans une telle situation. Pendant ce travail de thèse, nous avons contribué à l'analyse des études INSPIRE 2 & 3, où 107 patients présentant une faible réponse immunitaire ont reçu des cycles (3 injections) répétés de r-hIL-7 (*Interleukine 7 recombinée humaine*).

Nous avons utilisé des modèles dynamiques basés sur des systèmes d'équations différentielles pour analyser l'effet de la r-hIL-7 exogène sur les cellules $CD4^+$ lors des trois études INSPIRE. Un modèle mathématique, avec un modèle à effets mixtes appliqué sur les paramètres biologiques et un "modèle pour les observations" forment la structure de notre travail. Une estimation par maximum de vraisemblance basée sur une méthode de type Newton est combinée avec une estimation du maximum *a posteriori* dans un contexte semi-Bayésien.

Mots clés: Biostatistique, cellules T $CD4^+$, équations différentielles, essais cliniques, Interleukine 7, modélisation, VIH.